U. S. ARMY
TRANSPORTATION RESEARCH COMMAND
FORT EUSTIS, VIRGINIA

TCREC TECHNICAL REPORT 61-15

RESULTS OF WIND-TUNNEL TEST OF A FULL-SCALE FUSELAGE-MOUNTED, TIP-TURBINE-DRIVEN LIFT FAN

VOLUME 2

Additional 30 Hours of Wind Tunnel Tests
September-December 1960

Task 9R38-01-020-02
Contract DA 44-177-TC-584

April 1961

prepared by :

GENERAL ELECTRIC COMPANY
Flight Propulsion Laboratory Department
Cincinnati 15, Ohio

DISCLAIMER NOTICE

When Government drawings, specifications, or other data are used for any purpose other than in connection with a definitely related Government procurement operation, the United States Government thereby incurs no responsibility nor any obligation whatsoever; and the fact that the Government may have formulated, furnished, or in any way supplied the said drawings, specifications, or other data is not to be regarded by implication or otherwise as in any manner licensing the holder or any other person or corporation, or conveying any rights or permission, to manufacture, use, or sell any patented invention that may in any way be related thereto.

ASTIA AVAILABILITY NOTICE

Qualified requestors may obtain copies of this report from

Armed Services Technical Information Agency
Arlington Hall Station
Arlington 12, Virginia

The information contained herein will not be used for advertising purposes.

The findings and recommendations contained in this report are those of the contractor and do not necessarily reflect the views of the Chief of Transportation or the Department of the Army.

HEADQUARTERS
U. S. ARMY TRANSPORTATION RESEARCH COMMAND
Fort Eustis, Virginia

FOREWORD

This report is the second of a three-volume series on the fan-in-fuselage model wind tunnel tests at the NASA-Ames Research Center 40' x 80' wind tunnel. The estimated STOL performance shown in Section V is preliminary and may be revised in Volume 3. The reader is encouraged to review the procedure used to separate fan lift from aircraft lift as described in Section V.

This Command concurs in the recommendations set forth in Section VII. The references listed in Section VIII include additional reports that have been produced under Contract DA 44-177-TC-584.

FOR THE COMMANDER:

APPROVED BY:

John W. White
JOHN W. WHITE
USATRECOM, Project Engineer

Earl A. Wirth
EARL A. WIRTH
CWO-4 USA
Adjutant

Task 9R38-01-020-02
Contract DA 44-177-TC-584
April 1961

RESULTS OF WIND TUNNEL TESTS OF A FULL SCALE FUSELAGE MOUNTED, TIP TURBINE DRIVEN LIFT FAN

Volume 2

Additional 30 Hours of Wind Tunnel Tests

September-December 1960

Prepared By:
GENERAL ELECTRIC COMPANY
Flight Propulsion Laboratory Department
Cincinnati 15, Ohio

for
U. S. ARMY TRANSPORTATION RESEARCH COMMAND
FORT EUSTIS, VIRGINIA

TABLE OF CONTENTS

LIST OF ILLUSTRATIONS

LIST OF TABLES

I SUMMARY

Contract DA-44-177-TC-584 with the Army requires that, in addition to bi-monthly technical progress reports, comprehensive reports of major work phases be prepared and submitted to the contracting officer. Previous reports submitted under this requirement are:

X353-5 Fan Design Report, May 30, 1960

Fabrication, Test and Analysis of a Tip-Turbine VTOL Propulsion System (Report of Phase I, Static Tests, Fuselage Mounted X353-5) TREC 60-42, August 31, 1960.

Results of Wind Tunnel Tests of a Full Scale Fuselage Mounted Tip Turbine Driven Lift Fan (X353-5) Phase II Volume 1 of 3, TREC 61-15, January, 1961.

This is the required report for another major portion of Phase II contract work. It includes additional results for the full scale fuselage mounted X353-5 lift fan obtained during a second test of 30 hours duration in the Ames 40' X 80' wind tunnel. The report includes:

- Modifications to test equipment (Section II)
- New instrumentation (Section III)
- Test procedures and results (Section IV)
- Analysis of test results, conclusions and discussion of any problems encountered (Section V)
- Hardware Inspection Results (Section VI)

- Program Recommendations (Part VII)

The basic test data obtained for every test point are tabulated in Appendix A. A few items of summary:

Fan operating time - 29 hours, 44 minutes
Data points recorded - 824
Range of Variables tested -

- Tunnel speed	0 to 100 Knots
- Angle of attack	-8° to +16°
- Fan speed	0 to 2640 RPM (100%)
- Exit louver angle	-1° to +49°
- Wing flap angle	0°, 30°, 40°
- Tail position	0.2 and 0.4 b/2 above extended wing chord plane
- Tail configuration	With and without full span, split flap
- Tail incidence angle	0° to 25°
- Pitch reaction control	0 to +5000 Ft. Lbs.
- J85 engine speed	0 to 16,500 RPM (100%)
- J85 turbine discharge bleed	6% of J85 inlet flow
- Tunnel temperature	52° to 102°F

Analyses of the results are presented in considerable depth defining fan hover performance and variation with flight speed, comparing fan powered with basic aircraft performance and calculating various transition performance characteristics and configuration requirements for cases of maximum acceleration, maximum climb, controlled descent, unaccelerated level flight and short take off (with and without overloads). A few items of performance conclusions are listed below:

AERODYNAMIC

- The basic aircraft (fan not operating) exhibited a more favorable static longitudinal stability derivative for the case with the fan inlet duct open than with the duct closed off ($\partial C_M/\partial C_L$ = -0.22 versus -0.14).

- Throughout a flight speed range sufficient for take off transition, the level of total pressure at the rotor face was equal to the zero flight speed level plus 100% of the flight dynamic head.

- Neither angle of attack nor angle of yaw had an appreciable effect on inlet performance over a wide range of the variables. Combined high angle of attack and large angle of yaw caused inlet performance to drop to a level equivalent to operating without an inlet vane.

*- Measured fan performance at hover was 7050 pounds lift at 100% speed ($\beta = 0^\circ$).

*- The general characteristics of interaction lift and drag were similar. Both coefficients ($C_{L\ int}$ and $C_{D\ int}$) decreased with increased V_P/V_{tip} ratio and β, and were not influenced by angle of attack variations in the range of $\alpha = -4^\circ$ to $+8^\circ$. The maximum interaction lift measured was equivalent to a $C_L = 0.37$.

*- During transition, there is little or no interaction lift at the maximum conversion speed, but the drag of the aircraft is increased by an additional $C_D = 0.06$.

- Tail downwash was not significant except when the exit louver angle was set at 0°. The tail position (i.e., high vs. low) made only a slight difference in the results. Increased downwash experienced with the tail in the low position varied with V_P/V_{tip} from 2° to $1/2^\circ$.

---

* Denotes where conclusion given here may be somewhat more encompassing or different from that listed in Volume I and should therefore be considered as superseding.

- Pitching moment coefficient decreased at the very high velocity ratios indicating that the maximum trim control criterion will be determined at low velocity ratios (normally encountered in take off transition).

* - Aside from the nose up pitching moment due to vectoring the fan discharge, the largest contributions to nose up moment resulted from negative pressures on the top of the fuselage ahead of the fan and on the bottom of the fuselage behind the fan. The contribution from each of these low pressure zones appeared to be about equal.

* - In the transition analyses the following results were calculated: -

. The maximum trim control requirement (in addition to the tail lift) was about 7% of gross weight, in terms of reaction control force located at the tail, and was required for either the case of maximum acceleration or maximum climb.

. Maximum acceleration was shown to be 0.29 g during level flight. The time from hover to conversion speed was 32 seconds and required a distance of 3340 feet.

. Maximum deceleration was -0.28 g during level flight. The time from conversion to hover was about 42 seconds and required a distance of 2900 feet.

. Maximum rate of climb was 1380 fpm at Vp = 65 knots ($\theta = 12^{\circ}$).

. A landing transition at constant attitude required approximately 60 seconds and a distance of 4000 feet.

- Analysis of short take off* ground run followed by airplane rotation to maximum climb condition to clear a 50 foot obstacle showed the following distances:

Take Off Weight / Max. Installed Lift	Distance to Clear 50 Foot Obstacle
1.0	509
1.1	862
1.2	1195

MECHANICAL

- Angle of attack did not affect rotor stress characteristic except for a slight increase when the wing was stalled.

- Yaw had a negligible influence on rotor stress.

- Crossflow and β variations did not influence blade flexural and torsional modes of vibration.

- Increased crossflow and β setting did slightly increase the cosine 2θ mode in the rotor at normal fan operating speeds, but the values were low relative to running limits.

- Running stress limits were exceeded transiently during deceleration through the rotor critical speed at 60 knots flight speed with exit louvers at 35°; however, this value was within the absolute limit.

- Up to 40 knots, stress levels were unaffected by removal of the inlet vane. At 60 knots and above, both flexural and torsional modes increased slightly.

*The analysis of the STO performance is based on data obtained with an installation height to fan diameter ratio = 3.0. A more complete STOL analysis will be presented in Volume 3 which will include ground effect test results with h/d_F values of 0.9 and 1.5.

- Torque band stress (tangential) was reduced for the design used in this test; however, 6 tangential cracks were noted in the bands after about 22 hours of testing. Continued testing showed no new cracks or propagation in completing the 30 hours of testing.

- Redesign of the torque band will be required to eliminate the crack incidence.

- Hardware inspection after disassembly showed no other significant deficiency, and the hardware was generally in excellent condition.

II WIND TUNNEL MODEL

AIRCRAFT* MODIFICATIONS

In order to improve the model and to extend the test variables, some changes were made for this test period:

Flaps - Flaps initially extended from 20% to 100% of the wing semi-span distance. During this testing, they extended from 20% to 60% of the wing semi-span, and were adjustable to 40°.

Ailerons - The part of the flaps from 60% to 100% of the wing semi-span were converted to ailerons which could be preset at 0°, ±15° and ± 30° to provide lateral control force.

Drag Shape - A streamlined body was placed behind the J85 engine and elbow to reduce flow separation in that area and to reduce the yaw force due to asymmetric drag present at high tunnel and fan speed conditions. The J85 engine mounts were also covered with streamlined fairings.

FAN MODIFICATIONS

Fan Serial Number 001 was overhauled for use in this test program. It is the same fan used in the immediately preceding wind tunnel test program for this same fan-in-fuselage model (see Reference 10 for a discussion of the teardown inspection results). Several parts were replaced as follows: -

Forward Frame:

1. Trunnion mount bolts (to assure maximum locking action).
2. Six pieces of scroll seal (cut to longer length to provide more overlap).

*Figure 1, Appendix B shows the aircraft model dimensions and general specifications. This supersedes Figure 3, page 14 in Volume 1, and is based on measured rather than drawing dimensions.

Rotor:

1. Two covers (replacing one with a crack indication and another with a loose locknut).
2. Disc tie bolt nuts (to assure maximum locking action).
3. Retainer pin locking tabs (expendable).
4. Forward and aft torque bands (the aft torque band was replaced to retain a pair with identical operating history).

Failure of the forward torque band was discussed in detail in Reference 10. A design change incorporated in this assembly was based on the incidence of cracks only at the joint of adjacent carriers, the failure location being an indication that the discontinuity caused by individual carriers is not reflected in the basic design analysis which considers the boundary conditions to be identical at all torque band attachment ears.

The absence of cracks in the torque transmission attachment ears was an indication that the calculated steady-state stresses and the measured axial bending vibratory stresses at these ears were within the stress range properties of the band material. The design change was a method of reducing the steady state stresses and effectively redistributing the vibratory bending stresses away from the ear-band radius at the adjacent carrier joint. The change consisted of a small machined tab which was bolted across the carrier joint. The construction of the tab included a tapered "foot" to bear against the band as shown in Figure 2* during steady state loadings.

In addition to the tab, all indications of intergrannular attack at the ear-band radius were removed, and the torque band strain gages were relocated to measure axial bending vibratory stresses in line with the carrier joint.

*All Figures and performance curves are located in Appendix B.

The completely assembled rotor is shown in Figure 3.

Scroll:

1. Serial Number 001 scroll was used in place of Serial Number 002. This was done to make Serial Number 002 available for a concurrent test program using Fan 002 at Evendale which will be reported separately.*
2. The scroll end mounts were also interchanged.

ENGINE CHANGE

The most significant change in the test equipment from the previous program was the substitution of a J85-7** for the J85-3 engine. The J85-7 is a more advanced version of the J85 missile engine with a significantly higher cycle pressure ratio due to an additional compressor stage. The engine change allowed fan operation up to 100% fan speed.

With the J85-3, the scroll/engine area mismatch was so large that about 13% turbine discharge bleed was required to operate the engine within temperature limits. With the J85-7 and the scroll selected for powering the fan used in this test program, an area mismatch still required about 6% bleed. The basic engine power however is sufficiently in excess of specification so that 100% fan speed was still achievable even with this amount of bleed.

*The effect of this scroll change on fan turbine efficiency will be discussed in Section V of this report.

** S/N 235 - 003

IV TEST PROCEDURES AND RESULTS

Table 1 gives a summary of the test runs and the range of variables encompassed. Table 2 shows the breakdown of fan operating time as a function of speed and fan turbine inlet temperature. The testing reported herein was accomplished with Fan Serial Number 001 - Build-Up #3. The testing was conducted with essentially the same procedures described in Volume 1, Section V.

MEASUREMENT ACCURACIES

The velocity probe located on the nose of the aircraft was used to obtain a calibration between velocity measured upstream of the model and velocity near the model.

As expected, the velocity measured by the probe at low velocity ratios was considerably higher (as much as 50%) than the velocity used for calculation of the airplane coefficients. This was especially true for exit louver angles of 0°. Figure 6 shows the ratio of the two velocities as a function of velocity ratio (V_P/V_{tip}) and exit louver angle. The velocity as measured by this probe is corrected by a ratio obtained during runs with the fan off. This ratio was measured as $q_{tunnel}/q_{probe} = 1.08$, and is caused by the combination of blockage and other inaccuracies such as wall effect (i.e., proximity of probe to the nose of the aircraft). The readings obtained from this velocity probe were used only as a qualitative means of understanding the relatively high interaction drag phenomenon encountered at low velocity ratios at $\beta = 0°$ which was observed during the previous test period and also during this testing. In order to be consistent with any other similar data, the tunnel velocity, as measured by the conventional tunnel velocity measurement instrumentation, has been used in all quantitative calculations unless clearly stated otherwise.

TABLE 1

SUMMARY OF TEST RUNS

Run No.	Date	V_p Knots	α Deg.	R_F RPM	δ Deg.	i_t Deg.	RC In. Hg.	β Deg.	ψ Deg.	PURPOSE OF RUN
1	10/28	60	-4 to +16	0	0	Off	0	90	0	Checkout of model and aircraft polar.
2	10/31	20 - 60	-4 to +16	1630 - 1700	0	Off	0	0	0	Powered aircraft polar and stall determination at various velocity ratios.
3	10/31	20 - 60	0	2500 - 2530	0	Off	0	0 - 40	0	Powered aircraft performance as a function of exit louver setting and velocity ratio at high fan speeds - horizontal tail off.
4	11/1	0	0	2330 - 2640	0	Off	0	0 - 40	0	Static fan performance versus exit louver position-overhead door opened.
5	11/1	80 - 100	0	2470 - 2520	0	Off	0	0 - 40	0	Continuation of Run #3 at higher velocity ratio.
6	11/1	60	-4 to +16	0	0	0 - Hi pos.	0	90	0	Aircraft polar-power off.
7	11/1	20 - 100	0	2400 - 2500	0	0 - Hi pos.	0	0 - 35	0	Same as Runs #3 and #5, but with tail on.
8	11/2	20 - 80	-8 to +16	1330 - 1720	30	0 - Hi pos.	0	0	0	Powered aircraft polar, stability and stall investigation.
9	11/2	30 - 80	-8 to +14	1690 - 1760	30	0 - Hi pos.	0	20 - 35	0	Powered aircraft polar, stability at various exit louver settings.
10	11/2	40	-4 to +14	0	30	0 - Hi pos.	0	90	0	Aircraft polar-power off.
11	11/2	20 - 80	-4 to +14	0	30	0 - Hi pos.	0	90	0	Aircraft polar-power off.
12	11/3	20 - 100	-5 to +8	2350 - 2540	30	13-21 Hi pos.	9.3 - 11.8	-1 - +40	0	Trim aircraft at 6500 Lbs. G.W.
13	11/3	60	-4 to +12	0	30	0 - Lo pos.	0	90	0	Aircraft polar-power off, tail low position.
14	11/4	0	0	2600 - 2640	30	0 - Lo pos.	0	0 - 15	0	High speed fan performance-overhead doors opened.
15	11/4	20 - 80	0	1630 - 2500	0	0 - Lo pos.	0	0 - 49	0	Same as Runs #3 and #5 except for flap and tail position; also high exit louver angles at high velocity ratio.
16	11/4	20 - 80	-8 to +14	1640 - 1700	30	0 - Lo pos.	0	0	0	Same as Run #8 except with tail in low position.
17	11/4	0	0	0	30	0 - Lo pos.	0 - 11.2	0	0	Calibration of pitch reaction control
18	11/4	40 - 60	-8 to +14	0	30	0-24 Lo pos.	0 - 11.9	0	0	Aircraft polar, low tail position sweep and pitch reaction control effectiveness at different forward speeds.
19	11/4	20	0	0	30	0-24 Lo pos.	0	0	0	Tail sweep at 20 knots.
20	11/7	20 - 80	-8 to +12	1680 - 2450	40	0-25 Hi pos.	0 - 9.5	0 - 28	0	Powered aircraft polar and trim at 6500 Lbs. G.W.
21	11/7	20 - 80	-8 to +14	0	40	0 - Hi pos.	0	90	0	Aircraft polar-power off.
22	11/8	60 - 100	-4 to +10	2400 - 2520	30	0-15 Hi Lift Tail	0 - 9.9	24 - 40	0	Trim aircraft at 9000 Lbs. (STOL).
23	11/8	40 - 80	0	0	30	0-18 Hi Lift Tail	0	90	0	High lift tail sweep and calibration.
24	11/8	60	8	0	30	0 - Hi pos.	0	90	-16 to +16	Yawler-power off.
25	11/9	20	-8 to +16	1670 - 1720	30	0 - Hi pos.	0	0 - 35	-16 to +8	Yawler-power on, 20 knots.
26	11/10	40	0 to +14	1160 - 1720	30	0 - Hi pos.	0	0 - 35	-16 to +8	Yawler-power on, 40 knots.
27	11/10	60	-8 to +14	0	30	0 - Hi pos.	0	90	-16 to +8	Polar at various yaw angles - power off.
28	11/14	20	0	1690 - 1730	30	0-20 Hi pos.	0	0 - 35	0	Tail downwash investigation.
29	11/14	40	-8 to +10	1700 - 1720	30	0 - Hi pos.	0	20 - 35	0	Stability at louver settings of 20 and 35 degrees.
30	11/14	60	-8 to +10	1680 - 1710	30	0 - Hi pos.	0	0	-16 to 0	Yawler at 60 knots.
31	11/14	80	-8 to +10	1690 - 1720	30	0 - Hi pos.	0	0	-16 to 0	Yawler at 80 knots.
32	11/14	60	-8 to +10	1690 - 1700	30	0 - Hi pos.	0	20 - 35	0	Stability at louver settings of 20 and 35 degrees.
33	11/15	0 - 100	0	1160 - 2400	30	0 - Hi pos.	0	0 - 35	0	High crossflow to through flow ratio stress investigation at high velocity ratios; comparison of door closed and opened static performance.
34	11/15	20 - 80	0	1690 - 1730	30	0 - Hi pos.	0	0 - 35	0	Inlet louvers removed; inlet loss and fan and aircraft performance with crossflow.
35	11/15	30 - 60	-8 to +14	1660 - 1700	30	0 - Hi pos.	0	0	0	Polar-power on with inlet louver removed.
36	11/16	20 - 40	-8 to +14	0	30	0-20 Hi pos.	0	90	0	Power off polar-fan inlet opened, and high tail position calibration.
37	11/16	60 - 80	-8 to +16	0	30	0-16 Hi pos.	0	90	0	Same as Run #36 at 60 - 80 knots.
38 to 48	11/16 to 11/18	0 - 60	-4 to +16	0	30	0 - Hi pos.	0	90	-16 to 0	Aileron effectiveness calibration; roll reaction control effectiveness, power off.

TABLE 2
SUMMARY OF LIFT FAN OPERATING TIME
(Fan Serial Number 001)

Speed Range, N_F (Per cent)	B/U #1[a] Even.	B/U #2[b] Even.	B/U #2[b] Ames.	B/U #3 Ames	Total
0 - 24	5:02	4:08	-	-	9:10
25 - 49	2:43	7:23	5:08	4:10	19:24
50 - 74	9:52	5:57	12:01	16:43	44:33
75 - 89	1:29	2:11	3:08	1:06	15:49
90 - 100	-	-	-	7:45	
TOTAL	19:06	19:39	20:17	29:44	88:56
Temp. Range, $T_{t_{5.1}}$ (Deg. F)					
0 - 599	8:20	5:09	-	-	13:29
600 - 799	1:57	1:49	-	5:05	9:01
800 - 899	7:49	7:05	:28	15:17	30:39
900 - 999	1:00	4:39	14:22	1:21	21:22
1000 - 1200	-	:57	5:27	8:01	14:25
TOTAL	19:06	19:39	20:17	29:44	88:56
Data Points	71	66	348[c]	539[c]	1024

[a] Reference 5

[b] Reference 10

[c] Not including basic airplane data with fan off which represents an additional 476 data points.

The test results are presented in Table A-2, Appendix A. The following items in this table are direct readings (incorporating appropriate calibration): tunnel speed (V_p), fan speed (N_F), tunnel temperature, aircraft angle of attack (α), exit louver angle (β), tail incidence angle (i_t), reaction control output (RC), flap deflection angle (δ_f), engine speed (N_{J85}) and exhaust gas temperature (EGT). The other items in the table have been converted from direct measurements by means of the relationships outlined in the list of definitions and symbols in Table A-1, Appendix A. These calculations were accomplished as follows:

- All the force data (lift, drag and moments) were reduced on the IBM 704 computer operated by NASA-Ames. The standard 40' X 80' wind tunnel calculation program was used with proper constants applied for this particular configuration.

- The internal fan performance data reduction was accomplished at Evendale also using an IBM 704 computer and an existing lift fan program deck.

- All other fan/aircraft performance calculations were made manually as described in the section on analysis of results, where appropriate.

V ANALYSIS OF RESULTS

A. GENERAL CONSIDERATIONS

J85 Engine:

The J85-7 engine used during this test develops a considerably higher power level than the -3 engine used previously. In addition, the control utilizes a continuously variable compressor bleed schedule throughout the speed range which provides more stall margin and a wider fan speed operating range. Due to the change of scrolls, an area mismatch between the scroll and the engine discharge still existed and, throughout most of the runs, approximately 6% of the turbine discharge weight flow was bled off. This paragraph deals with the operating characteristics of the engine which are not as encountered with a normal engine installation that does not require turbine discharge bleed, and the operating characteristics are therefore different than described in engine manuals. The fan performance can, of course, be expressed as a function of available horsepower and actually becomes independent of the gas generator. The total available horsepower at stations 5.1 and 5.4 is shown in Figure 7 as a function of engine speed. The losses in the elbow (including diffuser) and scroll were assumed to be the same as for all previous tests and are plotted as a function of station 5.1 Mach number in Figure 8. The turbine discharge temperature as a function of engine speed is shown in Figure 9 .

Bleed Thrust:

Because of the reduction in bleed requirements by approximately a factor of two, the bleed thrust was reduced by a factor of 4, or it was at most around 25 pounds, and is disregarded in all the analyses (moment caused by this thrust is also disregarded).

Turning Angle:

Based on an extensive analysis of hover data (by calculating the turning angle from horizontal and vertical thrust measurements), the actual turning angle, β_V, of the exit louvers was 3.2° more than the physical angle, β. (This was reported as approximately 3° in Volume 1 and, because it is a function of the assembly of the exit louvers and the tolerances in all the actuator linkages, this will be a slightly different value for each fan.)

B. BASIC AIRCRAFT PERFORMANCE (Fan Off)

The Aircraft Drag:

Aircraft drag was high for the reasons described in Volume 1. Some small changes were made on the installation to reduce yaw oscillations at high flight speeds; however, the effect on drag was small. For comparison, the values of C_D as measured at zero lift conditions are shown in Table 3 below (fan inlet and exit closed).

TABLE 3

VARIATION OF C_{Do} WITH A/C CONFIGURATION

Flap Position	Tail Position	C_{Do}	Test Phase
0°	Off	0.100	1st
0°	High	0.105	1st
0°	High	0.110	2nd
15°	Off	0.115	1st
15°	High	0.120	1st
30° (Full Span)	Off	0.150	1st
30° (Full Span)	High	0.155	1st
30° (.2 - .6 b/2)	High	0.145	2nd
30° (.2 - .6 b/2)	Low	0.160	2nd
30° (.2 - .6 b/2)	High	0.155*	2nd
40° (.2 - .6 b/2)	High	0.170	2nd

*Data obtained with inlet hole uncovered.

Because of the change in flap configuration, only the $\delta = 0°$ case for the first and second test periods is directly comparable (i.e., 0.105 versus 0.110).

Aircraft polars (C_L vs. C_D, α and C_M) are plotted in Figures 10 through 14 which take into account the configuration changes incorporated for this test period.

Lift:

Lift characteristics are similar to the ones obtained during the first phase of Ames testing. Maximum lift coefficient with 30° flaps (tail-on, high position) was about 1.5, and with 40° flaps about 1.4.

Tail Downwash and Tail Control Effectiveness:

Three different tail configurations were tested:

1. High tail position (same as during previous test period) located 0.4 b/2 above the wing chord plane.
2. Low tail position located 0.2 b/2 above the wing chord plane.
3. High lift tail in same location as number 1 with a full span split flap set at 30° (see sketch below).

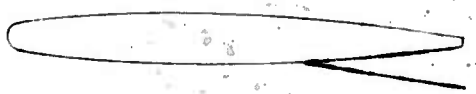

The change in moment coefficient due to the tail, ΔC_M, is plotted in Figure 15. Adding the split flap to the tail located in the high position resulted in a 47% increase in $\Delta C_{M\ max}$. As far as actual ability to produce pitch control moment, the low and high tail positions were about equal. The low tail position however encountered approximately 2° more downwash (3° vs. 1°) so that a tail incidence angle schedule for equivalent tail control power would be 2° offset from a high tail schedule.

During the previous test, the downwash was determined from a comparison of test runs with the tail on and off, and these results were used again for this report in determining the $\Delta C_M - i_t$ relationship for the high tail positions in Figure 15.

The low tail configuration added to the program during this test period was tested only with the wing flap angle set at 30° (0.2 to 0.6 b/2), and there is no corresponding tail off data for direct comparison. The tail downwash for this configuration was obtained from an estimated value of C_M at $\alpha = 0°$ and $\delta_f = 30°$ corresponding to a tail off condition as follows:

- From the previous test period

C_M @ $\alpha = 0°$, $\delta_f = 0° = +0.08$

C_M @ $\alpha = 0°$, $\delta_f = 30°$ (full span) $= -0.21$

The ΔC_M between the 0° and 30° (full span) flap cases is, therefore, -0.29. Since only approximately 57% of the wing area is influenced by the 0.2 to 0.6 span flaps, the tail off C_M for this new wing configuration is estimated as: $0.08 + [0.57 \times (-0.29)] = -0.09$.

Due to large scatter in pitching moment data, the attempt at trying to determine tail downwash variation with angle of attack had to be abandoned.

Ailerons:

Aileron effectiveness as a function of aileron angle is shown in Figure 16.

Static Longitudinal Stability (Fan Off):

Table 4 shows a comparison of the static longitudinal stability derivatives, $\partial C_M/\partial C_L$, for the various flap configurations tested. Apparently, uncovering the fan inlet hole (exit louvers still fully closed) reduces the inherent instability of the fuselage (refer to Appendix B-I, Volume 1).

TABLE 4

COMPARISON OF LONGITUDINAL STABILITY DERIVATIVES

Flap Position (Deg.)	Tail Position	$\partial C_M/\partial C_L$
0	High	-0.17
30	High	-0.14
30	Low	-0.13
30	High	-0.22*
40	High	-0.16

* Data obtained with inlet hole uncovered.

C. FAN AERODYNAMIC PERFORMANCE

Fan Inlet Performance:

The face of the fan rotor is over four feet below the edge of the inlet when installed in the test model, and is normal to the flight path. At zero flight speed there is a small inlet total pressure decrease between ambient and the face of the rotor due to duct friction and vane losses. During the previous testing program in this wind tunnel, it was found that, throughout transition, the pressure level at the rotor face was equal to the zero flight speed value plus 100% of the flight dynamic head.

These earlier tests were conducted primarily at zero angle of attack and yaw so that it was an objective of this test period to determine the effect on the inlet performance of varying these parameters. Comparative data are shown in Figures 17, 18, and 19, with the inlet loss expressed as a fraction of average inlet duct dynamic pressure. Also indicated in Figure 17 is the effect of removing the inlet vane. The inlet loss was so small at zero and low flight speeds that the effect of the vane in these regions was not distinguishable in the data. However, the importance of the vane becomes clear at higher flight speeds since it extends the low loss range to higher values of the flight velocity to fan tip velocity ratio (V_P/V_{tip}). This, in effect, increases the flight speed at which net forward thrust becomes zero and therefore, increases the margin of conversion speed above airplane stall speed.

Angle of attack had a negligible influence on inlet performance at negative angles and up to 4° positive angle. At 8°, however, the low loss range was significantly decreased indicating the onset of inlet separation at a lower velocity ratio. Yaw, on the other hand, did not by itself result in greatly changed inlet performance, even at very high angles on the order of 16°; the characteristics noted were probably due to changes in vane end effects as the yaw angle varied. The direction of yaw (i.e., with or against fan rotation) made no difference in the results. The combined influence of yaw and high positive angles of attack was more severe than either alone, and most noticeably so at the higher velocity ratios. The particular combination of -8° yaw and +8° angle of attack showed rapidly deteriorating performance such that, at the higher velocity ratios, a loss level was measured equivalent to that obtained where no vane was employed. Figure 20 is a summary plot showing the relative influence of these various configurations.

For the relatively low angles of attack required in accomplishing transitions with this airplane model, the loss levels measured appear to be very satisfactory.

The data in Figures 17 through 20 have all been adjusted to correspond to 100% fan speed, although they were obtained at approximately 65% speed. In essence, the adjustment is to the V_P/V_{tip} parameter to account for the variation in the ratio of the fan axial (or through-flow velocity) to fan tip speed with fan speed. Figure 21 is data taken from the previous test period, and shows the characteristic of inlet duct flow coefficient* with fan speed. This parameter very nearly integrates the effects of Reynolds number change, fan efficiency change and fan energy absorption change due to blade untwist, all of which are a function of fan speed. An additional effect of Mach number on the fan performance is very small, and can be neglected since the fan is of a relatively low pressure ratio design.

The result of these combined influences is that at low fan speeds, the axial velocity to fan tip speed ratio is lower than at higher fan speeds; this causes the inlet loss versus V_P/V_{tip} based on low fan speed data to be somewhat pessimistic. The correction is therefore applied to V_{tip} to reduce it proportionately or, in effect, shift the loss curves of $\bar{\omega}$ versus V_P/V_{tip} to the right (i.e., higher V_P/V_{tip} ratios). This adjustment can be made by recalculating the V_P/V_{tip} ratio as follows:

$$(V_P/V_{tip} \text{ measured at part speed}) \quad K = V_P/V_{tip} \text{ equivalent at 100\% fan speed}$$

$$\text{where } K \text{ is } 1 + \frac{\Delta \Phi_{oo}}{\Phi_{oo} \text{ at part speed}} = \frac{\Phi_{oo} \text{ at 100\% speed}}{\Phi_{oo} \text{ at part speed}}$$

*Duct flow coefficient at station 10.2 is $\Phi_{oo} = C_{Z\ 10.2}/V_{tip}$ where $C_{Z\ 10.2}$ is the inlet duct average velocity.

From Figure 17, it would appear that the effect of increasing exit louver angle setting was to increase the inlet loss. In fact, however, this is the effect of fan throttling which reduces through-flow velocity with increased β for a given speed or, in other words, reduces the flow coefficient. It is more precise but less convenient to replot the inlet loss data against an abscissa defined as the ratio of flight speed to fan inlet duct velocity. This was done in Figure 22, and as would be expected, the 0° and 35° β data collapse into a single line; data plotted in this manner make it possible to apply inlet results obtained with this fan to similar installations, but using different fan designs since the losses are shown as a function of duct velocity which is independent of the source of the flow. For the specific model tested, it is more convenient to use the more easily obtained relationships shown in Figures 17 through 20.

Inlet performance was efficient in terms of recovering flight dynamic pressure. This can be clearly seen by Figure 23; the pressure at the face of the rotor is lower than ambient by the static inlet losses (duct friction and vane), and the difference between the line representing ambient plus flight dynamic pressure and the line representing the pressure at the face of the rotor is constant throughout the transition range indicating full recovery of flight dynamic pressure. At the high flight speeds as the inlet losses increase, this difference increases indicating a reduction in ram recovery. Another manner of viewing this same performance is to define a ram efficiency which includes the static inlet loss or $\eta_R = 1 - \Delta P_t/q$, where ΔP_t is the total pressure difference between ambient plus flight dynamic pressure and the pressure at the face of the rotor. Since there is a static loss, this is obviously indeterminate at zero q values, and increases with flight speed until the point is reached where the inlet separates and losses begin to increase. This is shown in Figures 24 and 25.

Fan System Performance:

During the previous test program, it was estimated that the change in inlets between earlier static tests at Evendale and the wind tunnel program appeared to have resulted in an increase in fan performance at hover of approximately 4% in thrust; this was based on inlet pressure measurements.

Data were taken during this most recent test period with the throat section of the tunnel open to atmosphere (entire roof of tunnel open, refer to Volume 1, Figure 5) to obtain a valid zero V_p force measurement minimizing tunnel effects. This apparently relieved some tunnel effect, and the measured thrust increase over Evendale results was about 3.5% and correlated with the better inlet performance. This is attributable to the change from a 6% radius ratio bellmouth employing a cascade of six spanwise vanes to the 23.5/6%* bellmouth and single curved vane. Table 5 shows the actual performance values measured.

TABLE 5

FAN PERFORMANCE COMPARISON - EVENDALE VERSUS AMES

Test Configuration	Total Thrust Measured At 100% Speed (Lbs.)	Estimated Total Thrust At Design HP Based on Using Scroll, S/N 2 (Lbs.)
Evendale:		
6% bellmouth with cascade	6810	6950
6% bellmouth without cascade	7000	7140
Ames:		
23.5/6% bellmouth with curved vane	7050	7190

*23.5/6% stands for a bellmouth with a 6% radius ratio (i.e., bellmouth radius divided by inlet duct diameter) on the sides and back and a 23.5% radius ratio at the leading edge.

Note that in Table 5, the estimated thrust at design horsepower is qualified as based on using scroll, serial number 2.

The fan speed actually obtainable in this testing using scroll, serial number 1, with the design horsepower was only 99.5% of design speed compared to the Evendale result of 101% discussed in Reference 5. This results from scroll No. 1 having a poorer alignment with the turbine flow passage and also modified nozzle diaphragms (trailing edges relieved to increase the effective nozzle area) which affects the turbine vector diagram and, in turn, turbine efficiency. Turbine efficiency calculations based on fan internal performance data indicate the turbine efficiency penalty for scroll No. 1 is approximately 6% relative to scroll No. 2. This fully accounts for the change in fan speed - available horsepower relationship noted. (6% additional power from the turbine would increase the fan speed by approximately 2%.)

Figure 26 presents the fan performance characteristics at hover.

Establishing hover performance accurately is important for determining maximum VTOL capability of the system, but more specifically in this analysis, it is important in calculating that part of total measured lift at any flight speed which can be attributed to the fan; these calculations of fan performance are all extrapolations of hover performance. The wind tunnel balance system measures over-all performance at any flight speed and is therefore, not dependent upon knowing fan performance per se. But, in order to accurately determine interaction effects, the fan performance must be accurately identified. It is in this regard that this report differs from the analysis in Volume 1. Figure 27 shows the change in fan performance in terms of static lift coefficient (H_L) as a function of fan speed. The interaction analysis herein will be more accurate than in Volume 1 and should be considered to supersede that work.

In order to establish the accuracy level of these thrust measurements at hover, Table 6 was developed using data from both Evendale and Ames configurations. It can be seen from the "maximum variation" column that the accuracy of lift data (F_y) is less influenced by changing the test configuration or test location than is horizontal thrust data (F_x). This is as would be expected when considering the influence of ram drag on the F_x data. For example, a ten knot wind either at the Evendale open air facility or due to induced flow in the wind tunnel can cause a variation of as much as $\pm$ 250 pounds in horizontal thrust at hover conditions. At Evendale, it is necessary to know both wind velocity and direction; in the wind tunnel the direction is known, but the velocity on the airplane upper surface relative to measured tunnel velocity at low flight speeds has been shown* to be different. These conditions make it difficult to calculate the ram effect accurately. Measurement tolerances of $\pm$ 1 1/2% lift and $\pm$ 4% thrust appear to be proper. Here again, it must be pointed out that these accuracies refer only to segregating fan performance, and are not to be confused with accuracies of total lift and drag (or thrust) measurements of the airplane via the tunnel balance system which remain as outlined in Volume 1.

Fan performance in this report is the actual measured performance at Ames during this latest test period, Run #4, since the fan speed, thrust and tunnel speeds are felt to be more accurately known for this run than for any other test period.

Determination of Fan Performance as a Function of Flight Speed:

The difference between measured performance of the fan/aircraft system and the sum of the individual fan and aircraft contributions that can be calculated at any flight condition has been termed performance interaction; that is, an effect of the fan on the basic aircraft

*See Section IV

TABLE 6

FAN THRUST VARIATION AT CONSTANT FAN SPEED WITH EXIT LOUVER ANGLE FOR THREE TEST CONFIGURATIONS

	Ames 30 Hr. Test $\approx 95\% N_F/\sqrt{\theta}$			Evendale J85-3 $\approx 90\% N_F/\sqrt{\theta}$			Evendale 401 Burner. $\approx 90\% N_F/\sqrt{\theta}$			Maximum Variation Among Configurations		
β	$F/F_{\beta=0}$	$F_y/F_{\beta=0}$	$F_x/F_{\beta=0}$	$F/F_{\beta=0}$	$F_y/F_{\beta=0}$	$F_x/F_{\beta=0}$	$F/F_{\beta=0}$	$F_y/F_{\beta=0}$	$F_x/F_{\beta=0}$	$\Delta F/F$	$\Delta F_y/F$ Per cent	$\Delta F_x/F$
0	1.000	0.999	0.049	1.000	0.998	0.061	1.000	1.000	0.000	0	0.2	6.1
10	1.000	0.972	0.232	-	-	-	-	-	-	-	-	-
20	0.980	0.897	0.394	0.983	0.905	0.384	0.945	0.882	0.339	3.8	2.3	5.5
30	0.928	0.775	0.509	0.942	0.782	0.526	0.906	0.776	0.467	3.6	0.7	5.9
35	0.880	0.694	0.540	0.909	0.706	0.572	0.866	0.695	0.519	4.3	1.2	5.3
40	0.802	0.583	0.550	0.833	0.589	0.590	0.779	0.576	0.524	5.4	1.3	6.6

performance or of the aircraft on the basic fan performance, or both. Fan/aircraft performance is as accurate as the wind tunnel force balance system; the accounting for the various contributors to this performance is difficult. There is no known method of separating fan performance from airplane performance in a physical manner in a wind tunnel; i.e., by separate thrust measurements.* This is due to the inability to determine where the fan inlet ends and the aircraft surfaces begin, or to isolate interactions physically. However, even the analytical approach used herein could be improved by greatly expanding the internal fan instrumentation.

The basic airplane performance as a function of flight speed (with the fan off and the holes covered) is well defined; therefore, the key to accurate calculation of interaction effects is the accuracy with which the fan performance is known as a function of flight speed.

Specifically, what is needed is a relationship of fan thrust with exit louver angle and V_p/V_{tip} ratio. As described in Volume 1, Section VII-A, a relationship of measured total thrust to an ideal momentum thrust (based on station 10.6 total pressure and measured fan weight flow) was determined to be $F_{measured}/F_{10.6} = 0.96$ during static runs conducted at Evendale. This relationship was assumed to hold constant for all velocity ratios at $\beta = 0°$. This is a reasonably valid assumption as long as the fan to fan turbine thrust ratio does not change appreciably (e.g., a 1% error in total thrust would require a 10% change in fan turbine thrust). Also, it was assumed that the loss coefficients of stators and exit louvers are not affected materially by crossflow; and that the total thrust change as a function of exit louver angle at constant $HP_{5.4}$ is the same at any value of velocity ratio as at static conditions represented by Figures 28a and 28b. This latter assumption is valid if the rate of change of rotor efficiency ratio with throttling is independent of velocity ratio. This has been well verified. (See Figure B-4V-5, Volume 1 where

*In the sense that measuring rotor thrust is not considered to be sufficient to provide the basis for determining total fan thrust contribution as a function of V_p/V_{tip}.

it is apparent that changes in efficiency with throttling are linear throughout the velocity ratio range tested.) Using the above assumptions, fan performance characteristics as a function of velocity ratio and louver angle were obtained and are shown in Figures 29 through 33.

For calculation of fan ram drag, the fan weight flow variation with velocity ratio, β and fan speed as shown in Figures B-IV-6, B-IV-7 and B-IV-8, Volume 1, were used. J85 ram drag was obtained from J85 flow measured in the bellmouth. The tunnel velocity measurement upstream of the test section was used in all ram drag calculations.

There are considerable data at high fan speeds for determining fan performance up to velocity ratios, V_p/V_{tip}, of 0.3. There was a limited amount of higher velocity ratio data obtained between 0.3 and 0.5 (equivalent to 213 knots at 100% fan speed) but, in order to remain within the 100 knot limit on the test airplane, these data were obtained at near idle conditions on the fan. The rotor pressure ratio is so low near idle that assessing station 10.6 thrust is inaccurate. In order to estimate fan performance at velocity ratios above 0.3 V_p/V_{tip}, data obtained up to 0.3 velocity ratio was extrapolated. The extrapolation procedure and results are explained more fully in Appendix A.

Some results of fan speed variation at constant horsepower as a function of velocity ratio and β angle were reported in Volume 1. Considerable additional high fan speed data obtained during this phase of testing provides a more complete and more accurate picture, and supersedes the previous results. These fan speed characteristics as a function of velocity ratio and exit louver angle at constant horsepower are shown in Figure 34. It is apparent in the range of 0° - 20° β that fan speed at constant $HP_{5.4}$ is constant for all β and V_p/V_{tip} values. At hover and at low velocity ratios, increasing β beyond 20° unloads the fan resulting in a fan speed increase; as velocity ratio is

increased, however, the fan absorbs more power resulting in a fan speed decrease accompanying throttling beyond 20° β. This change in characteristic can be shown on the fan operating map (see sketch below) where the fan operating point shifts along a constant horsepower line to the right as a result of ram recovery and to the left as the result of throttling with the exit louvers. At hover and at low velocity ratios, the throttling occurs between points A and B and; at high velocity ratios, the throttling occurs between points C and A.

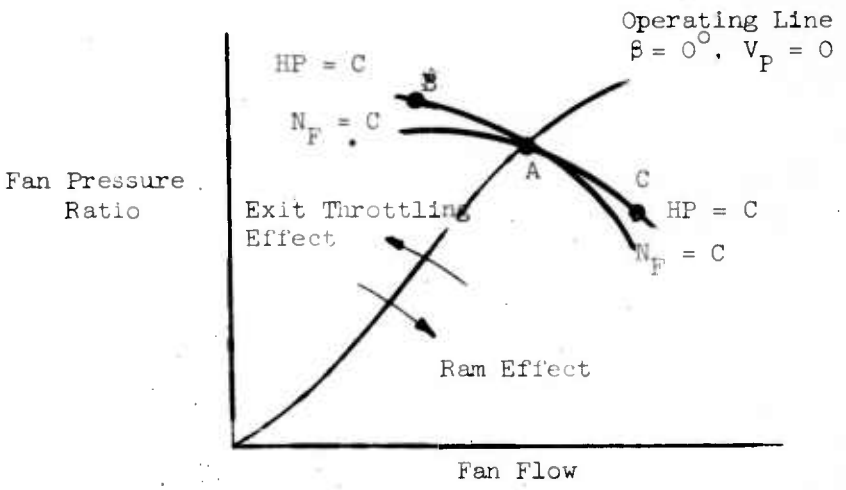

Figure 35 shows the fan speed characteristics as a function of flight speed and β. It is obtained at constant J85 throttle setting corresponding to 100% N_F at β = 0° and V_P = 0 and applies 100% J85 inlet ram recovery.

D. FAN POWERED AIRCRAFT PERFORMANCE

Performance Coefficients:

Since performance in the flight regime from hovering through transition is necessarily a function of the fan performance, a set of relationships to non-dimensionalize fan powered aircraft performance was developed. These coefficients are described in Volume 1, and lend themselves more readily to studies of the various approaches to transition. The conventional airplane coefficients C_L, C_D, C_M are used extensively as well, and are interchangeable with these derived coefficients.

In order to convert from one system to the other, the relationships in Table 7 hold. Since geometric parameters are involved, a general conversion as well as one specifically appropriate to this airplane model are given. Basically, the new coefficients differ from conventional coefficients due to being based on the fan dynamic pressure instead of flight dynamic pressure, for example:

$$C_L = \frac{2\,L_T}{\rho\,S_w\,(V_p)^2} \quad \text{whereas} \quad H_L = \frac{L_T}{\rho\,A_F\,(V_{tip})^2}$$

TABLE 7

CONVERSION RELATIONSHIPS - AIRCRAFT COEFFICIENTS

To Convert From	To	MULTIPLY BY (For General Case)	MULTIPLY BY (For Specific Model Tested)
C_L	H_L	$\frac{(V_P/V_{tip})^2 S_w}{2 A_F}$	$7.023 (V_P/V_{tip})^2$
C_D	H_D	Ditto	Ditto
C_M	H_M	$\frac{(V_P/V_{tip})^2 S_w \bar{c}}{2 A_F l_t}$	$2.339 (V_P/V_{tip})^2$
H_L	C_L	$\frac{2 A_F}{(V_P/V_{tip})^2 S_w}$	$0.1424 \left[\frac{1}{(V_P/V_{tip})^2}\right]$
H_D	C_D.	Ditto	Ditto
H_M	C_M.	$\frac{2 A_F l_t}{(V_P/V_{tip})^2 S_w \bar{c}}$	$0.4274 \left[\frac{1}{(V_P/V_{tip})^2}\right]$

Interaction Lift and Drag:

Interaction lift is defined for this analysis as the difference between the measured value of total lift and the sum of basic airplane lift and basic fan lift, corrected for ram recovery and exit louver throttling and vectoring effects.

Interaction drag is defined as the difference between the measured value of total drag and the sum of -

- Basic aircraft drag.

- Basic fan thrust, corrected for ram recovery and exit louver throttling and vectoring effects.

- Fan and engine ram drag.

Tables 8 and 9 are presented to show precisely the calculation routine. While interaction lift is defined and calculated similarly to interaction drag, it is more accurately known since fan lift as a function of exit louver angle is known with greater accuracy than thrust; also, tunnel velocity accuracy does not affect fan lift materially. Tunnel velocity measurement inaccuracies do affect aircraft lift, but this inaccuracy is present only at low tunnel speeds where wing lift is a very small contribution to total lift. Interaction lift is not calculated at velocity ratios below 0.075 V_p/V_{tip}. At this velocity ratio, a C_L change of 0.1 is equivalent to 85 pounds of lift, or slightly more than 1% of total fan lift which would be obscured in the measurement accuracy. Interaction lift as a function of both velocity ratio and exit louver setting was calculated as shown in Figure 36. The interaction lift with louver settings of 30°, 35° and 40° calculates to be very nearly equal to zero throughout the velocity range of 0.2 to 0.3. Interaction lift with β of 0° shows an increase up to velocity ratios of 0.15 and then decreases gradually. The maximum value of $C_{L\ int}$ was 0.38 at a velocity ratio of 0.17 and $\beta = 0°$. Some of this interaction lift might be explained by an increased velocity above the airplane model when exit louvers are set at low angles. Some of it can be due to the normal mirror effect in the tunnel as described in Volume 1, Section VII-C.

In general, the fan does produce a similar effect to a jet flap where, if the jet exhaust is at right angles to the airfoil camber line, the maximum induced lift is produced. Near conversion speed with the

TABLE 8

INTERACTION LIFT - CALCULATION ROUTINE

Conditions

Run #3, Reading #21
Fan Speed - 2480 RPM
Angle of Attack - 0°
Flap Angle - 0°
Exit Louver Angle 20°
Tunnel Temperature - 553°R
Tunnel Static Pressure - 29.70 In. Hg.
Tunnel Dynamic Pressure - q = 11.66 Lbs/Ft^2

1. Fan Tip Speed

$$V_{tip} = \frac{N_F(V_{tip} \text{ at } 100\% N_F)}{N_F \, 100} = \frac{2480\ (720)}{2640} = 676 \text{ Ft/Sec.}$$

2. Tunnel Velocity

$$V_P = \sqrt{\frac{2q}{\rho}} = \sqrt{\frac{2qTsRg}{Ps}} = \sqrt{\frac{2(11.66)\ 553\ (53.3)\ 32.2}{29.70\ (.491)\ 144}} = 102.6 \text{ Ft/Sec.}$$

3. Velocity Ratio

$$V_P/V_{tip} = \frac{102.6}{676} = 0.152$$

4. Basic Aircraft Lift

C_L = 0.05 from Figure 10

$L = C_L qSw = 0.05(11.66)250 = 146$ Lbs.

5. Fan Corrected Speed

$$\% \, N/\sqrt{\theta} = \frac{2480}{2640\left(\sqrt{\frac{553}{519}}\right)} 100 = 91.2\%$$

6. Fan Total Thrust at $\beta = 0°$ and $V_P/V_{tip} = 0$

F/δ = 5960 from Figure 26

$$F = 5960 \frac{(29.70)}{(29.92)} = 5920 \text{ Lbs.}$$

At $\beta = 20°$

$F_{\beta = 20°} = F_{\beta = 0°}$ (0.98) from Figure 28a = 5800 Lbs.

At $\beta = 20°$ and $V_P/V_{tip} = 0.152$

$$F = F_{\beta = 20°} \left[\frac{H_T \text{ at } V_P/V_{tip} = 0.152}{H_T \text{ at } V_P/V_{tip} = 0} \right] \quad \text{from Figure 29}$$

$$F = 5800 \left(\frac{0.337}{0.314} \right) = 6220 \text{ Lbs.}$$

7. Basic Fan Lift

$$F_y = F[\cos(\beta_V - \alpha)] = F(\cos 23.2°) = 5720 \text{ Lbs.}$$

8. Total Measured Lift 6312 Lbs.

$$L_{int} = L_T - (F_y + L)$$
$$= 6312 - (5720 + 146)$$
$$= 446 \text{ Lbs.}$$

Expressed as C_L

$$C_{L\ int} = \frac{446}{11.66\ (250)} = 0.15$$

Expressed as H_L

$$H_{L\ int} = 7.023\ (V_P/V_{tip})^2\ C_L = 0.025$$

TABLE 9

INTERACTION DRAG - CALCULATION ROUTINE

Conditions

Same point as used in Table 8

1. Basic Aircraft Drag

C_D = 0.11 from Figure 10

$D = C_D q S_W$ = 320 Lbs.

2. Fan Total Thrust

F_β = 20° and V_P/V_{tip} = 0.152 = 6220 Lbs. from Table 8

3. Fan Horizontal Thrust

$F_x = F[\sin(\alpha - \beta_V)] = -F(\sin 23.2°) = -2450$ Lbs.

4. Fan Ram Drag

$$D_R = \frac{W_F}{g} V_P$$

H_{DR} = .084 from Figure 32

$$\rho = P_S/RT_s g = \frac{29.70(.491)144}{53.3(553)32.2} = 0.00222 \text{ Slugs/Cu. Ft.}$$

$D_R = \rho A_F (V_{tip}) H_{DR} = 0.00222 (17.8) (676)^2 .084 = 1516$ Lbs.

5. Engine Ram Drag

$$\frac{W_{J85} V_P}{g} = \frac{42.0(102.6)}{32.2} = 134 \text{ Lbs.}$$

6. Total Measured Drag

D_T = -189 Lbs.

7. Interaction Drag

$D_{int} = D_T - [D + F_x + D_R + D_{RJ85}] = -189 - [320 - 2450 + 1516 + 134] = 291$ Lbs.

Expressed as C_D

$$C_{D\ int} = \frac{291}{11.66(250)} = 0.10$$

Expressed as H_L

$$H_{L\ int} = 7.023(V_P/V_{tip})^2\ C_D = 7.023(0.152)^2\ 0.10 = 0.016$$

high louver angle settings necessary at these conditions, there will be no appreciable interaction lift.

The interaction lift does not seem to be a function of angle of attack and appears as a constant additive throughout the normally linear C_L versus α range (see Figure 38). It does however decrease at high angles of attack of 8° or more. The value of interaction lift at maximum lift coefficient is of interest. For the 30° flap configuration, $C_{L\ max}$ for the basic aircraft was 1.5 and occurred at about 14° angle of attack. The change in $C_{L\ max}$ due to operating the fan is shown in Figure 39, plotted as a function of velocity ratio, and was obtained by plotting the locus of $\partial C_L/\partial \alpha = 0$ points from Figure 38 (less basic aircraft $C_{L\ max}$ of 1.5). It is apparent, by comparing the $\beta = 0°$ data from Figure 36 with Figure 39, that the interaction lift at angles of attack corresponding to $C_{L\ max}$ followed the same basic pattern as at 0° angle of attack; the magnitude was, however, less than 40% of the $\alpha = 0°$ effect.

During the previous testing period, static pressure measurements along several wing chord lines were taken at $\alpha = 0°$ conditions where the basic airplane wing $\bar{C}_L$ was equal to 0.07 with the fan off. The wing $\bar{C}_L$ calculated based on these pressure measurements indicates a significant increase when the fan is operating; this is, in essence, the interaction lift associated with the wing. Figure 37 replots this data for comparison with Figure 36 and shows that the pressure measurements on the wing account for a large amount of the calculated interaction lift, and show the same general characteristics of decreasing with β angle and V_p/V_{tip} ratio. The fact that Figures 36 and 37 are not identical can be viewed two ways:

1. Interaction lift is not only developed on the wings, but also on other sections of the airplane such that the combined characteristics calculated in Figure 36 result.

2. The interaction lift is only developed on the wings so that the total characteristic is as shown in Figure 37. This would require revising the method of calculating fan performance as a function of β and V_p/V_{tip}. While this may be the case, the best method available for calculating fan performance has been used.

The general characteristics of interaction drag variation with β and V_p/V_{tip} in the angle of attack range of -4° to +8° are similar to the interaction lift characteristics; that is, both V_p/V_{tip} and β increases are accompanied by decreases in interactions, but are not influenced by angle of attack changes. Figure 40 shows the calculated interaction drag characteristics which corresponds to interaction lift as shown in Figure 36.

The high values of interaction drag measured for low β settings could be explained by air velocities around the model that are higher due to blockage presented by the exhaust gases. In fact, velocities were calculated from the pitot static tube on the nose of the aircraft to be 40% higher than the upstream tunnel velocity measurement at a nominal setting of 20 knots and $\beta = 0°$. This can account for as much as 230 pounds of ram drag. On the other hand, vectoring the louvers may possibly act as an ejector causing the higher velocity to occur on the underside of the model and a corresponding reduction in velocity above the model. Due to the difficulties in evaluating interaction drag and the relatively small values of this quantity at velocity ratios below 0.1 V_p/V_{tip}, the values above 0.1 only are shown in Figure 40 (at 0.1 V_p/V_{tip} and full fan speed, a value of $C_D = 0.1$ is equivalent to 150 pounds of drag, or only slightly more than 2% of fan total thrust). It is apparent that with velocity ratios of 0.2 to 0.3 and exit louver angles of 30°, 35° and 40°, the interaction drag is equivalent to 0.06 C_D. In the same range of V_p/V_{tip} and β, interaction C_L varies between -0.04 to +0.04. While the data has been very repeatable at all test conditions during the 50 hours of testing conducted, the lack

of consistent trends as a function of the different variables leads to the suspicion that the accounting for interactions is somewhat in error. Items which would greatly influence this accounting are:

- Determination of velocity in the test section.
- Fan throttling characteristic as a function of flight speed.
- Tunnel wall effects at low velocity ratios.

The characteristics of $C_{L\ int}$ and $C_{D\ int}$ for $\beta \approx 20°$ appear to be most consistent, and it could be speculated that, at this vector angle, the blockage and tunnel air flow split above and below the model are closest to that which would occur if the fan were not operating. Also, the higher velocity ratio data is felt to yield more accurate conclusions as to interaction effects.

Application of these interaction effects to other configurations or even to this configuration outside of the wind tunnel may not be valid. However, for the configuration tested when it is in the tunnel, it can be concluded that during transition, there is little or no interaction lift at the maximum conversion speed, and that the drag of the aircraft is increased by an additional $C_D = 0.06$ (600 pounds at V_P = 111 knots and 100% N_F).

At velocity ratios and β settings corresponding to STO conditions, the interaction is a significantly favorable effect with $C_{L\ int}$ varying from 0.1 to 0.25 depending on the specific STO flight path.

Tail Downwash:

With the fan operating, tests were made with the tail in both a high and low position and with the wing angle of attack at 0° (δ_f = 0°). The tail downwash angle, ϵ, calculated from the change in pitching moment (tail on compared with the tail off) is shown in Figure 41

as a function of V_p/V_{tip} for $\beta = 0°$. Because of the scatter in pitching moment data, determination of tail downwash as a function of angle of attack was not attempted. However, for the tests made at 0° angle of attack ($\delta_f = 0°$), some consistency was found to determine that:

1. There was no measurable downwash in the plane of the tail with exit louvers closed more than 20°. This result was obtained with the tail in either the high or low position and was not expected This possibly indicates the downwash data was being adversely influenced by tunnel effects.

2. At $\beta = 0°$, an increase in downwash at low velocity ratios of as much as 10° due to operating the fan was indicated, but this diminished rapidly with increased V_p/V_{tip} approaching "fan-off" results. Only a slight difference could be ascertained by changing the tail to the low position, an increase in downwash being experienced which varied with increased V_p/V_{tip} from 2° to 1/2°.

The tail is located 3 wing chord lengths behind the wing 1/4 chord, and this distance could not be varied in the test, but is probably of considerable significance to the downwash results.

Pitching Moments:

The pitching moment characteristics are basically unchanged from those reported in Volume 1. Data were also obtained at higher velocity ratios (above 0.3) which are normal to a landing transition. These data indicate that the pitching moment coefficient decreases appreciably with increased V_p/V_{tip}, and that the maximum trim control will be determined by take-off transition requirements. The test results in coefficient form for lift, drag and moments are shown in Figures 42 through 56. These are the over-all fan powered aircraft performance results as a function of all the test variables.

The moment coefficients for $\beta = 0°$ and $35°$ intersect at about V_P/V_{tip} of 0.35, and further increases in velocity ratio result in a relative decrease in moments for $\beta = 35°$ as compared with $\beta = 0°$ (see Figure 42c). This is as would be expected since the moment contribution due to exit louver turning increases about 25% throughout the flight speed range for a constant fan speed and is equal to F_x (3.56) Ft. Lbs. The induced moments are however a function of ram drag (see Tables 9 and 11, Volume 1, and therefore increase proportional to flight speed. Vectoring louvers at high velocity ratios reduces pitching moments since fan flow (and correspondingly ram drag) is reduced such that induced moments decrease at a faster rate than the direct contribution from fan vectoring.

Pitching moment contributions due to fan operation were assessed and described in Volume 1. Some speculation was made at that time as to the magnitude of the various effects. Static pressure measurements around the fuselage during this part of the test provide some additional insight to the pitching moment analysis. When operating with no crossflow and exit louvers at the 0° position, the fan draws air equally from all directions, and the resulting pitching moment is zero, because pitching moment is always calculated about the fan center which is also the quarter chord of the wing. As soon as some forward velocity is present, the fan tends to draw the air in from the front more than from the sides and rear. This, of course, accounts for the major portion of the pitching moment. The additional phenomenon which was suspected during the first phase of testing was that, at the fan exit the static pressures in front of the fan discharge were higher than tunnel static, while behind it, they were lower. This was clearly shown by the static pressure data obtained on the underside of the fuselage (refer to Figure 5). The measurements obtained with these pressures in conjunction with wing static pressure measurements obtained during the previous test period allows a reasonably accurate account of the pitching moments on the whole aircraft.

The following discussion is concerned with Run #15, during which the pressure measurements on the fuselage were taken. The aircraft configuration was as follows:

- Flaps at zero degrees.

- Tail at zero incidence angle and in the low position.

Figures 57a through 57d show the static pressure distribution on the upper surface of the fuselage as a function of exit louver angle and velocity ratio, and Figures 58a through 58d show the same for the bottom surface of the fuselage. Looking at the top of the fuselage, Figures 57a through 57d, it is apparent that the stagnation point ($C_p = 1$)* behind the fan inlet was located very close to the inlet at all velocity ratios. Even at velocity ratios as low as approximately 0.07, the stagnation point was about 2 fan radii behind the centerline of the fan. This stagnation point varied from a radius ratio of 2 at a velocity ratio of 0.07 to 1.25 at a velocity ratio of 0.30. The pressure behind the stagnation point gradually approached the tunnel static pressure (or $C_p = 0$) 2 1/2 to 3 fan radii behind the fan. Forward of this point, the pressure coefficient, of course, rapidly decreased and became highly negative as the lip of the bellmouth was approached. A negative pressure coefficient persisted over all of the surface ahead of the fan and followed an exponential decay curve with distance from the fan; this was one of the larger contributors to the total pitching moment. The variation of the pressure coefficient level with β is also shown in Figures 57a through 57d which reflects the reduced fan axial velocity.

On the underside of the fuselage, ahead of the fan discharge, there was a positive pressure not quite approaching a stagnation point ($C_p \approx 0.7$). Behind the fan, the lowest pressure coefficient was approximately -1. There was a variation of the static pressure both

* $C_p = \dfrac{P_{sl} - P_{so}}{P_{to} - P_{so}}$

ahead and behind the fan with exit louver angle which decreased this contribution to the pitch-up moment as exit louver angle was increased.

Figures 59a and 59b showing the breakdown of total measured moment into the contributing sources were obtained in the following manner:

1. The values of fuselage static pressures were as shown in Figures 57a through 57d (the static pressure measurements were assumed to be representative of all points on the fuselage which were located at the same longitudinal station as the pressure tap used. The area used was the fuselage area projected onto a horizontal plane).

2. The value of wing moment contribution was as determined previously (see Figure B-II-21, Volume 1).

3. Moment due to exit louver vectoring was determined in the same manner as described in Volume 1, page 69.

4. Tail moment was obtained from the measured downwash as shown in Figure 41 and the $\Delta C_M - i_t$ relationship as shown in Figure 15 (low tail position).

5. Reviewing Figures 57a through 57d, it can be seen that on the upper surface, there are high negative pressure coefficients both in front and behind the fan. On the aft side, this high negative coefficient is confined to an area very close to the fan inlet. In the calculation, the moment contribution of this negative portion on the aft side was balanced out by an equivalent moment contribution from the forward side. In that way, the remaining forces aft of the inlet on the upper surface always represented a net positive moment (nose up).

6. The ram drag force was taken to act at a point 10% of the inlet duct diameter below the top of the inlet duct (and is referred to as inlet pitching moment).

7. J85 ram drag was taken to act 6.3 Ft. below the center of gravity.

It can be seen from Figure 59b that at low velocity ratios, the moment due to exit louver turning was the predominant contribution (this, of course, can be minimized by careful aircraft design in placing exit louvers relative to the center of gravity). The moments caused by static pressures on the top of the fuselage ahead of the fan and on the bottom of the fuselage behind the fan constituted the other large contributions and were approximately equal to each other.

The calculations did not always exactly account for the total measured moment; however, the value of the measured and the value of the total calculated moment were within 20% of each other. This is a very good correlation, considering that the large area of the fuselage, of necessity, could only be sparingly instrumented with static taps. Assuming the same limits of accuracy for each individual contributor to the pitching moment, the range of each in percentages of the total moment measured is shown in Table 10.

The static pressure surveys provide only a method of accounting for moment contributions. The total moment is caused by a sink (fan inlet) and a source of flow (fan discharge) operating in a crossflow. The air has to be turned 90° before entering the fan and the force required is proportional to the mass flow and initial velocity of the crossflow air and therefore, proportional to ram drag. The fan flow discharging into the crossflow stream is turned by the crossflow toward a horizontal direction. A method of calculating the amount

TABLE 10

PITCHING MOMENT CONTRIBUTIONS IN PER CENT OF TOTAL

$\frac{V_p}{V_{tip}}$	β	Fuselage Total	Forward Upper	Forward Lower	Aft Upper	Aft Lower	Exit Louvers	Wings	Tail $i_t = 0°$	Fan Inlet	J85 Ram Drag
.073	0	40 to 60	23 to 35	2	1	15 to 21	11 to 17	4 to 6	14 to 22	14 to 22	-4 to -6
.073	35	23 to 35	9 to 13	2 to 4	2	10 to 16	48 to 72	2	3 to 5	6 to 8	-2
.147	0	46 to 70	28 to 42	2	2	15 to 23	6 to 8	5 to 7	14 to 20	14 to 20	-4 to -6
.147	35	32 to 48	15 to 21	2 to 4	3 to 5	12 to 18	36 to 54	2 to 4	6 to 8	7 to 11	-3 to -5
.227	0	52 to 78	23 to 35	8 to 14	1	19 to 29	3 to 5	7 to 9	11 to 15	12 to 18	-4 to -6
.227	35	34 to 50	15 to 23	3 to 5	1	14 to 22	34 to 50	4 to 6	4 to 6	9 to 13	-4 to -6
.302	0	54 to 80	21 to 31	11 to 17	1	21 to 31	2 to 4	7 to 9	10 to 14	12 to 18	-4 to -6
.302	35	40 to 60	20 to 28	6 to 8	2 to 4	13 to 19	24 to 36	5 to 7	6 to 8	10 to 14	-4 to -6

of pitching moment contribution due to this is not available;* however, it is apparent that by preturning this source flow (e.g., with the exit louvers), this pitching moment contribution will be diminished. In the limit when the source flow is ejected parallel to the crossflow stream, there would be no external pitching moment contribution. This correlates with the measured reduction in induced pitching moment with louver vector angle which is more than would be calculated by the measured fan flow reduction and corresponding ram drag reduction.

Static Longitudinal Stability (Fan On):

Static longitudinal stability defined as the partial derivative of pitching moment coefficient with respect to lift coefficient was comparable to the value for the unpowered aircraft at conditions where exit louvers were set at 0° (see Figure 60). The value of this derivative with exit louver settings of 20° and 35° was less favorable as can be seen from the same Figure. The stability appeared to decrease with flap angle; in other words, the airplane showed highest stability with the lowest setting of flaps. For example, compare Figure B-III-12 from Volume 1, with Figure 60 from this report. The 30° flap data is more believable, as it showed a tendency of the stability derivative to be poorer at the low velocity ratios and increasing to approach the basic unpowered aircraft stability as the velocity ratio increased. This is as would be expected, since tail downwash and other fan induced effects become smaller with velocity ratio increase. Some limited data obtained with no flaps during this test generally agrees with the no flap data obtained during the previous test period; e.g., high values of stability at low velocity ratios, decreasing as velocity ratios increased. Data obtained around trim point settings was inconsistent due in large

*Reference 8 qualitatively discusses the induced moment due to interaction of the existing jet and the free-stream flow.

part to the tail being operated very nearly stalled in order to obtain maximum control power. Small increases in angle of attack from a trim condition caused the tail to stall as observed by some static pressures measurements on the tail horizontal surface which were monitored during test to determine the stall condition. This resulted in unfavorable stability. Control power available versus that required for trim conditions is discussed in the section on transition analysis. The variation in aircraft pitching moment coefficient with angle of attack and velocity ratio is shown in Figure 61 for $\beta = 0°$ and Figure 62 for $\beta = 20°$ and $35°$. The data shows considerable scatter which can be expected with the relatively low accuracy of moment measurement in the tunnel when the fan is operating (see Section VI, Volume 1).

Aircraft Performance with Inlet Vane Removed:

The inlet performance with the vane removed was described in a previous section. The gross performance of the airplane however was only slightly different from performance with the inlet vane installed. For an aircraft configuration using the high tail position and a 30° flap angle tested to 0.286 V_p/V_{tip}, the significant results are listed below (comparing Figures 49 and 56 with Figures 55a and 55b):

1. Pitching moment was slightly less ($\approx 5\%$).

2. Lift and drag were essentially unchanged for all α and β values.

3. Longitudinal stability was unchanged.

It is apparent that up to the velocity ratios tested, which are sufficient for transition, there was very little, if any, penalty in over-all aerodynamic performance caused by removal of the inlet vane. More data at higher velocity ratios and at high fan speeds

for extending take off conversion speeds with the inlet vane removed would be required to assess the actual penalties in aerodynamic and mechanical performance under these conditions. At first it may appear inconsistent that, in spite of the high inlet losses experienced without the inlet vane at high velocity ratios, the over-all performance remained essentially unchanged. As far as lift is concerned, as velocity ratio is increased, the fan contribution to total lift diminishes rapidly and changes in fan performance do not influence the over-all results to a large degree. Over-all drag, on the other hand, is a function of ram drag, aircraft drag, gross thrust and any interactions that may be present. Reduced inlet performance decreases both ram drag and gross thrust. Since the reduction in inlet performance occurs at high velocity ratios where ram drag is large, there is a trade off in ram drag and gross thrust which results in practically constant net thrust. Theoretical cycle analysis of the fan operating at constant speed and any given flight velocity indicates that around 20° β, inlet efficiency has no affect on the net thrust of the fan; below 20° β, inlet recovery actually reduces net thrust; above 20° β, inlet recovery increases net thrust slightly. At louver settings above 35°, the improvement in net thrust with inlet recovery becomes more significant. This analysis however does not take into account any changes in fan efficiency as a function of distortion in the inlet and, therefore, it is very likely that at higher velocity ratios than tested, the gross performance without the vane would decrease significantly relative to the performance with the vane installed.

The pitching moment decrease at high velocity ratios results directly from the fan weight flow and consequent ram drag decrease caused by removal of the inlet vane.

Transition Analyses:

The aerodynamic characteristics of the airplane and lift fan test configuration shown in Figures 46 through 56 were cross-plotted to obtain Figures 63 through 65 for seven velocity ratios. These curves are used exclusively as the basis for the various transitions presented. Throughout the transition discussion, the lift characteristics measured in the tunnel were used for the configuration with 30° flap angle (0.2 to 0.6 b/2); the measured drag was reduced by a drag coefficient (C_D) of 0.065 based on wing area (see Section VII-B, Volume 1 for basis). For the moment evaluation, the exit louvers are assumed to be at the aircraft center of gravity so that there is no pitching moment contribution from thrust vectoring.

The aircraft gross weight is assumed to be 7000 Lb., but for the purpose of evaluating STOL performance, 10% and 20% overloads were also analyzed.

The performance equations listed in Table 11 summarize the various transition flight conditions investigated.

Transition Analyses:

The aerodynamic characteristics of the airplane and lift fan test configuration shown in Figures 46 through 56 were cross-plotted to obtain Figures 63 through 65 for seven velocity ratios. These curves are used exclusively as the basis for the various transitions presented. Throughout the transition discussion, the lift characteristics measured in the tunnel were used for the configuration with 30° flap angle (0.2 to 0.6 b/2); the measured drag was reduced by a drag coefficient (C_D) of 0.065 based on wing area (see Section VII-B, Volume 1 for basis). For the moment evaluation, the exit louvers are assumed to be at the aircraft center of gravity so that there is no pitching moment contribution from thrust vectoring.

The aircraft gross weight is assumed to be 7000 Lb., but for the purpose of evaluating STOL performance, 10% and 20% overloads were also analyzed.

The performance equations listed in Table 11 summarize the various transition flight conditions investigated.

TABLE 11

TRANSITION EQUATIONS OF MOTION

Flight Condition	Equations of Motion
1. Level unaccelerated flight.	$-\rho A_F (V_{tip})^2 H_D = \frac{G.W.}{g} \frac{dV_P}{dt} = 0$ $\rho A_F (V_{tip})^2 H_L = G.W.$
2. Level accelerated flight and level decelerated flight.	$-\rho A_F (V_{tip})^2 H_D = \frac{G.W.}{g} \frac{dV_P}{dt}$ $\rho A_F (V_{tip})^2 H_L = G.W.$
3. Constant speed climb.	$-\rho A_F (V_{tip})^2 H_D - G.W. \sin \theta = \frac{G.W.}{g} \frac{dV_P}{dt} = 0$ and $\rho A_F (V_{tip})^2 H_L = G.W. \cos \theta$
4. Accelerated climb and decelerated descent.	$-\rho A_F (V_{tip})^2 H_D - G.W. \sin \theta = \frac{G.W.}{g} \frac{dV_P}{dt}$ $\rho A_F (V_{tip})^2 H_L = G.W. \cos \theta$
5. S.T.O.L.	
a. Ground run	$-\rho A_F (V_{tip})^2 H_D - \mu (G.W. - \rho A_F (V_{tip})^2 H_L) = \frac{G.W.}{g} \frac{dV_P}{dt}$ or $-H_D - \mu H_{G.W.} + \mu H_L = \frac{H_{G.W.}}{g} V_P \frac{dV_P}{dx}$
b. Distance for rotation.	$X_2 = V_P \left(\frac{\tan^{-1} H_D/H_L}{\omega} \right)$ where $\omega = \frac{\Delta G.W.}{G.W.} \frac{g}{V_P}$
c. Distance to climb out	$X_3 = \frac{50 - X_2 \sin 1/2 (\tan^{-1} H_D/H_L)}{\tan H_D/H_L}$

Unaccelerated Level Flight:

It is possible to hold the airplane at a steady forward speed in level flight with a combination of wing lift and fan power over the complete speed range from hover to conversion by a suitable choice of angle of attack (α) and louver setting (β). With a gross weight of 7000 Lb., then $H_L = 7000/\rho A_F (V_{tip})^2$. For the fan speed which corresponds to a hover lift of 7000 Lb., $H_L = 0.315$ and, if the fan speed is held constant, it is only necessary to select an α and β schedule at several velocity ratios, V_P/V_{tip}, representing the transition which will satisfy both $H_L = 0.315$ and $H_D = 0$.

For the seven velocity ratios arbitrarily selected, α and β combinations have been determined for this type of take off transition and are plotted as a function of forward speed in Figure 66. This type of flight path can also be accomplished with fan speed as an additional variable. In this case, the value of H_L will be 0.315 at hover, but will vary throughout the transition to satisfy the total lift = 7000 Lb. requirement. A different α and β schedule will then be required to satisfy the H_L schedule and $H_D = 0$ criteria.

Acceleration and Deceleration in Level Flight:

For maximum acceleration, the minimum value of H_D (i.e., the largest negative number) is selected which satisfies the H_L requirement. For the case where H_L is maintained constant at 0.315 (fan speed constant), the α and β schedule corresponding to a maximum acceleration in level flight is shown in Figure 67.

From the equation of motion for accelerated level flight shown in Table 11.

$$dt = \frac{G.W.}{g} \left(\frac{1}{-\rho A_F (V_{tip})^2 H_D} \right) d V_P$$

Since H_D varies with V_P for this type of flight path

$$\frac{G.\ W.}{g} \left(\frac{1}{-\rho\ A_F\ (V_{tip})^2\ H_{D\ min}} \right)$$

is plotted as a function of V_P in Figure 67, and the area under the curve for any velocity interval can be measured, yielding the time to accelerate between two flight speeds.* Similarly, the distance required to accelerate to any speed can be obtained by measuring the area under the velocity time curve and this is also shown in Figure 67. Maximum acceleration as a function of forward speed can be calculated directly from the equation of motion and is plotted in Figure 67.

A similar procedure may be used to decelerate for landing in level flight. The primary difference from an accelerating transition is that the velocity ratio for a given flight speed is higher since the fan is operating at reduced power settings for most of the landing transition.

Assuming a maximum deceleration rate of 0.3 g or

$$-\left(\frac{H_D}{H_L} g \right)_{max} = -0.3$$

allows an α and β schedule to be selected for decelerated level flight. For this transition, α was maintained at zero and the fan speed, β schedule, deceleration rate, horizontal distance and time as a function of flight speed are plotted in Figure 68.

*The time interval for the last 10 knots of a transition to maximum conversion speed (zero acceleration point) is taken based on the average acceleration for the last 10 knots.

Constant Speed Climb:

If V_P, the speed along the flight path, is held constant and the flight path inclined at an angle θ to the horizontal, $V_C = dh/dt$ is the rate of climb (vertical component of velocity). The equation of motion for a constant speed climb is given in Table 11 and $\theta = \tan^{-1} H_D/H_L$.

For a constant 100% fan speed condition, to select the maximum climb angle, it is necessary to determine by iteration the largest negative value of H_D at each velocity ratio which satisfies both $H_L = 0.315 \cos \theta$ and $-H_D = 0.315 \sin \theta$ from Figures 63 and 64. This is similar to the procedure used in defining maximum acceleration in level flight, except that the excess thrust used to accelerate the aircraft in level flight is now used to climb. The α and β schedules for this condition and the rate of climb and climb angle as a function of flight speed are shown in Figure 69.

Accelerated Climb and Decelerated Descent:

Two methods of approach could be used to solve the equation of motion. The rate of climb could be maintained constant, or the climb angle could be held constant and the rate of climb varied. Whichever method was used, the boundaries of the problem are defined by the acceleration in level flight (i.e., zero climb angle) and the constant speed climb (i.e., maximum rate of climb). It can be seen that an infinite number of accelerated climb paths are available in between these two limiting paths.

The descent is accomplished in a similar manner, but for this case, the gross weight component acting along the flight path (G.W. $\sin\theta$) tends to accelerate the aircraft downwards. The equation of motion is exactly the same as for the accelerated climb, but in this case,

dh/dt is negative. Since this is a deceleration, it was assumed that it would occur following a conversion from conventinal flight to fan powered flight and the analysis was carried out as for the level acceleration, commencing with a low fan speed.

For a constant rate of descent, θ is known and $H_L = 0.315 \cos \theta (V_{tip}/V'_{tip})^2$.* An iteration process at each flight speed to determine N_F, α and β can be followed to satisfy the $\geq$ -0.3 g criterion as follows:

1. Select N_F and $\therefore (V_{tip}/V'_{tip})^2$.
2. Calculate H_L
3. Determine α from rate of descent and given flight speed for a constant attitude.
4. Obtain β and H_D which corresponds to the calculated values of α and H_L from Figures 70a through 71c.
5. Solve the relationship

$$\frac{\rho A_F (V'_{tip})^2 H_D + G. W. \sin \theta}{H_L \cos \theta}$$

6. Repeat the process by changing fan speed until the solution to the above relationship approaches a minimum value, but not less than -0.3.

Figures 70a through 71c are similar to Figures 63 and 64, except that they were extended to include the higher velocity ratios; and

---

* Correction factor for varying fan speed see page 51, Volume 1

the data at other than $\alpha = 0°$ above $0.3\ V_P/V_{tip}$ is extrapolated. Data at low velocity ratios above $\alpha \approx 16°$ was also estimated to enable the analysis to cover the entire landing sequence.

For the decelerated descent flight path, the α and β schedule, fan speed and deceleration rate are plotted in Figure 72. If the equation of motion is written in the form

$$dt = \frac{d\,V_P}{-g\left(\frac{H_D \cos\theta}{H_L} + \frac{dh}{dt}/V_P\right)},$$

the term

$$\frac{1}{-g\left(\frac{H_D \cos\theta}{H_L} + \frac{dh}{dt}/V_P\right)}$$

can be evaluated for several values of V_P and plotted against V_P. Then the area under the curve between any two values of V_P is the time required to slow down from the higher to the lower speed.

A plot of velocity as a function of time is shown in Figure 72. The area under this curve yields the distance needed for decelerating the aircraft, and a velocity - distance curve is also shown in Figure 72 .

If it is assumed that the airplane will be at ground level when a speed of 10 knots is attained, a step-by-step procedure from this point can be followed to determine a speed - altitude curve. This is also shown in Figure 72.

Short Take Off Analysis:

Three load conditions, lift equal gross weight and 10% and 20% overload were investigated for short take off to clear a 50 foot obstacle. This can be represented by the relationship -

Total distance (X) = Ground run distance (X_1) + distance required for rotation to climb out angle (X_2) + distance required to climb out (X_3).

For the ground run during take off, the equation of motion is shown in Table 11. If G.W. is arbitrarily set equal to

$$\rho A_F (V_{tip})^2 H_{G.W.}$$

then this equation can be divided by $\rho A_F (V_{tip})^2$ yielding

$$H_D - \mu(H_{G.W.} - H_L) = H_{G.W.}/g \; d^2 x/dt^2$$

where μ is the rolling coefficient of friction assumed to be 0.03.

Since $V_P = dx/dt$

then $d^2x/dt^2 = d V_P/dt = d V_P/dx \; dx/dt$

or $d^2x/dt^2 = V_P \, d V_P/dx$

Therefore, $H_D - \mu H_{G.W.} + \mu H_L = \dfrac{H_{G.W.}}{g} V_P \dfrac{d V_P}{dx}$

H_D and H_L will vary as a function of V_P and the variables in the above equation can be separated to yield

$$dx_1 = \frac{H_{G.W.} V_P dV_P}{g(H_D - \mu H_{G.W.} + \mu H_L)}$$

or ground roll distance (X_1) = $\displaystyle\int_0^{V_P \text{ at take off}} \frac{H_{G.W.} V_P dV_P}{g(H_D - \mu H_{G.W.} + \mu H_L)}$

The term $\dfrac{H_{G.W.} V_P}{g(H_D - \mu H_{G.W.} + \mu H_L)}$ can be plotted against V_P using the values of H_D and H_L from Figures 63 through 64 for $\alpha = 0°$ and the following β schedule:*

*The β schedule selected is based on several trial solutions and appears to yield near optimum STO performance.

Take Off Weight / Max. Installed Lift	β Setting
1.0	30°
1.1	30°
1.2	35°

By measuring the area under this curve from zero to the take off speed, the ground roll distance was obtained. This curve is plotted for the three gross weight values in Figure 73.

The rotation to an optimum climb path imposes an additional weight increment due to centrifugal force $\Delta G.W. = G.W./g\ \omega V_p$ where ω is the rate of rotation in radians/sec. For straight and level flight the H_L values required for zero, 10% and 20% overload are 0.315, 0.346 and 0.378 respectively at 100% fan speed. For the rotational motion, an additional increment in H_L will then be required to overcome the centrifugal force component. In order to maintain exit louver angle constant throughout the take off, it is necessary to review Figures 63 through 64 to determine the flight speed at the end of ground run sufficient to provide the lift coefficient H_L necessary for both lift off and rotation and at the same time to provide sufficient thrust for climb.

A small part of the H_L required is obtained from the tail lift. With the tail lift, the lowest flight speed which satisfied each weight condition was 35, 60 and 60 knots respectively.

The rotation and climb can be accomplished in many ways, primarily dependent on the angle of attack selected at the end of the ground run. An approximate analysis indicated that for the lift equal gross weight condition, selection of $\alpha = +4°$ at the beginning of rotation was about optimum (in terms of shortest distance to complete the STO). For these conditions, $H_D = -0.065$ and H_L at lift off was 0.351 (0.315 from Figure 70b and 0.036 from interpolation of Figures 65a and 65b).*

*Figure 65 is data plotted with the tail off. Providing tail power to trim this moment is equivalent to adding H_L to the system equal to H_M since the tail moment = Ll_t and $H_M = Ll_t/\rho A_F(V_{tip})^2 l_t = H_L(l_t/l_t)$.

The rate of rotation $\omega = \Delta G.W.g/G.W.\ V_P$ (where $\Delta G.W.$ is proportional to H_L at lift off minus H_L in level flight or 0.351 - 0.315) was 3.5°/sec. The climb out angle given by $\tan^{-1} H_D/H_L$ would be about 10.5°. The rotation is therefore completed in about three seconds in a distance of 180 feet (assuming V_P is essentially constant). The height gained during rotation would approximate 180 tan $\theta/2$ = 16.5 feet.

For the remaining 33.5 feet to clear the obstacle, retaining the climb out angle at 10.5° at constant V_P, $X_3 = 33.5/\tan\theta = 189$ feet. The total STO distance then taking the ground roll distance (X_1) from Figure 81 would be

$$X = 140 + 180 + 189 = 509 \text{ Feet.}$$

Table 12 shows the results of the analysis, including the 10% and 20% overload conditions. Figure 74 also shows this relationship.

TABLE 12
SHORT TAKE OFF DISTANCE AS A FUNCTION OF TAKE OFF WEIGHT

	α* (Deg.)	β (Deg.)	ω (°/Sec.)	θ (Deg.)	X_1 (Ft.)	X_2 (Ft.)	X_3 (Ft.)	X (Ft.)
With Tail Trim:								
Lift = G.W.	+4	30	3.5	10.5	140	180	189	509
10% O.L	0	30	3.1	9.7	422	300	140	862
20% O.L.	+4	35	0.78	9.0	330	865	-	1195
Without Tail Trim:								
Lift = G.W.	+4	20	2.4	5.5	219	128	460	807
10% O.L.	+3	25	1.7	5.0	531	270	447	1248
20% O.L.	+2	25	0.78	4.3	665	550	400	1615

*α refers to the angle of attack during rotation.

It should be noted that these STO analyses are conservative to the extent that no advantage has been taken for the possibility of applying a variable β schedule during the ground run.

Pitch Control Requirements During Transition:

The out-of-balance pitching moment is plotted in Figures 75, 76, and 77 for three flight conditions: maximum climb, maximum acceleration, and a constant attitude descent. These were all determined from test data with the tail off. For the purpose of this moment analysis, the louvers were assumed to be located at the center of gravity and consequently, there is no moment from turning the flow. A high lift (split flap) tail using a maximum pitching moment coefficient of 0.7* was used to determine the available control moment and additional control moment required.

It can be seen that when the tail is used to provide a nose down moment for control, an additional lift force will be developed not included in previous transition calculations. This lift force will have a peak value close to 2000 pounds which means, in effect, that the previous performance estimates are, to some extent, pessimistic at the high speed end since these points are based on zero tail lift.

The main effect on these calculations will be that the time to speed and time to altitude will be improved due to the additional thrust available from trading lift for thrust.

In reviewing Figures 75 through 77, it can be seen that the maximum additional control required occurs for either the maximum acceleration or maximum climb case, and, assuming the pitch reaction control is located as shown in Figure 3, Volume 1, this would represent a force equivalent to approximately 7% of the gross weight. If pitch control were located in both the tail and nose of the aircraft and the fan center of lift relocated relative the aircraft center of gravity, this additional control requirement could be reduced to

*Equivalent C_{Lt} = 1.17

approximately 3 1/2% of gross weight. Because of the lower fan speeds required during landing, the additional moment required is only about 50% of that required for take off.

E. MECHANICAL PERFORMANCE

Rotor:

A detailed mode analysis of the rotor vibratory stresses has been made and the data are presented in Tables 13, 14, 15 and 16. These results show the rotor stress characteristics as a function of fan speed, tunnel speed, β and yaw angle. Angle of attack did not affect the rotor stress relationships except in the region where the wing stalled. In this region, blade stresses increased slightly and began to amplitude modulate. Since yawing the airplane resulted in stalling the wing at lower angles of attack, the blade stresses increased slightly and began to modulate at this same lower angle of attack. The effect of removing the inlet vane is also shown in the tables. In many cases it is not possible to determine the exact change in stress resulting from a variation of α, β, ψ, etc. since fan speed is not held constant. Nearby resonances whose amplitudes are a function of speed make it impossible to pin down the exact stress change without extremely detailed data reduction process. The rather small stress changes observed do not warrant such an analysis.

The rotor blade stress analysis was made using three gages - 90B2, 51B3 and 51B5 (refer to page 92, Volume 1 for the gage location specification. Blade 90 was also used for the analysis in Volume 1 These three gages were the most important to the analysis, and fortunately, they were functioning properly throughout the test. Gage 90B2 responds primarily to the cosine $n\theta$ and the first torsional modes. The first flexural stress response of this gage is less than 40% of the first flexural stress read on other gages. Gage 90B2 is located near the trailing edge just above the dovetail on the concave side of the blade. Gage 51B5 responds almost exclusively to the first flexural mode. The gage is located just below the tip tang

TABLE 13

DYNAMIC ROTOR BLADE STRESSES AS A FUNCTION OF V_P, β AND N_F

Point	Gage No.	Speed (RPM)	Tunnel Vel. (Knots)	β (Deg.)	Total Stress (psi sa)	1st Flexural Stress (psi sa)	1st Torsional Stress (psi sa)	Cosine 2θ Stress (psi sa)
1	90B2	2550	20	0	3200	750	1800	750
2	90B2	2490	100	40	5700	750	1800	3750
3	90B2	2306	100	40	8000	1000	1250	6000
4	51B5	2500	40	0	2500	750	1000	-
5	51B3	2550	20	0	2200	500	1000	1000
6	51B3	2490	100	40	3500	500	1000	2400
7	51B3	2306	100	40	5500	1500	1000	3800

TABLE 14

DYNAMIC ROTOR BLADE STRESSES AS A FUNCTION OF YAW AND TUNNEL VELOCITY

Point	Gage No	Speed (RPM)	Tunnel Vel. (Knots)	ψ (Deg.)	α (Deg.)	β (Deg.)	Total Stress (psi sa)	1st Flexural Stress (psi sa)	1st Torsional Stress (psi sa)	Cosine 3θ Stress (psi sa)
1	90B2	1710	20	0	0	0	5000	700	2700	1700
2	90B2	1704	20	+8	0	0	5000	-	2700	1700
3	90B2	1690	20	-16	0	0	4100	-	1800	2000
4	90B2	1690	60	0	0	0	4500	700	1500	2000
5	90B2	1697	60	-16	0	0	5200	1000	2700	1700
6	90B2	1700	80	0	0	0	5200	1200	2700	1200
7	90B2	1705	80	-16	0	0	5200	1200	2700	1200
8	51B5	1690	20	-16	0	0	2200	1200	500	0
9	51B5	1690	60	0	0	0	2200	2000	-	0
10	51B5	1697	60	-16	0	0	3000	2500	-	0
11	51B5	1700	80	0	0	0	3500	2700	-	0
12	51B5	1705	80	-16	0	0	3500	2700	-	0
13	51B3	1710	20	0	0	0	4500	1200	2500	700
14	51B3	1704	20	+8	0	0	4200	1200	2000	800
15	51B3	1690	20	-16	0	0	3500	800	1500	900
16	51B3	1690	60	0	0	0	3500	1700	1700	800
17	51B3	1697	60	-16	0	0	4300	2000	2000	900
18	51B3	1700	80	0	0	0	3500	1500	2100	700
19	51B3	1705	80	-16	0	0	4300	1800	2500	700

TABLE 15

DYNAMIC ROTOR BLADE STRESSES WITH THE INLET VANE REMOVED AS A FUNCTION OF TUNNEL VELOCITY

Point	Gage No.	Speed (RPM)	Tunnel Vel. (Knots)	α (Deg.)	β (Deg.)	Total Stress (psi sa)	1st Flexural Stress (psi sa)	1st Torsional Stress (psi sa)	Cosine 3θ Stress (psi sa)
1	90B2	1700	20	0	0	4800	700	1900	1500
2	90B2	1697	30	0	0	5000	900	1500	1700
3	90B2	1695	40	0	0	4000	800	1200	1700
4	90B2	1710	60	0	0	4700	700	2200	1700
5	90B2	1725	80	0	0	5500	1300	1700	2000
6	51B5	1700	20	0	0	2000	1300	400	-
7	51B5	1697	30	0	0	2000	1300	400	-
8	51B5	1695	40	0	0	2000	1300	400	-
9	51B5	1710	60	0	0	3000 peaks to 4200	2500 peaks to 3500	400	-
10	51B5	1725	80	0	0	4200 peaks to 5200	3200 peaks to 4500	600	-
11	51B3	1695	40	0	0	3200	1500	1500	500
12	51B3	1710	60	0	0	4500	2200	2200	700
13	51B3	1725	80	0	0	6300 peaks to 7500	3000 peaks to 4000	3700 peaks to 4700	700

TABLE 16

DYNAMIC ROTOR BLADE STRESSES WITH THE INLET VANE REMOVED AS A FUNCTION OF β AND TUNNEL VELOCITY

Point	Gage No.	Speed (RPM)	Tunnel Vel. (Knots)	α (Deg.)	β (Deg.)	Total Stress (psi sa)	1st Flexural Stress (psi sa)	1st Torsional Stress (psi sa)	Cosine 3θ Stress (psi sa)
1	90B2	1700	20	0	0	4800	700	1900	1500
2	90B2	1745	20	0	35	3700	700	1200	1200
3	90B2	1710	60	0	0	4700	700	2200	1700
4	90B2	1740	60	0	35	4700	1000	1000	1500
5	90B2	1725	80	0	0	5500	1300	1700	2000
6	90B2	1720	80	0	20	5700	1300	2000	1300
7	51B5	1700	20	0	0	2000	1300	400	-
8	51B5	1745	20	0	35	2200	1400	400	-
9	51B5	1710	60	0	0	4200 peak	3500 peak	400	-
10	51B5	1740	60	0	35	4200 peak	3300 peak	400	-
11	51B5	1725	80	0	0	5200 peak	4500 peak	600	-
12	51B5	1720	80	0	20	5200 peak	4500 peak	600	-
13	51B3	1710	60	0	0	4500	2200	2200	700
14	51B3	1740	60	0	35	5000	3000	2500	700
15	51B3	1725	80	0	0	7500 peak	4000 peak	4700	700
16	51B3	1720	80	0	20	7500 peak	4000 peak	4000 peak	500

and it reads the highest flexural stress of any gage on the blade. Gage 51B3 responds to flexural, torsional and the cosine nθ modes. It does not read the highest stress in the blade for any mode, but it reads over 70% of the maximum stress for any mode. This gage is located 5.5 inches from the dovetail on the leading edge concave side.

The following table lists the various resonant speeds for the blades and system modes.

TABLE 17

BLADE RESONANT SPEEDS AND SYSTEM MODES

Speed RPM	Mode	Excitation
1690	3θ	3/rev
1705	First torsional	16/rev
1800	First flexural	8/rev
1980	4θ	4/rev
2100	5θ	5/rev
2100	2θ	2/rev
2350	6θ	6/rev
2380	First torsional	12/rev

Table 13 shows the change in blade stress* as a function of crossflow, exit louver angle and fan speed.

The 1st flexural, 1st torsional and cosine 2θ stresses need not add up to the total stress for two reasons: the stresses in the various modes are vector quantities and the stress level is so low that the noise level of the gage, recording and playback system can introduce small errors.

Crossflow and β variations above 2300 RPM resulted only in a change in the magnitude of the cosine 2θ stress. Any change in the flexural or torsional mode stresses was a function of speed only (i.e., proximity to the resonant speed). Gage 90B2 had the largest increase in the 2θ stress as was expected. The increase between points 1 and 2 in Table 13 is 3000 psi in the 2θ mode. When speed is decreased 200 RPM holding the same configuration as point 2, the 2θ stress increases 2250 psi point 3. This is a result of speed moving closer to 2100 RPM, the cosine 2θ resonant speed.

The torsional mode was found to be independent of crossflow velocity and β angle by comparing decelerations through the torsional resonance speed (2380 RPM) for β = 0° and 20 knots, and β = 35° and 100 knots. The maximum torsional stress gage, 90B2, showed 5000 psi at both conditions. The only exception to the above general statement occurred at 40° β setting and tunnel velocities of 40 knots and below with fan speeds near 2500 rpm. The torsion stress increase was highest at 30 knots, even though speed was moving away from the torsional resonance. This increase was small, 1250 psi and the cause has not been thoroughly investigated. The flexural mode at 1800 RPM was also found to be independent of crossflow and β angles during the first Ames test.

* All stress values in this report are single amplitude (sa)

The cosine 2θ mode stresses are shown in Figure 78 as a function of flight speed and louver angle for the normal fan operating speeds. These values are low relative to a running limit of 14,500 psi since the operating speed is not near the 2100 resonance speed. Also shown in Figure 78 are the peak cosine 2θ mode stresses observed during transients through the resonant speed at various tunnel velocities and β angles. The peaks always were higher during deceleration than during acceleration. Transients were not obtained above 60 knots; however, running limits* were exceeded at 60 knots when the exit louvers were at 35° setting.

Yaw from +8° to -16° had very little effect on blade stresses as shown in Table 14. Factoring out the change in stress due to resonances changing as a function of speed, yaw produced 500 psi or less stress variation. It is somewhat deceiving to say yaw does not affect blade stress since at some larger yaw angle the inlet vane will cease to function properly and the blade stress as a result of inlet distortion will increase much like the stresses increase when the inlet louver is removed.

With the inlet vane removed and up to and including 40 knots tunnel velocity, there was no change in stress levels. At 60 knots and above, the stress changes are shown in Table 15. In general, the absence of the inlet louver increased both the flexural and torsional blade stresses at crossflow velocities of 60 knots and above. The type of vibration changes from a pure resonant type with a constant amplitude to a separated flow type of vibration with rapidly modulating amplitudes. The separated flow exciting force could come either from the separated inlet or from the inlet air angles, being such that the air is separating on the blade airfoil. Closing the exit louvers to 35° at 1700 RPM without the inlet louver did not change the blade stress at any crossflow velocity as long as speed was held constant as shown in Table 16.

*Running Limits = $\frac{\text{Absolute Limits}}{1.56}$ (see Table 12, Volume 1).

The addition of the tab at the carrier ends did two things:

1. Change the frequency of the cosine $n\theta$ modes.

2. Lowered the torque transmission stresses.

The cosine $n\theta$ mode changes are shown below:

TABLE 18

CHANGE IN COSINE $n\theta$ MODES WITH TORQUE BAND DESIGN CHANGE

Mode	RPM - No Tab	RPM - With Tab
2θ	2080	2100
3θ	1520	1690
4θ	1680	1980
5θ	1800	2100
6θ	2000	2350

The tangential torque band stress at 2250 RPM was reduced from 10,000 psi to 6,800 psi. If the data from the previous testing were extrapolated to 2600 RPM, that torque band stress would be 12 to 15,000 psi; with the tab, the stress at 2600 RPM was 5,500 psi. The addition of the tab provided another friction surface between carrier and, therefore, more torque was transmitted through the carriers instead of the torque band.

No significant changes from the results reported in Volume 1 in stator or louver stresses or fan vibration and rotor bearing characteristics were noted throughout the test.

Torque Band Failure:

Component inspection following 23 hours of testing revealed cracks in the fan rotor torque bands. Specifically, cracks had occurred in both bands and, as in the previous test period, were located at the joint of adjacent turbine bucket carriers. This time, however, the cracks were situated near the axial center of the band and were oriented circumferentially in-line with the band components. Consideration of location and orientation of the cracks resulted in a decision to continue testing to observe crack propagation and incidence as a function of test time and test conditions.

Subsequently, eight hours of tests were conducted at rotor speeds up to 87% with no new cracks occurring or propagation of existing failure areas. The test plan was completed without compromise.

Analysis of the failure has been concerned with the following items:

1. Study of stresses recorded during test and a comparison of vibratory stresses in the band at the torque transmitting attachment point with those measured at the joint of adjacent carriers.

   Strain gage sensors were applied to both torque bands in an attempt to record and measure vibratory stresses in the band at the center of the bucket carrier (torque transmitting attachment point) and at the joint of adjacent carriers. (Gage location however was chosen to monitor stresses adjacent to the attachment ear (B/U #2 failure) and did not cover the failure areas in this test.) Tapes of stresses recorded during these tests do not show a significant change in level between the two locations. The maximum stress level tended to be slightly lower than measured in the previous tests (8 - 9 ksi versus 10 ksi).

2. Support Tab Fit-Up - Component inspection has shown that the cracks in the band were coincident with the toe on the support tab added as a fix for this testing. It was felt that the stack-up variation in tab-band fit-up during rotor assembly which produced cold clearances smaller than design (0.010) may have resulted in high radial shear and bending loading in the band at the support tab toe. Data taken during assembly and confirmed in teardown showed that the tab-band clearance ranged from 0.002 to 0.018 inches across the total of 72 tabs assembled to the fan rotor. There is no correlation however between this clearance and the band failure locations.

Forward Band	Failure Location	Clearance
	Tab 22	0.012 - 0.014
	27	0.008 at weld
	32	0.007
	36	0.010 at weld
Aft Band	Tab 5	0.010 at weld

Further inspection during teardown indicates that all tabs on the forward side of the carrier had been in contact with the band during test.

3. Comparison of the Steady-State Stresses in the Forward Band Relative to the Aft Band - Torque band analyses using measured temperature gradients show a significant reduction in steady-state stresses and hence, an increase in permissible vibratory stress on the aft band component.

Measured vibratory stresses from identical gage locations show nearly equal stress levels on the two components. It is felt that the aft band failure must be regarded as a material deficiency in the heat affected weld area or the interaction

between the support tab and cold assembly clearance relative to the band. The aft band did not show marks of tab-band contact that were evident on the forward band.

4. Shutdown Transients - Analysis of shutdown transients to determine feasibility of limiting stresses has been completed. There is no indication that this condition would result in high amplitude, low cycle fatigue.

5. Teardown Inspection Results - Component teardown and inspection have been completed. Flourescent penetrant and optical inspection have confirmed the original data. A total of five* cracks were noted: 4 cracks in the forward band; 2 in parent metal; and 2 in heat affected weld zones; one crack in the aft band in a heat affected weld area. At least two of the support tabs in failure locations show evidence of shear damage of the tab carrier support rabbet indicating severe radial loading.

The theory of failure resulting from this investigation is built on the interaction of the torque bands with the rotor system axial vibration. As the rotor is accelerated through these modes, the axial displacement of the bands about their maximum inertia axis results in a radial motion of the unsupported band lips. Construction of the rotor permits this displacement to occur only at the joint of adjacent bucket carriers and the radial movements of the lip is a vibratory stress not sensed at the other attachment location. The addition of the support tabs in the system was an attempt to provide support for the band at this location and effectively redistribute the vibratory loading away from the attachment ears and inherent stress concentration areas. The support tabs did result in a redistribution of loading, but the assembly stack-up and inability of the support to contain the radial motion

*Subsequent metallurgical analysis in the laboratory identified a sixth crack in the aft band.

of the overhung lip resulted in high shear loading and bending about the support tab toe. This combined loading in the band caused fatigue failure in that area.

A design change to correct this problem has resulted in two new configurations, each of which will be demonstrated in future fan tests.

6. The louvers, lever arms and pushrod were zygloed. One slight crack in a corner weld on louver #37 was found; this has been benched out.

7. The instrumentation was completely removed at teardown.

8. Figure 82 shows a crack propogation in the sawcut of the support ring between the fan and turbine stators due to thermal grcwth; this has been stop drilled.

SCROLL

1. No visible wear observed in any section of the scroll; the mounts, hangar brackets and several partition weld areas were spot zyglo checked.

ROTOR

1. The disc and shafts were magnafluxed, no cracks.

2. Two tabs on the aft retainer ring had indications in several spot welds. These were observed at previous zyglo before build-up; no new cracks are indicated.

3. Platforms were zygloed and are in good condition.

4. Blades show no nicks or dents in the airfoils; magnaflux was satisfactory. Dovetails and tangs showed no signs of fretting. The blades were completely cleaned, including removal of all strain gage instrumentation.

5. Carriers were cleaned and zygloed, no cracks. Several pieces from the bucket shroud were missing on teardown (Figure 83). These probably broke off during the shroud rub. Carriers show no new foreign object damage other than what was observed before build-up.

6. All pins zyglo tested satisfactorily. The amount of pin bow varied between 0.004 inches to 0.006 inches. Carrier holes were scored by pin removal and will be polished. Larger pins will be required for improved fit in next build-up.

7. Torque band cracks that were found during tests (after 20 hours) were also apparent from zyglo inspection after disassembly. A total of six were found (4 in the forward band and 2 in the aft band).

8. The tabs that were added to provide additional support for the torque bands were zygloed and three had crack indications near the heel. Six others removed from assembly prior to zyglo had visible cracks in the same area.

9. The covers were zygloed and were all satisfactory.

VII RECOMMENDATIONS

The nature of the work under contract DA 44-TC-584 is such that specific individual recommendations are made in the regular and continuing working relationships between the contractor, TRECOM and NASA-Ames. Such recommendations are usually presented in correspondence and in the bi-monthly technical progress reports and are not restated here. Also, in the body of this report, individual technical recommendations are incorporated in the technical discussions of which they are appropriately an inseparable part.

The intent of this part of the report is to summarize the major program recommendations relating to the continuation of the work. These are:

A. Complete the wind tunnel testing of this lift fan in the fuselage configuration by conducting tests of airplane - lift fan interaction in ground effect take off and ground effect hover, with the objective of increased understanding of tail downwash, lift variations, longitudinal stability and control, reingestion and fan mechanical performance.

B. Complete the concurrent fan-in-wing static test program.

C. Complete, as planned, the program for wind tunnel testing of the fan-in-wing configuration, plus the associated inlet development and engineering analysis work as described in the January 4, 1961 contract amendment. This program will cover approximately 75 hours of testing, including inlet performance; fan mechanical performance (steady state and transient); effectiveness of thrust spoiling, vectoring and ailerons for roll/yaw control; longitudinal and directional stability and static derivatives and trim control requirements; tail downwash; ground effect hover and transition; and reingestion and circulation patterns.

D. Begin the Flight Research Vehicle Program, as currently proposed, including the early selection of the airframe manufacturer, and the initiation of the propulsion system and aircraft programs. This will permit hardware design and procurement to proceed while the results of items A, B and C above are being obtained and used to define the ground and flight tests of the flight research program. In this way, orderly and continuous progress can be made toward the demonstration of a lift-fan powered airplane in free flight.

VIII. REFERENCES

1. Corning, Gerald, Supersonic and Subsonic Airplane Design, Second Edition, Edwards Brothers, Inc., Ann Arbor, Michigan, 1953.

2. Hickey, D. H., and Ellis, D.R., Wind-Tunnel Tests of a Semispan Wing With a Fan Rotating in the Plane of the Wing, NASA Technical Note D-88, October 1959.

3. Hoerner, S.F., Dr., Fluid-Dynamic Drag, Published by the Author, 1958, Library of Congress Catalog Card Number 57-13009.

4. *Kelly, M.W., Large-Scale Wind-Tunnel Studies of Several VTOL Types, Ames Research Center.

5. Kuhn, R. E., and Naeseth, R.L., Tunnel-Wall Effects Associated with VTOL-STOL Model Testing, NASA, Langley Research Center, Langley Field, Va., March 1959.

6. *Maki, R.L., and Hickey, D.H., Aerodynamics of Fan-in-Fuselage Model, Ames Research Center.

7. Pope, Alan, Wind-Tunnel Testing, Second Edition, John Wiley and Sons, Inc., New York, 1954

8. *Spreemann, K. P., Induced Interference Effects on Jet and Burried Fan VTOL Configurations in Transition, Langley Research Center.

---

* From NASA Conference on V/STOL Aircraft (a compilation of papers presented), Langley Research Center, Langley Field, Virginia, November 17-18, 1960.

9. Switzer, J.R., VTOL Wing-Fan Model Tests, Flight Propulsion Laboratory Department, General Electric Company, Cincinnati 15, Ohio, 1958.

10. Theodorsen, Th., Dr., Theoretical Investigation of Ducted Propeller Aerodynamics, Volume 1, USATRECOM Contract No. DA 44-177-TC-606, Project No. 9R38-01-017-24, Republic Aviation Corporation, Farmingdale, New York, August 10, 1960.

11. Fabrication, Test and Analysis of a Tip-Turbine Lift-Fan VTOL Propulsion System for U.S. Army Transportation Research Command Fort Eustis, Virginia, TREC Technical Report 60-42, Contract No. DA44-177-TC-584, Project No. 9R38-01-017-04, Flight Propulsion Laboratory Department, General Electric Company, Cincinnati 15, Ohio 1960.

12. Results of Wind-Tunnel Tests of a Full-Scale Fuselage-Mounted Tip-Turbine-Driven Lift Fan, TREC Technical Report 61-15, Volume 1, Contract No. DA 44-177-TC-584, Project No. 9R38-01-020-02, Flight Propulsion Laboratory Department, Cincinnati 15, Ohio January 1961.

APPENDIX A

METHOD FOR ESTIMATING FAN PERFORMANCE ABOVE V_P/V_{tip} OF 0.3

A considerable number of test points were obtained at high fan speeds up to velocity ratios of 0.3 and fan performance was calculated as described in Section V-C. At velocity ratios above 0.3 only a few data points were obtained and only at reduced fan speeds (in order not to exceed the 100 knot limit on the model). This makes the calculation of fan performance at these high velocity ratios by the method described in Section V-C impractical.

Fan performance can be estimated above V_P/V_{tip} = 0.3 by the use of the parameter $\eta_R(V_P/V_{tip})^2$, which is reasonably well known up to velocity ratios of 0.5. Fan performance changes with crossflow are due to the relative change of the pressure levels at the fan inlet and fan exit. As long as this difference between these two levels is known, the performance of the fan can be estimated. The quantity $\eta_R(V_P)^2$ is proportional to the difference in levels of fan inlet and fan exit pressures; dividing by $(V_{tip})^2$ nondimensionalizes this quantity so that it can be applied to any fan speed. The plot of $\eta_R(V_P/V_{tip})^2$ is shown in Figure 84, and shows that between velocity ratios of 0.3 and 0.5, this quantity does not change appreciably. From this, it can be concluded that fan performance between 0.3 and 0.5 V_P/V_{tip} is essentially constant (i.e., the ram recovery is just sufficient to maintain constant thrust with increases in V_P/V_{tip} above 0.3) and equal to the calculated performance at 0.3 V_P/V_{tip}. This conclusion is most likely optimistic since distortion of the inlet increases as velocity ratio increases and therefore, fan efficiency will be affected adversely. The parameter $\eta_R(V_P/V_{tip})^2$ can also be used in estimating X353-5 fan performance with other inlets if the inlet performance is known in terms of η_R versus $V_P/C_{Z\ 10.2'}$ and the distortion patterns are similar to the Ames fuselage inlet.

TABLE A-1

DEFINITIONS AND SYMBOLS

A_f — Fan exit area = 17.8 Sq. Ft.

AR — Wing aspect ratio, b^2/S_w = 5.

b — Wing span = 35.36 Ft.

c — Local wing chord, Ft.

$\bar{c}$ — Mean wing chord, S_w/b = 7.07 Ft.

d — Diameter, Ft.

C_D — Drag coefficient D/q S_w (based on tunnel q)

C_{Di} — Induced drag coefficient, C_L^2/π AR e

C_{Do} — Drag coefficient at zero lift.

C_{Dw} — Drag coefficient based on wetted area.

c.g. — Center of Gravity.

C_L — Lift coefficient, L/q S_w (based on tunnel q)

$\bar{C}_L$ — Lift coefficient calculated from wing static pressure distribution.

$$\frac{1}{2}\int_{-1}^{1} \frac{c_a}{\bar{c}} \frac{c}{\bar{c}}\, d\left(\frac{y}{b/2}\right)$$

$C_{L\,max}$ — Maximum lift coefficient at $\Delta C_L/\Delta\alpha = 0$.

C_{Lt} — Horizontal tail lift coefficient.

C_ℓ — Rolling moment coefficient, $\frac{\text{Roll Force}}{q\ b\ S_w}$ (based on tunnel q)

C_M — Pitching moment coefficient, M/q S_w c_{mac} (based on tunnel q)

c_a — Wing section lift coefficient.

$\bar{C}_M$ — Pitching moment coefficient calculated from wing static pressure distribution.

ΔC_M — Change in moment coefficient due to change in tail incidence.

c_{mac} — Mean aerodynamic chord $\int_{-b/2}^{b/2} \frac{c^2\, dy}{S_w}$ = 7.33 Ft.

C_z — Fan average axial (or through flow) velocity, Ft/Sec.

D — Basic aircraft drag (fan off-holes covered), Lbs.

D_{int} — Interaction drag, Lbs.

D_b — Ram drag, Lbs.

D_T — Total measured drag (fan on), Lbs.

e — Oswald efficiency = 0.8 (assumed)

F — Total fan thrust, Lbs.

F_{J85} — Thrust from J85 bleed gas

F_x — Horizontal component of fan thrust, F [sin (α - β_v)] Lbs.

F_y — Vertical component of fan thrust, F [cos (β_v - α)] Lbs.

g — Acceleration due to gravity = 32.2 Ft/Sec^2.

G.W. — Aircraft gross weight, Lbs.

H_D — Drag coefficient, $D_f/\rho\ A_f\ (V_{tip})^2$ (based on fan q)

H_{DF} — Drag coefficient, $F_d/\rho\ A_f\ (V_{tip})^2$

H_{DB} — Drag coefficient, $H_{DF} - H_{DB}$

H_{DB} — Drag coefficient, $D_b/\rho\ A_f\ (V_{tip})^2$

$H_{G.W.}$ — Coefficient, $G.W./\sigma A_f (V_{tip})^2$

H_L — Lift coefficient, $L_f/\rho\ A_f\ (V_{tip})^2$ (based on fan q)

H_{LF} — Lift coefficient, $F_y/\rho\ A_f\ (V_{tip})^2$

H_M — Moment coefficient, $M_f/\rho\ A_f\ (V_{tip})^2\ l_t$ (based on fan q.

HP — Horsepower

H_T — Thrust coefficient, $F/\rho\ A_f\ (V_{tip})^2$

h — Height of the bottom of the fuselage above the ground, Ft.

i_t — Tail incidence angle.

L — Basic aircraft lift (fan off - holes covered), Lbs.

L_{int} — Interaction lift, Lbs.

l_{PRC} — Pitch reaction control moment arm = 25.5 Ft.

L_T — Total measured lift (fan on), Lbs.

l_t — Tail moment arm = 22 Ft.

M — Basic aircraft pitching moment (tail off, power off), Ft. Lbs.

M_β — Pitching moment due to exit louver vectoring, Ft. Lbs.

$M_{D,\ J85}$ — Pitching moment due to J85 ram drag.

M_{int} — Interaction pitching moment, Ft. Lbs.

M_{J85} — Pitching moment due to J85 bleed thrust, Ft. Lbs.

M_T — Total measured pitching moment (fan on), Ft. Lbs.

M_t — Pitching moment due to tail, Ft. Lbs.

N_f — Fan speed, RPM or % of design = 2640 RPM at 100%.

N_{J85} — Engine speed, RPM or % of design = 16,500 RPM at 100%.

P — Pressure, lbs/Sq. In.

P_{ss} — Local static pressure, lbs/Sq. In.

P_{to} — Tunnel total pressure, lbs/Sq. In.

P_{so} — Tunnel static pressure, lbs/Sq. In.

q — Tunnel dynamic pressure, lbs/Sq. Ft.

RC — Reaction control output, Cycles/Sec.

S_t — Horizontal tail gross area = 50 Sq. Ft.

S_w — Wing gross area = 250 Sq. Ft.

T — Temperature °R or °F.

V_p — Tunnel or airplane velocity, Knots.

V_{tip} — Fan blade tip speed = 780 Ft/sec or 465.6 knots at 2640 RPM

V_p/V_{tip} — Velocity ratio parameter (nondimensional).

V_{stall} — Airplane stall speed (fan off), Knots.

W — Weight flow, Lbs./Sec.

y — Spanwise location from center line of the aircraft, Ft.

α — Angle of attack, Degrees.

β — Indicated exit louver angle, Degrees.

β_v — Effective exit louver turning angle, Degrees.

δ — Pressure correction parameter, $P_{ambient}/14.696$.

δ_f — Wing flap angle, Degrees.

ϵ — Tail downwash angle, Degrees.

η_R — Fraction of tunnel velocity head recovered by fan inlet (includes static loss).

θ — Temperature correction parameter, $T_{ambient}/518.7$.

ρ — Mass Density, Slugs/Cu. Ft.

$\bar{\omega}$ — Loss coefficient in per cent of fan inlet velocity head at the face of the rotor.

ψ — Aircraft yaw angle.

SUBSCRIPTS

c — Corrected.

f — Denotes fan.

f — Denotes flap or frontal area.

p — Denotes airplane.

s — Denotes static.

t — Denotes total or tail.

u — Uncorrected.

w — Denotes wing or wetted area.

10.1; 5.3 etc. — Denotes measurement plane identification.

TABLE A-2

AMES TEST RESULTS

Point No. - Consecutive	Point No. - Per Run	Run No.	Tunnel Speed (V_p) - Knots	Tunnel Dynamic Pressure (q) - Lbs/sq.ft.	Fan Speed (N_p) - RPM	Tunnel Temp. °F	Angle of Attack (α_f) - degrees	Exit Louver Angle (δ_j) - degrees	Horizontal Tail Incidence Angle (i_t) - degrees	Ejection Control Setting (EC) - CPS	Wing Flap Angle (δ_f) - degrees	Engine Speed (N_{gg}) - RPM	Exhaust Gas Temp (EGT) - °F	Total Lift (L_T) - Lbs.	Total Drag (D_T) - Lbs.	Total Pitch Moment (M_T) - Ft. Lbs.	Lift Coefficient (C_L)	Drag Coefficient (C_D)	Pitch Moment Coefficient (C_M)	Lift To Drag Ratio (L_T/D_T)	Barometer In. Hg.	Velocity Ratio ($V_p/\sqrt{gD}$)	Lift Coefficient (Π_L)	Drag Coefficient (Π_D)	Pitch Moment Coefficient (Π_M)
1	1	2	20	1.05	1704	90	-4.00	0	Off	Off	0	14310	TNC	2706	92	2758	10.309	.3505	1.4326	29.413	30.02	.066	.314	.010	.014
2	2			1.00	1701		-2.00					14330		2698	157	3114	10.792	.6280	1.6989	17.185		.064	.310	.018	.016
3	3			.98	1700	91	.00					14320		2724	245	2416	11.183	1.0000	1.346	8.316		.063	.314	.028	.012
4	4			1.29	1702	90	2.00					14340		2749	371	3142	8.524	1.1504	1.3268	7.410		.073	.317	.042	.016
5	5			1.29	1698	91	4.00					14320		2743	462	3204	8.505	1.4326	1.3549	5.937		.073	.320	.054	.017
6	6			1.29	1692		6.00					14340		2830	629	3617	8.775	1.9504	1.5294	4.499		.073	.332	.073	.019
7	7			1.29	1690	92	8.00					14330		2784	696	3171	8.633	2.1581	1.3407	4.000		.073	.327	.081	.016
8	8			2.97	1686	90	-4.00					14330		2676	396	5617	3.604	.533	1.0326	5.136		.112	.318	.061	.010
9	9			2.97	1693		-2.00					14370		2719	470	4445	3.662	.6330	.8163	5.785		.111	.318	.055	.023
10	10			2.97	1687		.00					14350		2918	587	5095	3.930	.7906	.9357	4.971		.112	.346	.069	.027
11	11			2.97	1689		2.00					14360		2999	689	4774	4.039	.9279	.8768	4.353		.112	.346	.069	.025
12	12			2.97	1684		4.00					14320		3138	789	5563	4.226	1.0626	1.0216	3.977		.112	.372	.093	.030
13	13		30	2.97	1684		6.00					14340		3231	892	5507	4.352	1.2013	1.0115	3.622		.112	.384	.106	.029
14	14			2.97	1686		8.00					14340		3265	1007	5624	4.397	1.3562	1.0329	3.242		.112	.388	.119	.030
15	15			2.97	1689		10.00					14360		3349	1106	5851	4.510	1.4896	1.0747	3.028		.112	.397	.131	.031
16	16			2.97	1690		12.00					14360		3415	1207	5721	4.599	1.6256	1.0508	2.829		.111	.399	.141	.030
17	17			2.97	1691		14.00					14370		3499	1327	5927	4.712	1.7872	1.0885	2.637		.111	.410	.155	.031
18	18			3.01	1688	94	16.00					14350		3728	1492	6539	4.954	1.9827	1.1850	2.499		.112	.441	.176	.035
19	19		40	5.21	1698		-4.00					14380		2918	727	7022	2.240	.5582	.7352	4.014		.148	.345	.085	.037
20	20			5.21	1698		.00					14390		3295	875	7444	2.530	.6718	.7794	3.766		.148	.389	.103	.040
21	21			5.21	1692	95	4.00					14370		3689	1087	8139	2.832	.8345	.8522	3.394		.148	.438	.128	.043
22	22			5.21	1693		6.00					14320		3901	1169	8059	2.995	.8975	.8437	3.337		.148	.463	.138	.043
23	23			5.21	1682		8.00					14390		4112	1290	9140	3.157	.9904	.9570	3.188		.150	.497	.155	.050
24	24			5.21	1685		10.00					14380		4623	1421	9106	3.423	1.0910	.9534	3.000		.149	.512	.171	.049
25	25			5.21	1685		12.00					14400		4387	1527	8904	3.368	1.1724	.9323	2.873		.149	.528	.183	.048
26	26			5.21	1669		14.00					14370		4373	1749	8176	3.357	1.3428	.8560	2.500		.151	.533	.213	.045
27	27			5.21	1650		16.00					14380		4341	1972	6137	3.486	1.5140	.6425	2.303		.153	.571	.248	.035
28	28		60	11.08	1688	96	-4.00					14410		3074	1493	10475	1.110	.5390	.5157	2.059		.217	.365	.177	.056
29	29			11.08	1697		.00					14430		4138	1596	12874	1.494	.5762	.6338	2.593		.216	.487	.188	.068
30	30			11.08	1699		4.00					14400		5046	1742	14257	1.822	.6289	.7019	2.897		.216	.594	.205	.076
31	31			11.08	1687		8.00					14420		6009	1971	15276	2.169	.7116	.7521	3.049		.217	.713	.234	.082
32	32			11.62	1684		10.00					14420		6168	2218	14837	2.123	.7635	.6965	2.781		.224	.744	.268	.081
33	33			11.68	1660		12.00					14440		6423	2388	15281	2.200	.8178	.7137	2.690		.227	.792	.294	.085
34	34			11.68	1665							14420		-	-	-	-	-	-	-		.227	.819	.321	-
35	35			11.68	1646		16.00					14420		6298	2987	14198	2.157	1.0229	.6631	2.108		.228	.784	.375	.080

TABLE A-2
(Continued)
AMES TEST RESULTS

Point No. - Consecutive	Point No. - Per Run	Run No.	Tunnel Speed (V_o) - Knots	Tunnel Dynamic Pressure (q) - Lbs/sq.ft.	Fan Speed (N_F) - RPM	Tunnel Temp. °F	Angle of Attack (α_c) - degrees	Exit Louver Angle (δ_e) - degrees	Horizontal Tail Incidence Angle (i_t) - degrees	Reaction Control Setting (RC) - CFM	Wing Flap Angle (δ_f) - degrees	Engine Speed (N_{JET}) - RPM	Exhaust Gas Temp. (EGT) - °F	Total Lift (L_T) - Lbs.	Total Drag (D_T) - Lbs	Total Pitch Moment (M_T) - Ft. Lbs.	Lift Coefficient (C_L)	Drag Coefficient (C_D)	Pitch Moment Coefficient (C_M)	Lift To Drag Ratio (L_T/D_T)	Barometer In. Hg.	Velocity Ratio ($V_o/\sqrt{g_c p/\rho}$)	Lift Coefficient (Π_L)	Drag Coefficient (Π_D)	Pitch Moment Coefficient (Π_M)
36	36	2	60	1.17	2287	98	0.00	0	Off	Off	0	16140	NC	4921	324	5091	16.824	1.1077	2.3736	15.188	30.02	.072	-	-	-
37	1	3	20	1.33	1425	66	0.00	0	Off	Off	0	13280	NC	2126	294	3189	6.394	.8842	1.3081	7.231	30.00	.087	.340	.047	.023
38	2			1.31	1730	66						14350		1984	315	-5741	6.058	.9618	-2.3905	6.298		.071	.215	.034	-
39	3			1.29	2270	68						15870		5142	388	4432	15.944	1.2031	1.8657	13.253		.053	.312	.024	-
40	4			1.17	2453	71						16250		5892	364	4724	20.144	1.2444	2.2023	16.187		.047	.319	.019	-
41	5			1.39	2548	73						16500		6390	450	5799	18.388	1.2950	2.2757	14.200		.049	.320	.022	.013
42	6			1.35	2545	77		20				16500		5854	-1805	12684	17.345	-5.3481	5.1252	-3.243		.049	-.300	-.092	.029
43	7			1.70	2570	78		30				16500		5186	-2644	17616	12.202	-6.2212	5.6524	-1.961		.055	.258	-.131	.039
44	8			1.60	2580	81		35				16500		4683	-3038	18057	11.708	-7.5950	6.1561	-1.541		.053	.233	-.151	.040
45	9			1.68	2617	82		40				16500		3951	-3234	17926	9.407	-7.7009	5.8203	-1.222		.054	.192	-.157	.039
46	10		30	3.05	2520	85		0				16500		6411	843	6747	8.408	1.1056	1.2066	7.605		.075	.336	.044	.016
47	11			2.82	2515			20				16500		5927	-1417	15494	8.407	-2.0059	2.9970	-4.183		.073	.314	-.075	.037
48	12			3.09	2533	86		30				16500		5156	-2346	18525	6.686	-3.0369	3.2702	-2.202		.075	.269	-.122	.043
49	13			2.88	2558			35				16500		4564	-2755	18778	6.339	-3.8264	3.5566	-1.657		.072	.234	-.141	.043
50	14			2.86	2595	87		40				16500		3762	-2967	18548	5.262	-4.1497	3.5376	-1.268		.071	.188	-.148	.042
51	15		40	5.32	2500	89		0				16500		6580	1190	9920	4.947	.8947	1.0171	5.529		.101	.355	.064	.024
52	16			5.21	2485	90		20				16500		6033	-1035	17655	4.632	-.7946	1.8484	-5.829		.100	.330	-.056	.044
53	17			5.03	2500			30				16500		5130	-2020	20027	4.080	-1.6064	2.1719	-2.540		.098	.277	-.109	.049
54	18			5.21	2535	91		35				16500		4411	-2356	21057	3.387	-1.8088	2.2047	-1.872		.098	.232	-.123	.050
55	19			5.11	2570			40				16500		3713	-2590	20613	2.906	-2.0274	2.2003	-1.434		.096	.189	-.132	.047
56	20		60	11.70	2483	93		0				16500		7582	2060	16679	2.592	.6838	.7776	3.791		.154	.431	.097	.043
57	21			11.66	2480			20				16500		6312	-169	22812	2.165	-.0648	1.0672	-33.397		.151	.349	-.010	.057
58	22			11.49	2489	92		30				16500		5287	-1244	24753	1.841	-.4331	1.1751	-4.250		.149	.288	-.067	.061
59	23			11.64	2511	93		35				16500		4621	-1581	25937	1.588	-.5433	1.2155	-2.923		.149	.249	-.085	.063
60	24			11.86	2547			40				16500		3785	-1833	25672	1.277	-.6182	1.1807	-2.065		.148	.197	-.095	.061
61	1	4	0	0	2334	68		0	Off	Off	0	16110	NC	5454	-276	671	NA	NA	NA	NA	29.97	NA	.326	-.016	.001
62	2				2465			0				16350	1130	5931	-295	396							.317	-.015	.000
63	3				2461			0				16540	1160	6202	-269	1052							.333	-.014	.002
64	4				2434			10				16480	1200	6109	-1071	10749							.334	-.058	.026
65	5				2544			20				16490	1200	5778	-2177	10309							.290	-.109	.023
66	6				2568	70		30				16490	1200	5063	-3046	14925							.249	-.150	.033
67	7				2602			35				16490	1200	4632	-3296	17125							.222	-.158	.037
68	8				2645			40				16490	1200	4038	-3473	16977							.187	-.161	.035
69	9				2451	81		0				16490	1190	5983	-346	1872							.330	-.019	.004
70	10				2502	84		0				16510	NC	6661	1228	10020							.352	-.065	.024

TABLE A-2
(Continued)
AMES TEST RESULTS

Point No. - Consecutive	Point No. - Per Run	Run No.	Tunnel Speed (V_o) - Knots	Tunnel Dynamic Pressure (q) - Lbs/sq.ft.	Fan Speed (N_2) - RPM	Tunnel Temp. °F	Angle of Attack (α_c) - degrees	Exit Louver Angle (δ_j) - degrees	Horizontal Tail Incidence Angle (i_t) - degrees	Reaction Control Setting (RC) - CPS	Wing Flap Angle (δ_{wf}) - degrees	Engine Speed (N_{GG}) - RPM	Exhaust Gas Temp. (EGT) - °F	Total Lift (L_T) - Lbs.	Total Drag (D_T) - Lbs.	Total Pitch Moment (P_{M_T}) - Ft. Lbs.	Lift Coefficient (C_L)	Drag Coefficient (C_D)	Pitch Moment Coefficient (C_{P_M})	Lift To Drag Ratio (L_T/D_T)	Barometer In. Hg.	Velocity Ratio ($V_o/\sqrt{Eg}$)	Lift Coefficient (C_L)	Drag Coefficient (C_D)	Pitch Moment Coefficient (C_{P_M})
71	1	5	80	20.62	2504	88	0.00	0	Off	Off	0	11760	NC	8830	3303	23952	1.713	.6019	.6336	2.84	30.10	.198	.472	.165	.058
72	2			20.51	2502			20				16530		6578	745	30500	1.283	.1453	.8112	8.83		.198	.354	.039	.074
73	3			20.48	2478	91		30				16500		5305	-326	31765	1.036	-.0637	.8461	-16.27		.301	.294	-.018	.079
74	4			20.60	2485			35				16540		4680	-731	32710	.909	-.1419	.8661	-6.40		.201	.238	-.040	.081
75	5			20.69	2521	95		40				16500		3807	-1033	31138	.736	-.1997	.8209	-3.68		.199	.204	-.055	.075
76	6		100	32.40	2484			0				16520		9362	4233	32059	1.156	.5226	.5397	2.21		.260	.546	.247	.084
77	7			31.97	2487	97		20				16520		6981	1787	36942	.873	.2236	.6303	3.90		.251	.386	.098	.092
78	8			32.61	2467			30				16520		5729	702	38261	.703	.0861	.6400	8.16		.254	.318	.038	.096
79	9			32.39	2468	98		35				16520		5177	305	36909	.639	.0377	.6216	16.97		.255	.291	.017	.094
80	10			32.45	2494			40				16520		4154	-32	34721	.512	-.0039	.5837	-129.81		.252	.228	-.0017	.086
81	1	6	60	11.76		71	-4.14	90	On	Off	0		NA	-775	392	1227	-.264	.1340	.0620	-1.96	30.13	NA	NA	NA	NA
82	2						-2.06							-318	351	509	-.108	.1195	.0257	-.90					
83	3			11.80			.03							165	326	-282	.056	.1105	-.0141	.50					
84	4			11.70			2.11							619	313	-651	.212	.1074	-.0345	1.97					
85	5			11.76			4.20							1086	319	-930	.369	.1098	-.0503	3.36					
86	6			11.92			6.28							1590	337	-1452	.534	.1157	-.0768	4.61					
87	7			11.68			8.37							2027	359	-1731	.694	.1274	-.0943	5.44					
88	8			11.66			10.46							2503	430	-2366	.859	.1441	-.1367	5.96					
89	9			11.72			12.54							2982	450	-2950	1.018	.1632	-.1570	6.23					
90	10			11.76			14.62							3405	546	-3938	1.158	.1982	-.2051	5.84					
91	11			11.72			16.00							3338	755	-4622	1.139	.2697	-.2372	4.22					
92	1	7	20	1.17	1730	69	0.00	0	On	Off	0	14400	NC	2971	334	3512	10.157	1.1419	1.6375	8.89	30.10	.067	.323	.036	.017
93	2			1.35	2248	71						15870		5021	428	5261	14.877	1.2681	2.1257	11.73		.055	.325	.027	.015
94	3			1.27	2463	73						16350		5929	432	6081	18.674	1.3606	2.6118	13.72		.049	.319	.023	.014
95	4			1.17	2466	75		20				16350		5499	-1740	12170	18.800	-5.9487	5.6741	-3.16		.047	.297	-.094	.029
96	5			1.33	2508	76		35				16340		4381	-2912	17528	13.176	-8.7579	7.1069	-1.50		.049	.227	-.151	.041
97	6		30	2.97	2445	77		0				16330		6044	791	8866	8.140	1.0653	1.6284	7.64		.076	.331	.043	.022
98	7			2.88	2430	81		20				16340		5515	-1274	15455	7.660	-1.7694	2.9272	-4.32		.075	.309	-.071	.039
99	8			3.13	2470	82		35				16340		4289	-2517	18225	5.481	-3.2166	3.1761	-1.70		.078	.234	-.137	.045
100	9		40	5.46	2418	85		0				16340		6234	1129	11818	4.567	.8271	1.1807	5.52		.105	.356	.064	.030
101	10			5.46	2410	86		20				16330		5747	3124	99181	4.210	2.2886	-9.9086	1.84		.106	.331		
102	11			5.15	2450			35				16330		4202	-2184	20303	3.264	-1.6963	2.1505	-1.92		.101	.234	-.121	.051
103	12		60	11.68	2409	88		0				16330		7154	1956	17632	2.450	.6699	.9235	3.65		.155	.413	.138	.046
104	13			11.76	2398	89		20				16330		5945	-60	23202	2.022	-.0204	1.0762	99.08		.156	.347	-.003	.061
105	14			11.76	2422			35				16330		4291	-1365	25562	1.457	-.4635	1.1837	-3.14		.155	.245	-.078	.066

TABLE A-2
(Continued)
AMES TEST RESULTS

Point No. - Consecutive	Point No. - Per Run	Run No.	Tunnel Speed (V_T) - Knots	Tunnel Dynamic Pressure (q) - Lbs/sq.ft.	Fan Speed (N_{FAN}) - RPM	Tunnel Temp. °F	Angle of Attack (α_T) - degrees	Bolt Linear Angle (ζ_T) - degrees	Horizontal Tail Incidence Angle (i_t) - degrees	Aeration Control Setting (DC)	CPS Wing Flap Angle (δ_{WF}) - degrees	Engine Speed (N_{RPM}) - RPM	Exhaust Gas Temp. (EGT) - °F	Total Lift (C_{L_T}) - Lbs.	Total Drag (D_T) - Lbs.	Total Pitch Moment (C_{m_T}) - Ft. Lbs.	Lift Coefficient (C_L)	Drag Coefficient (C_D)	Pitch Moment Coefficient (C_m)	Lift To Drag Ratio (C_L/C_D)	Barometer in. Hg.	Velocity Ratio (V_p/V_{AIR})	Lift Coefficient (C_L)	Drag Coefficient (C_D)	Pitch Moment Coefficient (C_m)
106	15	7	80	20.70	2404	90	0.00	0	0	OFF	0	16340	NC	8309	2933	27872	1.606	.5668	.7345	2.83	30.00	.207	.482	.170	.073
107	16			20.74	2409	90		20				16340		6133	839	31370	1.183	.1618	.8251	7.31		.207	.356	.049	.083
108	17			20.72	2409	90		35				16350		4342	-536	32960	.838	-.1035	.8672	-8.10		.207	.252	-.031	.087
109	18		100	32.72	2415	91		0				16350		8951	4298	33985	1.094	.5254	.5666	2.08		.260	.519	.249	.089
110	19			32.66	2417			20				16360		6593	1948	37651	.807	.2386	.6288	3.38		.260	.382	.113	.099
111	20			32.66	2404			35				16360		4799	428	39360	.588	.0524	.6574	11.21		.261	.281	.025	.105
112	21			32.84	2306			40				16360		3847	296	34934	.469	.0361	.5803	12.99		.273	.244	.019	.101
113	1	8	20	1.55	1705	75	-8.00	0	0	OFF	30	14330	NC	2277	-15	3301	7.166	-.0387	1.1616	-185.13	30.00	.079	.313	-.002	.017
114	2			1.31	1703	76	-6.00					14320		2754	36	2997	8.609	.1099	1.2678	76.50		.073	.313	.004	.015
115	3			1.31	1696	77	-4.00					14330		2836	144	2879	8.660	.4397	1.1986	19.69		.073	.325	.016	.015
116	4			1.25	1697	78	-2.00					14330		2850	233	3030	9.120	.7456	1.3310	12.23		.071	.326	.027	.016
117	5			1.29	1695	79	.00					14330		2943	372	3496	9.126	1.1535	1.4782	7.91		.073	.338	.043	.018
118	6			1.31	1697	80	2.00					14330		2965	474	3534	9.053	1.4473	1.4716	6.25		.073	.340	.054	.018
119	7			1.25	1693		4.00					14330		2988	588	3182	9.562	1.8816	1.3887	5.08		.071	.341	.067	.017
120	8			1.35	1692	81	6.00					14330		3100	748	3140	9.185	2.2163	1.2688	4.14		.075	.361	.087	.017
121	9			1.29	1695		8.00					14330		3117	839	2950	9.665	2.6016	1.2476	3.71		.073	.358	.096	.015
122	10			1.29	1692		10.00					14330		3145	960	2776	9.752	2.9767	1.1737	3.27		.073	.363	.111	.015
123	11			1.35	1694	82	12.00					14330		3235	1100	2985	9.585	3.2593	1.2060	2.94		.075	.376	.128	.016
124	12			1.31	1688		14.00					14330		3259	1203	2731	9.951	3.6733	1.1371	2.70		.074	.379	.140	.014
125	13		30	3.15	1693	83	-8.00					14340		2777	312	5244	3.526	.3962	.9082	8.90		.114	.321	.036	.028
126	14			2.97	1688	84	-6.00					14340		2883	387	5485	3.883	.5212	1.0074	7.45		.111	.336	.045	.029
127	15			2.94	1691		-4.00					14340		3029	469	4751	4.121	.6381	.8815	6.45		.111	.355	.055	.025
128	16			2.97	1691		-2.00					14340		3200	557	5339	4.319	.7502	.9806	5.74		.111	.374	.065	.028
129	17			3.03	1684		.00					14340		3325	679	4664	4.349	.8964	.8397	4.89		.113	.391	.080	.025
130	18			2.97	1687		2.00					14340		3422	784	4467	4.609	1.0559	.8205	4.36		.112	.403	.092	.024
131	19			2.92	1687	85	4.00					14340		3559	882	4679	4.875	1.2082	.8749	4.20		.111	.438	.104	
132	20			2.90	1688		6.00					14340		3670	1012	4354	5.062	1.3959	.8189	3.62		.111	.432	.119	.023
133	21			3.05	1690		8.00					14340		3837	1159	4205	5.032	1.5200	.7520	3.31		.113	.447	.135	.022
134	22			2.86	1690		10.00					14340		3936	1262	4085	5.505	1.7650	.7790	3.11		.109	.461	.148	.022
135	23			2.97	1690		12.00					14340		4041	1402	4044	5.442	1.8882	.7522	2.88		.113	.472	.164	.022
136	24			2.88	1687	86	14.00					14340		4077	1511	3857	5.663	2.0986	.7306	2.69		.110	.482	.178	.021
137	25		40	5.13	1690		-8.00					14350		2861	584	6909	2.231	.4554	.7347	4.89		.147	.336	.069	.037
138	26			5.28	1683		-4.00					14350		3435	799	7237	2.602	.6053	.7470	4.29		.150	.408	.095	.039
139	27			5.15	1691		.00					14350		3900	954	6518	3.029	.7410	.6904	4.08		.147	.456	.112	.034
140	28			5.19	1689		4.00					14350		4360	1213	6021	3.360	.9349	.6328	3.59		.148	.515	.163	.032

TABLE A-2
(Continued)
AMES TEST RESULTS

Point No. - Consecutive	Point No. - Dat Sch.	Run No.	Tunnel Speed (V_∞) - Knots	Tunnel Dynamic Pressure (q) - Lbs/sq.ft.	Fan Speed (N_p) - RPM	Tunnel Temp. °F	Angle of Attack (α_s) - degrees	Exit Louver Angle (δ_e) - degrees	Horizontal Tail Incidence Angle (i_t) - degrees	Ejection Control Setting (EC) - CPS	Wing Flap Angle (δ_f) - degrees	Engine Speed ($N_{2(R)}$) - RPM	Exhaust Gas Temp. (EGT) - °F	Total Lift (C_L) - Lbs.	Total Drag (C_D) - Lbs.	Total Pitch Moment (C_m) - Ft. Lbs.	Lift Coefficient (C_L)	Drag Coefficient (C_D)	Pitch Moment Coefficient (C_m)	Lift To Drag Ratio C_L/C_D	Barometer In. Hg.	Velocity Ratio $V_\infty/\sqrt{Rlg}$	Lift Coefficient (C_L)	Drag Coefficient (C_D)	Pitch Moment Coefficient (C_m)
141	29	8	60	5.35	1690	87	8.00	0	0	Off	30	14350	WC	4917	1481	5914	3.697	1.1135	.6064	3.32	30.00	.150	.579	.175	.032
142	30			5.17	1686		10.00					14350		5109	1608	5758	3.953	1.2441	.6075	3.17		.148	.603	.190	.031
143	31			5.13	1671		12.00					14350		5236	1808	6821	4.083	1.4097	.5127	2.89		.149	.632	.218	.026
144	32			5.15	1668		14.00					14360		4980	2060	4503	3.868	1.6000	.4770	2.41		.148	.601	.249	.025
145	33		60	11.66	1703	86	-8.00					14380		2939	1495	11948	1.008	.5129	.5590	1.96		.219	.337	.172	.062
146	34			11.84	1699		-4.00					14370		4211	1596	11160	1.423	.5392	.5142	2.63		.222	.489	.185	.059
147	35			11.88	1695		.00					14370		5442	1780	10277	1.832	.5993	.4719	3.05		.223	.636	.208	.055
148	36			11.66	1695		4.00					14380		6632	1976	10603	2.275	.6779	.4960	3.35		.221	.775	.231	.056
149	37			11.64	1682		8.00					14380		7594	2297	9633	2.610	.7893	.4514	3.30		.222	.901	.272	.052
150	38			11.86	1676	87	10.00					14380		7803	2603	8681	2.632	.8779	.3992	2.99		.225	.932	.311	.047
151	39			11.39	1677		12.00					14380		7455	2899	7547	2.618	1.0181	.3614	2.57		.221	.893	.347	.041
152	40		80	20.78	1712	86	-8.00					14400		3142	2505	17198	.605	.4822	.4515	1.25		.291	.359	.286	.089
153	41			20.70	1712		-4.00					14400		5085	2537	15903	.983	.4902	.4192	2.00		.290	.579	.289	.082
154	42			20.78	1712		.00					14400		6905	2733	13940	1.329	.5261	.3659	2.52		.291	.789	.312	.072
155	43			20.86	1713		4.00					14400		9007	2996	13083	1.727	.5745	.3421	3.00		.292	1.030	.344	.068
156	44			20.88	1694		8.00					14400		10469	3296	11929	2.006	.6314	.3116	3.17		.295	1.222	.384	.063
157	45			20.88	1703		10.00					14400		10875	3642	10973	2.083	.6977	.2867	2.98		.293	1.250	.419	.057
158	46			20.72	1720		12.00					14400		11024	3948	8760	2.128	.7622	.2306	2.79		.290	1.248	.447	.045
159	47			20.96	1345		-4.00					12730		3846	2275	12830	.734	.4342	.3339	1.69		.371	.705	.417	.107
160	48			20.86	1335		.00					12700		5684	2327	10160	1.090	.4462	.2657	2.44		.373	1.067	.437	.087
161	49			20.86	1336		4.00					12700		7485	2469	8738	1.435	.4734	.2285	3.03		.373	1.404	.463	.075
162	50			20.76	1329		8.00					12700		9019	2615	6336	1.738	.5039	.1665	3.44		.374	1.703	.494	.054
163	51	CALIBRATION																							
164	1	9	30	2.97	1711	86	-8.00	20	0	Off	30	14440	WC	2317	-778	8736	3.121	-1.0478	1.6044	-2.97	30.00	.110	.265	-.089	.045
165	2			2.88	1711	86	-4.00					14430		2645	-616	8629	3.674	-.8556	1.6343	-4.29		.108	.302	-.070	.045
166	3			2.94	1708	86	.00					14430		3012	-383	7743	4.098	-.5211	1.4366	-7.86		.110	.344	-.044	.040
167	4			2.94	1711	87	4.00					14430		3297	-154	7454	4.486	-.2095	1.3830	-21.40		.110	.377	-.018	.039
168	5			2.97	1707	87	8.00					14430		3683	43	7871	4.960	.0579	1.4455	85.65		.110	.423	.005	.041
169	6		60	5.34	1718	87	-8.00					14430		2294	-424	10000	1.718	-.3176	1.0215	-5.41		.147	.260	-.048	.052
170	7			5.28	1709	87	-4.00					14430		2848	-258	9789	2.158	-.1955	1.0113	-11.03		.147	.326	-.029	.051
171	8			5.19	1709	87	.00					14430		3407	-67	9950	2.626	-.0516	1.0457	-50.85		.146	.390	-.008	.052
172	9			5.28	1710	87	4.00					14430		3981	151	9602	3.016	.1144	.9920	26.36		.147	.455	.017	.050
173	10			5.21	1707	87	8.00					14430		4470	337	9930	3.432	.2587	1.0396	13.26		.146	.514	.039	.052
174	11			5.34	1710	87	10.00					14430		4394	424	18992	3.291	.3176	1.9401	10.36		.148	.503	.049	.099
175	12			5.24	1699	87	12.00					14430		4311	530	21369	3.291	.4046	2.4327	8.13		.147	.500	.061	.123

TABLE A-2
(Continued)
AMES TEST RESULTS

Point No. - Consecutive	Point No. - Per Run	Run No.	Tunnel Speed (V_o) - Knots	Tunnel Dynamic Pressure (q) - Lbs/sq.ft.	Fan Speed (N_p) - RPM	Tunnel Temp. °F	Angle of Attack (α_w) - Degrees	Exit Louver Angle (δ_e) - Degrees	Horizontal Tail Incidence Angle (i_t) - Degrees	Reaction Control Setting (RC) - CPS	Wing Flap Angle (δ_f) - Degrees	Rotor Speed ($P_{.83}$) - RPM	Exhaust Gas Temp. (EGT) - °F	Total Lift (L_T) - Lbs.	Total Drag (D_T) - Lbs.	Total Pitch Moment (C_{M_T}) - Ft. Lbs.	Lift Coefficient (C_L)	Drag Coefficient (C_D)	Pitch Moment Coefficient (C_M)	Lift To Drag Ratio (L_T/D_T)	Barometer In. Hg.	Velocity Ratio ($V_o/V_{.83}$)	Lift Coefficient (C_L)	Drag Coefficient (C_D)	Pitch Moment Coefficient (C_M)
176	13	9	40	5.09	1693	67	12.00	20	0	Off	30	14430	RC	4311	530	23369	3.291	.4046	2.4327	8.13	30.00	.146	.481	.088	.117
177	14		60	11.76	1726		-8.00	35				14450		1325	-340	15124	.451	-.1156	.7015	-3.89		.217	.149	-.038	.077
178	15			11.68	1728		-4.00					14450		2415	-260	15030	.827	-.0890	.7019	-9.28		.216	.270	-.029	.076
179	16			11.70	1722		.00					14450		3597	-123	14605	1.230	-.0421	.6809	-29.24		.217	.406	-.014	.075
180	17			11.78	1728		4.00					14450		4666	108	15321	1.584	.0367	.7095	43.20		.217	.522	.012	.078
181	18			11.70	1726		6.00					14450		5254	191	13885	1.796	.0653	.6473	27.50		.217	.590	.021	.071
182	19			11.66	1728		8.00					14450		5741	323	13680	1.969	.1108	.6403	17.77		.216	.646	.036	.070
183	20			11.96	1726		10.00					14450		6420	502	11286	2.147	.1679	.5148	12.78		.219	.721	.056	.057
184	21			11.55	1721		12.00					14440		6363	766	12299	2.204	.2653	.5808	8.30		.216	.719	.086	.063
185	22			11.45	1717		14.00					14450		5895	1033	11680	2.059	.3609	.5565	5.70		.216	.669	.117	.060
186	23		80	20.74	1725	86	-8.00					14470		983	482	19061	.190	.0930	.5013	2.03		.288	.111	.054	.097
187	24			20.76	1725		-4.00					14470		2928	538	18043	.564	.1037	.4741	5.44		.288	.328	.060	.092
188	25			20.74	1727		.00					14470		4737	672	16867	.914	.1296	.4436	7.04		.288	.531	.075	.086
189	26			20.74	1738		4.00					14470		6767	924	14787	1.305	.1782	.3889	7.32		.286	.748	.102	.074
190	27			20.84	1753		8.00					14470		8583	1299	13357	1.647	.2493	.3496	6.60		.285	.933	.140	.066
191	28			20.70	1754		10.00					14470		9154	1530	15004	1.769	.2957	.3954	5.98		.283	.934	.166	.074
192	29			20.59	1766		12.00					14470		9498	1792	16419	1.845	.3481	.4350	5.30		.281	1.016	.182	.080
193	30			20.55	1731		14.00					14230		9305	2155	15251	1.811	.4195	.4048	4.31		.286	1.036	.240	.077
194	31	CALIBRATION																							
195	1	10	40	6.13	0	66	-3.88	90	0	Off	30		NC	342	284	979	.223	.1858	.0826	1.20	30.03	NA	NA	NA	NA
196	2			6.13			.27							787	257	62	.514	.1702	-.0044	3.01					
197	3			6.18			4.42							1205	277	-828	.780	.1849	-.0882	4.21					
198	4			6.18			6.48							1401	296	-1077	.907	.1992	-.1126	4.55					
199	5			6.18			8.55							1604	314	-1222	1.038	.2133	-.1280	4.86					
200	6			6.13			10.56							1610	306	2285	1.051	.2099	.1830	5.00					
201	7			6.06			12.58							1662	411	1984	1.097	.2825	.1573	3.88					
202	8			6.01			14.54							1515	465	3395	1.008	.3189	.2885	3.16					
203	9	CALIBRATION																							
204	1	11	20	1.27	0	66	-3.94	90	0	Off	30	0	NA	38	44	-126	.120	.1387	-.0566	.86	30.03	NA	NA	NA	NA
205	2			1.31			.26							160	44	-292	.489	.1366	-.1312	3.57					
206	3			1.31			4.44							273	46	-431	.834	.1469	-.1954	5.67					
207	4			1.31			6.54							331	52	-612	1.011	.1683	-.2743	6.00					
208	5			1.31			8.62							379	59	-596	1.157	.1926	-.2704	6.00					
209	6			1.31			10.66							405	72	-634	1.237	.2341	-.2880	5.28					
210	7			1.31			12.68							415	97	-825	1.267	.3111	-.3681	4.07					

TABLE A-2
(Continued)
AMES TEST RESULTS

Point No. - Consecutive	Point No. - Per Run	Run No.	Tunnel Speed (V_∞) - Knots	Tunnel Dynamic Pressure (q) - lbs/sq.ft.	Fan Speed (N_p) - RPM	Tunnel Temp. °F	Angle of Attack (α_w) - degrees	Exit Louver Angle (δ) - degrees	Horizontal Tail Incidence Angle (i_t) - degrees	Reaction Control Setting (RC) - CPR	Wing Flap Angle (i_{wf}) - degrees	Engine Speed (N_{25}) - RPM	Ambient Gas Temp. (AGT) - °F	Total Lift (L_w) - lbs.	Total Drag (D_w) - lbs.	Total Pitch Moment (M_w) - Ft. lbs.	Lift Coefficient (C_L)	Drag Coefficient (C_D)	Pitch Moment Coefficient (C_M)	Lift To Drag Ratio (L_w/D_w)	Barometer In. Hg.	Velocity Ratio ($V_\infty/\sqrt{\theta}$ kts)	Lift Coefficient (C_L)	Drag Coefficient (C_D)	Pitch Moment Coefficient (C_M)
211	8	11	20	1.27	0	66	14.65	90	0	Off	30	0	NA	386	121	-1169	1.216	.3948	-.5243	3.07	30.03	NA	NA	NA	NA
212	9		40	5.93		65	-3.96							113	197	+452	.076	.1329	-.0431	.57					
213	10			5.26			.23							575	177	-791	.437	.1364	-.0905	3.20					
214	11			5.26			4.44							1092	200	-1443	.830	.1585	-.1657	5.23					
215	12			5.26			6.53							1320	226	-1671	1.004	.1812	-.1928	5.53					
216	13			5.26			8.64							1567	248	-1861	1.192	.2018	-.2161	5.90					
217	14			5.21			10.74							1819	281	-2931	1.383	.2315	-.3308	5.97					
218	15			5.13			12.78							1917	356	-2925	1.472	.2935	-.3348	5.91					
219	16			11.70		64	14.81							1950	425	-2453	1.520	.3529	-.2903	4.30					
220	17		60	11.78			-3.97							161	417	-611	.055	.1426	-.0296	.38					
221	18			11.70			.23							1283	408	-2921	.436	.1403	-.1437	3.10					
222	19			11.62			4.42							2316	446	-2591	.792	.1583	-.1362	5.00					
223	20			11.82			6.52							2859	498	-3090	.984	.1804	-.1641	5.45					
224	21			11.86			8.63							3485	574	-3547	1.179	.2072	-.1866	5.69					
225	22			11.82			10.72							4011	642	-4230	1.353	.2335	-.2208	5.79					
226	23			11.66			12.80							4448	749	-4521	1.505	.2745	-.2379	5.48					
227	24			20.86			14.76							4168	930	-5164	1.430	.3381	-.2693	4.23					
228	25		80	20.86			-3.97							327	759	-1112	.063	.1456	-.0303	.43					
229	26			20.86			.23							2204	722	-3251	.423	.1401	-.0932	3.01					
230	27			20.84			4.43							4185	805	-4784	.802	.1604	-.1407	5.00					
231	28			20.84			6.52							5116	901	-5496	.982	.1819	-.1629	5.39					
232	29			20.63			8.62							6095	995	-6202	1.170	.2037	-.1850	5.74					
233	30			20.63			10.72							6988	1117	-6623	1.355	.2337	-.2014	5.79					
234	31			20.51			12.79							7689	1315	-7259	1.491	.2756	-.2209	5.40					
235	32			20.51			-							7952	1594	-8237	-	-	-	-					
236	33			20.51			15.80							7744	1758	-9086	1.510	.3641	-.2710	4.14					
237	34	CALIBRATION																							
238	1	12	20	1.27	2540	76	-2.00	3	21	145	30	16520	NC	6654	-84	1649	20.957	-.2646	.7083	-79.21	29.88	NC	NC	NC	NC
239	2			1.41	2535	78	-5.00					16530		6459	-380	368	18.323	-1.0780	.1425	-16.99					
240	3			1.41	2534		-5.00	-1				16510		6487	-13	-485	18.403	-.0369	-.1877	499.00					
241	4			1.23	2528	81	-2.00					16530		6490	300	-62	21.106	.9756	-.0273	21.63					
242	5			1.27	2528	82	.00					16500		6540	596	137	20.598	1.8772	.0589	10.97					
243	6		30	3.01	2540	84	-5.00					16510		6844	362	-1068	9.095	.4811	-.1936	18.90					
244	7			3.03	2453	85	-5.00	3				16380		6383	-37	611	8.426	-.0488	.1100	-172.51					
245	8			2.96	2444	86	-2.00					16380		6561	301	295	8.866	.4068	.0545	21.79					

TABLE A-2
(Continued)
AMES TEST RESULTS

Point No. - Consecutive	Point No. - Per Run	Run No.	Tunnel Speed (V_o) - Knots	Tunnel Dynamic Pressure (q) - Lbs/sq.ft.	Fan Speed (N_{FS}) - RPM	Tunnel Temp °F	Angle of Attack (α_w) - degrees	Exit Louver Angle - degrees	Horizontal Tail Incidence Angle (i_t) - degrees	Reaction Control Setting, CPS	Wing Flap Angle (δ_{FW}) - degrees	Engine Speed (N_{ENG}) - RPM	Exhaust Gas Temp. (EGT) - °F	Total Lift (L_T) - Lbs.	Total Drag (D_T) - Lbs.	Total Pitch Moment (M_T) - Ft. Lbs.	Lift Coefficient (C_L)	Drag Coefficient (C_D)	Pitch Moment Coefficient (C_M)	Lift To Drag Ratio C_L/C_D	Barometer In. Hg.	Velocity Ratio $V_o/\sqrt{kq}$	Lift Coefficient (C_L)	Drag Coefficient (C_D)	Pitch Moment Coefficient (C_M)
246	9	12	30	2.90	2445	87	2.00	3	21	0-145	30	16370	NC	6738	793	171	9.294	1.0938	.3229	8.49	29.88	NC	NC	NC	NC
247	10			3.01	2437	88	-5.00	10				16370		6016	-667	4480	7.995	-.8864	.8119	-9.01					
248	11			3.19	2434		-5.00	20				16380		6656	-1586	15147	8.346	-1.9887	2.5900	-4.19					
249	12			3.07	2430	90	-5.00		18			16380		6029	-110	1562	7.855	-.1433	.2775	-54.80					
250	13			3.07	2423		-5.00		14			16380		6104	-78	1792	7.953	-.1016	.3183	-78.25					
251	14			1.76	2425	91	-5.00	3	21			16370		5884	-582	406	13.373	-.8682	.1241	-15.60					
252	15		60	5.21	2422	92	-5.00					16360		6576	364	174	5.049	.2795	.0182	18.06					
253	16			5.24	2411	93	-5.00	8		165		16380		6475	-77	889	4.943	-.0588	.0925	-84.09					
254	17			5.24	2412	94	-2.00					16380		6904	280	1195	5.270	.2137	.1244	24.63					
255	18			5.24	2414		2.00					16370		7362	749	3080	5.620	.5718	.3206	9.82					
256	19			5.24	2410		-5.00	0				16370		6614	668	-990	5.049	.5099	-.1031	9.91					
257	20			5.36	2404	95	-5.00	20				16380		5972	756	-53923	4.473	.5663	-5.5082	7.89					
258	21		30	2.98	2403	96	-5.00	8				16370		5872	-489	1877	7.935	-.6608	.3459	-12.00					
259	22		50	8.24	2401	97	-5.00					16370		6933	454	-701	3.366	.2204	-.0464	15.27					
260	23		60	11.68	2403		-5.00					16370		7494	959	-2866	2.566	.3284	-.1339	7.81					
261	24			11.74	2354	98	-5.00	17	20	155		16300		6559	100	650	2.235	.0341	.0302	65.59					
262	25			11.76	2357		-2.00					16310		7364	427	3050	2.505	.1452	.1415	17.24					
263	26			11.68	2357		2.00					16300		8430	846	5070	2.887	.2897	.2368	9.96					
264	27			11.68	2359	99	-5.00	10				16300		7011	760	-727	2.401	.2603	-.0340	9.22					
265	28			11.57	2349		-5.00	25				16290		5817	-687	3089	2.011	-.2375	.1456	-8.46					
266	29		50	11.45	2376		-5.00	17				16290		4673	-1391	4561	1.632	-.4859	.2173	-3.35					
267	30		70	8.24	2440	100	-5.00					16300		6194	-371	1338	3.007	-.1801	.0886	-16.69					
268	31		80	16.01	2350	101	-5.00					16310		6950	647	-1410	1.736	.1616	-.0480	10.74					
269	32			20.74	2362		-5.00	26				16300		7363	1218	-3298	1.420	.2349	-.0867	6.04					
270	33			20.74	2397		-5.00		18			16400		6505	258	347	1.255	.0498	.0091	25.21					
271	34			20.55	2393		-2.00					16410		7971	488	137	1.552	.0950	.0036	16.33					
272	35			20.74	2397		2.00	20				16410		9707	1000	4804	1.872	.1929	.1264	9.70					
273	36			20.92	2409		-5.00					16400		7255	829	-1412	1.387	.1585	-.0368	8.75					
274	37			20.74	2409		-5.00	35				16400		5433	-463	2108	1.048	-.0893	.0554	-11.73					
275	38		90	15.99	2392		-5.00	26				16410		6127	-315	3285	1.533	-.0788	.1121	-19.45					
276	39		70	26.73	2400	102	-5.00					16410		7006	816	-2343	1.048	.1221	-.0478	8.58					
277	40		100	33.01	2437		-2.00	40	13			16410		7490	485	-318	.908	.0588	-.0053	15.44					
278	41	CALIBRATION																							
279	1	13	60	11.70	0	58	-3.96	90	0	OFF	30	0	NA	229	478	730	.078	.1635	.0325	.47	30.00	NA	NA	NA	NA
280	2			11.66			.23							1243	470	-97	.426	.1629	-.0128	2.61					

TABLE A-2
(Continued)
AMES TEST RESULTS

Point No. - Consecutive	Point No. - Per Run	Run No.	Tunnel Speed (V_o) - Knots	Tunnel Dynamic Pressure (q) - Lbs/Sq.ft.	Fan Speed (N_p) - RPM	Tunnel Temp. °F	Angle of Attack (α) - degrees	Exit Louver Angle (δ) - degrees	Horizontal Tail Incidence Angle (i_t) - degrees	Reaction Control Setting (RC) - GM	Wing Flap Angle (δ_f) - degrees	Engine Speed (N_{gg}) - RPM	Exhaust Gas Temp. (EGT) - °F	Total Lift (C_L) - Lbs.	Total Drag (C_D) - Lbs.	Total Pitch Moment (C_M) - Ft. Lbs.	Lift Coefficient (C_L)	Drag Coefficient (C_D)	Pitch Moment Coefficient (C_M)	Lift To Drag Ratio (C_L/C_D)	Barometer In. Hg.	Velocity Ratio (V_o/V_{ref})	Lift Coefficient (C_L)	Drag Coefficient (C_D)	Pitch Moment Coefficient (C_M)
281	3	13	60	11.66	0	58	4.41	90	0	Off	30	0	NA	2258	507	-865	.775	.1795	-.0555	4.31	30.00	NA	NA	NA	NA
282	4			11.66			6.51							2803	548	-1341	.962	.1966	-.0814	4.89					
283	5			11.53			8.61							3288	594	-1637	1.141	.2182	-.0996	5.22					
284	6			11.53			10.71							3823	668	-2005	1.326	.2481	-.1206	5.34					
285	7			11.53			12.78							4206	766	-2443	1.459	.2855	-.1439	5.11					
286	1	14	0	.16	2600	52	0.00	10	0	Off	30	16460	1190	6878	-1193	6890	NA	NA	NA	NA	30.04	NC	NC	NC	NC
287	2			.20	2620			15				16460	1200	6572	-1774	7679									
288	3			0	2610			5				16460	1205	6969	-542	4941									
289	4			.30	2620	54		0				16480	1210	6916	-354	1091									
290	5			.08	2580	55		10				16310	1140	6635	-1228	8733									
291	1	15	20	1.31	1720	67		0	0	Off	0	14260	NC	2939	411	3858	8.974	1.2550	1.6065	7.15	30.02	.071	.320	.045	.019
292	2			1.35	1716				4			14260		2923	430	3704	8.661	1.2741	1.4966	6.79		.073	.321	.047	.018
293	3			1.35	1714				8			14270		2962	439	3280	8.776	1.3007	1.3254	6.74		.073	.327	.048	.016
294	4			1.33	1712	68			12			14270		2979	444	2711	8.959	1.3353	1.1120	6.70		.072	.329	.049	.014
295	5			1.35	1711	69			16			14270		3035	440	1604	8.993	1.3037	.6480	6.89		.073	.335	.049	.008
296	6			1.27	2240	70			0			15790		4910	480	5081	15.465	1.5118	2.1824	10.22		.054	.320	.031	.015
297	7			1.27	2501	72						16350		6112	531	6631	19.250	1.6724	2.8481	11.51		.049	.320	.028	.016
298	8			1.39	1686	76		20				14220		2561	-593	7700	7.370	-1.7065	3.0218	-4.31		.073	.273	-.063	.037
299	9			1.43	1715	77		35				14190		1870	-1212	9430	5.231	-	-	-		.078	-	-	-
300	10		30	2.94	2397	78		0				16170		5765	820	8038	7.844	1.1156	1.4913	7.03		.078	.333	.047	.021
301	11			2.97	2389	80		20				16180		5390	-1120	12622	7.259	-1.5084	2.3182	-4.81		.079	.314	-.065	.033
302	12			3.13	2430	81		35				16180		4071	-2442	18908	5.203	-3.1208	'3.2951	-1.66		.080	.231	-.138	.049
303	13		40	5.21	1700	82		0				14820		3373	956	8951	2.590	.7340	.9.71	3.52		.146	.388	.011	.047
304	14			5.28	1694			20				14820		2857	-90	11273	2.164	-.0682	1.1646	-31.74		.148	.332	-.011	.060
305	15			5.30	1773			35				14320		2024	-757	12582	1.528	-.5713	1.2949	-2.67		.147	.231	-.086	.065
306	16		60	11.70	1649			0				14130		3996	1661	14180	1.366	.5679	.6611	2.40		.229	.501	.208	.081
307	17			11.72	1648			20				14200		2931	623	16161	1.000	.2126	.7522	4.70		.227	.362	.077	.091
308	18			11.72	1634			35				14180		2138	-92	16094	.730	-.0314	.7491	-23.23		.226	.262	-.011	.090
309	19		80	20.63	1666	83		0				14200		4653	2513	19202	.902	.4873	.5077	1.85		.303	.578	.312	.100
310	20			20.92	1677			20				14210		3404	1367	21[illegible]	.651	.2614	.5480	2.49		.299	.406	.163	.114
311	21			20.70	1650			35				14200		2436	577	19674	.471	.1115	.5184	4.22		.302	.300	.071	.110
312	22			20.84	1700			40				14170		2024	398	18246	.388	.0764	.4776	5.08		.294	.235	.046	.096
313	23			20.72	1730			45				14170		1586	256	16245	.306	.0498	.4277	6.14		.288	.177	.029	.083
314	24			20.74	1760			49				14150		1311	213	14444	.253	.0411	.3799	6.15		.283	.142	.023	.071
315	25	CALIBRATION																							

TABLE A-2
(Continued)
AMES TEST RESULTS

Point No. - Consecutive	Point No. - Per Run	Run No.	Tunnel Speed (V_∞) - Knots	Tunnel Dynamic Pressure (q) - Lbs/sq.ft.	Fan Speed (N_F) - RPM	Tunnel Temp. °F	Angle of Attack (α_T) - degrees	Exit Louver Angle (LE) - degrees	Tail Incidence Angle (i_t) - degrees	Reaction Control Setting (RCS) - CPS	Flap Flap Angle (δ_f) - degrees	Engine Speed (N_{gg}) - RPM	Exhaust Gas Temp. (EGT) - °F	Total Lift (L_T) - Lbs.	Total Drag (D_T) - Lbs.	Total Pitch Moment (M_T) - Ft. Lbs.	Lift Coefficient (C_L)	Drag Coefficient (C_D)	Pitch Moment Coefficient (C_M)	Lift To Drag Ratio (L_T/D_T)	Barometer In. Hg.	Velocity Ratio (V_∞/V_{EJ})	Lift Coefficient (Ω_L)	Drag Coefficient (Ω_D)	Pitch Moment Coefficient (Ω_M)
316	1	16	20	1.27	1690	78	+4.00	0	0	Off	30	14230	NC	1414	-835	64887	4.4 4	-2.6299	27.8696	-1.69	30.06	.072	-	-	-
317	2			1.23	1694	79	+2.00					14240		2846	304	3882	9.155	.9886	1.7218	9.36		.071	.325	.035	.020
318	3			1.25	1686	80	.00					14250		2849	378	3691	9.117	1.2096	1.6108	7.53		.072	.333	.044	.019
319	4			1.23	1681	81	2.00					14280		2828	458	3619	9.19	1.6894	1.6050	6.17		.072	.329	.053	.019
320	5			1.25	1681	82	4.00					14240		2850	556	3454	9.120	1.7792	1.5072	5.12		.072	.333	.065	.018
321	6			1.25	1678	83	6.00					14240		2868	668	3413	9.17	2.1376	1.4894	4.29		.072	.335	.078	.018
322	7			1.27	1678		8.00					14240		2958	846	3142	9.31	2.6646	1.3497	3.49		.073	.347	.099	.017
323	8			1.27	1673		10.00					14280		3024	962	3120	9.524	3.0299	1.3400	3.14		.073	.361	.115	.017
324	9			1.27	1671	84	12.00					14240		2988	1024	3223	9.411	3.2252	1.3844	2.91		.073	.357	.122	.017
325	10			1.25	1674	85	14.00					14240		3012	1164	3157	9.638	3.7248	1.3776	2.58		.073	.359	.139	.017
326	11		30	2.99	1672	86	+8.00					14260		2605	323	5695	3.485	.4321	1.0389	8.06		.113	.311	.039	.031
327	12			2.92	1670	87	+4.00					14250		2894	435	5545	1.964	.5959	1.0359	6.65		.111	.345	.052	.030
328	13			2.92	1674		.00					14260		3164	672	6140	4.334	.9205	1.1470	4.70		.111	.378	.080	033
329	14			2.94	1668	88	4.00					14250		3371	871	5716	4.586	1.1850	1.0605	3.87		.112	.406	.105	.031
330	15			3.07	1672		6.00					14240		3548	1020	5656	4.623	1.3290	1.0050	3.47		.114	.403	.116	.029
331	16			3.07	1669		8.00					14250		3600	1126	5806	4.691	1.4671	1.0316	3.19		.114	.409	.128	.030
332	17			3.07	1672		10.00					14260		3717	1250	5515	4.843	1.6287	.9800	2.97		.112	.422	.142	.028
333	18			2.92	1669		12.00					14250		3771	1354	5140	5.166	1.8548	.9603	2.78		.119	.454	.163	.028
334	19			2.92	1668	89	14.00					14250		3843	1511	4793	5.264	2.0699	.8953	2.54		.112	.462	.182	.026
335	20		40	5.17	1668		+8.00					14250		2651	667	8000	2.051	.5161	.8724	3.97		.149	.318	.080	.045
336	21			5.21	1668		+4.00					14270		3242	770	8215	2.489	.5912	.8601	4.21		.150	.390	.092	.045
337	22			5.17	1667	90	.00					14250		3761	965	8211	2.910	.7466	.8663	3.89		.150	.454	.116	.045
338	23			5.21	1670		4.00					14260		4190	1182	8666	3.217	.9075	.9074	3.54		.150	.511	.144	.048
339	24			5.21	1667		8.00					14270		4687	1427	7774	3.598	1.0956	.8139	3.28		.150	.566	.172	.043
340	25			5.21	1666		10.00					14270		4676	1522	12083	3.590	1.1685	1.2651	3.07		.150	.567	.185	.066
341	26			5.17	1645		12.00					14270		4668	1734	11582	3.612	1.3416	1.2220	2.69		.151	1578	.215	.065
342	27		60	11.68	1684	91	+8.00					14290		2756	1505	13383	.944	.5154	.6250	1.83		.222	.328	.179	.072
343	28			11.64	1676		+4.00					14290		3948	1598	13836	1.357	.5491	.6484	2.47		.223	.473	.191	.075
344	29			11.68	1670	92	.00					14280		5119	1759	13200	1.753	.6024	.6165	2.91		.224	.617	.212	.072
345	30			11.64	1676		4.00					14280		6188	1979	13882	2.126	.6801	.6505	3.12		.223	.742	.237	.075
346	31			11.64	1666		8.00					14290		7204	2284	13591	2.476	.7849	.6369	3.15		.225	.77	.278	.075
347	32			11.64	1634		10.00					14290		7445	2549	13929	2.558	.8759	.6527	2.92		.226	.918	.314	.078
348	33			11.66	1651		12.00					14290		7542	2759	13139	2.587	.9465	.6147	2.73		.228	.441	.344	.074
349	34		80	20.72	1688	93	+4.00					14300		4758	2569	19431	.919	.4959	.5115	1.85		.296	.465	.305	.106
350	35			20.65	1686		.00					14300		6523	2718	18653	1.264	.5265	.4927	2.40		.296	.775	.323	.100

TABLE A-2
(Continued)
AMES TEST RESULTS

Point No. - Consecutive	Point No. - Per Run	Run No.	Tunnel Speed (V_∞) - Knots	Tunnel Dynamic Pressure (q) - Lbs/sq.ft.	Fan Speed (n_{FS}) - RPM	Tunnel Temp. °F	Angle of Attack (α_s) - degrees	Exit Louver Angle (δ_e) - degrees	Horizontal Tail Incidence Angle (i_t) - degrees	Reaction Control Setting (RCS) - CPS	Wing Flap Angle (δ_f) - degrees	Engine Speed (n_{RPM}) - RPM	Exhaust Gas Temp. (EGT) - °F	Total Lift (L_T) - Lbs.	Total Drag (D_T) - Lbs.	Total Pitch Moment (M_{CG_T}) - Ft. Lbs.	Lift Coefficient (C_L)	Drag Coefficient (C_D)	Pitch Moment Coefficient (C_M)	Lift To Drag Ratio (C_L/C_D)	Barometer In. Hg.	Velocity Ratio (V_e/V_∞)	Lift Coefficient (C_L)	Drag Coefficient (C_D)	Pitch Moment Coefficient (C_M)
351	36	16	80	20.72	1690	93	4.00	0	0	Off	30	14300	RC	8481	2965	18960	1.037	.5724	.4991	2.86	30.06	.295	1.002	.351	.101
352	37			20.78	1670		8.00					14300		9975	3221	17997	1.920	.6200	.4724	3.09		.299	1.206	.389	.098
353	38			20.67	1682		10.00					14300		10549	3580	17630	2.041	.6928	.4653	2.94		.296	1.257	.427	.095
354	39			20.70	1691		12.00					14300		10522	3837	15288	2.033	.7414	.4029	2.74		.295	1.243	.454	.082
355	40	CALIBRATION																							
356	1	17	0	0	0	0	0.00	90	0	0-47	30	0	NA	17	0	-455	NA	NA	NA	NA	30.06	NA	NA	NA	NA
357	2									83				46		-1218									
358	3									118				86	-1	-2333									
359	4									140				124	-2	-3274									
360	5									160				168	-4	-4484									
361	6									0-65				-33	-2	657									
362	7									92				-54		1274									
363	8									110				-77	-1	1960									
364	9									138				-121		3007									
365	10									153				-155	-1	3915									
366	11									165				-181	-1	4577									
367	1	18	40	5.26	0	78	.25	90	0	0	30	0	NA	614	200	-311	.467	.1541	-.0413	3.03	30.06	NA	NA	NA	NA
368	2			5.21			.27		4					663	198	-1188	.509	.1544	-.1342	3.29					
369	3			5.24			.29		8					715	206	-2265	.546	.1600	-.2464	3.41					
370	4			5.32			.32		12					791	221	-3747	.595	.1695	-.3958	3.51					
371	5			5.30		77	.33		14					831	221	-4315	.627	.1705	-.4563	3.67					
372	6			5.32			.34		16					843	227	-4574	.634	.1744	-.4813	3.63					
373	7			5.30			.36		18					884	238	-5423	.667	.1838	-.5710	3.63					
374	8			5.26			.37		20					901	247	-5948	.685	.1922	-.6301	3.56					
375	9			5.24			.37		22					900	253	-6164	.687	.1975	-.6550	3.47					
376	10			5.21			.33		24					801	276	-4238	.615	.2154	-.4556	2.85					
377	11			5.28		76	.25		0					626	203	-419	.474	.1559	-.0524	3.04					
378	12			5.26			.22			0-75				555	208	1069	.422	.1598	.1027	2.64					
379	13			5.24			.21			110				504	211	2091	.385	.1624	.2102	2.36					
380	14			5.21			.18			140				431	215	3525	.331	.1661	.3626	1.99					
381	15			5.21			.16			163				380	211	4911	.292	.1628	.5085	1.79					
382	16			5.24			.26			0-75				644	204	-1214	.492	.1580	-.1359	3.11					
383	17			5.24			.28			110				695	208	-2344	.531	.1614	-.2543	3.28					
384	18			5.24		75	.31			140				757	209	-3671	.578	.1626	-.3934	3.55					
385	19			5.26			.33			164				802	208	-5061	.610	.1616	-.5367	3.77					

Table A-2
(Continued)
AMES TEST RESULTS

Point No. - Consecutive	Point No. - Per Run	Run No.	Tunnel Speed (P_{t_2}) - Knots	Tunnel Dynamic Pressure (q) - Lbs/sq.ft.	Fan Speed (N_2) - RPM	Tunnel Temp. °F	Angle of Attack (α_w) - degrees	Exit Louver Angle (δ_e) - degrees	Horizontal Tail Incidence Angle (i_t) - degrees	Reaction Control Setting (RC) - CPR	Wing Flap Angle (δ_f) - degrees	Engine Speed (N_{2E}) - RPM	Exhaust Gas Temp. (EGT) - °F	Total Lift (L_T) - Lbs.	Total Drag (D_T) - Lbs.	Total Pitch Moment (M_T) - Ft. Lbs.	Lift Coefficient (C_L)	Drag Coefficient (C_D)	Pitch Moment Coefficient (C_M)	Lift To Drag Ratio (L_T/D_T)	Barometer In. Hg.	Velocity Ratio (V_e/V_{sub})	Lift Coefficient (C_L)	Drag Coefficient (C_D)	Pitch Moment Coefficient (C_M)
386	20	18	60	5.30	0	75	.34	90	4	0-164	30	0	NA	847	214	-	.6 9	.1653	-.6644	3.86	30.06	NA	NA	NA	NA
387	21			5.30			.32		0	158				786	212	-4874	.593	.1633	-.5131	3.61					
388	22			5.30			.36		8	158				896	219	-7032	.676	.1695	-.7369	3.98					
389	23			5.32			.39		12	158				973	232	-8447	.732	.1794	-.8803	4.07					
390	24			5.21			.41		16	158				995	234	-9171	.76	.1851	-.9750	4.12					
391	25			5.24		74	.57		0	0-160				394	214	-4598	.301	.1640	.4730	6.12					
392	26			5.24			.59		4					446	214	3502	.34	.1650	.3640	6.33					
393	27			5.24			.61		8					497	221	2568	.32	.1700	.2600	6.33					
394	28			5.24			.24		12					591	227	1094	.451	.1752	.1052	2.57					
395	29			5.21			.25		16					617	236	266	.474	.1833	.0186	2.58					
396	30			5.24		73	.30		20					733	263	-1750	.560	.2037	-.1931	2.74					
397	31			5.24			.30		22					745	271	-2164	.569	.2099	-.2363	2.71					
398	32			5.19			.29		24					699	309	-1542	.539	.2408	-.1725	2.23					
399	33		60	11.94			-8.13		0	Off				-744	526	771	-.249	.1768	.0400	-1.41					
400	34			11.76			-3.95							276	464	125	.094	.1579	.0040	.59					
401	35			11.74			.24							1299	456	-305	.443	.1572	-.0228	2.81					
402	36			11.76			.25		4					1389	463	-2643	.472	.1596	-.1318	2.96					
403	37			11.74			.27		8					1508	472	-4939	.514	.1633	-.2395	3.14					
404	38			11.70			.31		12					1677	492	-8099	.573	.1713	-.3887	3.34					
405	39			11.72			.32		16					1765	510	-9944	.602	.1774	-.4745	3.39					
406	40			11.76			.34		18					1863	539	-11860	.634	.1871	-.5624	3.38					
407	41			11.74			.35		20					1936	559	-13163	.660	.1945	-.6244	3.39					
408	42			11.62		72	.35		22					1909	602	-12613	.657	.2112	-.6048	3.11					
409	43			11.72			4.43		0					2343	502	-699	.800	.1773	-.0480	4.51					
410	44			11.68			8.61							3354	602	-1770	1.149	.2184	-.	5.25					
411	45			11.76			10.69							3822	697	-2188	1.300	.2528	-.1267	5.14					
412	46			11.64			12.76							4137	788	-2279	1.422	.2896	-.1344	4.90					
413	47			11.68			14.80							4379	933	-2190	1.500	.3404	-.1314	4.40					
414	48	CALIBRATION																							
415	1	19	20	1.37	0	72	.20	90	0	Off	30	0	NA	131	46	-35	.382	.1357	-.0215	2.81	30.06	NA	NA	NA	NA
416	2			1.41			.27		4					176	49	-358	.499	.1413	-.1482	3.53					
417	3			1.33			.26		8					164	48	-533	.493	.1466	-.2281	3.36					
418	4			1.27			.30		12					178	47	-890	.561	.1510	-.3931	3.71					
419	5			1.27			.31		16					184	47	-1028	.580	.1512	-.4527	3.83					
420	6			1.29			.31		18					188	54	-1068	.583	.1706	-.4629	3.41					

TABLE A-2
(Continued)
AMES TEST RESULTS

Point No. - Consecutive	Point No. - Dot Dia.	Run No.	Tunnel Speed (V_∞) - Knots	Tunnel Dynamic Pressure, (q) - Lbs/Sq.Ft.	Fan Speed (N_{FS}) - RPM	Tunnel Temp. °F	Angle of Attack (α_w) - degrees	Exit Louver Angle (δ) - degrees	Horizontal Tail Incidence Angle (i_t) - degrees	Emission Control Setting (EC) - CPR	Wing Flap Angle (δ_F) - degrees	Engine Speed (N_{2D}) - RPM	Exhaust Gas Temp. (EGT) - °F	Total Lift (L_T) - Lbs.	Total Drag (D_T) - Lbs.	Total Pitch Moment (M_{CG_T}) - Ft. Lbs.	Lift Coefficient (C_L)	Drag Coefficient (C_D)	Pitch Moment Coefficient (C_M)	Lift To Drag Ratio (L_T/D_T)	Barometer In. Hg.	Velocity Ratio (V_∞/V_{Jet})	Lift Coefficient (C_L)	Drag Coefficient (C_D)	Pitch Moment Coefficient (C_M)
421	7	19	20	1.27	0	72	.32	90	20	Off	30	0	NA	192	59	-1018	.605	.1892	-.4490	3.19	30.06	NA	NA	NA	NA
422	8			1.29			.31		22					189	60	-914	.586	.1892	-.3979	3.09					
423	9			1.31			.31		24					189	61	-911	577	.1896	-.3907	3.04					
424	10			2.97	1690	92	10.34		0					3265	1007	5114	4.397	1.5361	.8539	2.86					
425	1	20	20	1.27	2414	74	-4.00	0	25	0-100	40	16180	NC	6051	48	1282	1^.058	.1512	.5507	126.06	30.02	NC	NC	NC	NC
426	2		30	2.96	2420		-4.00		25	100		16170		6637	464	1833	5.939	.6249	.3366	14.30					
427	3			3.00	1727	77	-8.00		0	0		14340		3006	286	5868	3.995	.3801	1.0633	10.51		.107	.312	.030	.028
428	4			2.97	1710		-4.00					14360		3238	491	5754	4.361	.6613	1.0567	6.59		.108	.355	.054	.029
429	5			2.92	1710		.00					14340		3514	690	5020	4.814	.9452	.9377	5.09		.107	.385	.076	.025
430	6			2.92	1700	72	4.00					14350		3770	944	4715	5.164	1.2932	.8807	3.99		.107	.413	.103	.023
431	7			2.97	1707		6.00					14350		3950	1088	4582	5.320	1.4653	.8416	3.63		.108	.433	.119	.023
432	8			2.99	1714		8.00					14340		4073	1238	4649	5.449	1.6562	.8481	3.29		.108	.444	.135	.023
433	9			2.97	1712		10.00					14360		4119	1355	4732	5.547	1.8249	.8690	3.04		.108	.444	.146	.023
434	10			2.92	1710	74	12.00					14340		4189	1467	4446	5.738	2.0096	.8306	2.85		.107	.459	.161	.022
435	11		40	5.26	2400		-6.00	7	25	145		16220		6666	39	558	5.069	.0297	.0579	170.92		-	NC	NC	NC
436	12			5.15	1700	76	-8.00	0	0	0		14380		3082	644	7413	2.394	.5002	.7852	4.78		.143	.342	.072	.037
437	13			5.28	1698		-4.00					14380		3637	851	7518	2.755	.6447	.7767	4.27		.145	.406	.095	.038
438	14			5.17	1694	82	.00					14320		4036	1021	7291	3.123	.7899	.7693	3.95		.144	.454	.115	.037
439	15			5.13	1695		4.00					14380		4578	1256	6866	3.570	.9793	.7301	3.64		.143	.511	.140	.035
440	16			5.13	1696		6.00					14320		4747	1382	6385	3.701	1.0776	.6790	3.43		.143	.530	.154	.032
441	17			5.24	1698		8.00					14380		5084	1536	6387	3.881	1.1725	.6649	3.31		.144	.564	.171	.032
442	18			5.13	1695		10.00					14320		5216	1664	6244	4.067	1.2975	.6639	3.13		.143	.583	.186	.032
443	19			5.08	1678		12.00					14380		5400	1884	6110	4.277	1.4923	.6600	2.86		.144	.622	.217	.032
444	20		50	8.24	2404	83	-6.00	7	25	150		16250		7129	2533	-58100	3.461	1.2296	-3.8462	2.81		NC	NC	NC	NC
445	21		60	11.66	2406	86	-6.00	7	25	150		16240		7687	1061	-2876	2.633	.3634	-.1343	7.24					
446	22			11.72	2321		-6.00	17	24	150		16110		6586	79	611	2.248	.0270	.0285	83.36					
447	23			11.60	1698		-8.00	0	0	0		14340		3242	1564	13167	1.108	.5347	.6139	2.07		.216	.363	.175	.067
448	24			11.72	1693		-4.00					14340		4447	1664	12570	1.518	.5679	.5850	2.67		.223	.530	.198	.068
449	25			11.70	1693		.00					14340		5521	1854	11709	1.888	.6338	.5459	2.97		.217	.625	.209	.060
450	26			11.66	.688		4.00					14340		6679	2112	11437	2.291	.7245	.5350	3.16		.217	.758	.240	.059
451	27			11.70	1692		6.00					14350		7195	2255	11155	2.460	.7709	.5201	3.19		.217	.814	.255	.057
452	28			11.68	1686		8.00					14340		7740	2408	10334	2.651	.8247	.4826	3.21		.218	.884	.275	.073
453	29			11.66	1680		10.00					14350		7644	2706	15257	2.622	.9283	.7138	2.82		.218	.875	.310	.078
454	30			11.74	1675		12.00					14360		7731	3059	14974	2.634	1.0422	.6957	2.52		.220	.895	.354	.078
455	31		70	16.00	2319		-6.00	17	24	150		16120		6912	691	-1244	1.729	.1729	-.0424	10.00		NC	NC	NC	NC

TABLE A-2
(Continued)
AMES TEST RESULTS

Point No. - Consecutive	Point No. - Per Run	Run No.	Tunnel Speed (V_o) - Knots	Tunnel Dynamic Pressure (q) - Lbs/Sq. Ft.	Fan Speed (N_{FS}) - RPM	Tunnel Temp. °F	Angle of Attack (α_c) - degrees	Exit Louver Angle (δ_E) - degrees	Horizontal Tail Incidence Angle (i_t) - degrees	Reaction Control Setting (RCS) - CPR	Wing Flap Angle (δ_F) - degrees	Engine Speed (N_{ES}) - RPM	Exhaust Gas Temp. (EGT) - °F	Total Lift (L_T) - Lbs.	Total Drag (D_T) - Lbs.	Total Pitch Moment (M_T) - Ft. Lbs.	Lift Coefficient (C_L)	Drag Coefficient (C_D)	Pitch Moment Coefficient (C_M)	Lift To Drag Ratio (C_L/C_D)	Barometer In. Hg.	Velocity Ratio ($V_o/\sqrt{\theta}$)	Lift Coefficient (C_L)	Drag Coefficient (C_D)	Pitch Moment Coefficient (C_M)
456	32	20	80	20.78	2323	86	-6.00	17	24	0-150	40	16120	NC	7479	1272	-4439	1.442	.2453	-.1167	5.88	30.02	NC	NC	NC	NC
457	33			20.70	2303		-5.00	28	20	150		16120		6498	257	2009	1.253	.0496	.0528	25.28					
458	34			20.74	1697	89	-4.00	0	0	0		14380		5215	2683	18364	1.006	.5175	.4830	1.94		.289	.590	.303	.094
459	35			20.74	1700		.00					14380		7042	2858	16156	1.358	.5512	.4252	2.46		.288	.781	.321	.082
460	36			20.76	1698	89	4.00		0	0	40	14340	NC	8860	3061	15375	1.707	.5936	.4040	2.87	30.02	.289	1.014	.338	.079
461	37			20.76	1684		6.00					14320		9579	3240	14361	1.844	.6237	.3770	2.95		.291	1.097	.371	.074
462	38			20.74	1679	86	8.00					14300		10319	3351	13515	1.990	.6463	.3554	3.07		.291	1.184	.384	.070
463	39			20.76	1679		10.00					14320		11065	3702	11013	2.132	.7133	.2894	2.98		.292	1.277	.427	.058
464	40			20.72	1679		12.00					14330		11325	3973	9435	2.186	.7670	.2484	2.85		.291	1.300	.456	.049
465	41	CALIBRATION																							
466	1	21	20	1.31	0	62	-8.07	90	0	0[1]	40	0	NA	-43	54	-275	-.131	.1650	-.1121	-.79	30.33	NA	NA	NA	NA
467	2			1.27			-3.91							55	40	17	.173	.1263	.0040	1.37					
468	3			1.27			.00							163	44	-233	.513	.1410	-.1101	3.64					
469	4			1.25			4.46							270	48	-684	.864	.1605	-.2278	5.38					
470	5			1.31			6.53							328	51	-417	1.302	.1651	-.1930	6.06					
471	6			1.31			8.63							385	63	-563	1.176	.2052	-.2574	5.72					
472	7			1.31			10.71							435	87	-681	1.328	.2821	-.3094	4.70					
473	8			1.31			12.72							443	92	-211	1.353	.2979	-.1141	4.54					
474	9			1.29			14.66							400	129	+1022	1.240	.4143	-.4563	2.99					
475	10		40	5.26		61	-8.10							-247	233	178	-.188	.1775	.0221	-1.05					
476	11			5.28			-3.92							202	208	-540	.153	.1578	-.0588	.97					
477	12			5.24			.27							669	214	-835	.511	.1650	-.0969	3.09					
478	13			5.21			4.44							1068	272	-845	.820	.2151	-.1044	3.81					
479	14			5.24			6.51							1251	308	-259	.955	.2436	-.0454	3.92					
480	15			5.26		60	8.59							1444	396	-928	1.098	.3124	-.1175	3.51					
481	16			5.21			10.67							1639	443	-533	1.258	.3548	-.0802	3.54					
482	17			5.15			12.70							1681	447	458	1.306	.3630	.0232	3.59					
483	18			5.19			14.75							1826	445	-559	1.407	.3614	-.0861	3.89					
484	19		60	11.68			-8.11							-594	532	550	-.203	.1826	.0296	-1.11					
485	20			11.57			-3.92							416	474		.144	.1641	-.0324	.87					
486	21			11.66			.26							1393	472	+1494	.480	.1649	-.0796	2.91					
487	22			11.70			4.44							2405	528	+2560	.822	.1868	-.1353	4.40					
488	23			11.72			6.53							2894	582	+2927	.988	.2077	-.1554	4.75					
489	24			11.74			8.62							3407	645	+3650	1.161	.2323	-.1921	4.99					
490	25			11.70			10.66							3631	667	161	1.241	.2424	-.0166	5.12					

TABLE A-2
(Continued)
AMES TEST RESULTS

Point No. - Consecutive	Point No. - Per Run	Run No.	Tunnel Speed (V_∞) - Knots	Tunnel Dynamic Pressure (q) - Lbs/sq.ft.	Fan Speed (N_p) - RPM	Tunnel Temp. °F	Angle of Attack (α_c) - degrees	Left Louver Angle (δ_L) - degrees	Horizontal Tail Incidence Angle (i_t) - degrees	Reaction Control Setting (RC) - CPS	Wing Flap Angle (δ_{wf}) - degrees	Engine Speed (N_{25}) - RPM	Exhaust Gas Temp. (EGT) - °F	Total Lift (L_T) - Lbs.	Total Drag (D_T) - Lbs.	Total Pitch Moment (M_T) - Ft. Lbs.	Lift Coefficient (C_L)	Drag Coefficient (C_D)	Pitch Moment Coefficient (C_M)	Lift To Drag Ratio (C_L/C_D)	Barometer In. Hg.	Velocity Ratio (V_∞/V_{510})	Lift Coefficient (C_L)	Drag Coefficient (C_D)	Pitch Moment Coefficient (C_M)
491	26	21	60	11.60	0	60	12.74	90	0	Off	30	0	NA	4012	756	1333	1.383	.2785	.0359	4.96	30.33	NA	NA	NA	NA
492	27			11.53			14.73							3947	916	435	1.369	.3352	-.0060	4.08					
493	28		80	20.78			-8.11							-1099	966	778	-.212	.1864	.0245	-1.13					
494	29			20.84			-3.92							745	861	-959	.143	.1654	-.0279	.86					
495	30			20.67			.25							2410	840	-3145	.466	.1646	-.0920	2.83					
496	31			20.76			4.43							4214	944	-4678	.812	.1880	-.1387	4.31					
497	32			20.78		61	6.53							5127	1007	-4972	.987	.2029	-.1497	4.86					
498	33			20.82			8.61							5977	1133	-6052	1.148	.2299	-.1809	4.99					
499	34			20.88			10.68							6623	1240	-3490	1.269	.2525	-.1158	5.02					
500	35			20.80			12.75							7328	1346	84	1.409	.2773	-.0251	5.08					
501	36			20.76			14.78							7574	1619	-946	1.459	.3318	-.0532	4.38					
502	1	22	60	11.72	2431	70	3.00	24	12	0+150	30	16200	NC	9121	159	1962	3.113	.0543	.0913	57.36	30.33	NC	NC	NC	NC
503	2			11.66	2422	72	6.00					16210		9980	527	2020	3.424	.1808	.0945	18.93					
504	3			11.68	2426	73	8.00					16200		10575	835	2252	3.622	.2860	.1052	12.66					
505	4			11.68	2420	74	10.00					16200		11028	1118	2379	3.777	.3829	.1111	9.86					
506	5			11.76	2408	76	.00					16200		8050	-156	1709	2.738	-.0531	.0793	-51.60					
507	6		70	16.01	2406	77	3.00					16210		10013	796	-2423	2.502	.1989	-.0825	12.57					
508	7		80	20.74	2398	78	3.00					16200		11193	1474	-6248	2.159	.2843	-.1656	7.59					
509	8			20.76	2469	81	.00	31	15	0		16360		8966	341	346	1.728	.0657	.0091	26.29					
510	9			20.76	2469	82	4.00					16380		10785	918	1671	2.078	.1769	.0439	11.74					
511	10			20.78	2466	83	6.00					16370		11781	1180	4602	2.268	.2271	.1208	9.98					
512	11			20.82	2459	84	8.00					16340		12685	1520	4738	2.437	.2920	.1241	8.34					
513	12			20.72	2455		-4.00					16360		7035	-67	-1243	1.358	-.0129	-.0327	-105.00					
514	13		90	26.75	2449	86	.00					16370		10081	1099	-6777	1.507	.1643	-.1382	9.17					
515	14		100	32.80	2453	87	.00					16390		11464	1785	-13196	1.398	.2177	-.2195	6.42					
516	15			32.76	2480	88	-2.00		0			16390		6949	448	13200	.848	.0547	.2198	15.51					
517	16			32.74	2463	89	.00	40				16380		8527	603	12817	1.042	.0737	.2135	14.14					
518	17			32.70	2480	90	4.00					16370		11716	1057	9677	1.433	.1293	.1614	11.08					
519	18			32.70	2516		6.00					16380		13381	1456	5687	1.637	.1781	.0949	9.19					
520	19		90	26.97	2470	91	-2.00					16390		6205	-100	16315	.920	-.0148	.3300	-62.05					
521	20	CALIBRATION																							
522	1	23	40	5.24	0	75	.30	90	0	Off	30	0	NA	729	219	-4471	.556	.1701	-.4762	3.27	30.29	NA	NA	NA	NA
523	2						.34		4					834	236	-6198	.637	.1839	-.6576	3.46					
524	3						.36		8					897	254	-7532	.685	.1983	-.7974	3.45					
525	4						.28		12					937	270	-8247	.715	.2109	-.8724	3.39					

TABLE A-2
(Continued)
AMES TEST RESULTS

Point No. - Consecutive	Point No. - Run Sch.	Run No.	Tunnel Speed (V_∞) - Knots	Tunnel Dynamic Pressure (q) - Lbs/sq.ft.	Fan Speed (N_p) - RPM	Tunnel Temp. T_T	Angle of Attack (α_c) - degrees	Exit Louver Angle (δ_e) - degrees	Horizontal Tail Incidence Angle (i_t) - degrees	Reaction Control Setting (RC) - CPS	Wing Flap Angle (δ_f) - degrees	Engine Speed (N_{gg}) - RPM	Exhaust Gas Temp. (EGT) - °F	Total Lift (L_T) - Lbs.	Total Drag (D_T) - Lbs.	Total Pitch Moment (M_T) - Ft. Lbs.	Lift Coefficient (C_L)	Drag Coefficient (C_D)	Pitch Moment Coefficient (C_m)	Lift To Drag Ratio (C_L/C_D)	Barometer in. Hg.	Velocity Ratio ($V_\infty/\sqrt{g_c R T_T}$)	Lift Coefficient (C_L)	Drag Coefficient (C_D)	Pitch Moment Coefficient (C_m)	Yaw Angle (ψ) - Degrees
526	5	23	40	5.24	0	75	.36	90	16	Off	30	0	NA	876	312	-6693	.069	.2423	-.7097	2.76	30.29	NA	NA	NA	NA	
527	6						.40		14					982	289	-8781	.750	.2258	-.9286	3.34						
528	7		60	20.74			.30		0					2885	900	-17742	.556	.1765	-.4774	3.13						
529	8			20.76			.34		4					3266	969	-25287	.629	.1804	-.6766	3.30						
530	9			20.74			.36		8					3540	1034	-30574	.683	.2038	-.8174	3.35						
531	10						.37		10					3622	1066	-32530	.699	.2101	-.8691	3.33						
532	11						.38		12					3739	1102	-33712	.721	.2174	-.9006	3.31						
533	12						.38		14					3745	1173	-33972	.722	.2309	-.9075	3.12						
534	13			20.61			.38		16					3695	1263	-32277	.717	.2499	-.8682	2.87						
535	14			20.72			.37		18					3569	1334	-29882	.689	.2619	-.8000	2.63						
536	1	24	60	11.66	0	65	.23	90	0	Off	30	0	NA	1274	465	-696	.437	.1613	-.0411	2.71	30.32	NA	NA	NA	NA	0
537	2			11.78			.23							1291	503	-400	.438	.1726	-.0269	2.54						4
538	3			11.74		64	.22							1219	459	-544	.415	.1560	-.0478	2.62						8
539	4			11.64			.23							1233	503	-738	.424	.1745	-.0682	2.42						12
540	5			11.64			.22							1218	557	-94	.419	.1939	-.0620	2.16						16
541	6			11.64			.22							1209	422	-823	.415	.1466	-.0543	2.83						4
542	7			11.68			.22							1184	413	-1397	.405	.1430	-.0731	2.81						0
543	8			11.70			.22							1200	423	-1413	.410	.1462	-.0778	2.80						-4
544	9			11.68			.22							1183	453	-1317	.403	.1567	-.0838	2.58						-8
545	10			11.62			.21							1157	490	-1096	.398	.1701	-.0880	2.34						-12
546	11			11.64			.21							1158	564	-1214	.398	.1953	-.1229	2.03						-16
547	12			11.72			8.62							3399	565	-2968	1.160	.2053	-.1606	5.64						0
548	13			11.68			8.62							3384	585	-2862	1.159	.2126	-.1586	5.44						4
549	14			11.66			8.62							3388	634	-2842	1.162	.2301	-.1693	5.03						8
550	15			11.80		63	8.61							3400	698	-2846	1.153	.2490	-.1792	4.62						12
551	16			11.72			8.60							3307	757	-2427	1.129	.2702	-.1789	4.17						16
552	17			11.68			8.62							3382	564	-3088	1.158	.2056	-.1667	5.63						0
553	18			11.74			8.61							3382	559	-3221	1.152	.2028	-.1751	5.68						-4
554	19			11.76			8.61							3338	577	-3255	1.135	.2082	-.1836	5.45						-8
555	20			11.68			8.59							3221	609	-3625	1.103	.2199	-.2081	5.01						-12
556	21			11.72			8.58							3180	673	-3958	1.085	.2406	-.2461	4.51						-16
557	22			12.00			8.60							3400	700	-2905	1.133	.2453	-.1753	4.62						12
558	1	25	20	1.27	1714	61	.00	0	0	Off	30	14240	NC	3130	394	3448	9.858	1.2409	1.4811	7.94	30.33	NC	NC	NC	NC	0
559	2			1.27	1714	62	.00					14250		3069	410	3461	9.666	1.2913	1.5110	7.48						4
560	3			1.23	1707	63	.00					14250		3018	364	3180	9.815	1.1837	1.4652	8.29						8

TABLE A-2
(Continued)
AMES TEST RESULTS

Point No. - Consecutive	Point No. - Per Run	Run No.	Tunnel Speed (V_p) - Knots	Tunnel Dynamic Pressure (q) - Lbs/sq.ft.	Fan Speed (N_p) - RPM	Tunnel Temp. °F	Angle of Attack (α) - degrees	Exit Louver Angle (β) - degrees	Horizontal Tail Incidence Angle (i_t) - degrees	Reaction Control Setting (RC) - CPS	Wing Flap Angle (δ_f) - degrees	Engine Speed (N_{J85}) - RPM	Exhaust Gas Temp. (EGT) - °F	Total Lift (L_p) - Lbs.	Total Drag (D_p) - Lbs.	Total Pitch Moment (M_p) - Ft. Lbs.	Lift Coefficient (C_L)	Drag Coefficient (C_D)	Pitch Moment Coefficient (C_m)	Lift To Drag Ratio (L_p/D_p)	Barometer In. Hg.	Velocity Ratio (V_p/V_{tip})	Lift Coefficient (R_L)	Drag Coefficient (R_D)	Pitch Moment Coefficient (R_M)	Yaw Angle (ψ) - Degrees
561	4	25	20	1.25	1709	64	0.00	0	0	Off	30	14250	NC	3065	407	3736	9.808	1.3024	1.5800	7.53	30.33	NC	NC	NC	NC	-4
562	5			1.23	1710	65						14250		3054	398	3040	9.932	1.2943	1.2381	7.67						-8
563	6			1.34	1704	66	-8.00					14250		2778	-11	3208	8.293	-.0328	1.0527	-252.54						-8
564	7			1.23	1701		-4.00					14250		2860	154	3362	9.301	.5008	1.2524	18.57						-8
565	8			1.29	1699	68	4.00					14250		3111	642	3382	9.647	1.9907	1.3318	4.84						-8
566	9			1.25	1699		6.00					14250		3112	770	3365	9.958	2.4660	1.3454	4.04						-8
567	10			1.27	1697	69	8.00					14250		3180	910	3203	10.016	2.8661	1.2958	3.49						-8
568	11			1.23	1694		10.00					14250		3195	884	6406	10.390	2.8748	2.6915	3.61						-8
569	12			1.23	1695	70	12.00					14250		3213	1106	2949	10.449	3.5967	1.2056	2.90						-8
570	13			1.29	1693		14.00					14250		3388	1262	3400	10.505	3.9132	1.2534	2.68						-8
571	14			1.21	1692		16.00					14250		3356	1334	3381	11.094	4.4099	1.4021	2.51						-8
572	15			1.19	1693	71	0.00					14250		2887	387	3360	9.704	1.3008	1.3672	7.46						+12
573	16			1.31	1693	72						14250		2938	423	3617	8.971	1.2916	1.1942	6.94						+16
574	17			1.23	1695			20				14250		2687	-552	7263	8.722	-1.7951	2.8658	-4.85						+16
575	18			1.29	1720			35				14250		2073	-1161	8831	6.428	-3.6000	3.5921	-1.78						+16
576	19			1.29	1685	73	8.00	0				14250		3150	861	3449	9.767	2.6698	1.4583	3.65						0
577	20			1.27	1683	74	8.00					14250		3102	853	3409	9.770	2.6866	1.5252	3.63						4
578	21			1.27	1684		8.00					14250		3107	840	3071	9.786	2.6457	1.3908	3.69						8
579	22			1.29	1685		8.00					14250		3166	868	3747	9.817	2.6915	1.5591	3.64						-4
580	23			1.27	1685		8.00					14250		3134	865	2991	9.871	2.7244	1.1764	3.62						-8
581	24			1.27	1681		8.00					14250		3107	860	3245	9.786	2.7087	1.3701	3.61						-8
582	25			1.27	1680	75	8.00					14250		3077	825	3242	9.691	2.5984	1.1877	3.73						+12
583	26			1.34	1690		8.00	20				14240		3057	-173	6691	9.125	-.5164	2.6170	-17.67						+16
584	27			1.27	1713	76	8.00	35				14220		2442	-841	8543	7.691	-2.6488	3.5446	-2.90						+16
585	28			1.21	1678		-8.00	0				14250		2652	-8	3256	8.767	-.0264	1.4563	-331.50						+16
586	29			1.27	1681		-4.00					14250		2789	194	2762	8.784	.6110	.9999	14.37						+16
587	30			1.27	1680	77	4.00					14250		2980	640	3355	9.386	2.0157	1.1790	4.65						+16
588	31			1.31	1681		6.00					14250		3037	757	3585	9.273	2.3115	1.1268	4.01						+16
589	32			1.27	1675		10.00					14250		3106	939	2538	10.101	3.0537	.8922	3.30						+16
590	33			1.23	1677		12.00					14255		3131	1060	2604	10.182	3.4472	.9146	2.95						+16
591	34			1.27	1676		14.00					14260		3156	1180	2868	9.940	3.7165	1.0105	2.67						+16
592	35			1.17	1672		16.00					14260		3231	1291	3064	11.046	4.4137	1.2825	2.50						+16
593	1	26	40	5.24	1708	58	0.00	0	0	Off	30	14240	NC	3996	1037	8192	3.050	.7916	.8528	3.85	30.36	NC	NC	NC	NC	0
594	2			5.24	1712	60						14250		4077	1050	8226	3.112	.8015	.8823	3.88						4
595	3			5.24	1706	61						14260		4015	1050	8072	3.065	.8015	.8713	3.82						8

TABLE A-2
(Continued)
AMES TEST RESULTS

Point No. - Consecutive	Point No. - Per Run	Run No.	Tunnel Speed (V_∞) - Knots	Tunnel Dynamic Pressure (q) - Lbs/sq.ft.	Fan Speed (N) - RPM	Tunnel Temp. °F	Angle of Attack (α_w) - degrees	Left Louver Angle (δ_L) - degrees	Horizontal Tail Incidence Angle (i_t) - degrees	Reaction Control Setting (RCS) - SCM	Wing Flap Angle (δ_f) - degrees	Engine Speed (N_{eng}) - RPM	Exhaust Gas Temp. (EGT) - °F	Total Lift (L_w) - Lbs.	Total Drag (D_w) - Lbs.	Total Pitch Moment (C_{m_w}) - Ft. Lbs.	Lift Coefficient (C_L)	Drag Coefficient (C_D)	Pitch Moment Coefficient (C_m)	Lift To Drag Ratio (L_w/D_w)	Barometer In. Hg.	Velocity Ratio (V_∞/V_{ID})	Lift Coefficient (C_L)	Drag Coefficient (C_D)	Pitch Moment Coefficient (C_m)	Yaw Angle (ψ) - Degrees
596	4	26	60	5.28	1708	62	0.00	0	0	Off	30	14250	NC	4171	1045	7969	3.160	.7917	.7919	3.99	30.36	NC	NC	NC	NC	-4
597	5			5.30	1708	63						14240		4164	1062	7926	3.143	.8015	.7544	3.92						-8
598	6			5.24	1700	64	-8.00					14240		3068	670	8236	2.342	.5115	.7898	4.51						-8
599	7			5.19	1707		-4.00					14240		3536	824	7912	2.725	.6351	.7688	4.29						-8
600	8			5.16	1702	65	4.00					14230		4655	1306	7639	3.474	.9746	.7224	3.56						-8
601	9			5.19	1702	66	6.00					14240		4832	1411	7534	3.724	1.0875	.7203	3.42						-8
602	10			5.24	1697		8.00					14240		5059	1544	7259	3.862	1.1786	.6878	3.27						-8
603	11			5.09	1697		10.00					14230		5170	1667	7115	4.063	1.3100	.7094	3.10						-8
604	12			5.21	1689	67	12.00					14240		5279	1882	5739	4.053	1.4449	.5303	2.80						-8
605	13			5.21	1700		0.00					14250		4020	1056	7476	3.086	.8107	.7057	3.80						-12
606	14			5.21	1700	68						14240		4055	1099	7609	3.113	.8438	.6567	3.69						-16
607	15			5.28	1696	69		20				14230		3393	72	10943	2.570	.0545	1.0226	47.12						-16
608	16			5.24	1714			35				14230		2462	-546	11700	1.879	-.4168	1.1163	-4.50						-16
609	17			5.26	1685	70	3.00	0				14240		5027	1518	7035	3.823	1.1544	.7298	3.31						0
610	18			5.28	1687							14250		5002	1515	7279	3.789	1.1477	.7758	3.30						6
611	19			5.34	1686							14260		4939	1524	7046	3.700	1.1416	.7541	3.24						8
612	20			5.28	1685	71						14260		5036	1509	7308	3.814	1.1432	.7241	3.31						-4
613	21			5.28	1690	72						14250		5057	1523	7247	3.831	1.1538	.7039	3.32						-8
614	22			5.26	1693							14250		5004	1542	6607	3.820	1.1771	.6280	3.24						-12
615	23			5.26	1688							14240		4912	1556	6906	3.750	1.1878	.6030	3.15						-16
616	24			5.17	1668			20				14230		4511	461	3797	3.490	.3567	.9513	9.78						-16
617	25			5.26	1707			35				14210		3508	-208	11462	2.678	-.1588	1.0975	-16.86						-16
618	26			5.17	1679	73	-8.00	0				14230		1024	715	7841	2.340	.5532	.7122	4.22						-16
619	27			5.19	1680		-4.00					14230		3456	876	8190	2.664	.6751	.7462	3.94						-16
620	28			5.13	1680	74	4.00					14240		4418	1279	7402	3.445	.9973	.6687	3.45						-16
621	29			5.21	1680		6.00					14240		4666	1442	7048	3.582	1.1071	.5871	3.23						-16
622	30			4.95	1683		10.00					14250		4841	1598	6634	3.912	1.2913	.6156	3.03						-16
623	31			5.01	1680		12.00					14240		5130	1834	6326	4.096	1.4643	.5688	2.79						-16
624	32			5.01	1720	75	14.00					14230		4953	1980	6315	3.954	1.5808	.5558	2.50						-16
625	1	27	60	11.70	0	56	-8.15	90	0	Off	30	0	NA	-842	612	2421	-.288	.2100	.0977	-1.37	30.22	NA	NA	NA	NA	-8
626	2			11.70			-3.96							201	536	336	.069	.1833	.0295	.37						-8
627	3			11.70			.22							1229	499	-357	.420	.1722	-.0342	2.43						-8
628	4			11.74			4.42							2308	537	-1853	.786	.1887	-.1094	4.16						-8
629	5			11.78			6.51							2827	584	-2275	.960	.2069	-.1346	4.64						-8
630	6			11.78			8.60							3339	648	-3174	1.134	.2320	-.1777	4.88						-8

TABLE A-2
(Continued)
AMES TEST RESULTS

Point No. - Consecutive	Point No. - Per Run	Run No.	Tunnel Speed (V_∞) - Knots	Tunnel Dynamic Pressure (q) - Lbs/sq.ft.	Fan Speed (N_p) - RPM	Tunnel Temp. - °F	Angle of Attack (α_T) - degrees	Exit Louver Angle (δ_e) - degrees	Horizontal Tail Incidence Angle (i_t) - degrees	Ejection Control Setting (EC) - CPS	Wing Flap Angle (δ_f) - degrees	Engine Speed (N_{gg}) - RPM	Exhaust Gas Temp. (EGT) - °F	Total Lift (L_T) - Lbs.	Total Drag (D_T) - Lbs.	Total Pitch Moment (M_{cg_T}) - Ft. Lbs.	Lift Coefficient (C_L)	Drag Coefficient (C_D)	Pitch Moment Coefficient (C_m)	Lift To Drag Ratio (L_T/D_T)	Barometer in. Hg.	Velocity Ratio (V_∞/V_{ref})	Lift Coefficient (R_L)	Drag Coefficient (C_D)	Pitch Moment Coefficient (R_M)	Tip Angle (TA) - Degrees
631	7	27	60	11.70	0	56	10.66	90	0	Off	30	0	NA	3635	691	-74	1.243	.2506	-.0328	4.92	30.22	NA	NA	NA	NA	-8
632	8			11.66			12.73							4015	755	1338	1.377	.2766	.0310	4.97						-8
633	9			11.66			14.70							3810	886	249	1.307	.3198	-.0043	4.08						-8
634	10			11.70			-8.14							-787	688	2629	-.269	.2359	.0694	-1.14						-16
635	11			11.70			-3.97							190	600	1725	.065	.2052	.0232	.31						-16
636	12			11.74			.22							1232	598	-548	.420	.2054	-.0813	2.04						-16
637	13			11.74			4.41							2239	614	-1620	.763	.2146	-.1403	3.55						-16
638	14			11.74			6.52							2747	681	-2686	.936	.2402	-.1927	3.89						-16
639	15			11.74			8.58							3183	724	-2956	1.084	.2576	-.1339	4.21						-16
640	16			11.70			10.63							3447	753	-82	1.178	.2704	-.0695	4.35						-16
641	17			11.66			12.69							3762	894	-134	1.291	.3222	-.0683	4.00						-16
642	18			11.70			14.70							3815	993	479	1.304	.3553	-.0203	3.67						-16
643	19			11.66			-8.14							-776	603	3919	-.266	.2075	.1385	-1.28						8
644	20			11.70			-3.96							238	530	1256	.081	.1813	.0424	.44						8
645	21			11.78		57	.24							1316	531	-76	.447	.1822	-.0080	2.45						8
646	22			11.78			4.44							2425	575	-1449	.823	.2016	-.0974	4.08						8
647	23			11.76			6.52							2883	633	-2257	.981	.2242	-.1377	4.37						8
648	24			11.70			8.62							3405	697	-3187	1.164	.2509	-.1821	4.64						8
649	25			11.70			10.67							3678	743	1463	1.257	.2687	.0339	4.67						8
650	26			11.70			12.70							3859	855	1819	1.319	.3085	.0666	4.27						8
651	27			11.78			14.71							3950	930	1796	1.341	.3325	.0708	4.03						5
652	1	28	20	1.25	1700	59	0.00	0	0	Off	30	14210	NC	3079	415	3529	8.853	1.3280	1.5400	7.41	30.32	.070	.339	.046	.018	
653	2			1.37	1699				4			14210		3182	474	3438	9.291	1.3839	1.3690	6.71		NC	NC	NC	NC	
654	3			1.37	1700	60			8			14210		3325	441	4919	9.708	1.2876	1.9587	7.54						
655	4			1.27	1704				12			14210		3130	426	2419	9.858	1.3417	1.0389	7.34						
656	5			1.27	1696				16			14210		3119	424	2314	9.824	1.3354	.9940	7.35						
657	6			1.27	1690	61			20			14210		3156	442	1770	9.960	1.3921	.7602	7.14						
658	7			1.31	1698	62		20	0			14210		2799	-618	7403	8.547	-1.8870	3.0824	-4.52		.072	.312	-.019	.037	
659	8			1.27	1696				4			14210		2809	-609	6814	8.847	-1.9181	2.9267	-4.61		NC	NC	NC	NC	
660	9			1.25	1697				8			14210		2798	-638	6793	8.954	-2.0416	2.9644	-4.38						
661	10			1.25	1696				12			14210		2803	-600	7009	8.970	-1.9200	3.0588	-4.67						
662	11			1.23	1695	64			16			14210		2820	-619	5829	9.171	-2.0130	2.5849	-4.55						
663	12			1.23	1697				20			14210		2872	-602	5641	9.340	-1.9577	2.5015	-4.77						
664	13			1.35	1734	65		35	0			14210		2149	-1254	8846	6.367	-3.7156	3.5741	-1.71		.072	.233	-.136	.043	
665	14			1.27	1724	66			4			14210		2133	-1272	8843	6.718	-4.0063	3.7981	-1.67		NC	NC	NC	NC	

TABLE A-2
(Continued)
AMES TEST RESULTS

Point No. - Consecutive	Point No. - Dir. Run	Run No.	Tunnel Speed (P_{t_2}) - Knots	Tunnel Dynamic Pressure (q) - Lbs/sq.ft.	Fan Speed (n_{fp}) - RPM	Tunnel Temp. - °F	Angle of Attack (α_w) - degrees	Exit Louver Angle (α_{EL}) - degrees	Horizontal Tail Incidence Angle (i_t) - degrees	Aileron Control Setting (DEG)	CPS Wing Flap Angle (δ_{wf}) - degrees	Engine Speed (n_{gg}) - RPM	Ambient Gas Temp. (SAT) - °F	Total Lift (C_{L_w}) - Lbs.	Total Drag (C_{D_w}) - Lbs.	Total Pitch Moment (C_{M_w}) - Ft. Lbs.	Lift Coefficient (C_{L_w})	Drag Coefficient (C_{D_w})	Pitch Moment Coefficient (C_{M_w})	Lift To Drag Ratio (C_{L_w}/C_{D_w})	Barometer In. Hg.	Velocity Ratio (V_a/V_{sub})	Lift Coefficient (Π_L)	Drag Coefficient (Π_D)	Pitch Moment Coefficient (Π_M)	Yaw Angle (YY) - Degrees
666	15	28	20	1.25	1725	66	0.00	35	0	Off	30	14710	NC	2154	-1264	8222	6.893	-.0448	3.5881	-1.70	30.32	NC	NC	NC	NC	0
667	16			1.19	1726				12			14210		2193	-1261	7590	7.371	-.2387	3.4790	-1.73						
668	17			1.19	1723	67			16			14210		2207	-1263	7587	7.418	-.2654	3.4755	-1.74						
669	18			1.19	1722				20			14210		2199	-1236	7330	7.392	-.1546	3.3601	-1.77						
670	1	29	40	5.28	1707	64	-8.00	20	0	Off	30	14280	NC	2466	-428	10813	1.868	-.3242	1.1171	-5.76	30.30	.143	.262	-.046	.052	0
671	2			5.26	1705	65	-4.00					14280		3037	-268	10327	2.310	-.2038	1.0710	-11.33		.143	.324	-.029	.050	
672	3			5.13	1702		.00					14280		3552	-85	10371	2.770	-.0663	1.1028	-41.78		.142	.389	-.009	.052	
673	4			5.19	1700	66	4.00					14270		4097	139	10311	3.158	.1071	1.0837	29.47		.143	.444	.015	.051	
674	5			5.32	1699		6.00					14280		4407	278	10280	3.314	.2090	1.0541	15.85		.145	.489	.031	.052	
675	6			5.34	1697	67	8.00					14270		4627	392	10333	3.466	.2936	1.0555	11.80		.145	.511	.043	.052	
676	7			5.30	1696	68	10.00					14280		6856	516	9922	3.663	.3896	1.0212	9.40		.145	.540	.057	.050	
677	8			5.21	1715	69	-8.00	35				14250		1566	-997	12302	1.202	-.7655	1.2880	-1.57		.142	.169	-.107	.060	
678	9			5.21	1715	70	-4.00					14250		2113	-879	11369	1.622	-.6749	1.1903	-2.40		.142	.228	-.095	.055	
679	10			5.15	1714		.00					14260		2652	-747	11732	2.060	-.5802	1.2426	-3.55		.141	NC	-.081	.058	
680	11			5.17	1714	71	4.00					14270		3193	-569	11563	2.470	-.4402	1.2280	-5.61		.141	.347	-.062	.057	
681	12			5.24	1722		6.00					14250		3638	-473	12067	2.626	-.3611	1.2561	-7.26		.142	.369	-.051	.059	
682	13			5.24	1709	72	8.00					14250		3718	-372	11574	2.838	-.2840	1.2848	-9.99		.143	.399	-.040	.056	
683	14			5.17	1710		10.00					14260		3896	-272	11436	3.013	-.2104	1.2866	-14.31		.142	.423	-.030	.056	
684	1	30	60	11.68	1711	64	0.00	0	0	Off	30	14230	NC	3653	1768	10765	1.936	.6055	.5028	3.19	30.35	NC	NC	NC	NC	0
685	2			11.68	1702							14230		5718	1795	11430	1.958	.6147	.5182	3.18						4
686	3			11.68	1696							14230		5621	1817	11232	1.925	.6223	.4924	3.09						8
687	4			11.64	1695	65						14230		5555	1870	10338	1.909	.6426	.4244	2.97						12
688	5			11.68	1705	66						14230		5598	1975	9684	1.886	.6766	.3564	2.78						16
689	6			11.72	1699		-8.00					14230		3860	1561	12676	1.038	.5259	.5479	1.97						8
690	7			11.68	1698		-4.00					14230		4427	1613	11880	1.516	.5526	.5235	2.76						4
691	8			11.68	1694	67	.00					14230		5584	1838	10896	1.912	.6295	.4773	3.03						0
692	9			11.68	1686		4.00					14230		6728	2045	10160	2.304	.7003	.4695	3.29						-4
693	10			11.68	1685		6.00					14230		7298	2196	9262	2.497	.7514	.3986	3.32						-8
694	11			11.68	1679	68	8.00					14230		7810	2364	8665	2.675	.8027	.3707	3.33						-12
695	12			11.64	1687		10.00					14230		8054	2554	9582	2.768	.8777	.4156	3.15						-16
696	1	31	80	20.21	1705	62	0.00	0	0	Off	30	14240	NC	7061	2747	14199	1.398	.5437	.3832	2.57	30.40	NC	NC	NC	NC	0
697	2			20.57	1707	64						14240		7116	2767	13826	1.384	.5381	.3613	2.57						4
698	3			20.51	1708	65						14240		7015	2832	15377	1.368	.5523	.3816	2.47						8
699	4			20.00	1709							14240		6888	2840	15636	1.376	.5688	.3791	2.42						12
700	5			20.11	1708	66						14230		6917	2874	14550	1.376	.5915	.3860	2.32						16

TABLE A-2
(Continued)
AMES TEST RESULTS

Point No. - Consecutive	Point No. - Per Run	Run No.	Tunnel Speed (V_∞) - Knots	Tunnel Dynamic Pressure (q) - Lbs/sq.ft.	Fan Speed (N_{FAN}) - RPM	Tunnel Temp. - °F	Angle of Attack (α_T) - Degrees	Left Louver Angle (δ_{LL}) - Degrees	Horizontal Tail Incidence Angle (i_t) - Degrees	Reaction Control Setting (RCS) - OFF	Wing Flap Angle (δ_{WF}) - Degrees	Engine Speed (N_{GG}) - RPM	Exhaust Gas Temp. (EGT) - °F	Total Lift (L_T) - Lbs.	Total Drag (D_T) - Lbs.	Total Pitch Moment (M_T) - Ft. Lbs.	Lift Coefficient (C_L)	Drag Coefficient (C_D)	Pitch Moment Coefficient (C_m)	Lift To Drag Ratio (L_T/D_T)	Barometer In. Hg.	Velocity Ratio ($V_\infty/V_{1.0}$)	Lift Coefficient (C_L)	Drag Coefficient (C_D)	Pitch Moment Coefficient (C_m)	Yaw Angle (Ψ) - Degrees
701	6	31	80	20.69	1705	67	-8.00	0	0	Off	30	14240	NC	3239	2564	19518	.626	.4957	.4868	1.26	30.40	NC	NC	NC	NC	-8
702	7			20.28	1702		-4.00					14240		5073	2638	16543	1.001	.5203	.4173	1.92						-8
703	8			20.28	1703		0.00					14240		6916	2806	15213	1.364	.5535	.3857	2.46						-8
704	9			21.00	1697	68	4.00					14240		9135	3131	13658	1.740	.5964	.3305	2.91						-8
705	10			20.92	1704		6.00					14240		9887	3229	11938	1.890	.6174	.2899	3.06						-8
706	11			20.55	1718	69	8.00					14230		10605	3339	10199	2.064	.6499	.2509	3.17						-8
707	12			20.25	1720		10.00					14230		10948	3483	10782	2.163	.6880	.2637	3.14						-8
708	1	32	60	11.80	1696	63	-8.00	20	0	Off	30	14240	NC	2175	383	15252	.737	.1198	.7051	5.67	30.42	.216	.243	.043	.077	0
709	2			11.60	1691	64	-4.00					14240		3415	460	13643	1.178	.1586	.6416	7.42		.214	.380	.051	.069	
710	3			11.45	1687		0.00					14240		4410	645	12889	1.541	.2253	.6140	6.83		.213	.487	.083	.064	
711	4			11.45	1688	65	4.00					14240		5518	854	13072	1.928	.2983	.6227	6.46		.213	.610	.110	.065	
712	5			11.51	1691		6.00					14240		6110	1001	13632	2.123	.3479	.6461	6.10		.214	.686	.112	.069	
713	6			11.64	1694		8.00					14230		6748	1157	12277	2.319	.3976	.5753	5.83		.214	.749	.128	.062	
714	7			11.55	1685	66	10.00					14230		7035	1307	13317	2.436	.4526	.6289	5.38		.215	.787	.146	.067	
715	8			11.62	1697		-8.00	35				14230		1316	-357	16413	.453	-.1229	.7705	-3.68		.214	.146	-.040	.083	
716	9			11.62	1696		-4.00					14230		2426	-242	15085	.835	-.0833	.7081	-10.02		.214	.270	-.027	.076	
717	10			11.74	1697		0.00					14230		3635	-85	14222	1.239	-.0290	.6608	-42.76		.215	.400	-.009	.071	
718	11			11.74	1696	67	4.00					14220		4681	118	13977	1.595	.0402	.6494	39.66		.215	.515	.013	.070	
719	12			11.78	1696		6.00					14320		5304	228	13791	1.801	.0774	.6386	23.26		.216	.594	.026	.070	
720	13			11.68	1695		8.00					14220		5753	328	13698	1.973	.1123	.6397	17.54		.215	.636	.036	.069	
721	14			11.66	1691	68	10.00					14220		6215	488	13280	2.132	.1674	.6213	12.73		.215	.689	.054	.067	
722	1	33	0	1.00	1159	55	0.00	0	0	Off	30	11660	NC	1297	-62	357	5.188	-.2480	.1948	-20.91	30.01	NC	NC	NC	NC	0
723	2			1.00	1715	55						14310		2957	-150	579	11.828	-.6000	.3156	-19.71						
724	3			1.00	1147	56						11720		1303	-102	42	5.212	-.4080	.0230	-12.77						
725	4			1.00	1716	57						14290		2785	-251	90	11.140	-1.0040	.0490	-11.09						
726	5		80	20.76	1214	62						11820		5242	2200	9793	1.010	.4239	.2573	2.38		.400	1.134	.476	.096	
727	6			20.88	1210	63		20				11840		4547	1612	9078	.871	.3088	.2372	2.82		.402	.991	.351	.090	
728	7			20.76	1204	64		35				11840		3939	1088	8112	.759	.2096	.2131	3.62		.404	.870	.240	.081	
729	8		100	32.78	1230	65		0				11860		7330	3040	12359	.894	.3710	.2057	2.41		.497	1.551	.644	.118	
730	9			32.68	1237	66		20				11870		6552	2440	10800	.802	.2987	.1803	2.68		.494	1.375	.512	.103	
731	10			32.80	1214	67		35				11840		5764	1900	8425	.703	.2317	.1401	3.03		.504	1.254	.413	.082	
732	1	34	20	1.27	1163	62		0	0	Off	30	11730	NC	1530	278	1910	4.819	.8756	.8205	5.50	30.46	.103	.362	.066	.021	0
733	2			1.27	1696	63						14240		3055	346	2702	9.622	1.0898	1.1605	8.82		.070	.342	.039	.014	
734	3			1.37	1698	63		20				14240		2872	-656	6960	8.385	-1.9153	2.7712	-4.37		.071	.320	-.073	.035	
735	4			1.33	1729	64		35				14225		2203	-1296	8637	6.626	-3.8977	3.5422	-1.70		.070	.238	-.140	.042	

TABLE A-2
(Continued)
AMES TEST RESULTS

Point No. - Consecutive	Point No. - Per Run	Run No.	Tunnel Speed (V_∞) - Knots	Tunnel Dynamic Pressure (q) - Lbs/sq.ft.	Fan Speed (N_F) - RPM	Tunnel Temp. °F	Angle of Attack (α_s) - degrees	Left Louver Angle (δ) - degrees	Horizontal Tail Incidence Angle (i_t) - degrees	Reaction Control Section (RCS) - ON	Wing Flap Angle (δ_f) - degrees	Engine Speed (N_{gg}) - RPM	Exhaust Gas Temp. (EGT) - °F	Total Lift (L_T) - Lbs.	Total Drag (D_T) - Lbs.	Total Pitch Moment (Q_T) - Ft. Lbs.	Lift Coefficient (C_L)	Drag Coefficient (C_D)	Pitch Moment Coefficient (C_m)	Lift To Drag Ratio (L_T/D_T)	Barometer In. Hg.	Velocity Ratio (V_j/V_∞)	Lift Coefficient (C_L)	Drag Coefficient (C_D)	Pitch Moment Coefficient (C_m)	Yaw Angle (Y) - Degrees
736	5	34	30	2.97	1691	66	0.00	0	0	Off	30	14230	NC	3475	669	4289	4.686	.9010	.7878	5.19	30.46	.107	.381	.073	.022	0
737	6			2.90	1690	67		20				14240		3159	-403	7441	4.357	-.5559	1.3996	-7.83		.106	.358	-.046	.038	
738	7			3.05	1718	68		35				14240		2369	-1017	9543	3.107	-1.3338	1.7066	-2.32		.105	.261	-.112	.048	
739	8		40	5.24	1692	69		0				14260		4008	979	4736	3.060	.7473	.5972	4.09		.146	.457	.112	.038	
740	9			5.26	1689			20				14260		3588	-85	9191	2.729	-.0646	.9531	-42.21		.146	.409	-.010	.048	
741	10			5.19	1709			35				14250		2703	-747	10558	2.083	-.5757	1.1097	-3.61		.143	.301	-.083	.054	
742	11		60	11.70	1703	70		0				14270		5504	-275	67107	1.802	-.0960	3.1287	-20.01		.215	.622	NC	NC	
743	12			11.66	1699			20				14260		4348	655	11592	1.492	.2247	.5423	6.63		.215	.493	.074	.060	
744	13			11.70	1730			35				14270		3478	-56	12347	1.189	.0191	.5757	-62.10		.211	.380	-.006	.061	
745	14		80	20.82	1718	71		0				14230		6918	2562	11334	1.329	.4927	.7969	2.70		.286	.768	.284	.057	
746	15			20.74	1710			20				14180		5569	1480	12236	1.074	.2854	.3218	3.76		.286	.624	.166	.062	
747	16			20.70	1713			35				14150		4564	730	12563	.882	.1411	.3311	6.25		.286	.509	.081	.064	
748	1	35	30	2.87	1698	60	-8.00	0	0	Off	30	14225	NC	2926	259	5332	4.078	.3610	1.0135	11.29	30.47	.105	.328	.029	.027	0
749	2			2.84	1694	62	-4.00					14225		3180	446	4967	4.479	.6282	.9540	7.13		.104	.356	.050	.025	
750	3			2.69	1693	63	0.00					14225		3502	637	4122	5.207	.9472	.8358	5.49		.102	.394	.072	.021	
751	4			2.51	1693	64	4.00					14230		3636	842	4020	5.794	1.3418	.8737	4.31		.098	.411	.095	.021	
752	5			2.70	1689	65	6.00					14230		3789	1017	4153	5.613	1.5067	.8390	3.72		.103	.430	.115	.021	
753	6			2.64	1687		8.00					14230		3842	1143	4026	4.821	1.7318	.8319	3.36		.102	.438	.130	.021	
754	7			2.74	1685		10.00					14230		4046	1292	3868	4.907	1.8861	.7700	3.13		.103	.461	.147	.020	
755	8			2.65	1687	66	12.00					14230		4111	1419	3571	6.205	2.1419	.7350	2.83		.102	.469	.162	.019	
756	9			2.57	1684		14.00					14230		4036	1515	3391	6.282	2.3580	.7198	2.66		.101	.462	.173	.018	
757	10		40	4.87	1683	67	-8.00					14240		2981	605	7131	2.448	.4969	.7987	4.92		.142	.343	.070	.037	
758	11			5.06	1691	68	-4.00					14240		3544	803	6917	2.802	.6348	.7456	4.41		.143	.402	.091	.036	
759	12			4.87	1681	69	0.00					14240		3969	968	6551	3.244	.7951	.7337	4.08		.142	.456	.112	.034	
760	13			4.72	1684		4.00					14240		4409	1191	5741	3.736	1.0093	.6635	3.70		.138	.507	.137	.030	
761	14			5.00	1679	70	6.00					14240		4829	1364	6113	3.863	1.0912	.6669	3.54		.143	.560	.158	.032	
762	15			4.95	1680		8.00					14240		5031	1489	5483	4.065	1.2032	.6042	3.37		.142	.581	.172	.029	
763	16			5.00	1681		10.00					14240		4298	1640	-3446	3.438	1.3120	-.3759	2.62		.143	NC	-.189	NC	
764	17			4.85	1663		12.00					14240		5136	1889	5011	4.236	1.5579	.5636	2.71		.143	.606	.223	.027	
765	18			4.85	1664		14.00					14240		5034	2034	3881	4.195	1.6950	.4410	2.47		.141	.594	.240	.021	
766	19		60	11.31	1692	71	-8.00					14260		2946	1503	11511	1.042	.5316	.5552	1.96		.214	.337	.172	.060	
767	20			11.20	1689		4.00					14260		4164	1599	14152	1.487	.5711	.6893	2.60		.213	.479	.184	.074	
768	21			11.21	1686		0.00					14260		5315	1764	9921	1.897	.6294	.4828	3.01		.214	.614	.204	.052	
769	22			11.03	1691	72	4.00					14260		6498	1952	8273	2.356	.7079	.4091	3.32		.212	.747	.224	.043	
770	23			10.95	1697		6.00					14260		7105	2056	7895	2.595	.7518	.3933	3.45		.210	.810	.246	.041	

TABLE A-2
(Continued)
AMES TEST RESULTS

Point No. - Consecutive	Point No. - Per Run	Run No.	Tunnel Speed (V_o) - Knots	Tunnel Dynamic Pressure (q) - Lbs/sq.ft.	Fan Speed (N_p) - RPM	Tunnel Temp. °F	Angle of Attack (α') - degrees	Exit Louver Angle (β) - degrees	Horizontal Tail Incidence Angle (i_t) - degrees	Reaction Control Setting (RC) - CPS	Wing Flap Angle (δ_f) - degrees	Engine Speed (N_{GG}) - RPM	Exhaust Gas Temp. (EGT) - °F	Total Lift (L_T) - Lbs.	Total Drag (D_T) - Lbs.	Total Pitch Moment (M_T) - Ft. Lbs.	Lift Coefficient (C_L)	Drag Coefficient (C_D)	Pitch Moment Coefficient (C_M)	Lift To Drag Ratio (L_T/D_T)	Barometer In. Hg.	Velocity Ratio (V_o/V_{tip})	Lift Coefficient (H_L)	Drag Coefficient (H_D)	Pitch Moment Coefficient (H_M)	Yaw Angle (Ψ) - Degrees
771	24	35	60	11.17	1691	72	8.00	0	0	Off	30	14260	NC	7499	2253	8495	2.685	.8068	.4148	3.32	30.47	.213	.862	.259	.044	0
772	25			11.18	1698	73	10.00					14260		7872	2550	6432	2.816	.9123	.3138	3.08		.212	.897	.291	.033	
773	1	36	20	1.27	0	52	-8.12	90	0	Off	30	0	NA	-69	57	282	-.217	..1800	.1254	-1.20	29.99	NA	NA	NA	NA	0
774	2			1.27			-3.94							37	50	-122	.117	.1576	-.0548	.73						
775	3			1.27			.21							125	47	73	.394	.1495	.0239	2.63						
776	4			1.29			4.40							244	53	-75	.757	.1697	-.0463	4.45						
777	5			1.27			8.61							363	53	-337	1.143	.1791	-.1885	6.38						
778	6			1.27			10.61							361	48	238	1.137	.1947	.0800	5.84						
779	7			1.23			12.63							361	79	-63	1.174	.2697	-.0509	4.35						
780	8			1.31		53	14.63							387	130	-678	1.182	.4099	-.3053	2.88						
781	9		40	5.21			.22		0					545	194	-597	.418	.1506	-.0706	2.77						
782	10			5.24			.26		4					628	199	-2364	.479	.1540	-.2554	3.11						
783	11			5.24			.28		8					697	210	-3728	.532	.1629	-.3984	3.26						
784	12			5.24		54	.30		10					740	217	-4473	.565	.1686	-.4766	3.35						
785	13			5.26			.31		12					773	225	-5146	.588	.1741	-.5450	3.37						
786	14			5.24			.33		14					807	229	-5533	.616	.1783	-.5879	3.45						
787	15			5.19			.32		16					781	249	-5198	.602	.1953	-.5580	3.08						
788	16			5.19			.30		18					728	270	-4144	.561	.2110	-.4464	2.65						
789	17			5.28			.30		20					733	290	-3946	.555	.2226	-.4184	2.49						
790	18			5.26			-8.14		0					-354	234	561	-.269	.1786	..0634	-1.50						
791	19			5.19			-3.96							105	202	-99	.081	.1557	-.0120	.52						
792	20			5.24		55	.24							583	195	-796	.445	.1507	-.0915	2.95						
793	21			5.24			4.42							1044	215	-1490	.797	.1700	-.1705	4.68						
794	22			5.26			6.52							1275	236	-1741	.970	.1882	-.1994	5.15						
795	23			5.26			8.61							1499	263	-2148	1.140	.2121	-.2448	5.37						
796	24			5.26		56	10.69							1708	295	-2440	1.299	.2400	-.2782	5.41						
797	25			5.24			12.74							1831	365	-2751	1.398	.2968	-.3135	4.70						
798	26			5.19			14.78							1895	428	-2659	1.461	.3497	-.3078	4.17						
799	1	37	60	11.78	0	61	-8.14	90	0	Off	30	0	NA	-767	515	244	-.260	.1755	.0164	-1.48	29.91	NA	NA	NA	NA	0
800	2			11.68			-3.95							281	446	-1298	.096	.1528	-.0625	.63						
801	3			11.70			.24							1296	429	-2328	.443	.1485	-.117	2.98						
802	4			11.66			4.43							2340	472	-3694	.803	.1679	-.1884	4.78						
803	5			11.86			6.52							2868	523	-4080	.967	.1851	-.2064	5.22						
804	6			11.70			8.61							3367	575	-4665	1.151	.2089	-.2398	5.51						
805	7			11.68			10.70							3845	614	-4978	1.317	.2264	-.2580	5.81						

TABLE A-2
(Continued)
AMES TEST RESULTS

Point No. - Consecutive	Point No. - Per Run	Run No.	Tunnel Speed (V_o) - Knots	Tunnel Dynamic Pressure (q) - Lbs/sq.ft.	Fan Speed (N_f) - RPM	Tunnel Temp. °F	Angle of Attack (α) - degrees	Exit Louver Angle (δ) - degrees	Horizontal Tail Incidence Angle (i_t) - degrees	Reaction Control Nozzles (RCN) - DIR	Wing Flap Angle (δ_f) - degrees	Engine Speed (N_{SLS}) - RPM	Exhaust Gas Temp. (EGT) - °F	Total Lift (L_T) - Lbs.	Total Drag (D_T) - Lbs.	Total Pitch Moment (C_{M_T}) - Ft. Lbs.	Lift Coefficient (C_L)	Drag Coefficient (C_D)	Pitch Moment Coefficient (C_M)	Lift To Drag Ratio (L_T/D_T)	Barometer In. Hg.	Velocity Ratio (V_p/V_{tip})	Lift Coefficient (R_L)	Drag Coefficient (R_D)	Pitch Moment Coefficient (R_M)	Yaw Angle (γ) - Degrees
806	8	37	60	11.62	0	61	12.75	90	0	Off	30	0	NA	4064	709	-4359	1.399	.2623	-.2318	5.33	29.91	NA	NA	NA	NA	0.
807	9			11.70			14.78							4259	873	-4849	1.456	.3182	-.2543	4.57						
808	10			11.76		62	16.73							4034	1185	-6262	1.372	.4206	-.3171	3.26						
809	11		80	20.67			.26							2324	767	-4413	.450	.1503	-.1252	2.99						
810	12			20.74			.27		4					2666	791	-11572	.514	.1550	-.3143	3.31						
811	13			20.70			.30		8					2971	826	-17371	.564	.1626	-.4687	3.47						
812	14			20.74		63	.32		10					3079	849	-20048	.594	.1689	-.5388	3.51						
813	15			20.74			.33		12					3188	895	-22550	.615	.1761	-.6050	3.49						
814	16			20.70			.33		14					3180	965	-21688	.614	.1900	-.5834	3.23						
815	17			20.70			.32		16					3121	1032	-20078	.603	.2028	-.5408	2.97						
816	18			20.72			-8.14		0					-1366	913	531	-.264	.1769	.0191	-1.49						
817	19			20.84			-2.95							468	808	-2160	.090	.1552	-.0583	.57						
818	20			20.72			.26							2331	765	-4220	.450	.1496	-.1200	3.00						
819	21			20.80			4.43							4168	856	-6539	.802	.1702	-.1870	4.70						
820	22			20.84		64	6.53							5164	928	-7735	.991	.1873	-.2217	5.29						
821	23			20.82			8.62							6032	1029	-8439	1.159	.2102	-.2436	5.51						
822	24			20.72			10.71							6860	1151	-9329	1.324	.2384	-.2713	5.55						
823	25			20.70			12.77							7456	1355	-10103	1.441	.2811	-.2942	5.12						
824	26			20.72			14.78							7573	1631	-10931	1.462	.3347	-.3161	4.36						

LEGEND:

- D Reaction Nozzle Direction Down
- U Reaction Nozzle Direction Up
- NC Not Calculated
- NA Not Applicable
- – Erroneous

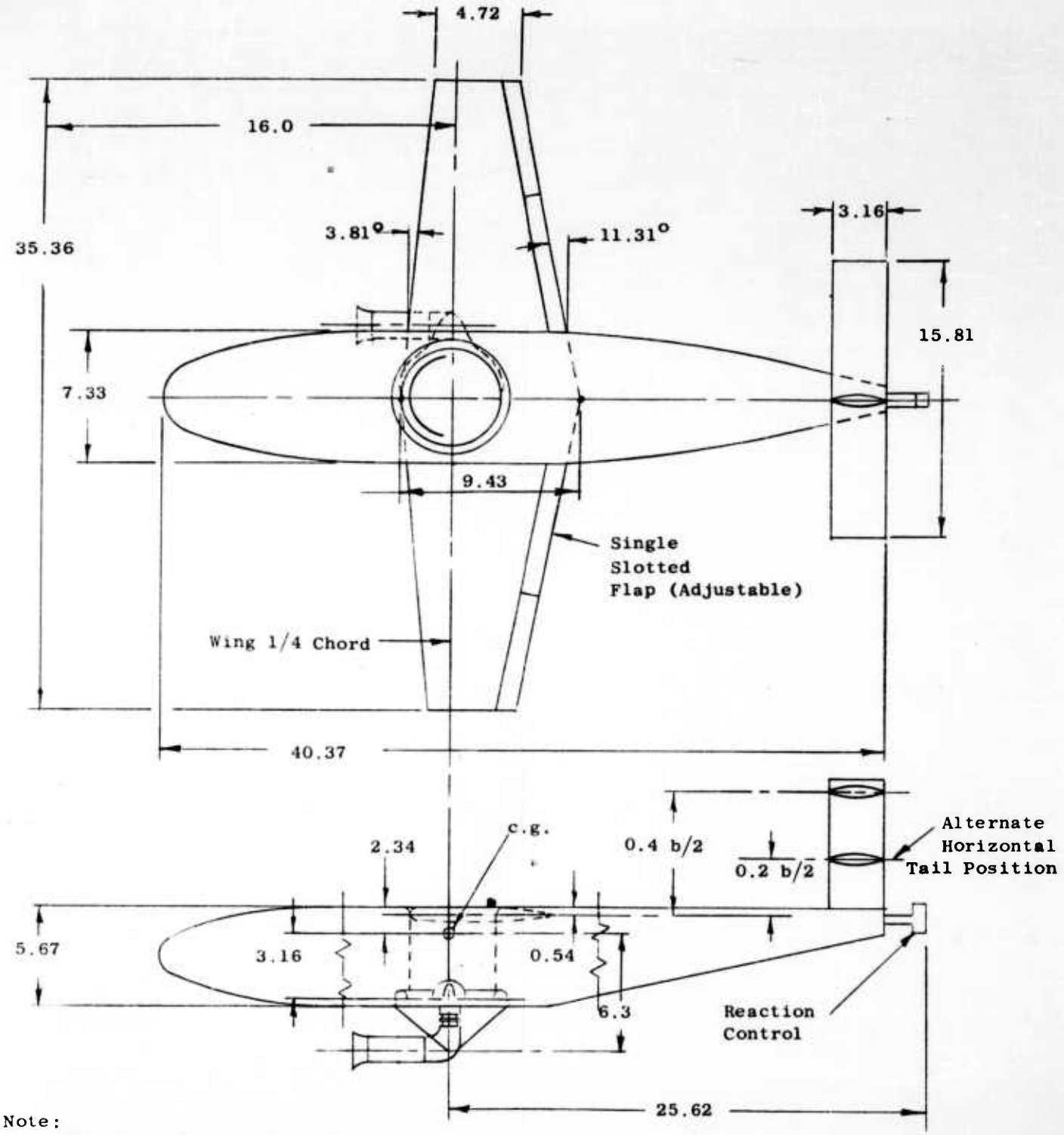

Note:
All Dimensions In Feet Unless
Otherwise Specified.

FIGURE 1. SKETCH OF NASA FULL-SCALE AIRCRAFT MODEL

GEOMETRIC DATA

WING

Area	250 Sq. Ft.
Aspect Ratio	5
Taper Ratio	0.5
Mean Aero. Chord	7.33 Ft.
Airfoil Section	NASA 63-210
Wing Loading	28 PSF.

HORIZONTAL TAIL

Area	50 Sq. Ft.
Aspect Ratio	5
Taper Ratio	1.0
Airfoil Section	NASA 63 A 012

VERTICAL TAIL

Area	25 Sq. Ft.
Aspect Ratio	2.5
Taper Ratio	1.0
Airfoil Section	NASA 63 A 015

C082602

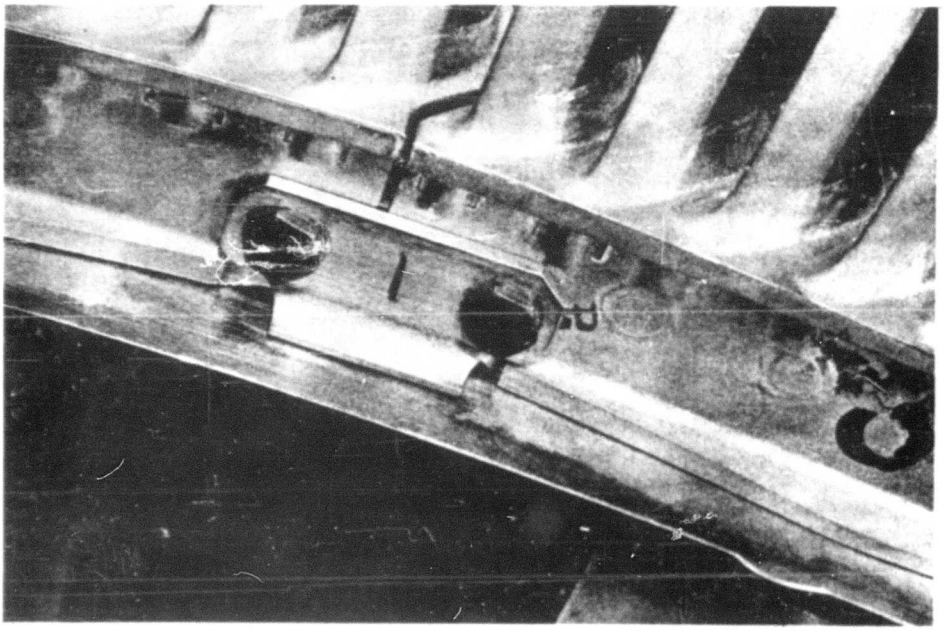

FIGURE 2 - CARRIER TAB INSTALLED

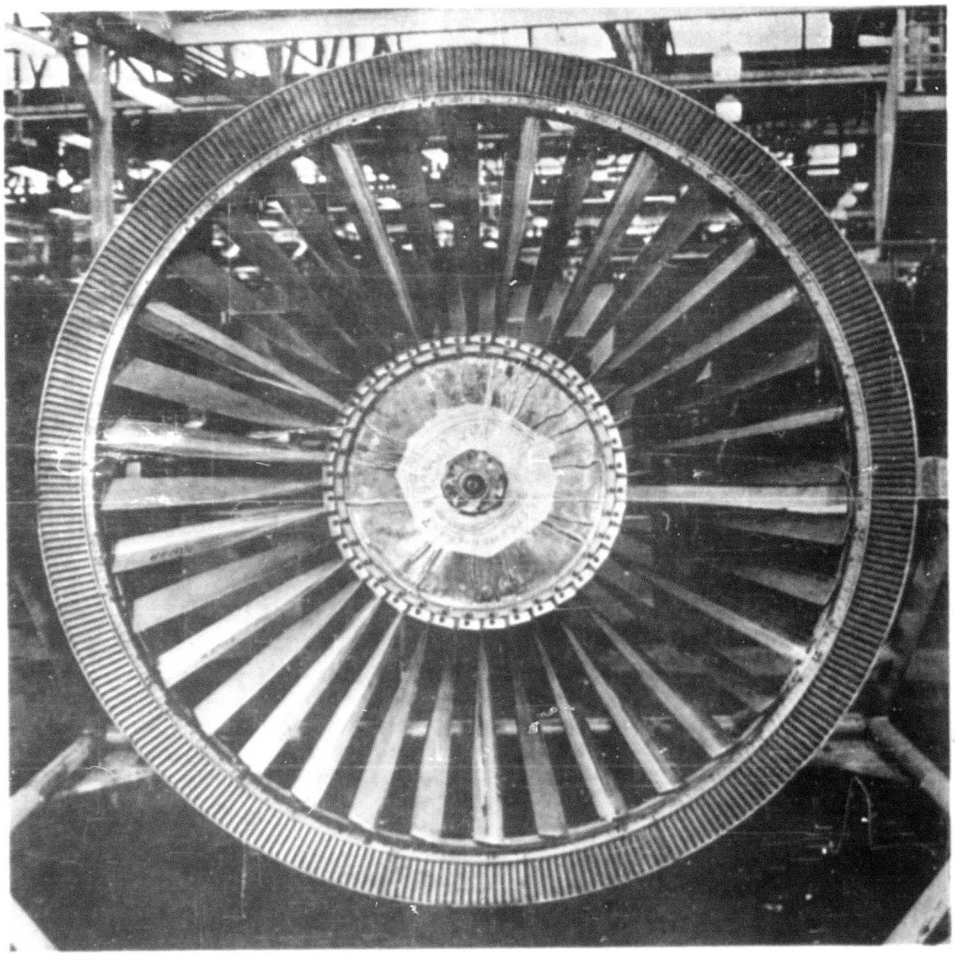

FIGURE 3 - ASSEMBLED ROTOR - BUILD-UP #3-001

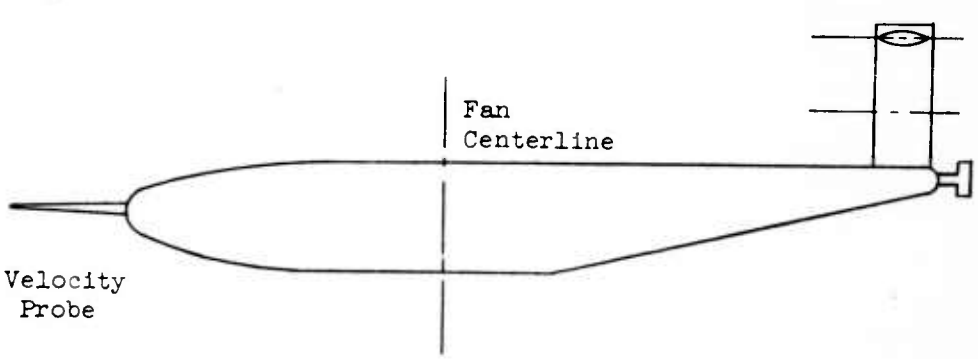

FIGURE 4 - VELOCITY PROBE LOCATION.

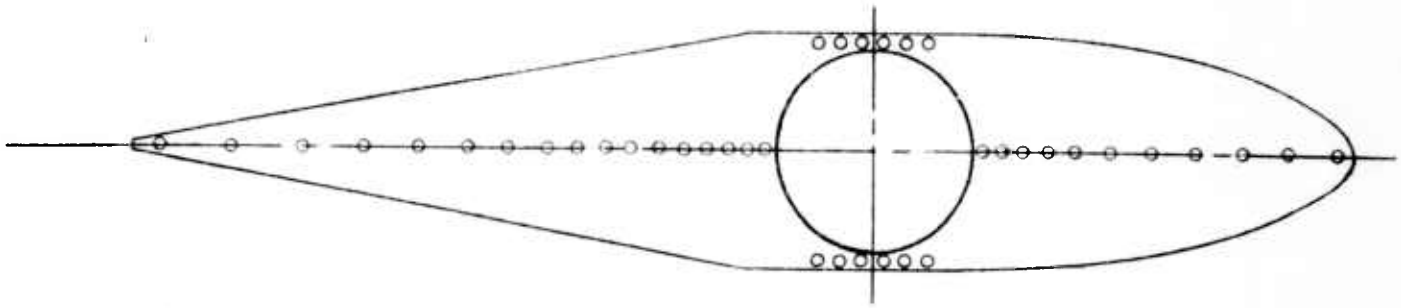

Bottom of Fuselage

NOTE:
Not to scale.

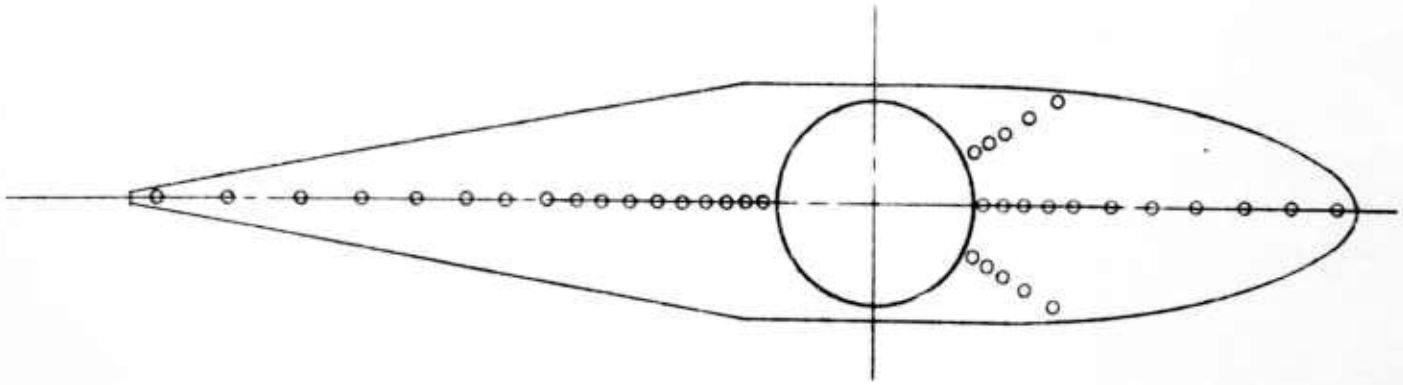

Top of Fuselage

FIGURE 5 - STATIC PRESSURE TAP LOCATIONS ON THE FUSELAGE

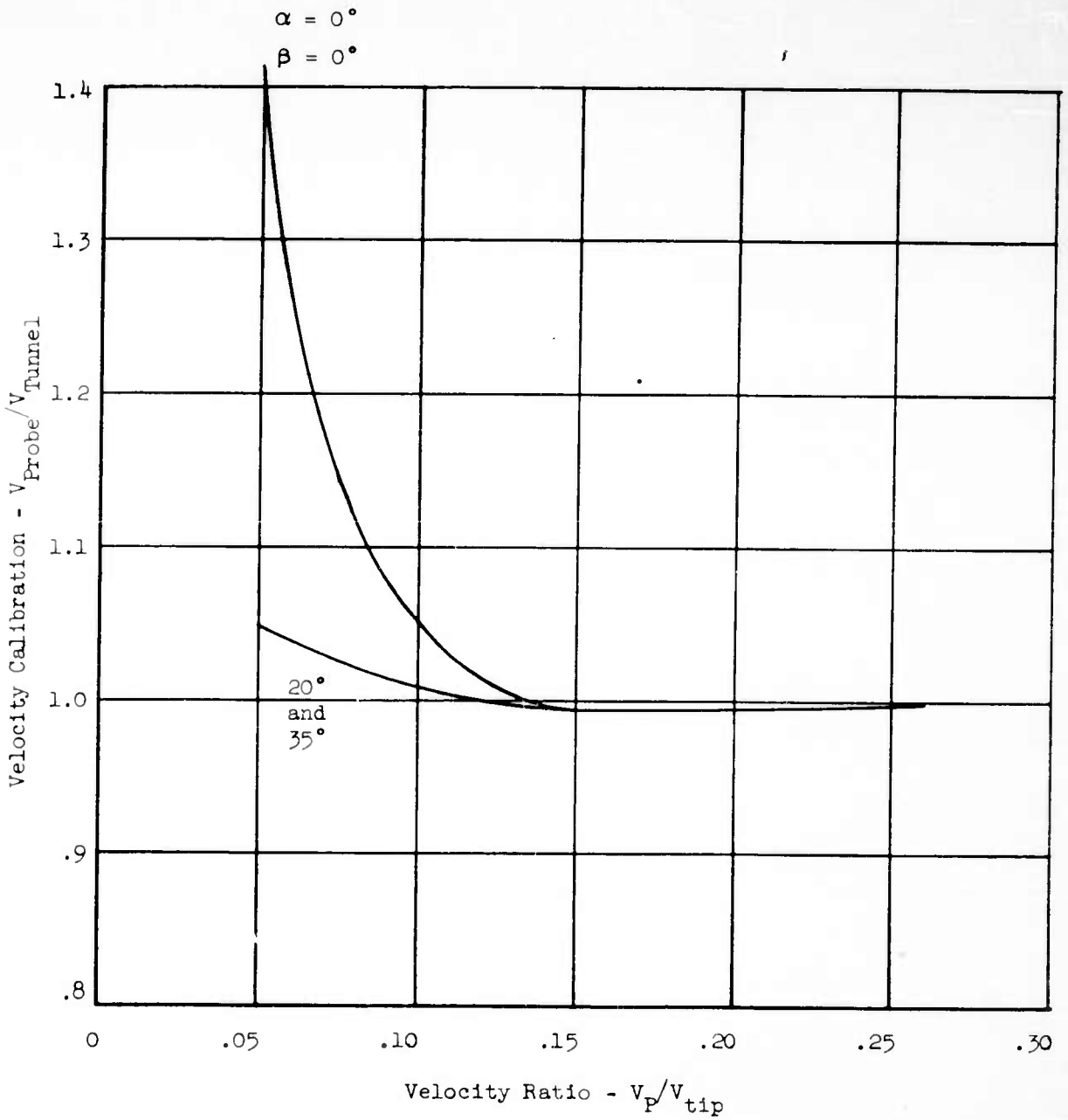

FIGURE 6 - VELOCITY CALIBRATION VS. VELOCITY RATIO.

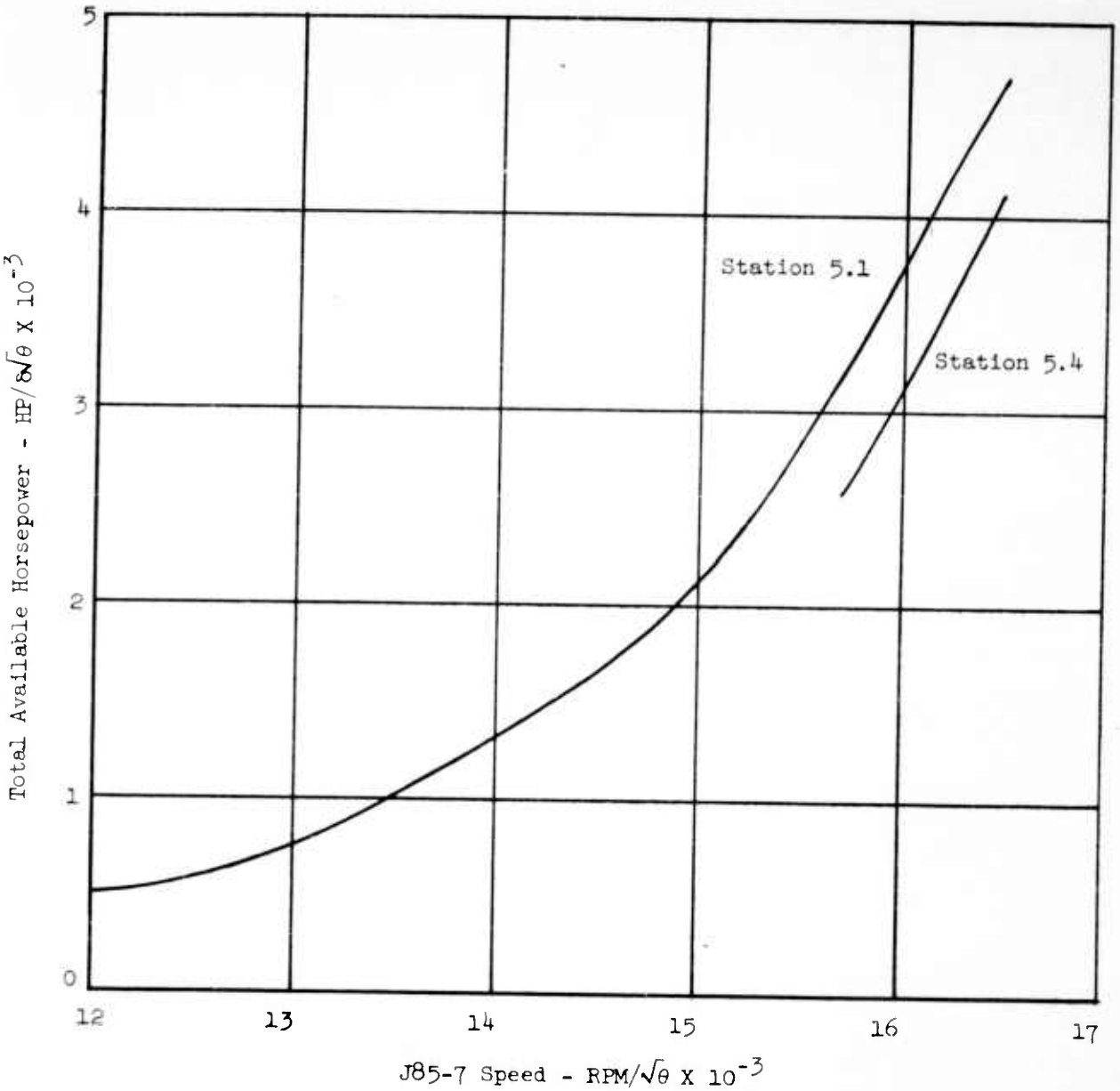

FIGURE 7 - TOTAL AVAILABLE HORSEPOWER VERSUS ENGINE SPEED

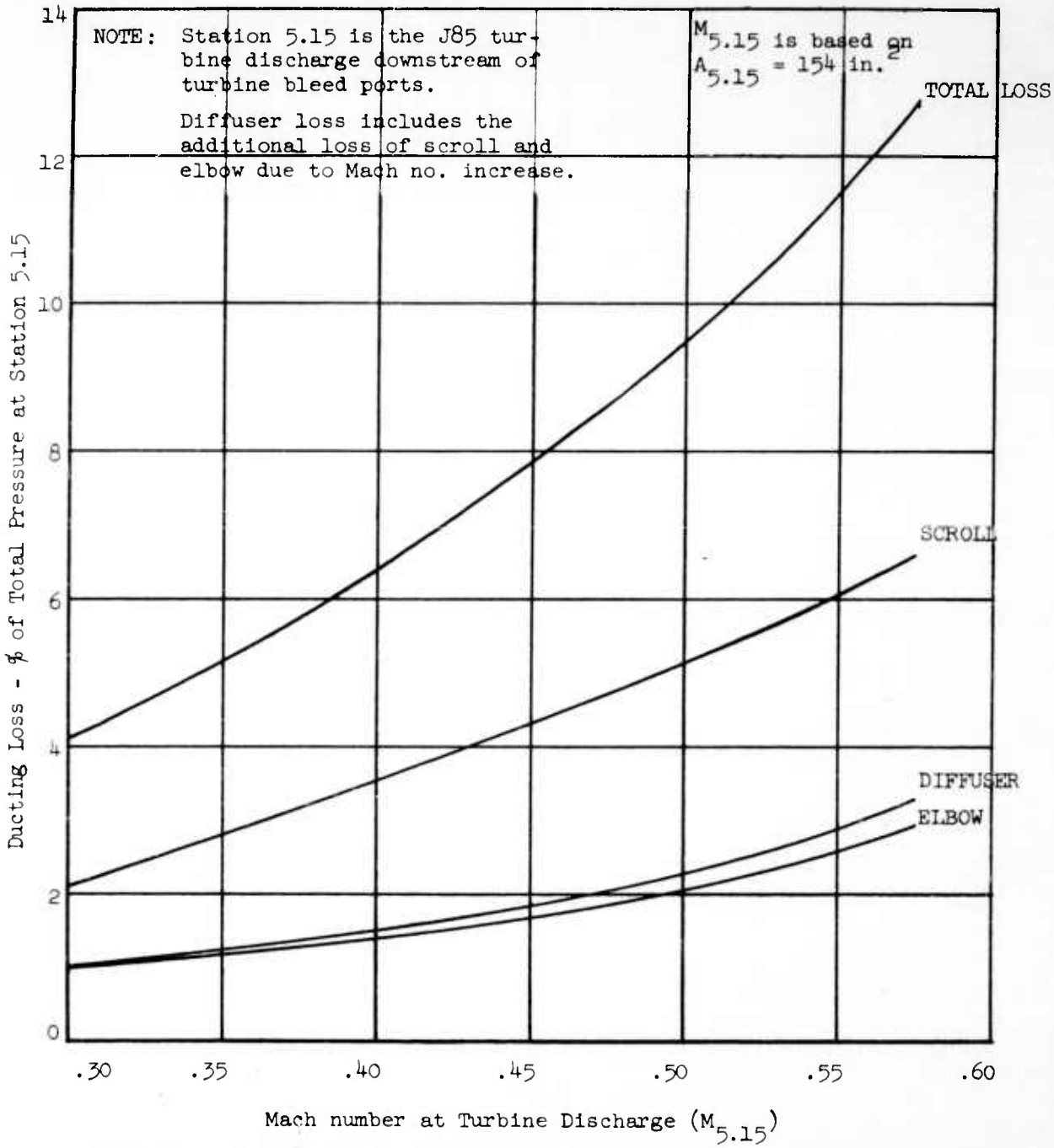

FIGURE 8 - DUCTING LOSSES VERSUS TURBINE DISCHARGE MACH NUMBER

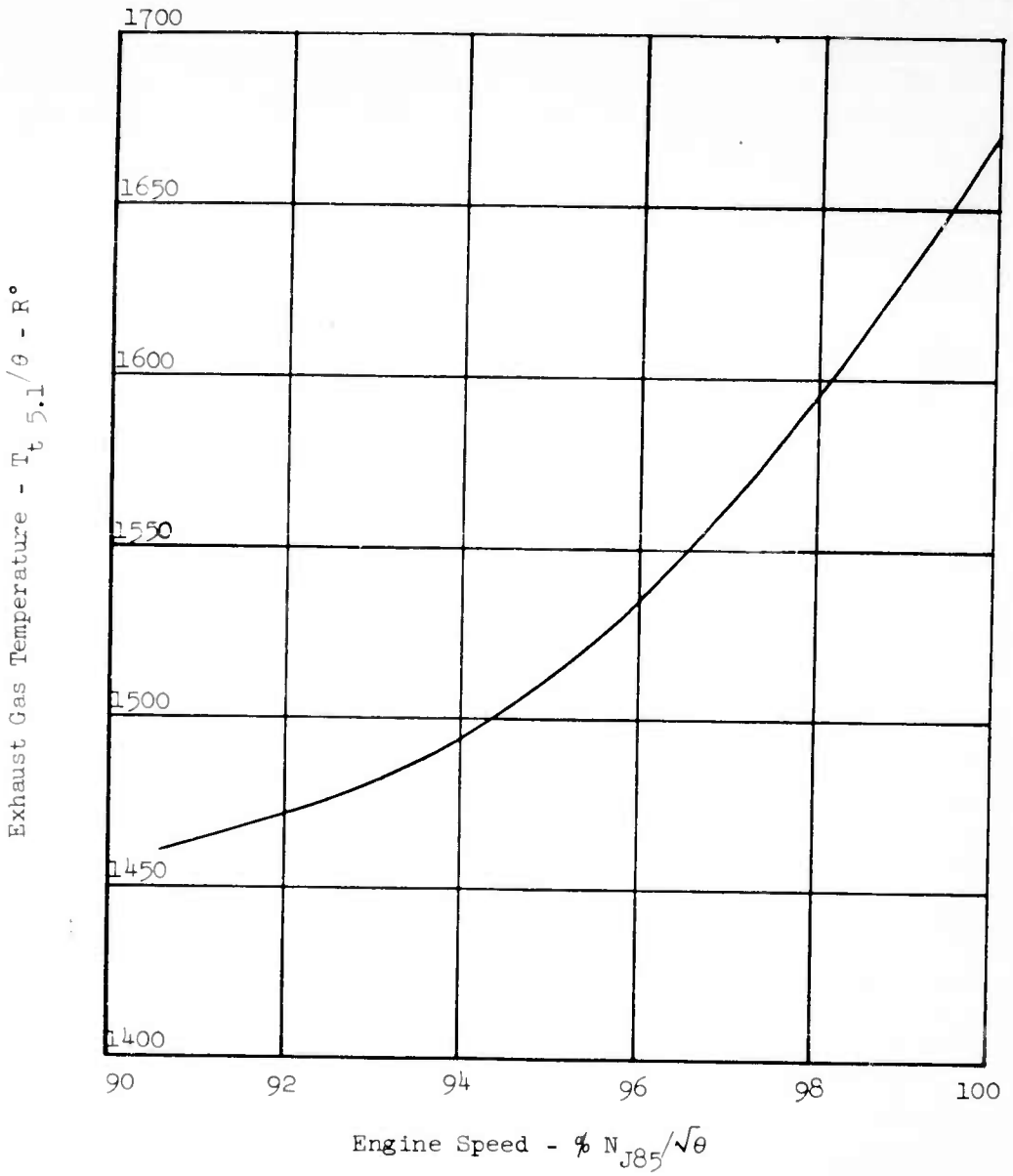

FIGURE 9 - EXHAUST GAS TEMPERATURE (EGT) VERSUS J85-7 SPEED

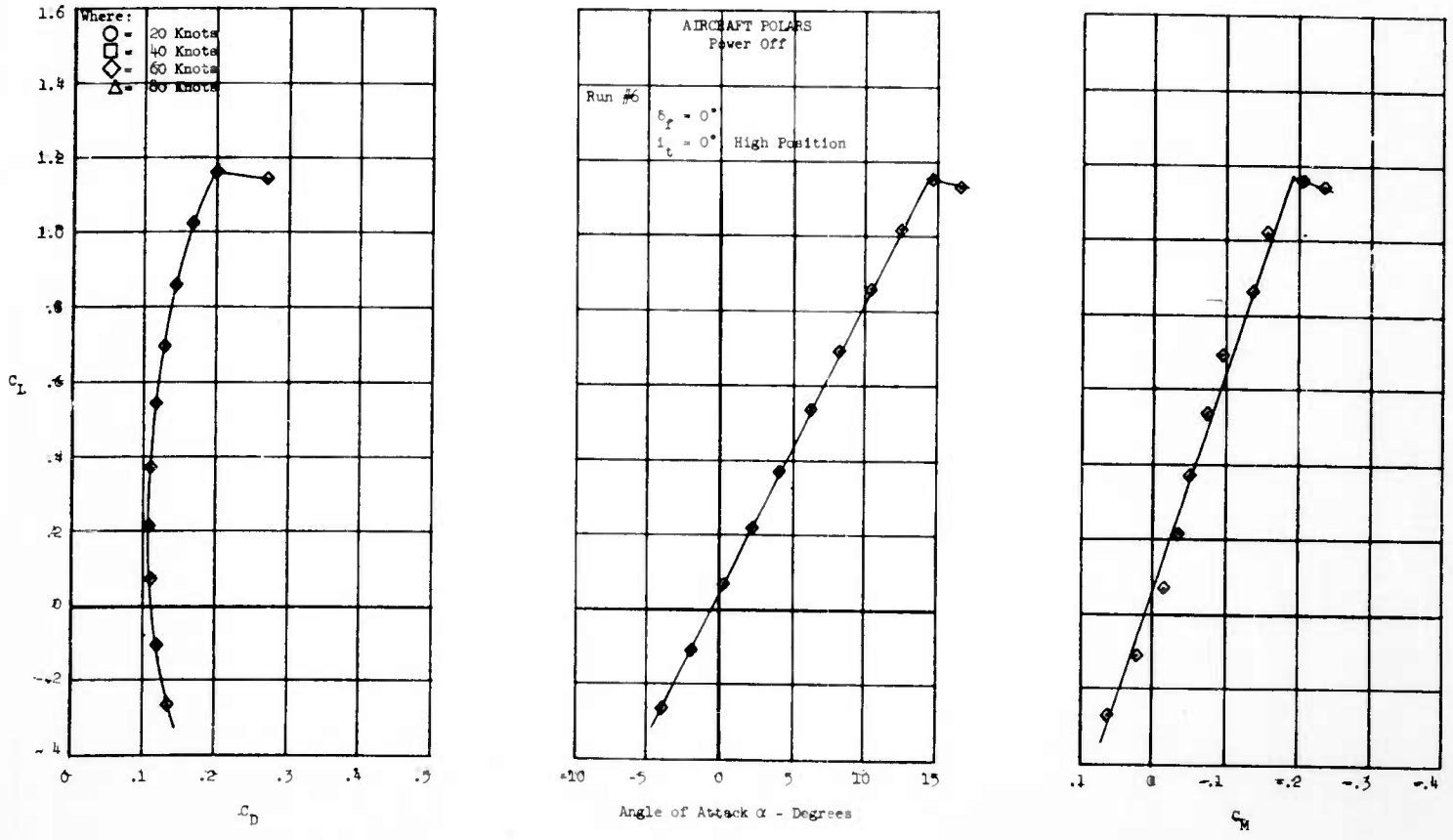

FIGURE 10 - UNPOWERED AIRCRAFT PERFORMANCE

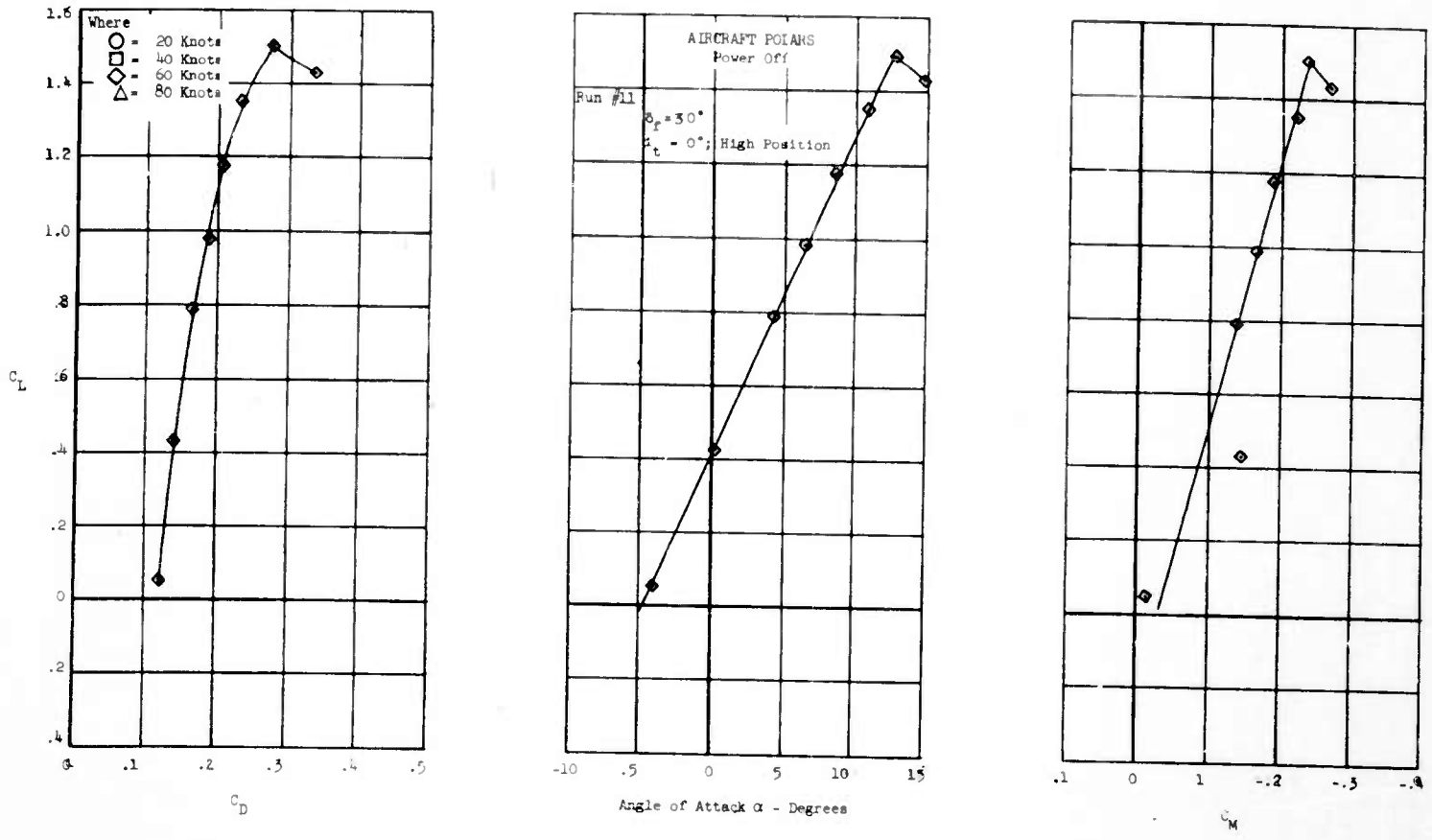

FIGURE 11 - UNPOWERED AIRCRAFT PERFORMANCE

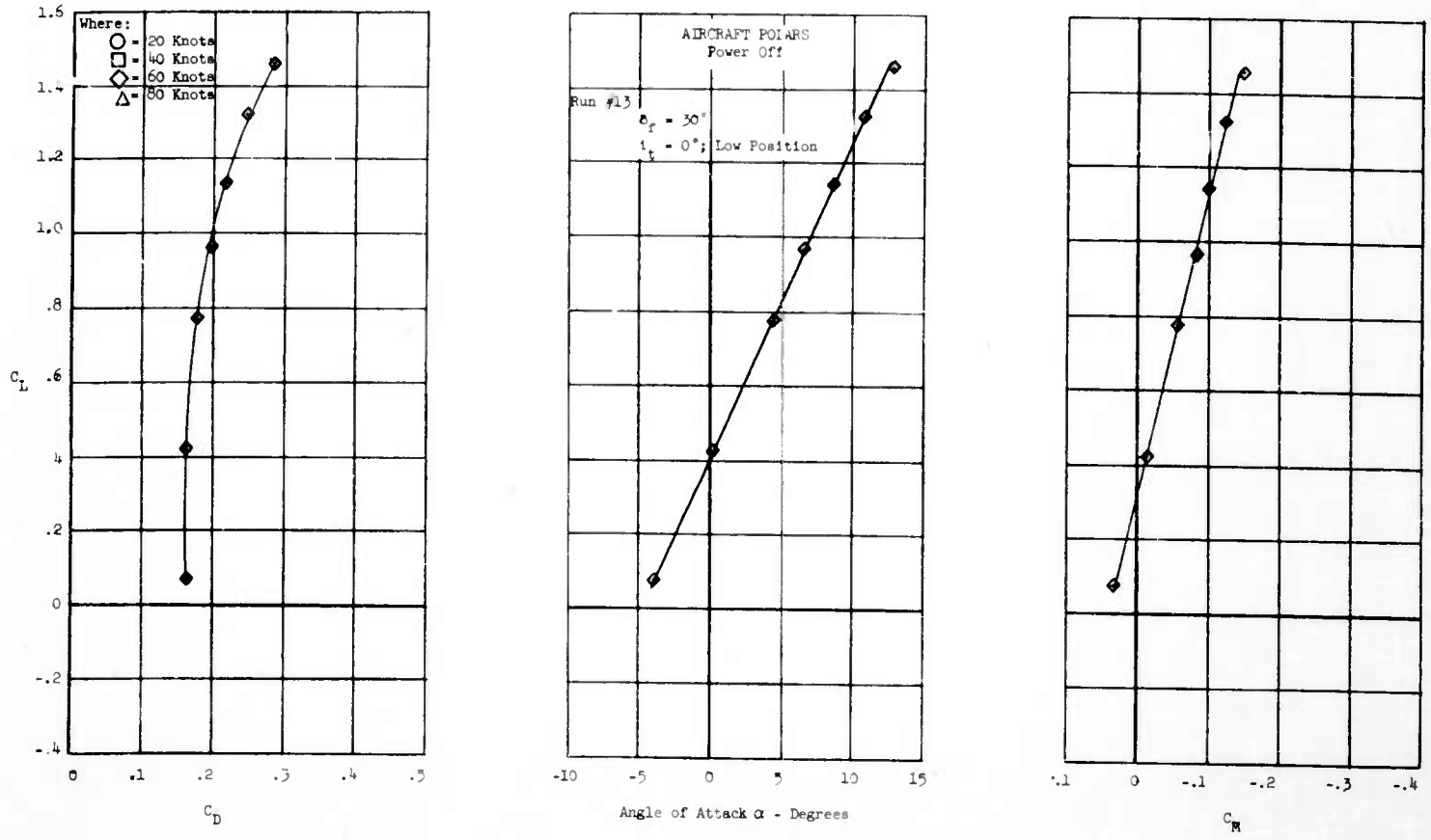

FIGURE 12 - UNPOWERED AIRCRAFT PERFORMANCE

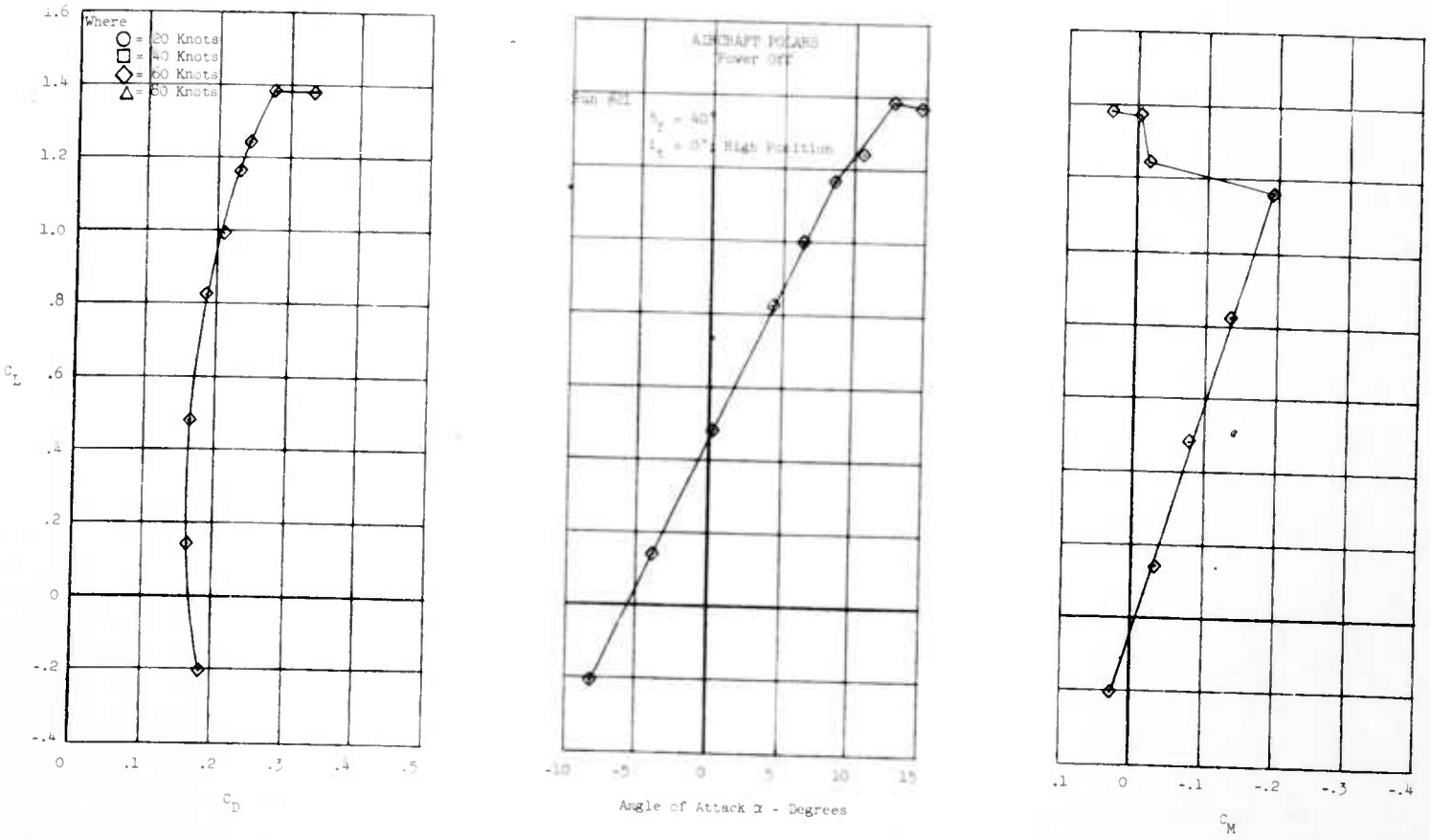

FIGURE 13 - UNPOWERED AIRCRAFT PERFORMANCE

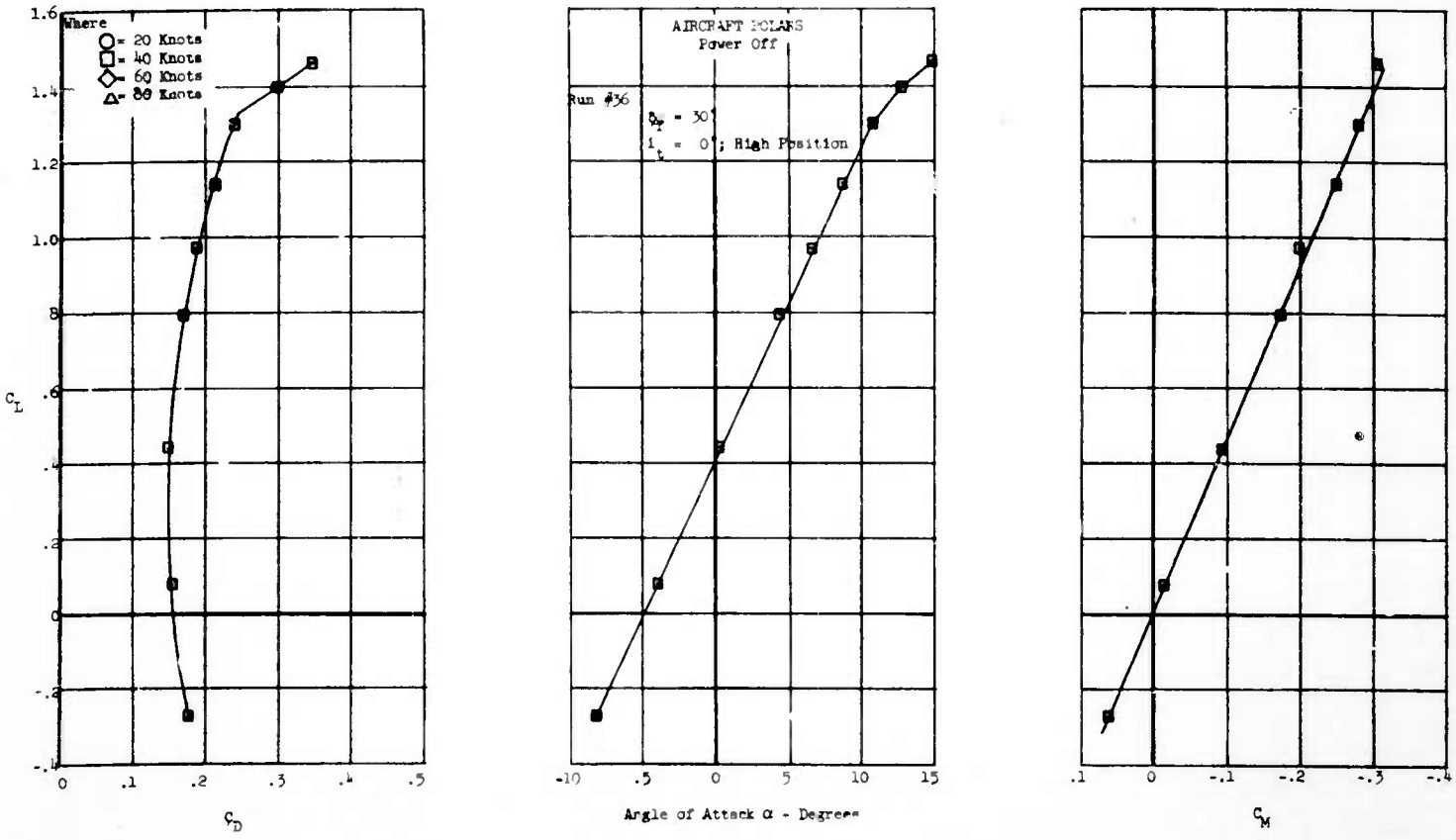

FIGURE 14 - UNPOWERED AIRCRAFT PERFORMANCE

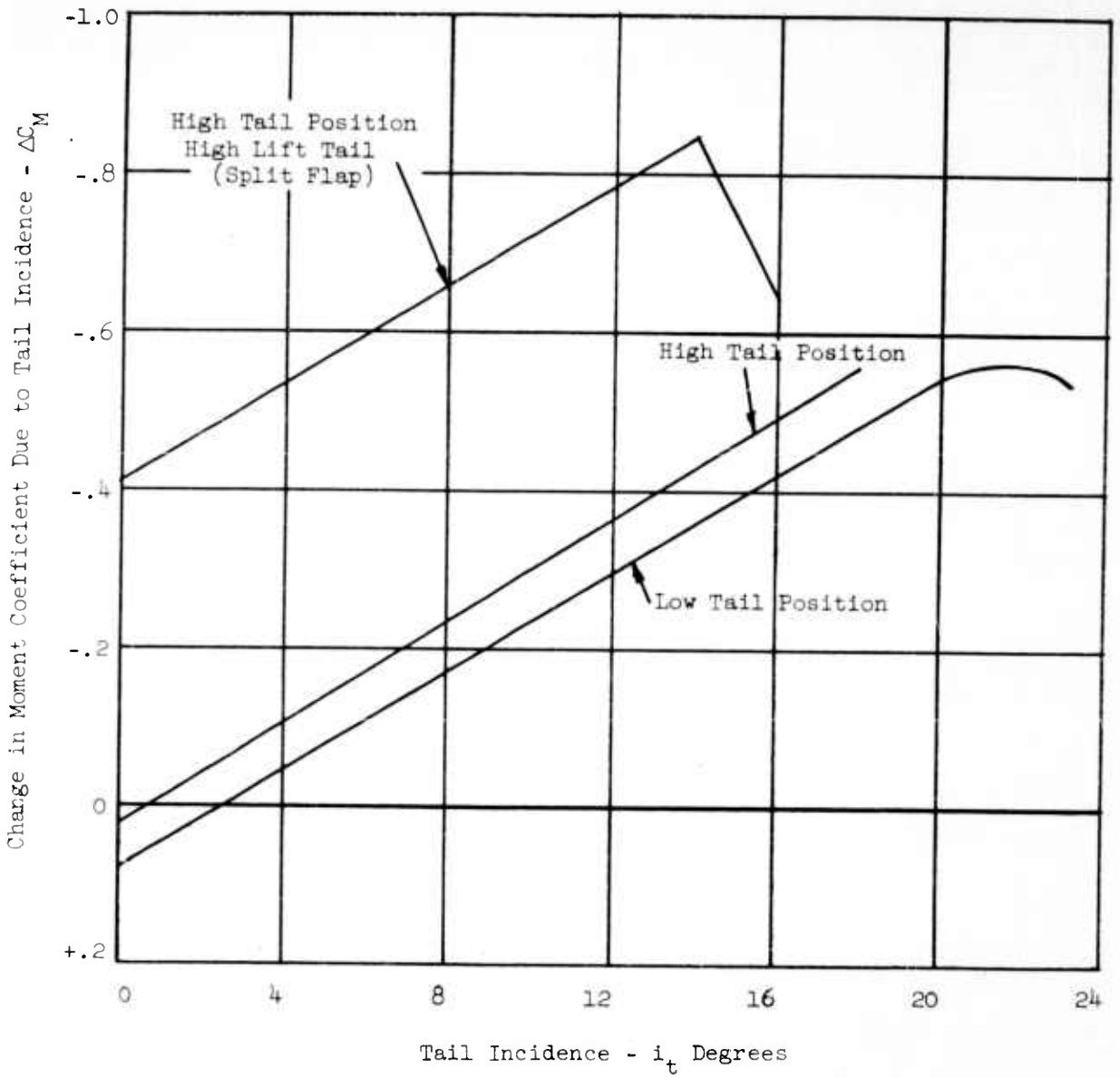

FIGURE 15 - HORIZONTAL TAIL EFFECTIVENESS

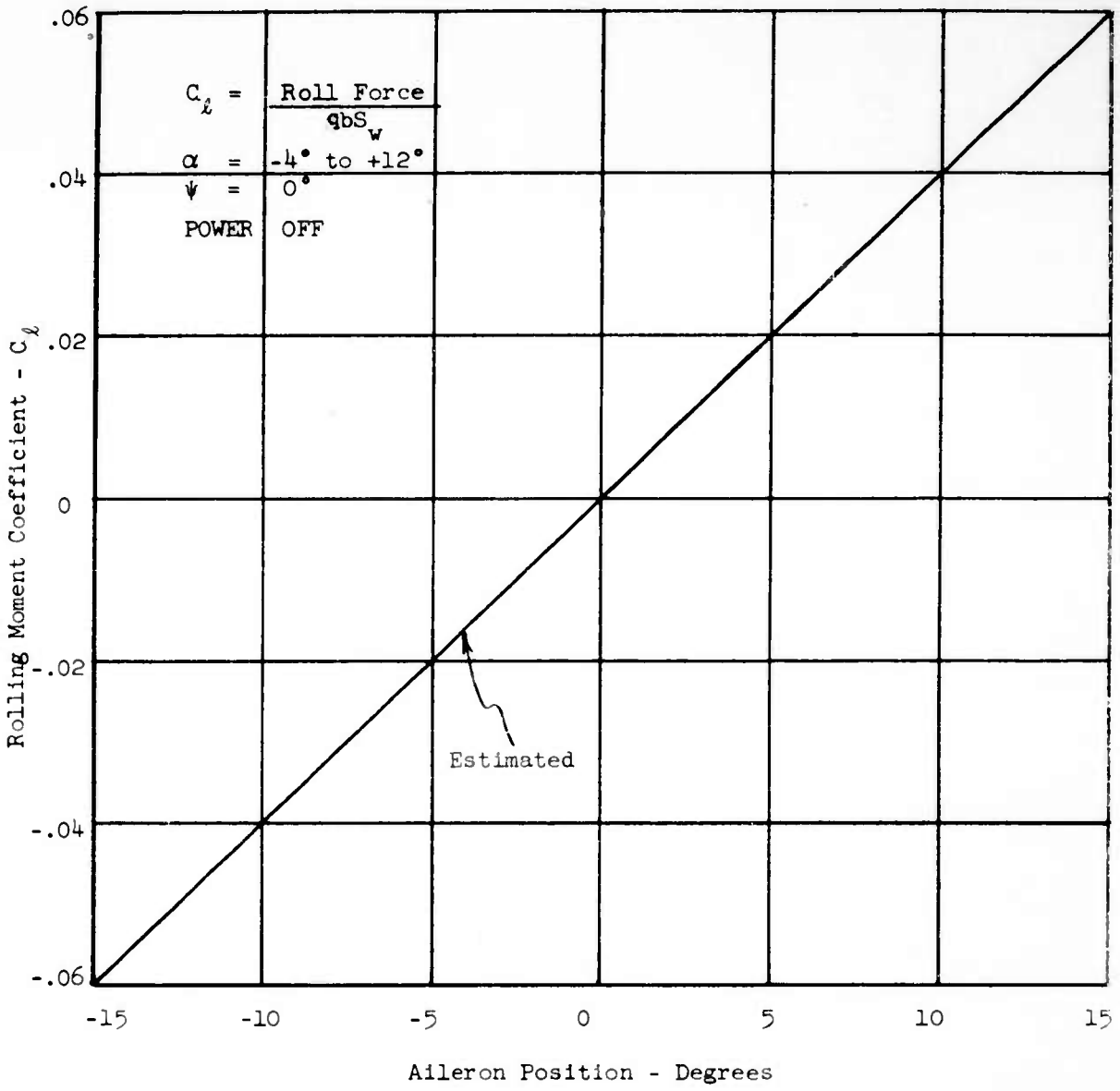

FIGURE 16 - ROLL COEFFICIENT VERSUS AILERON POSITION

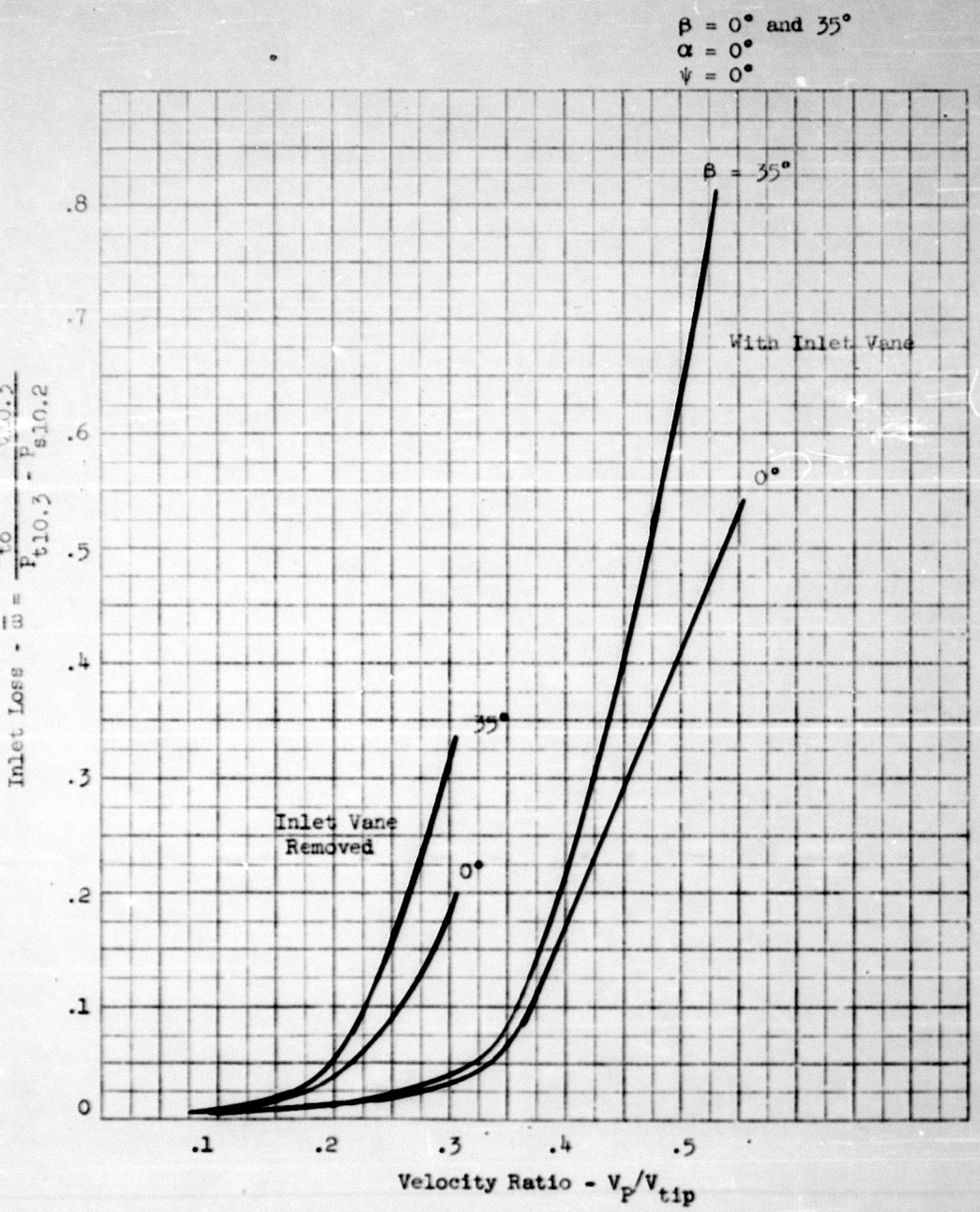

FIGURE 17 - FAN INLET LOSS VERSUS VELOCITY RATIO

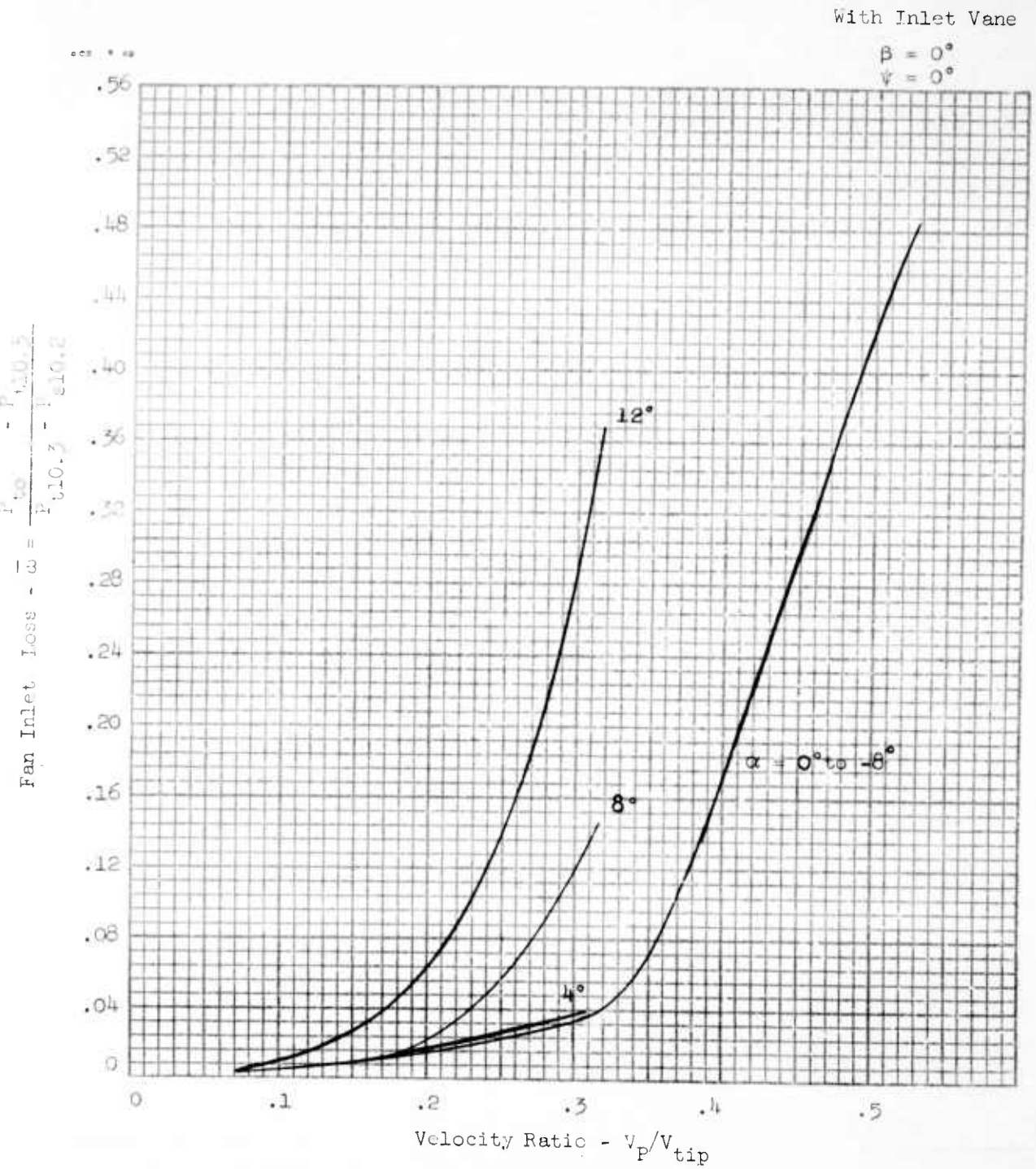

FIGURE 18 - FAN INLET LOSS VERSUS VELOCITY RATIO

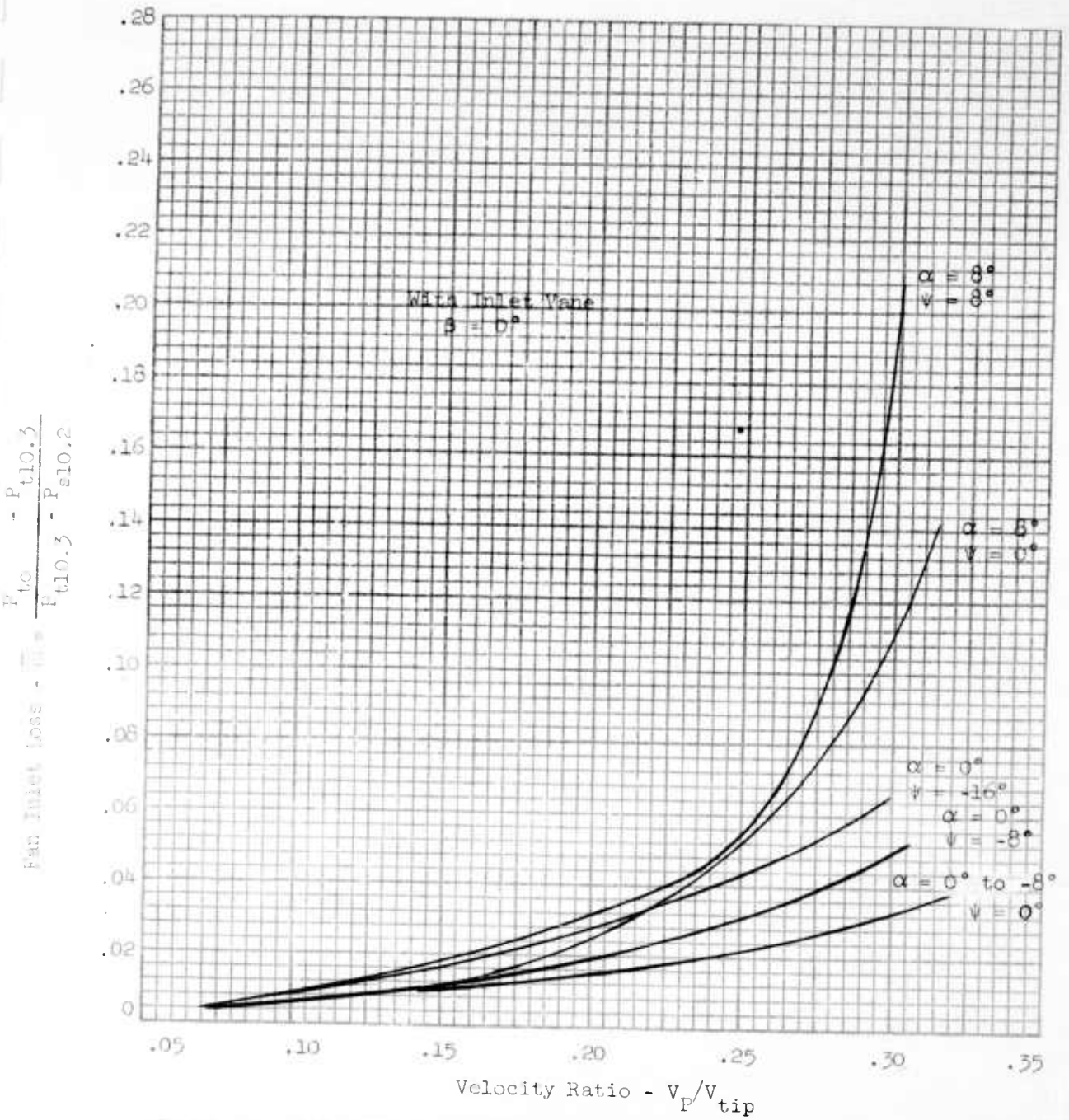

FIGURE 19 - FAN INLET LOSS VERSUS VELOCITY RATIO

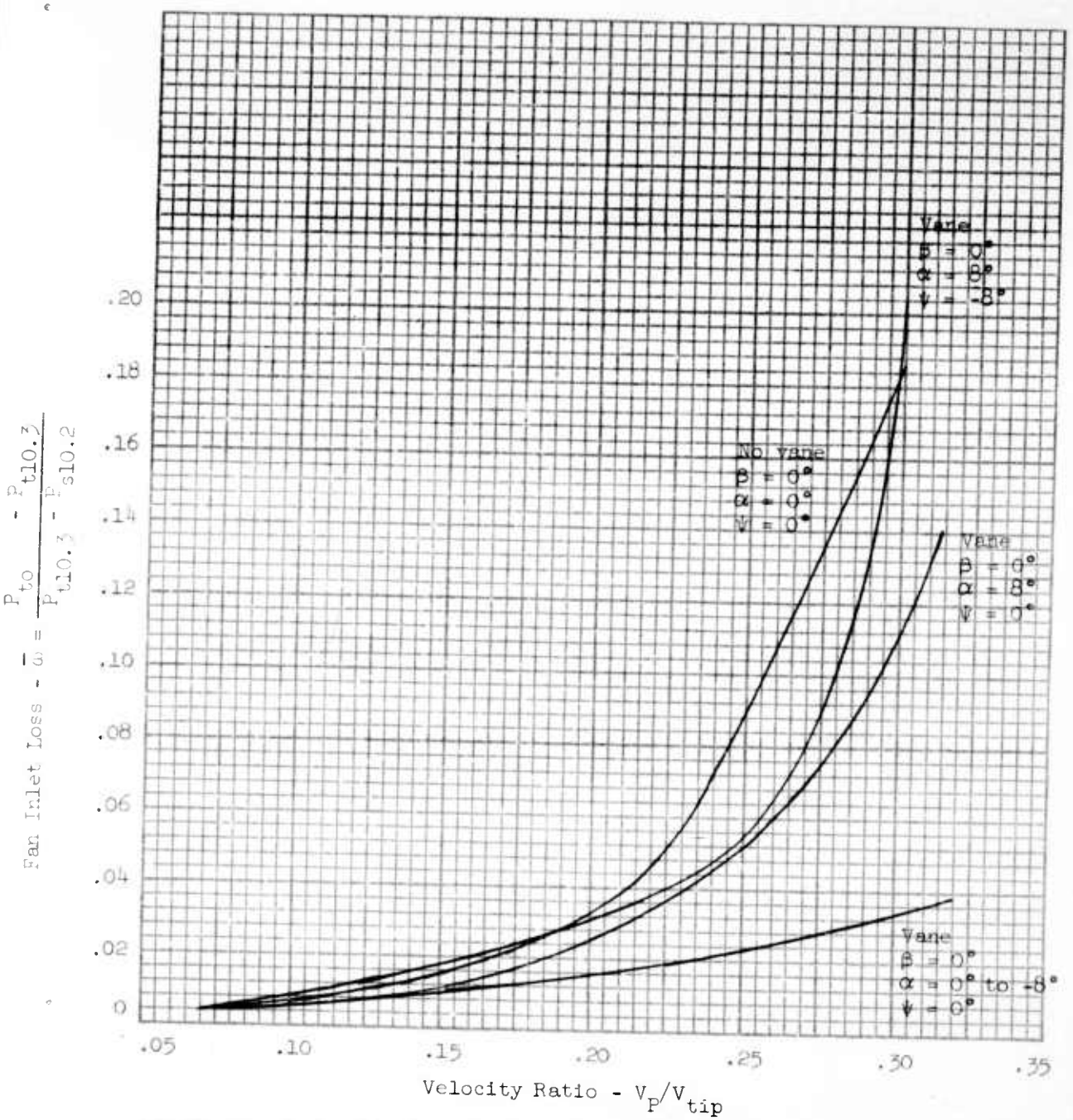

FIGURE 20 - FAN INLET LOSS VERSUS VELOCITY RATIO

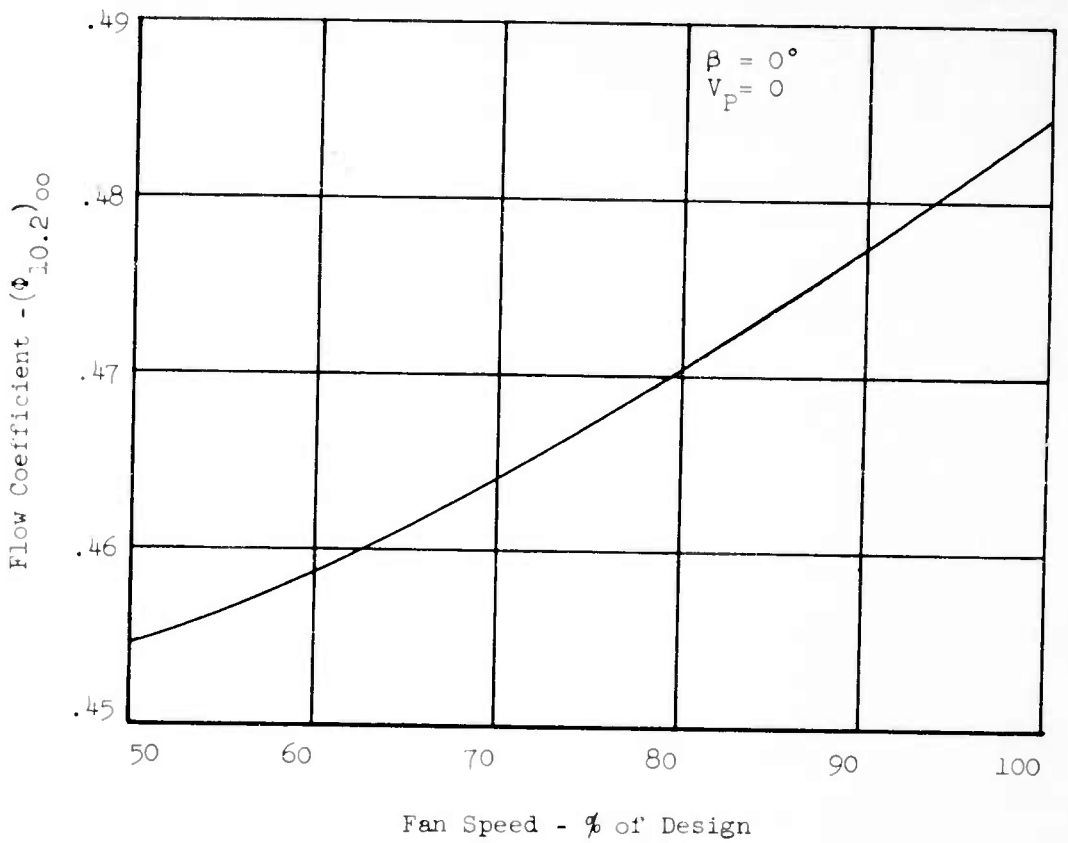

FIGURE 21 - STATIC FLOW COEFFICIENT FOR FAN INLET DUCT VERSUS FAN SPEED

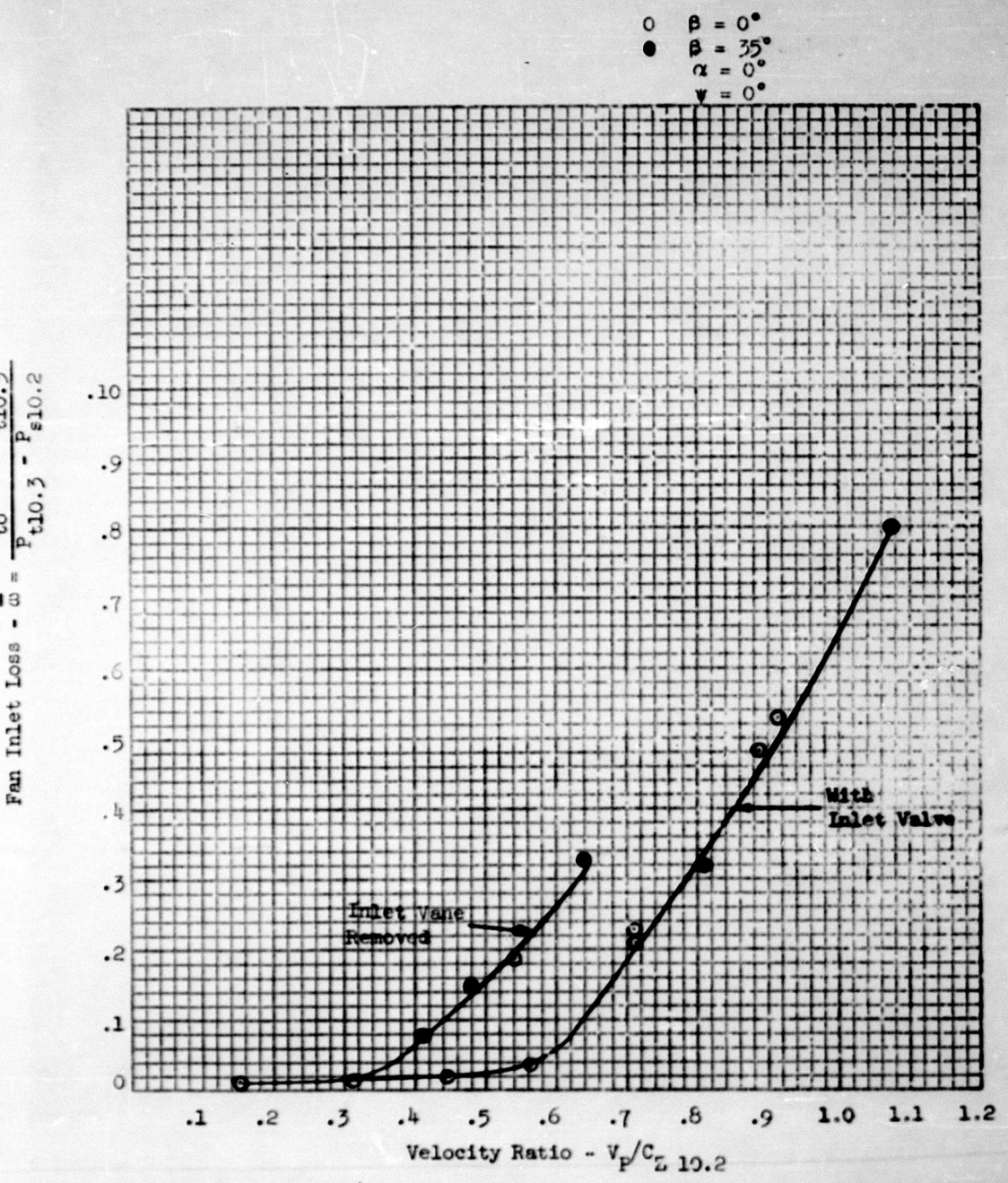

FIGURE 22 - FAN INLET LOSS VERSUS VELOCITY RATIO

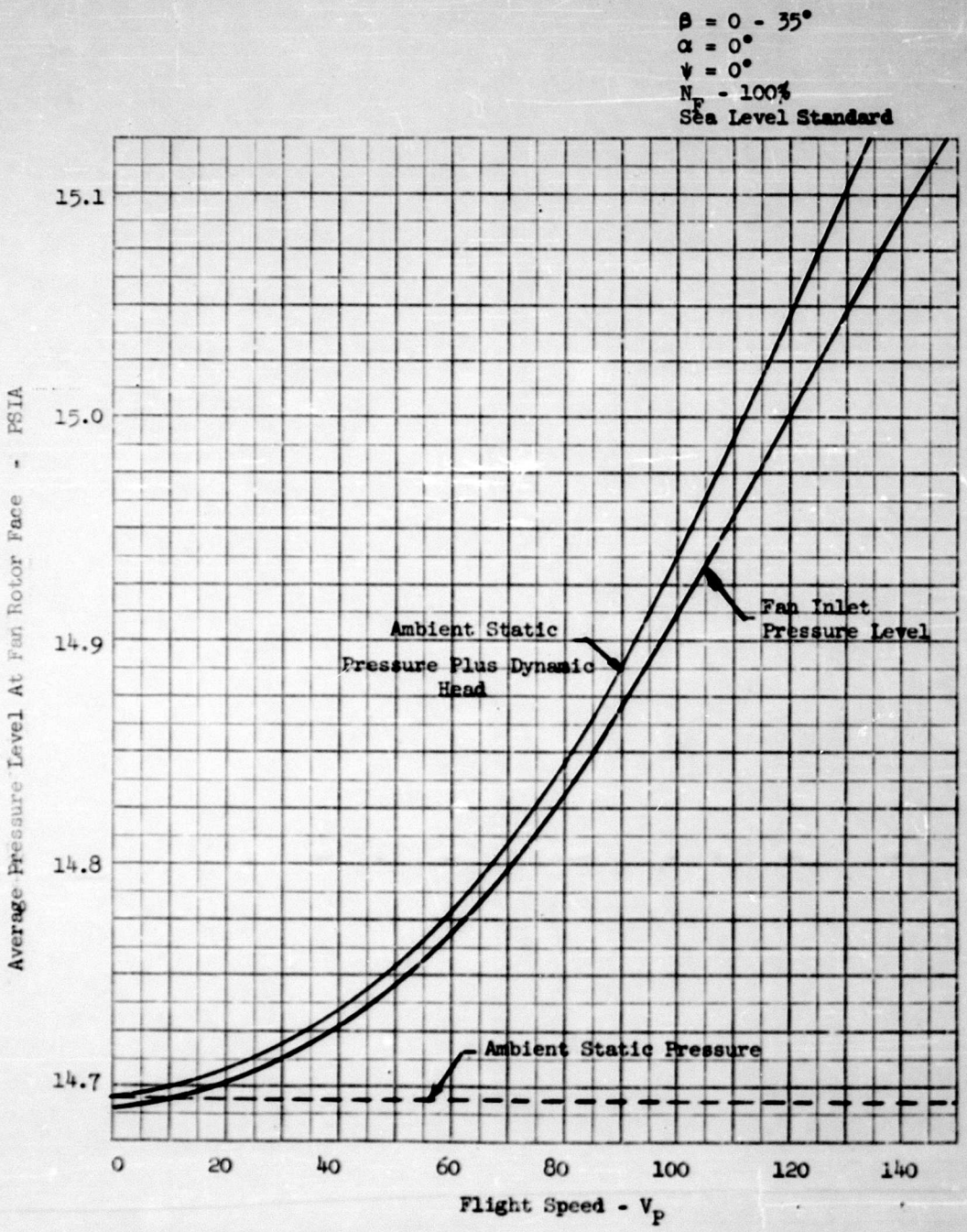

FIGURE 23 - FAN INLET PRESSURE VERSUS FLIGHT SPEED

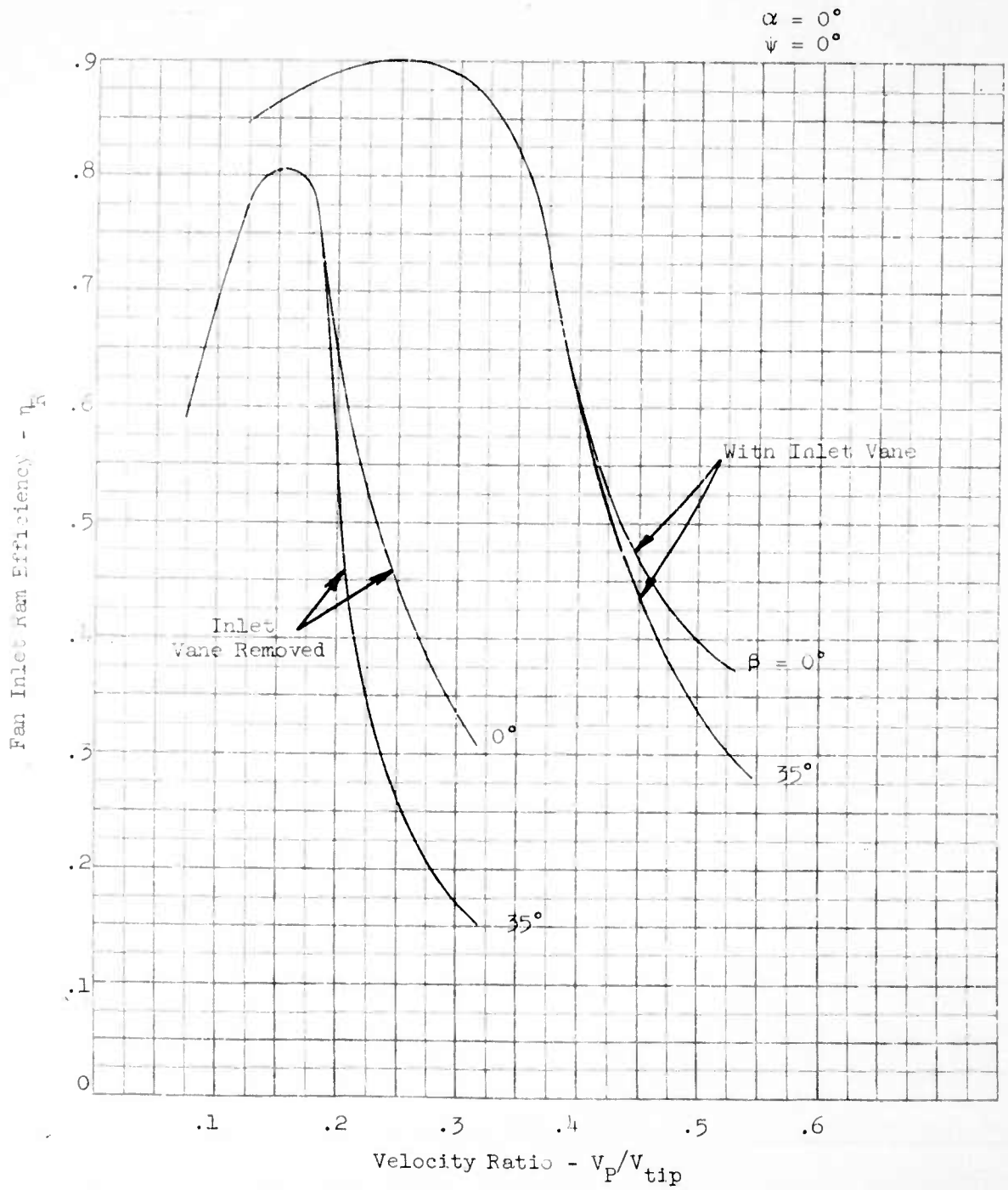

FIGURE 24 - FAN INLET RAM RECOVERY VERSUS VELOCITY RATIO

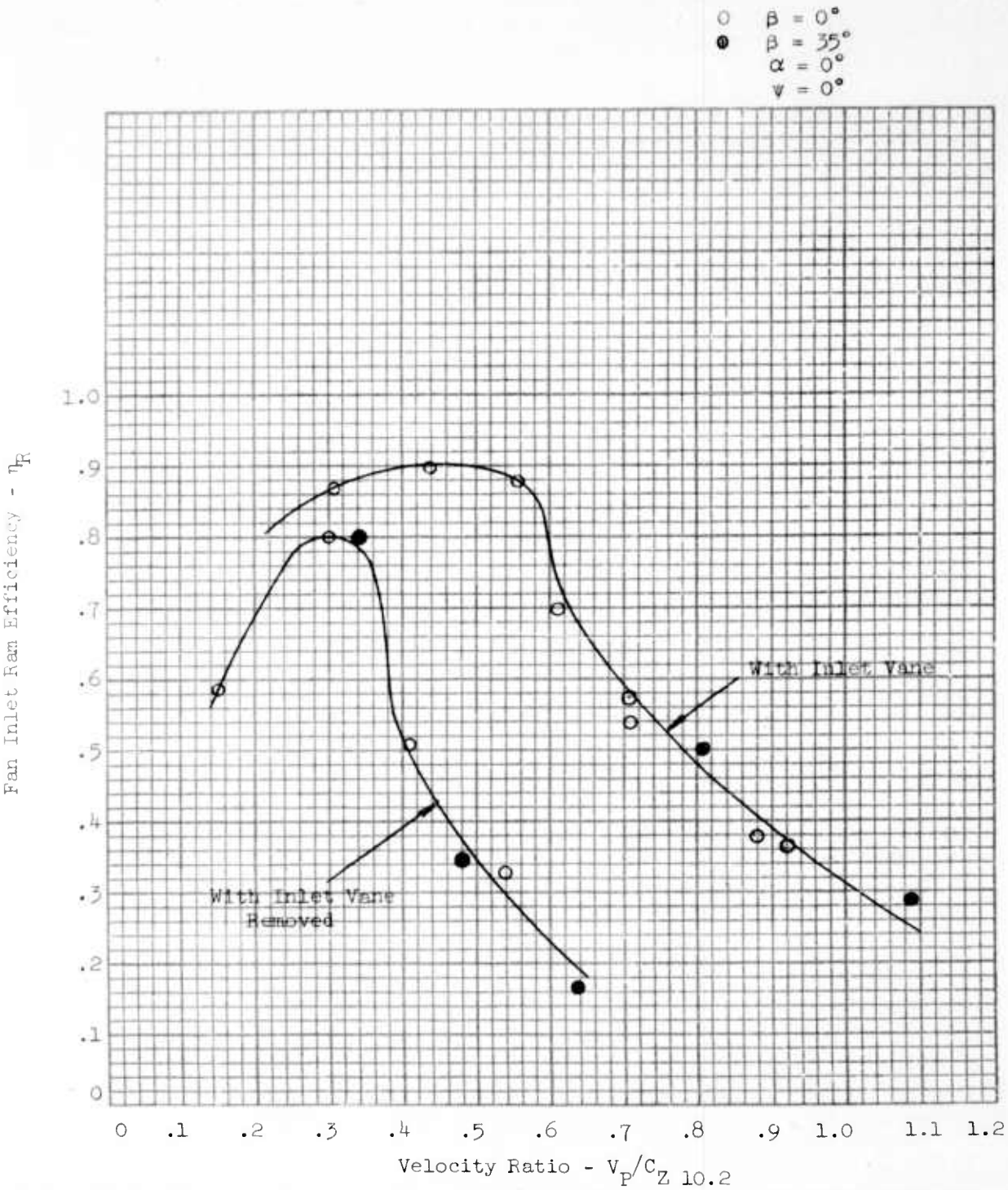

FIGURE 25 - FAN INLET RAM RECOVERY VERSUS VELOCITY RATIO

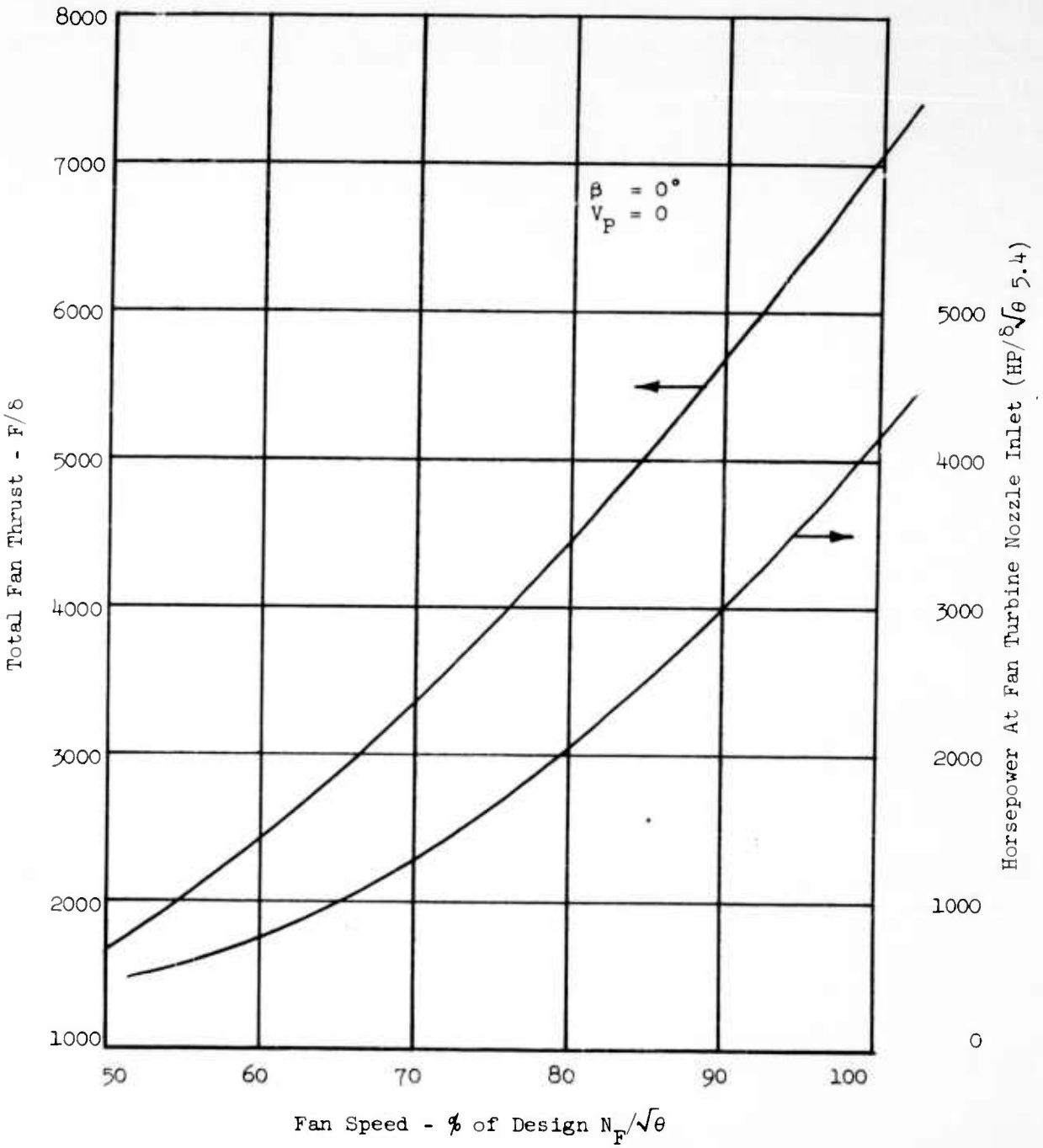

FIGURE 26 - TOTAL FAN THRUST AND ISENTROPIC HORSEPOWER VERSUS FAN SPEED

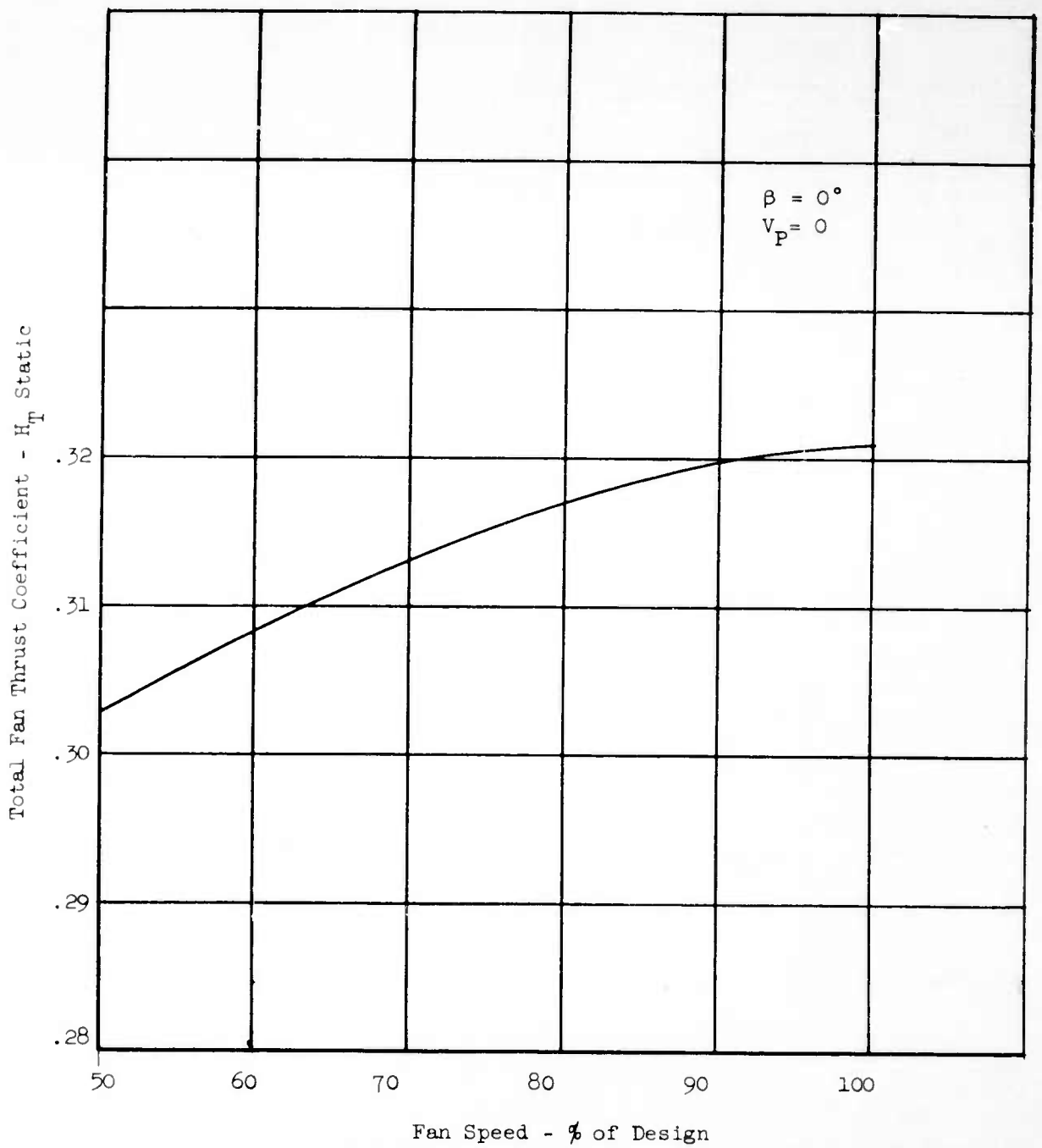

FIGURE 27 - TOTAL FAN THRUST COEFFICIENT VERSUS FAN SPEED

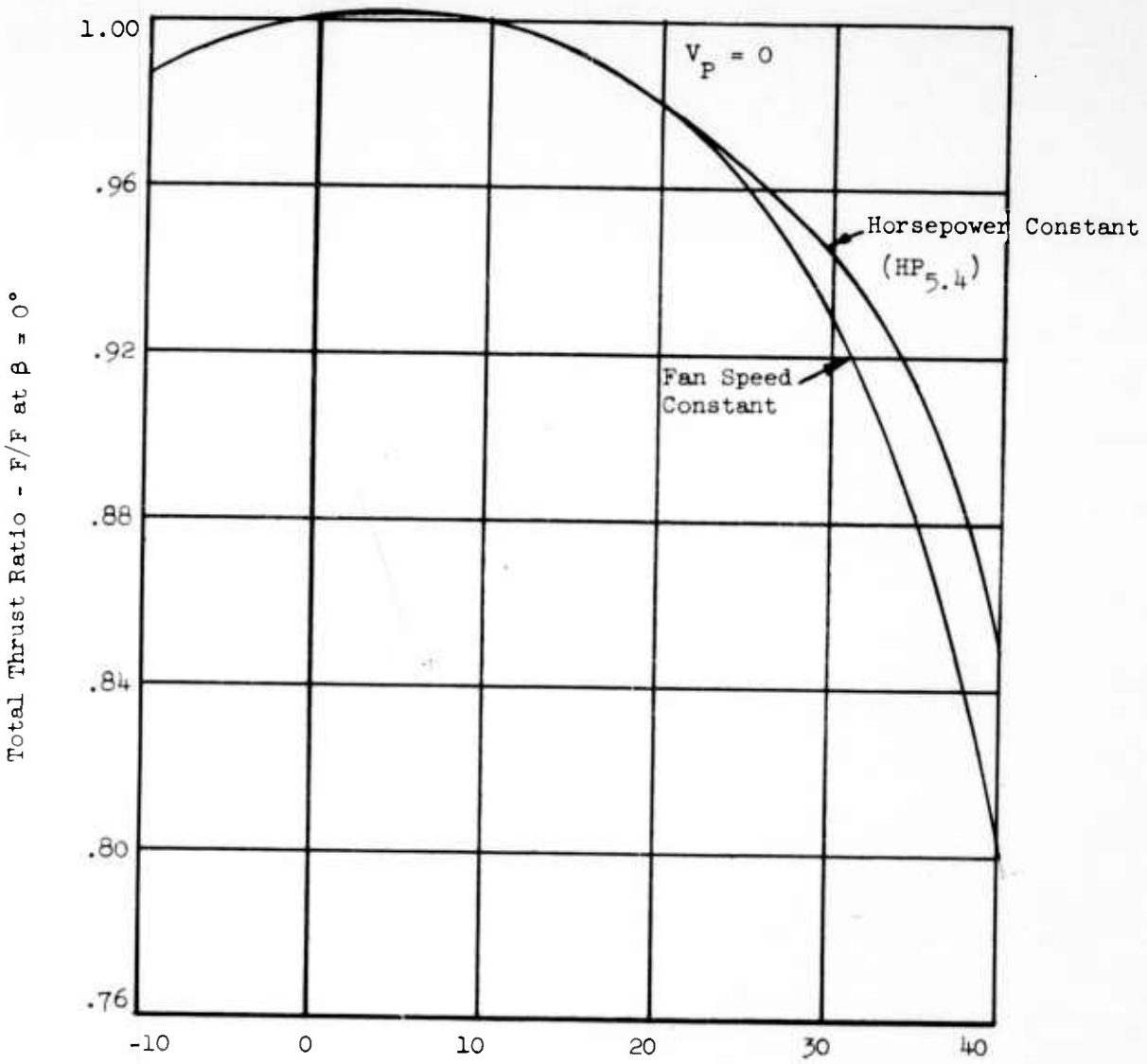

FIGURE 28a - TOTAL THRUST RATIO VERSUS INDICATED LOUVER ANGLE (β)

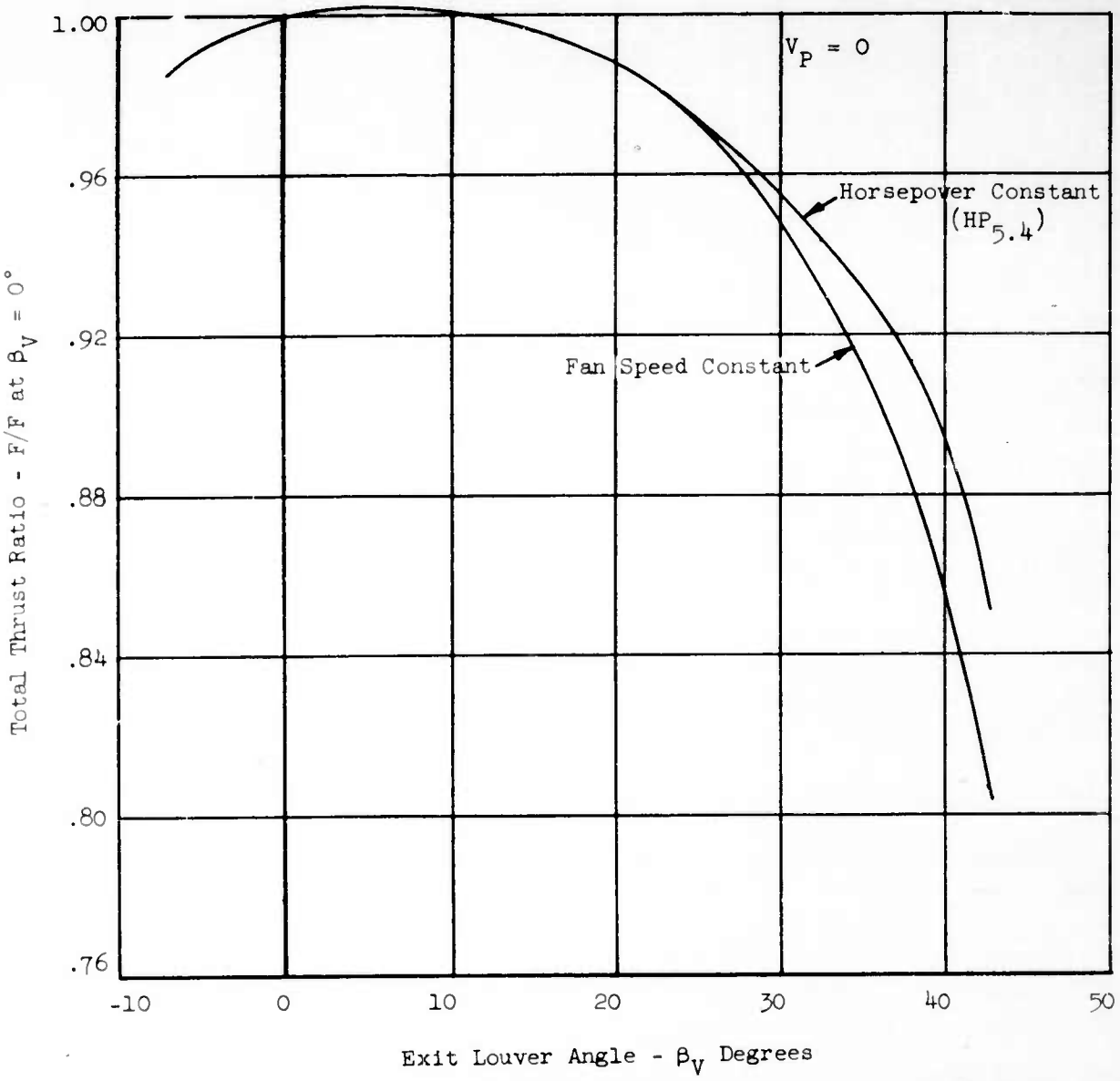

FIGURE 28b - TOTAL THRUST RATIO VERSUS ACTUAL TURNING ANGLE (β_V)

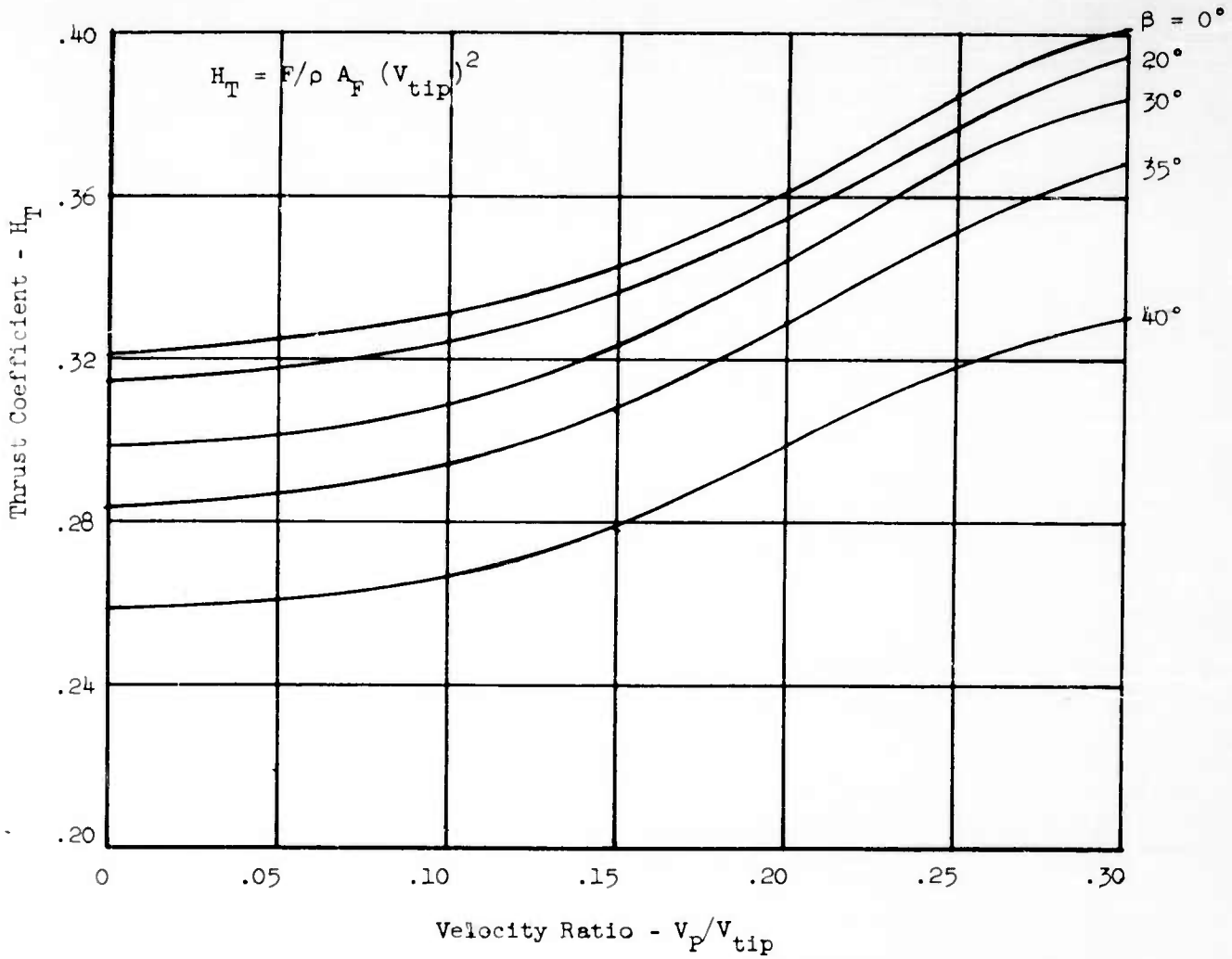

FIGURE 29 - TOTAL FAN THRUST COEFFICIENT (H_T) VS. VELOCITY RATIO.

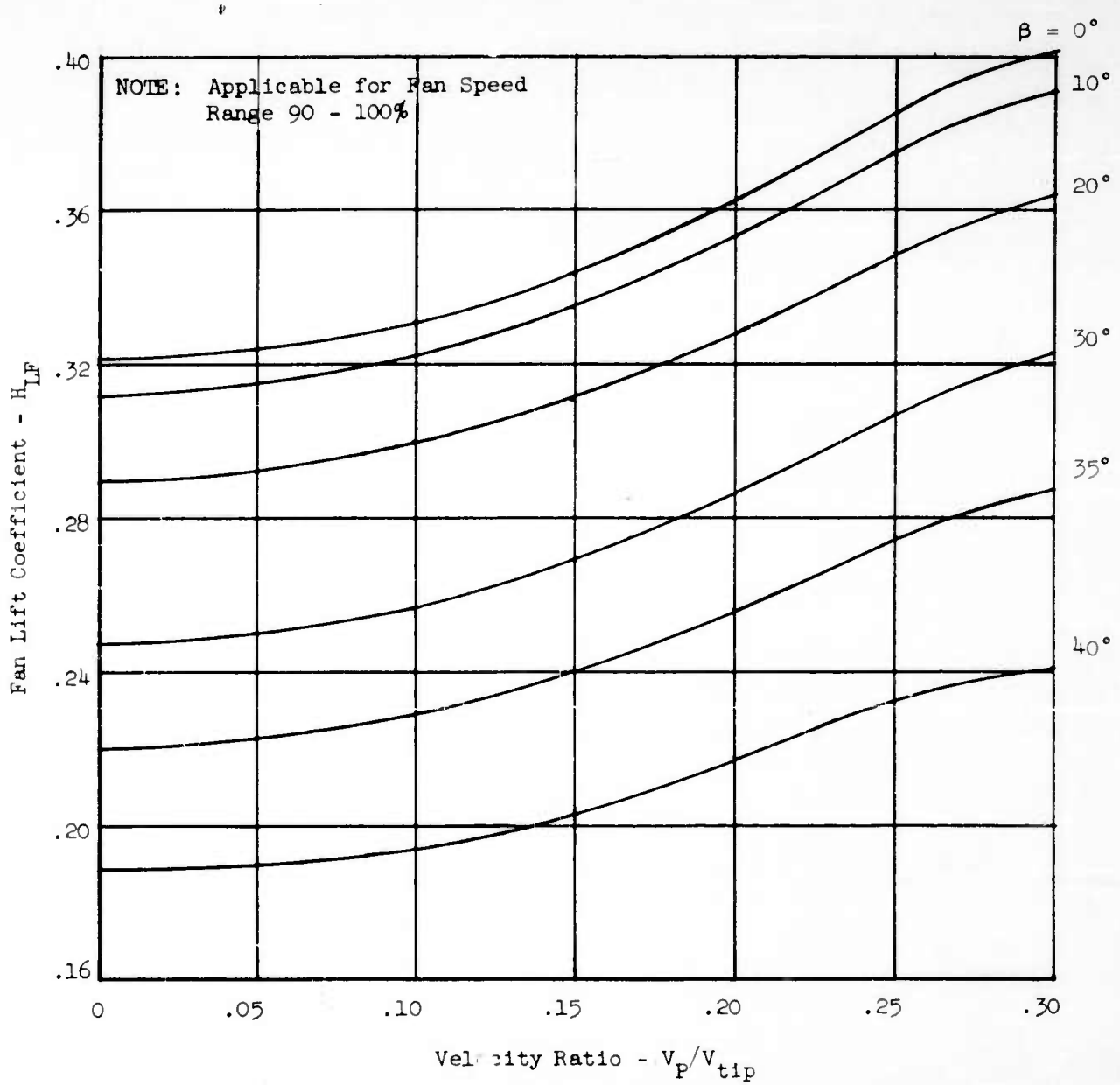

FIGURE 30 - FAN LIFT COEFFICIENT (H_{LF}) VERSUS VELOCITY RATIO

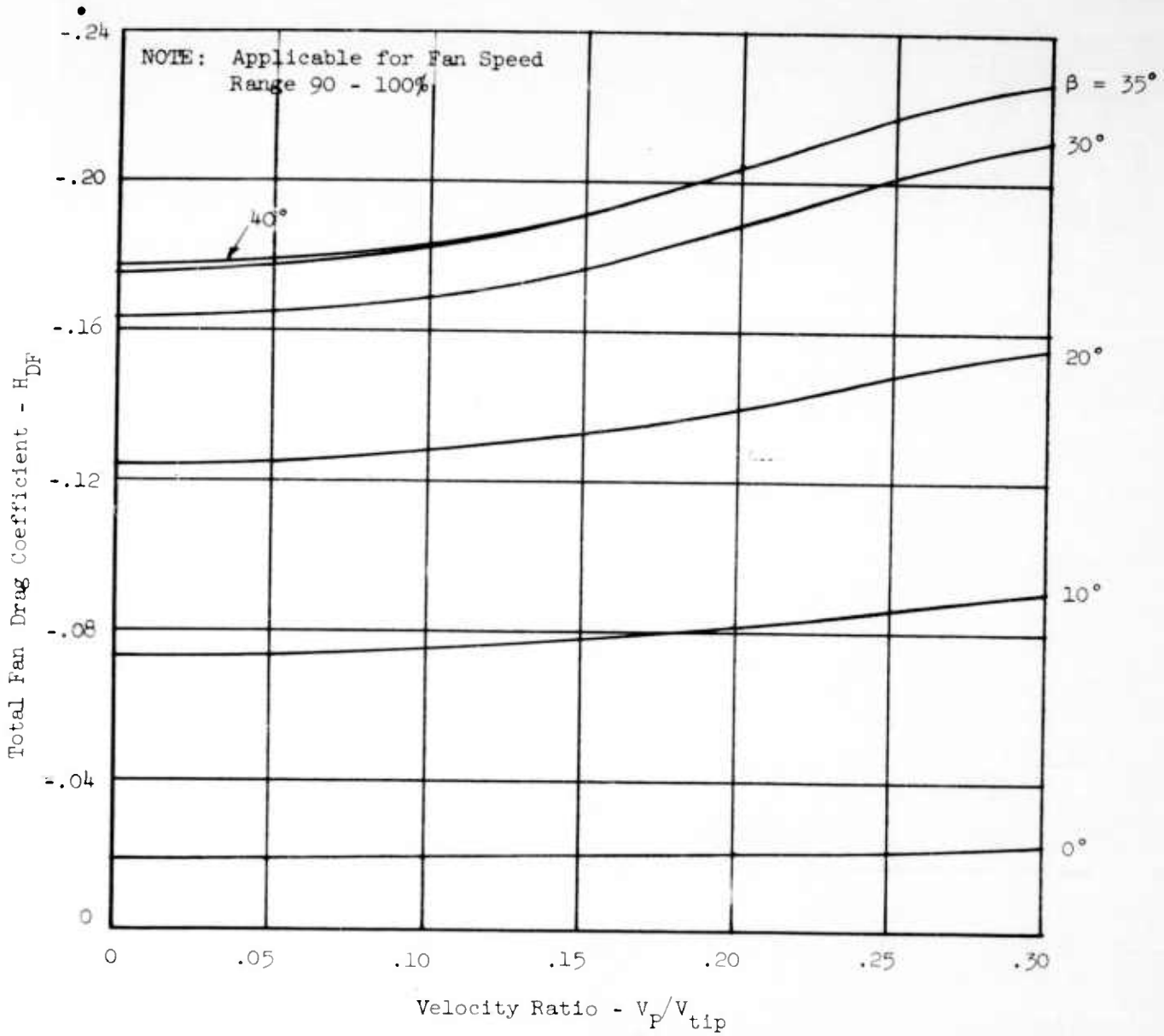

FIGURE 31 - TOTAL FAN HORIZONTAL DRAG COEFFICIENT (H_{DF}) VS. VELOCITY RATIO.

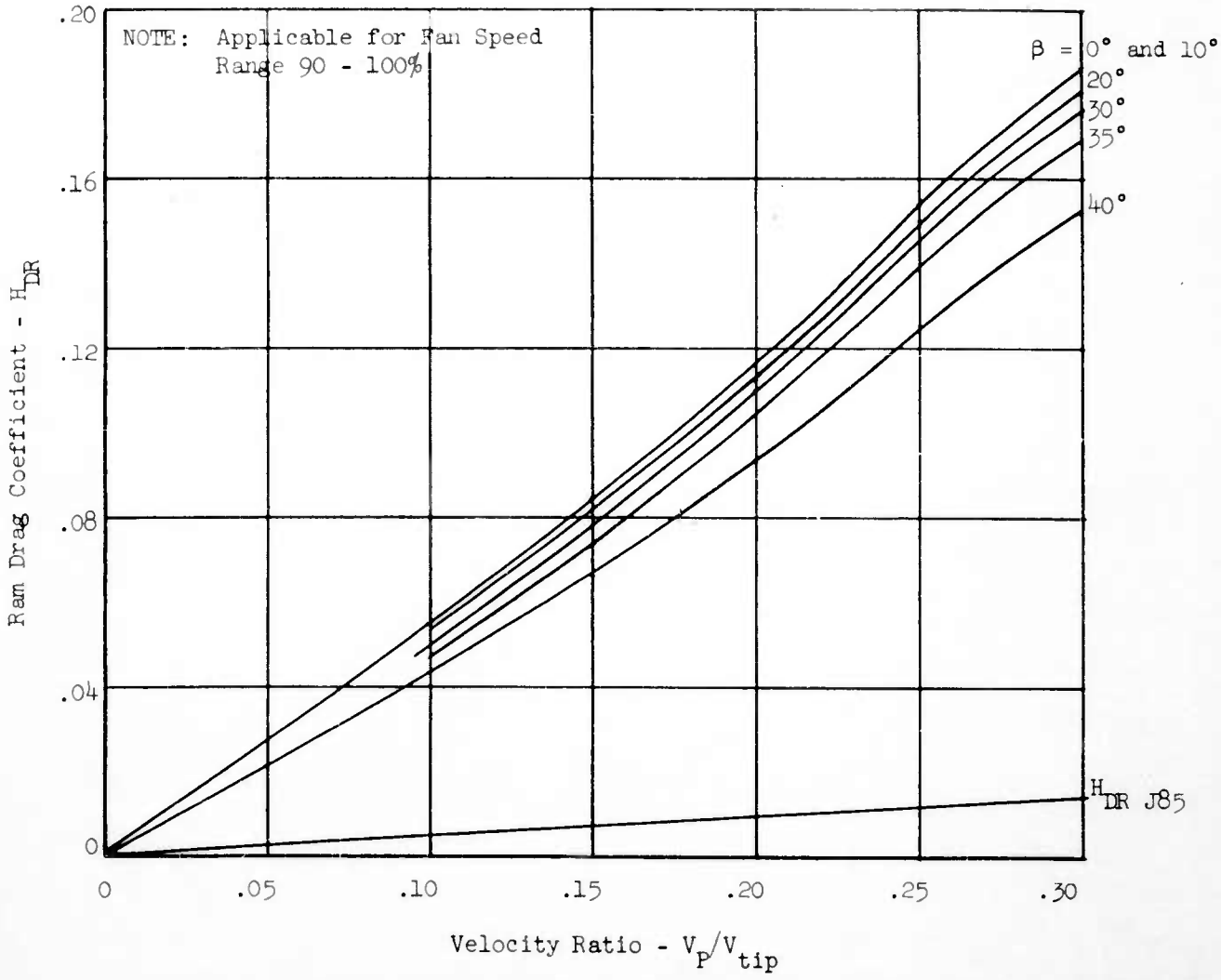

FIGURE 32 - FAN AND ENGINE RAM DRAG COEFFICIENT (H_{DR}) VERSUS VELOCITY RATIO

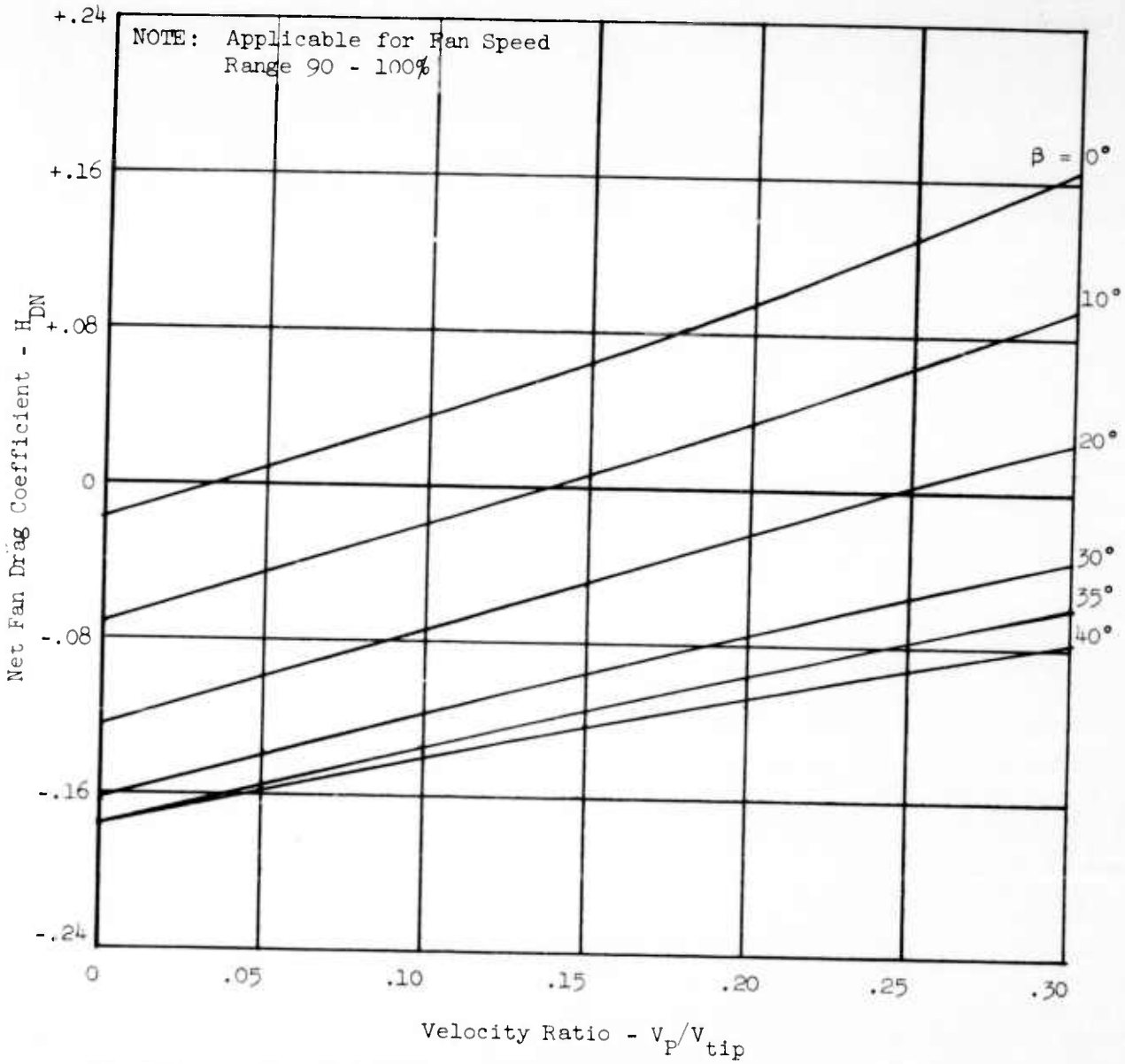

FIGURE 33 - NET FAN DRAG COEFFICIENT (H_{DN}) VERSUS VELOCITY RATIO

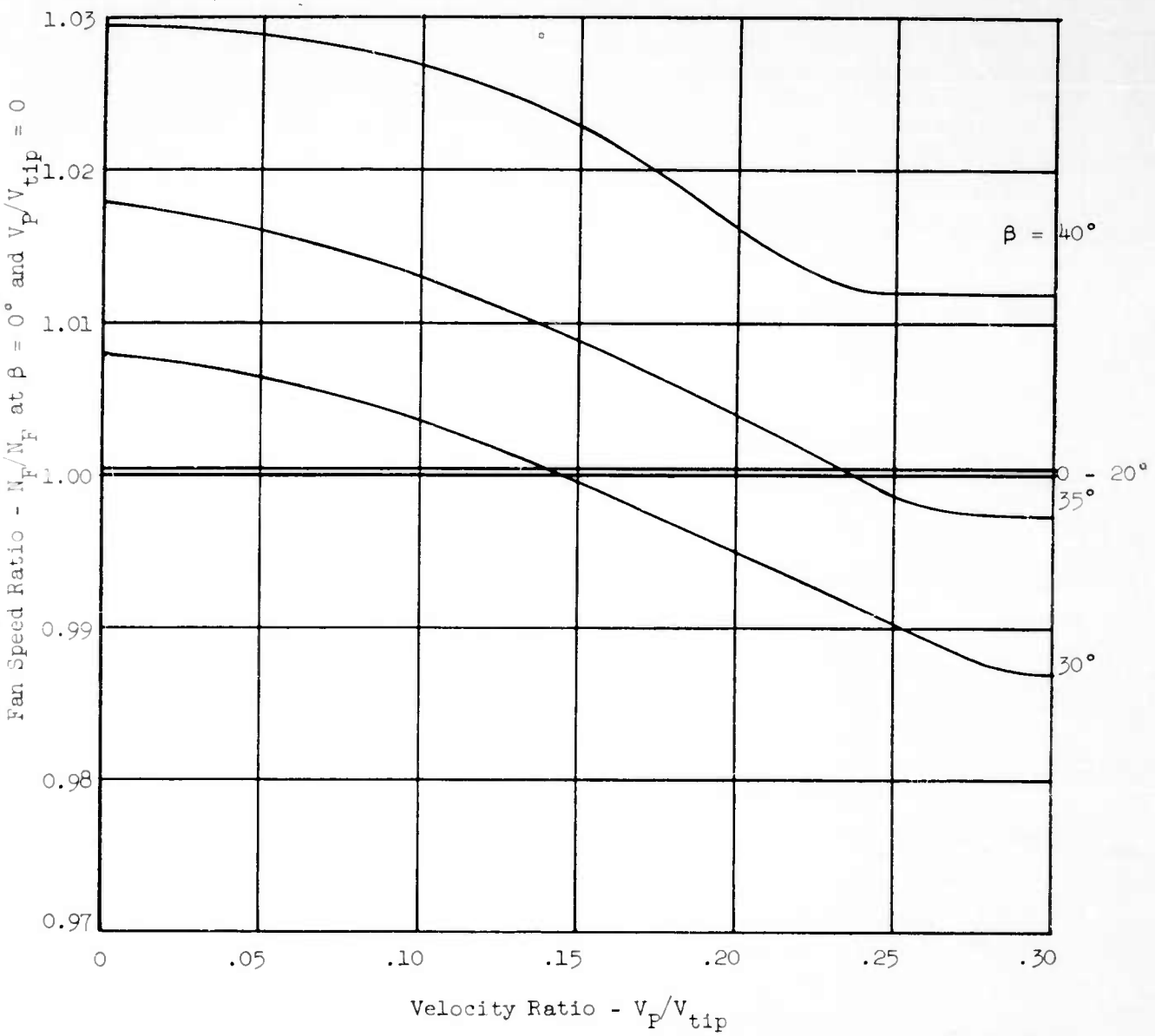

FIGURE 34 - FAN SPEED VARIATION AT CONSTANT HORSEPOWER VERSUS VELOCITY RATIO AND EXIT LOUVER ANGLE

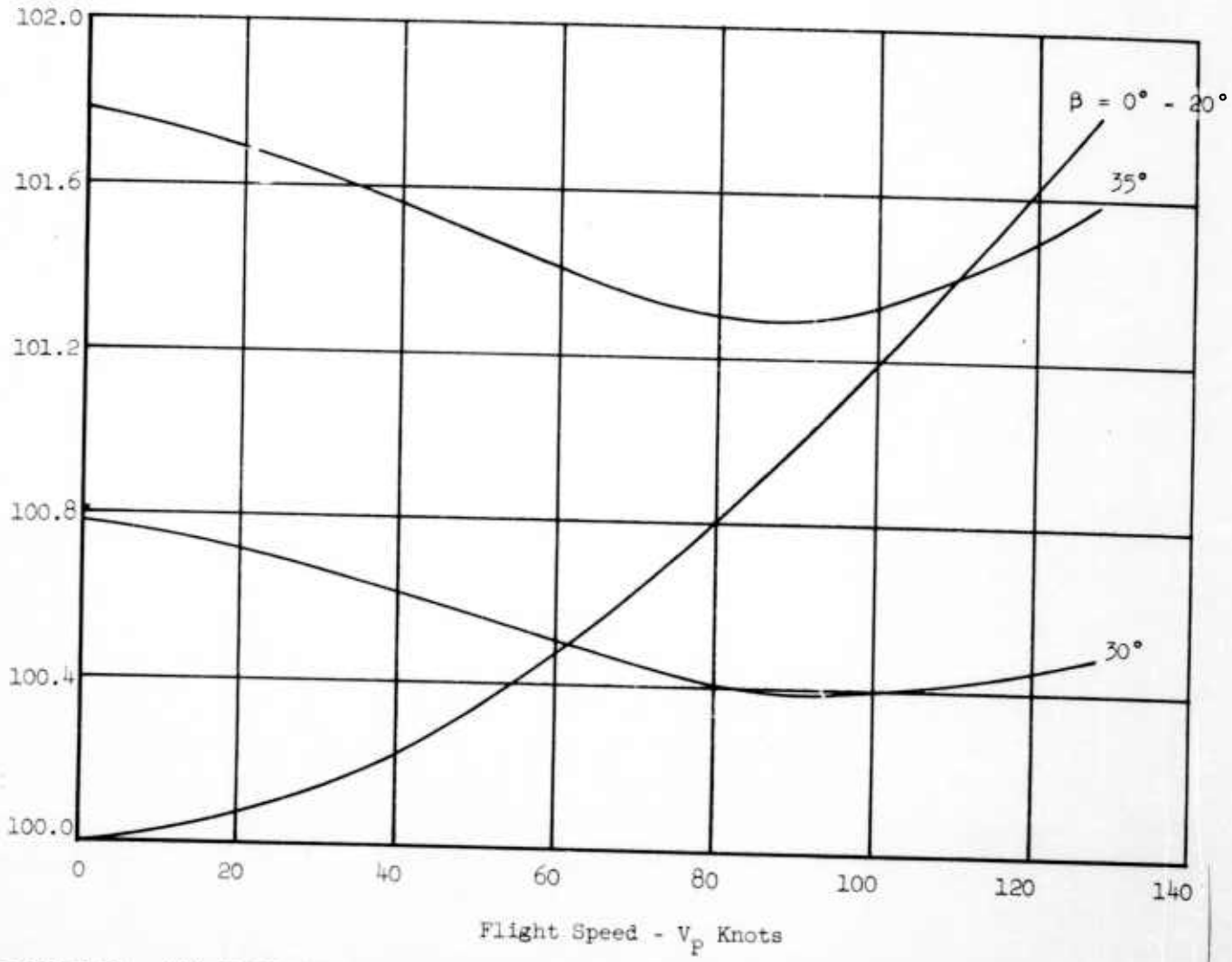

FIGURE 35 - FAN SPEED VARIATION VERSUS FLIGHT SPEED AND EXIT LOUVER ANGLE FOR CONSTANT J85 THROTTLE SETTING AND 100% J85 INLET RECOVERY

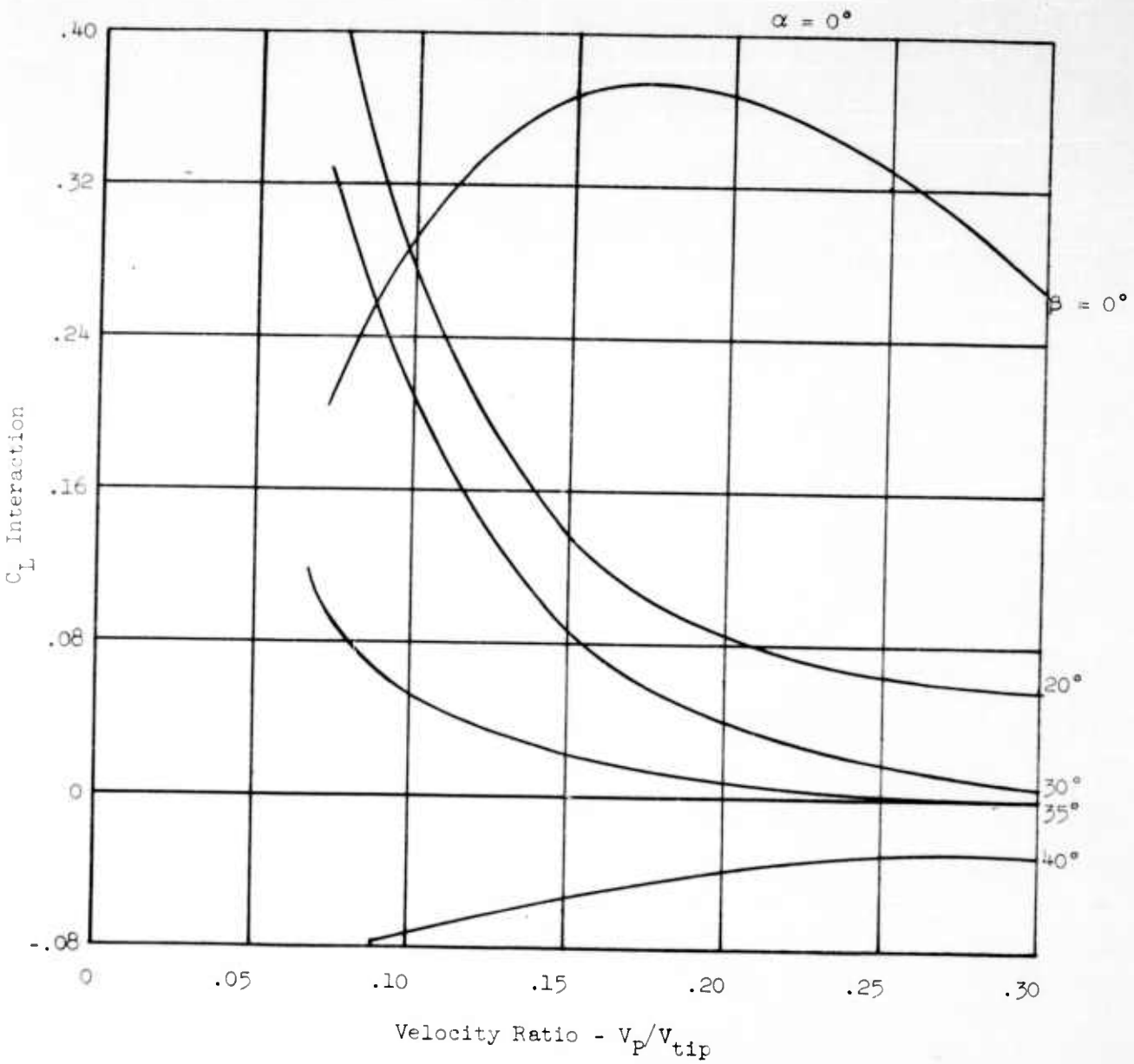

FIGURE 36 - INTERACTION LIFT VS. VELOCITY RATIO AND EXIT LOUVER ANGLE.

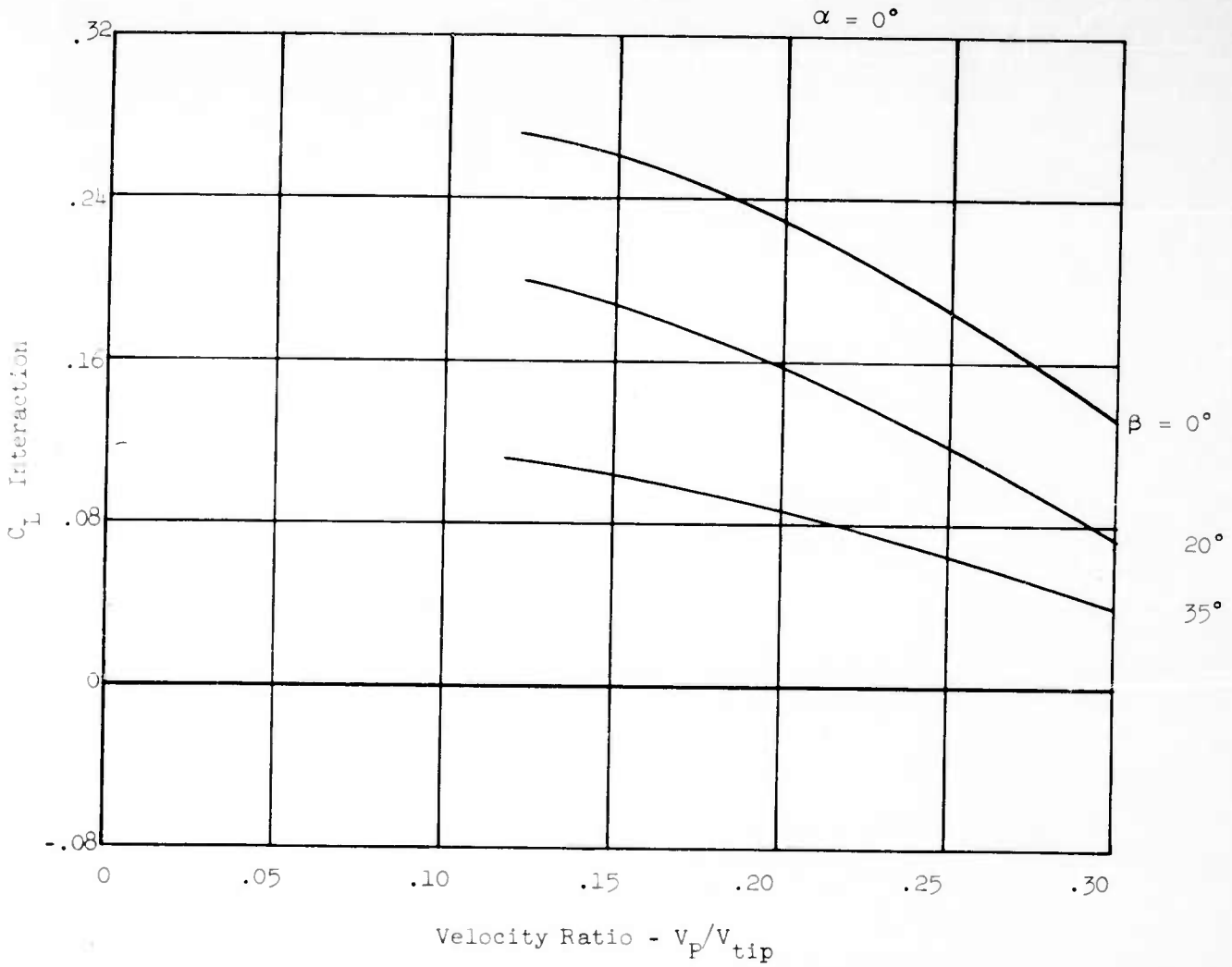

FIGURE 37 - INTERACTION LIFT (FROM WING STATIC PRESSURES) VERSUS VELOCITY RATIO AND EXIT LOUVER ANGLE

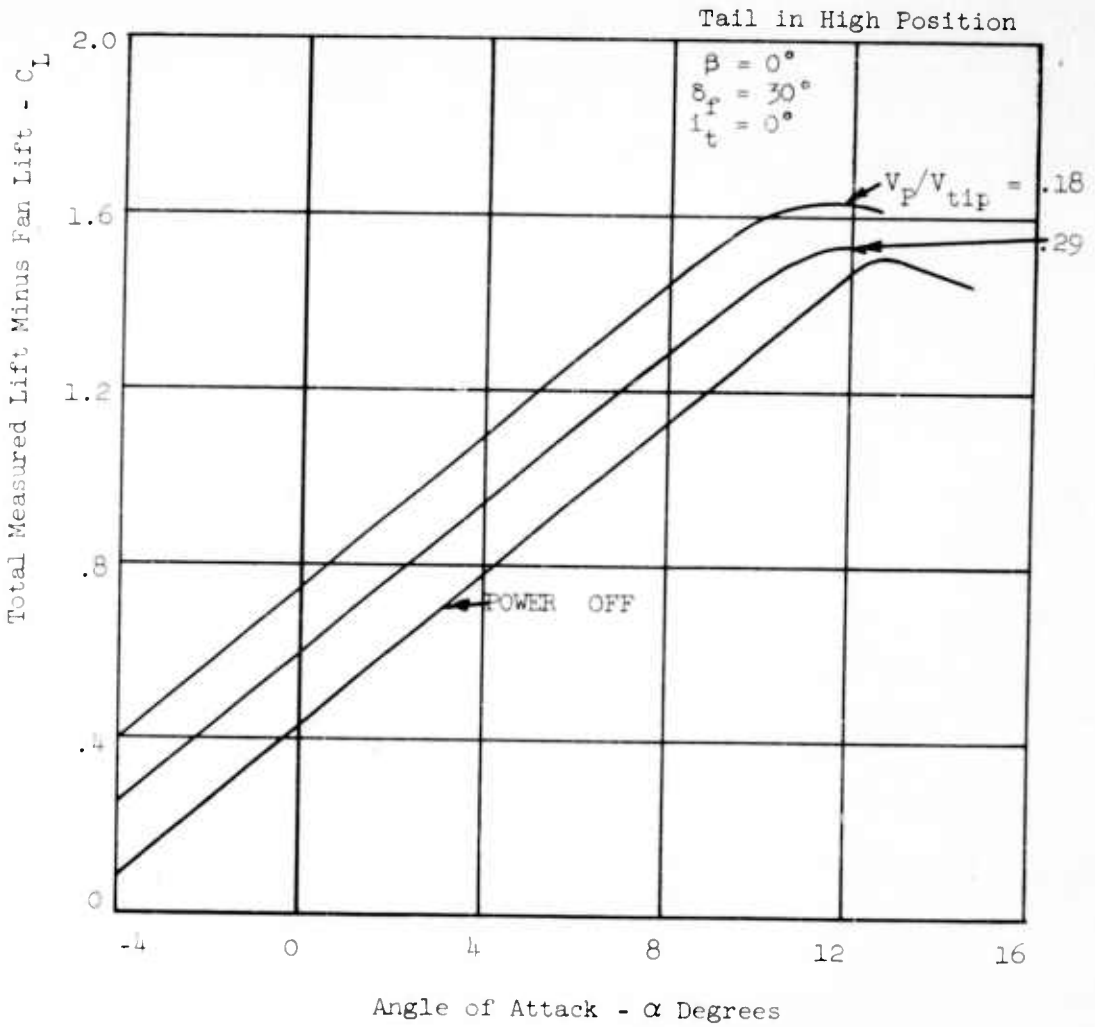

FIGURE 38 - TOTAL MEASURED LIFT MINUS FAN LIFT VERSUS ANGLE OF ATTACK AND VELOCITY RATIO

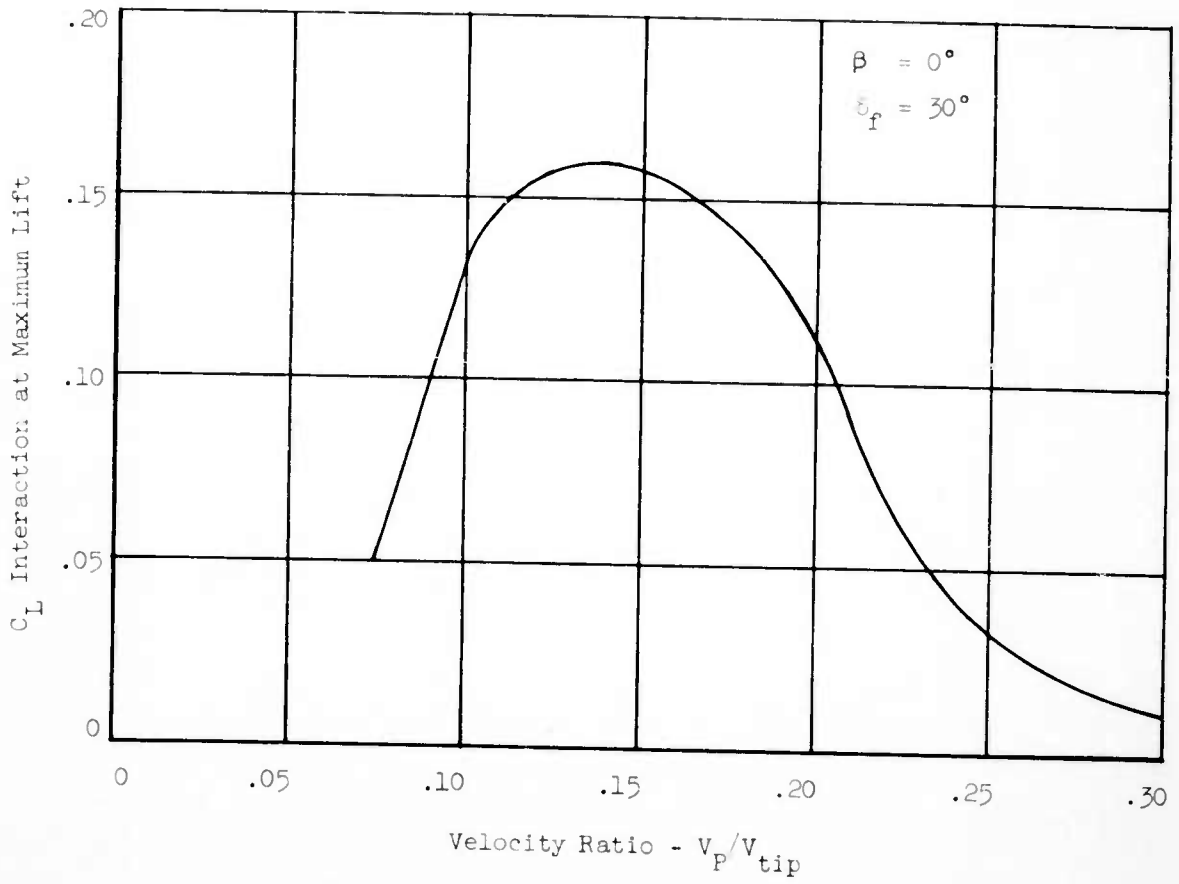

FIGURE 39 - INTERACTION LIFT AT MAXIMUM LIFT CONDITION VERSUS VELOCITY RATIO

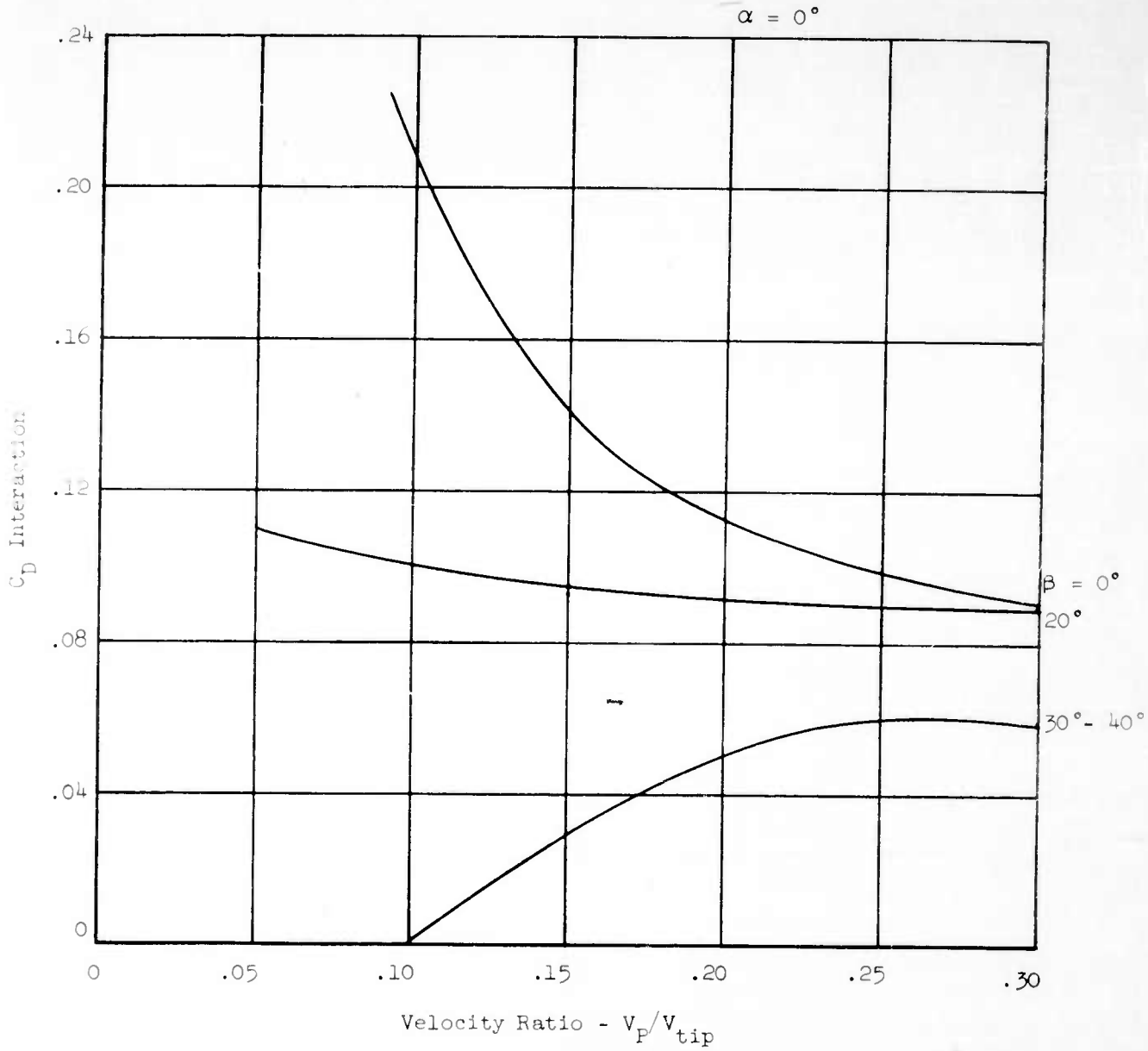

FIGURE 40 - INTERACTION DRAG VS. VELOCITY RATIO AND EXIT LOUVER ANGLE.

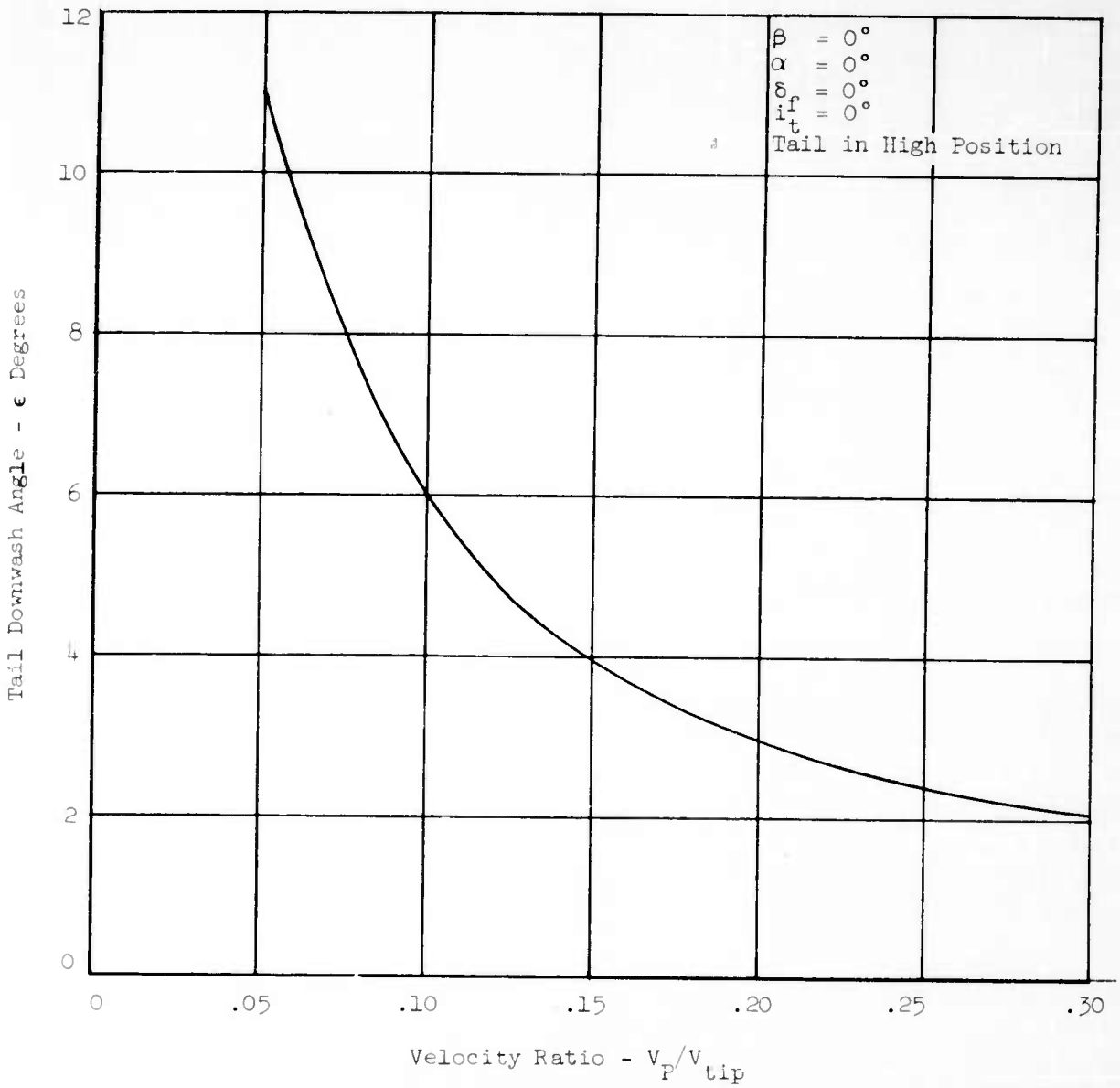

FIGURE 41 - TAIL DOWNWASH VERSUS VELOCITY RATIO

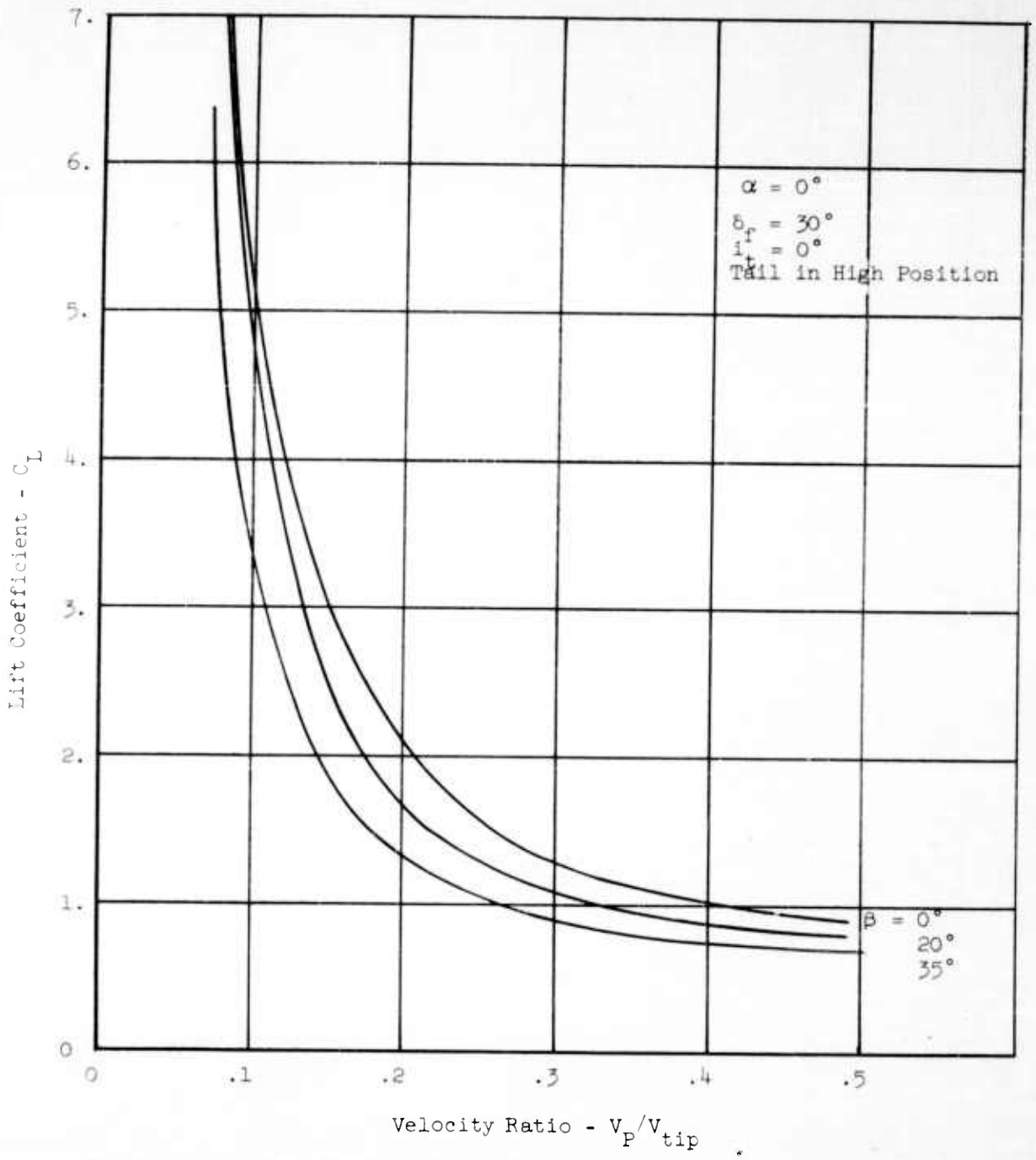

FIGURE 42a - LIFT COEFFICIENT VERSUS VELOCITY RATIO

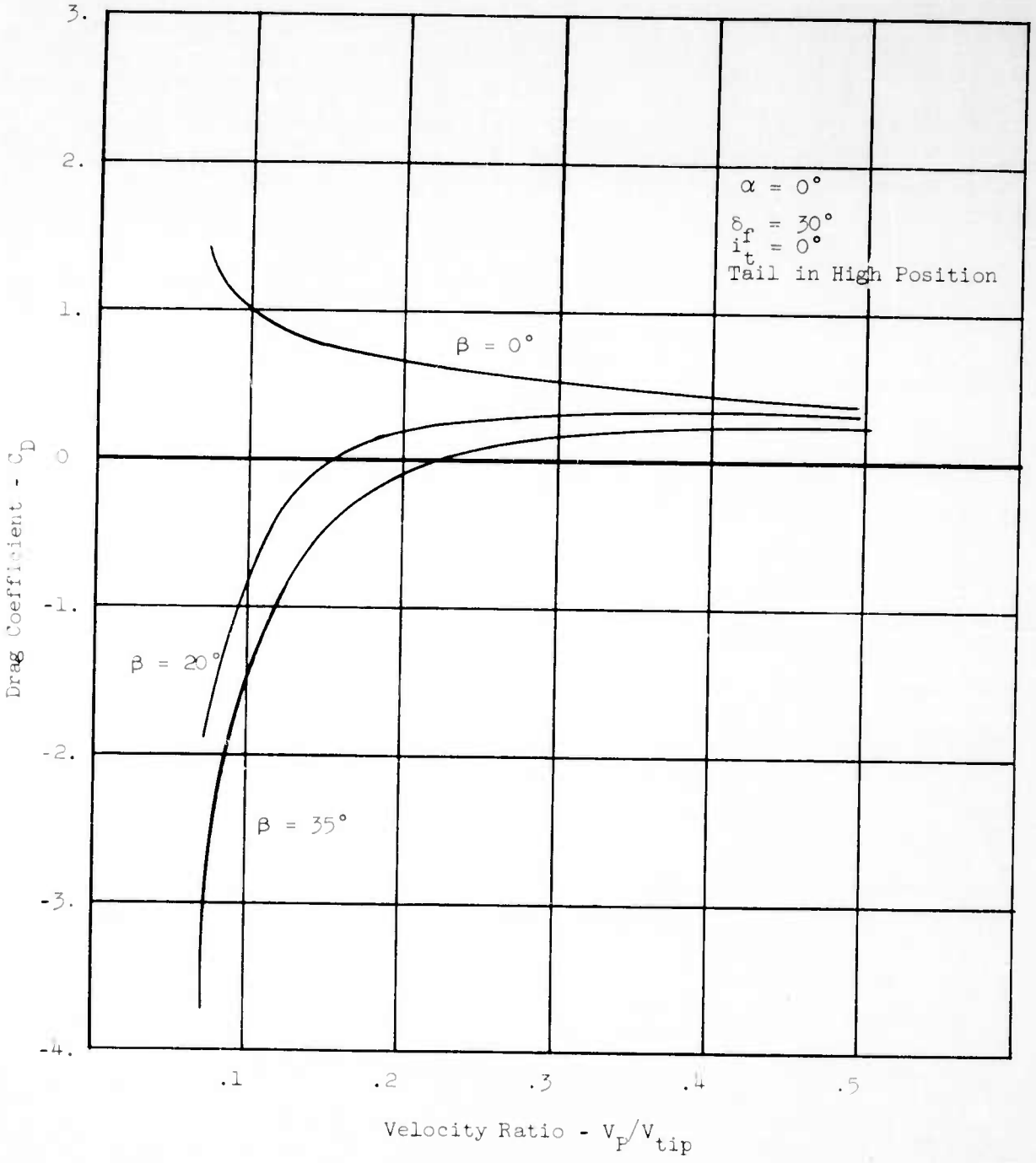

FIGURE 42b - DRAG COEFFICIENT VERSUS VELOCITY RATIO

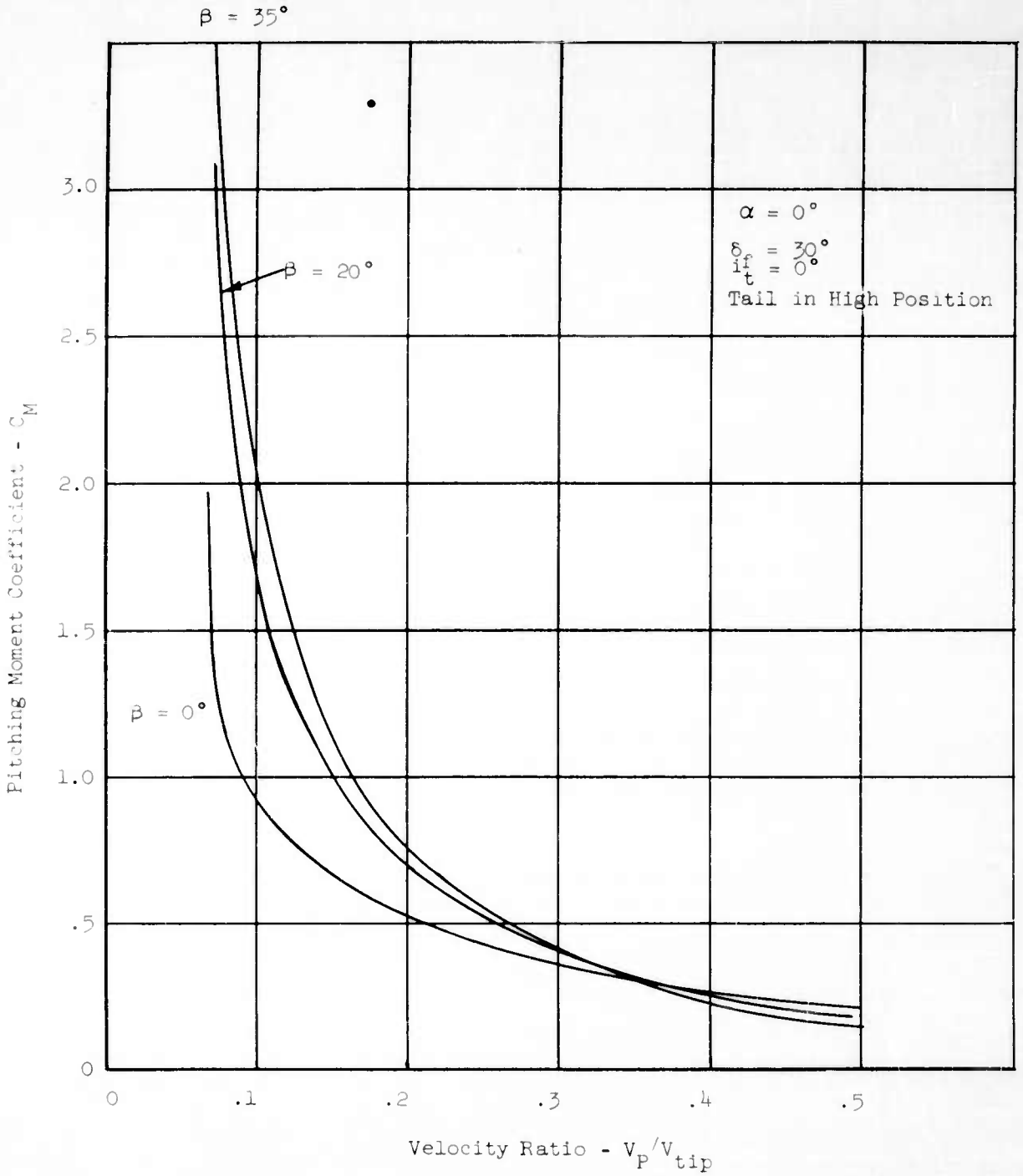

FIGURE 42c - PITCHING MOMENT COEFFICIENT VERSUS VELOCITY RATIO

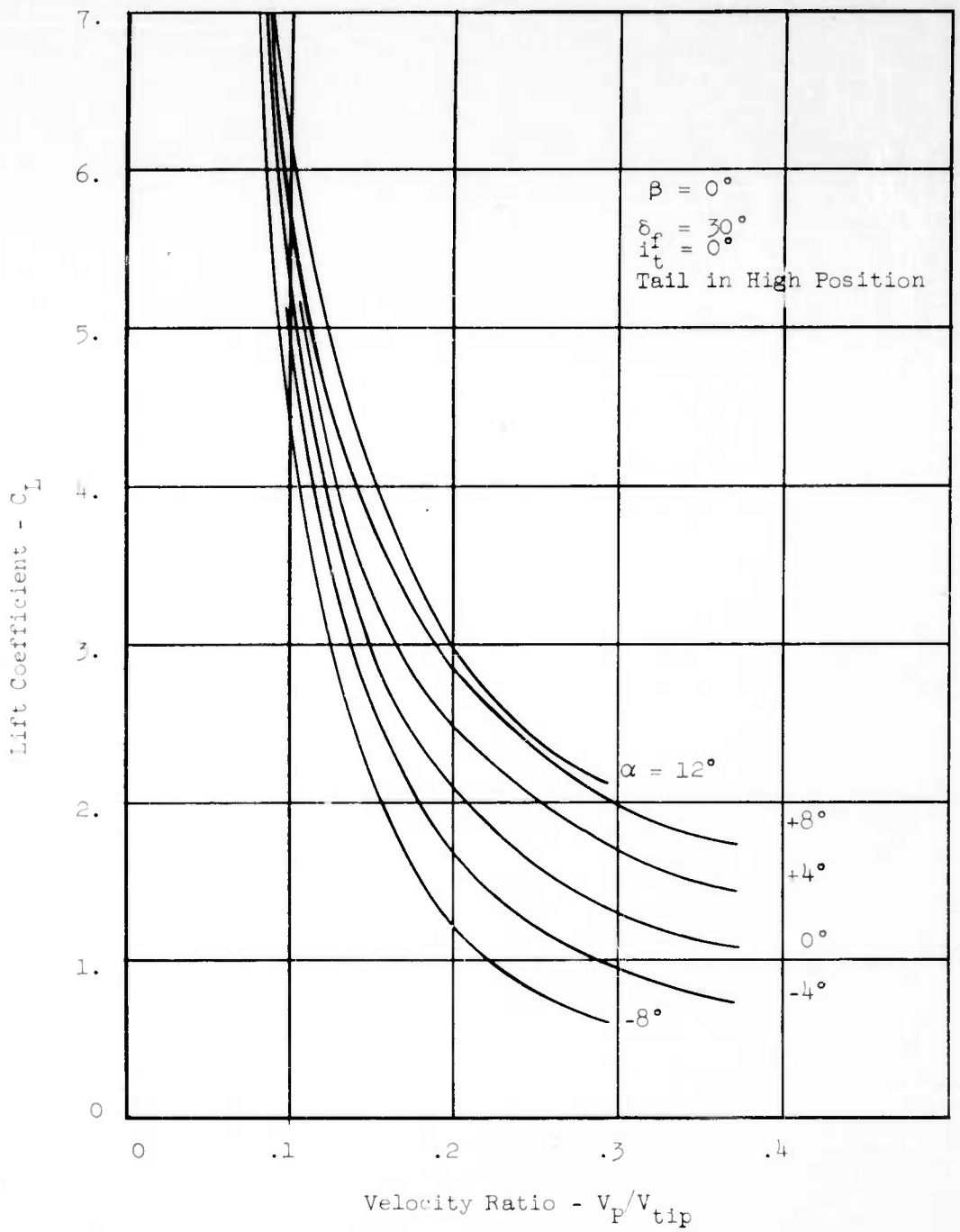

FIGURE 43a - LIFT COEFFICIENT VERSUS VELOCITY RATIO

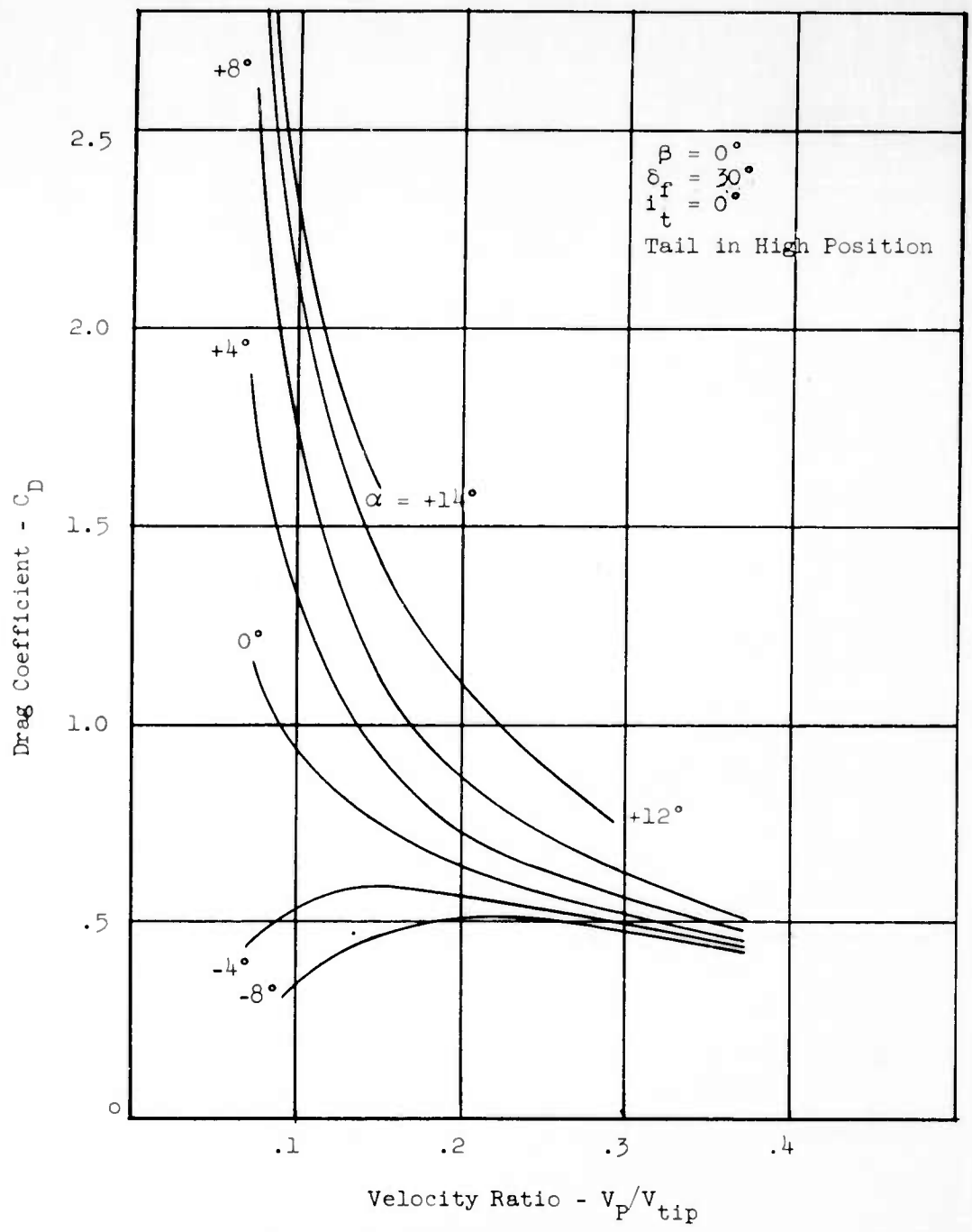

FIGURE 43b - DRAG COEFFICIENT VERSUS VELOCITY RATIO

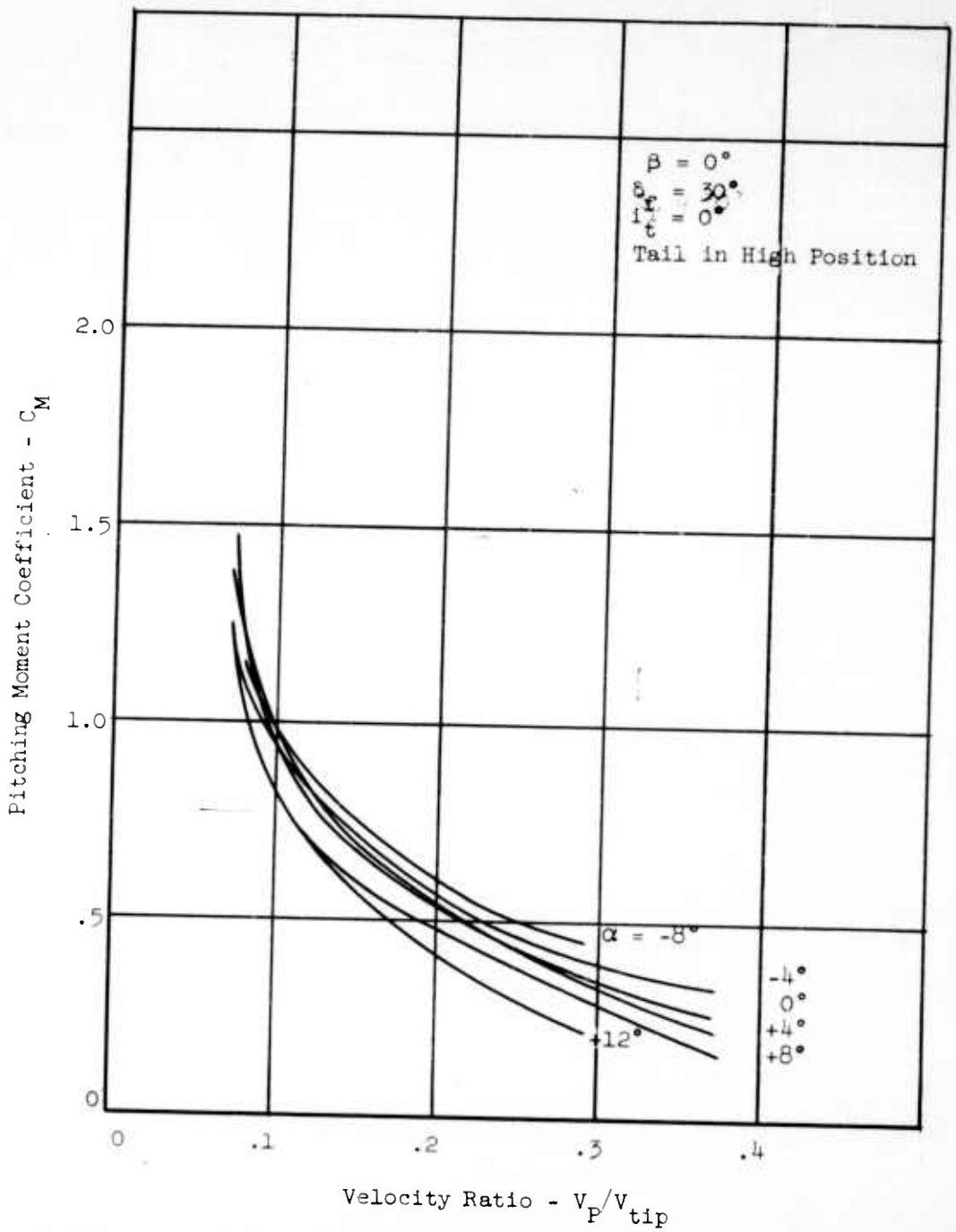

FIGURE 43c - PITCHING MOMENT COEFFICIENT VERSUS VELOCITY RATIO

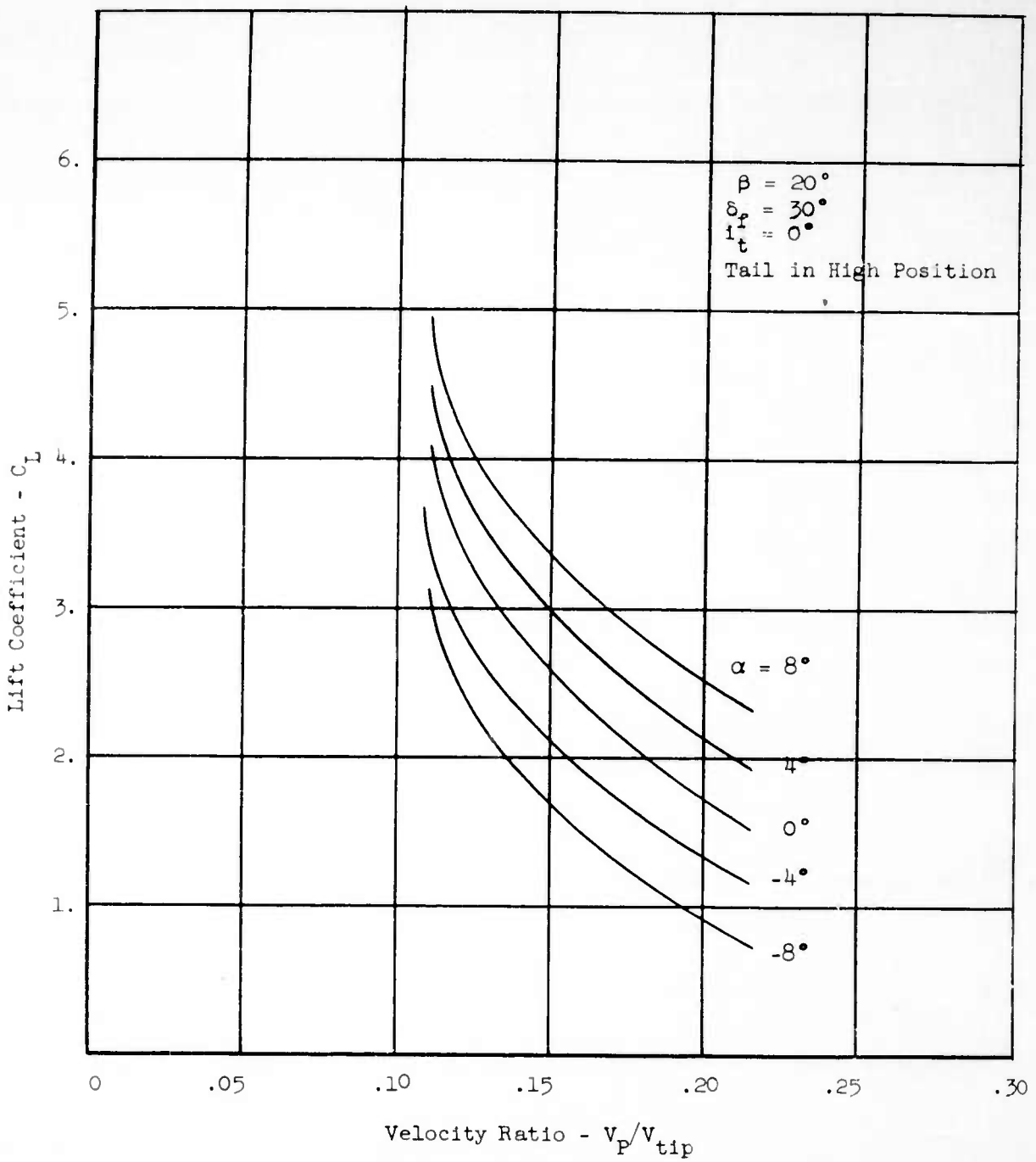

FIGURE 44a - LIFT COEFFICIENT VERSUS VELOCITY RATIO

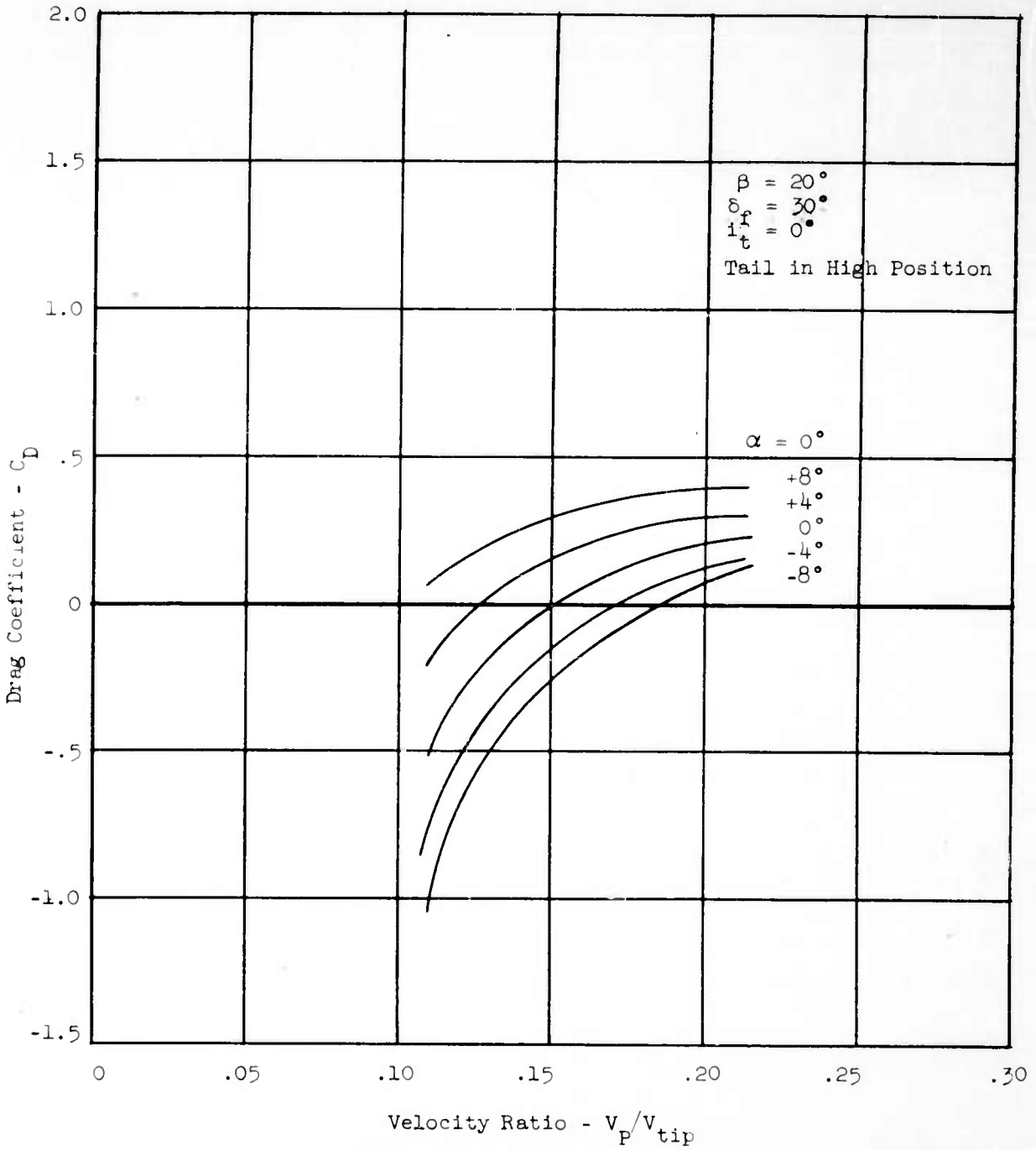

FIGURE 44b - DRAG COEFFICIENT VERSUS VELOCITY RATIO

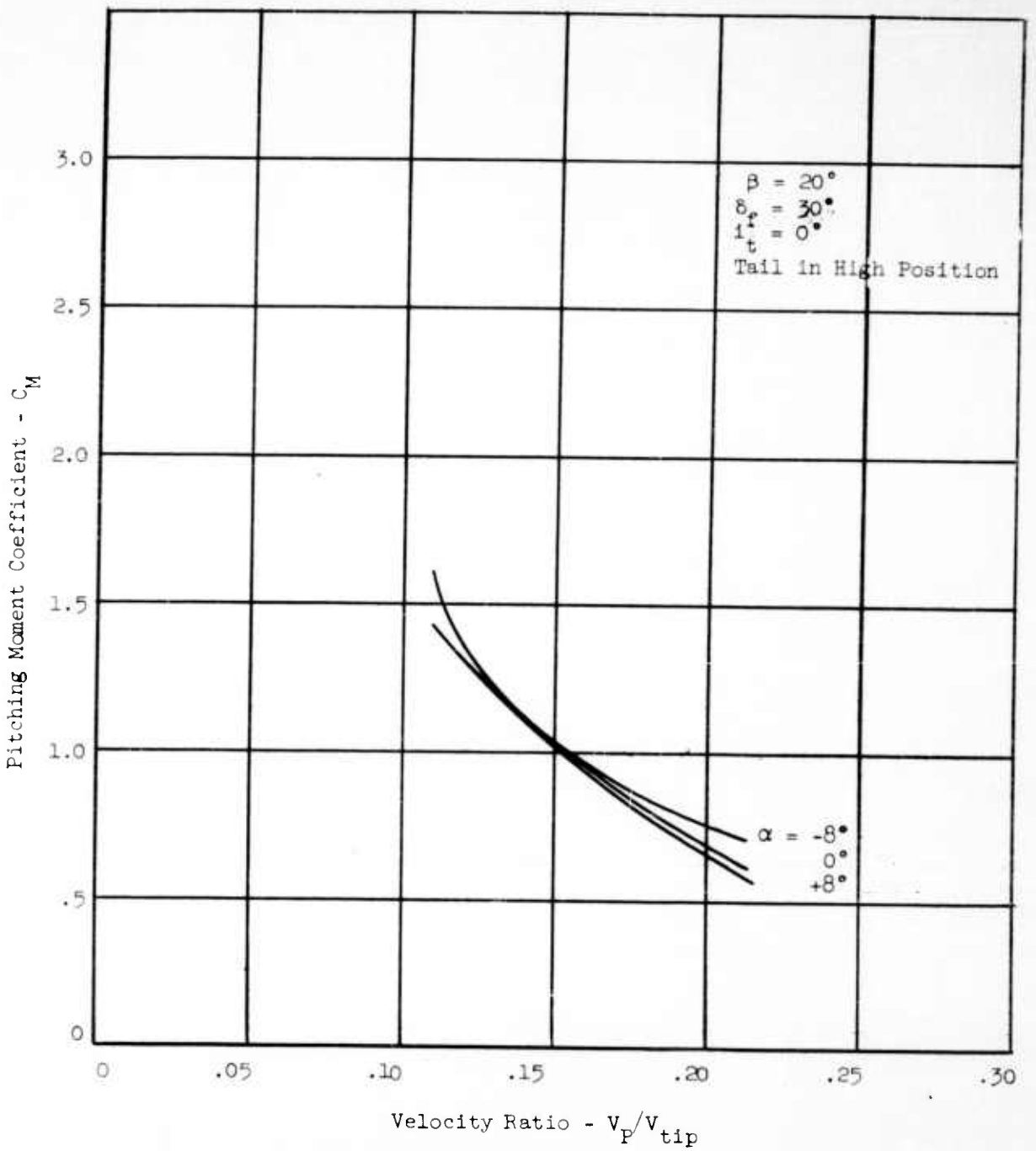

FIGURE 44c - PITCHING MOMENT COEFFICIENT VERSUS VELOCITY RATIO

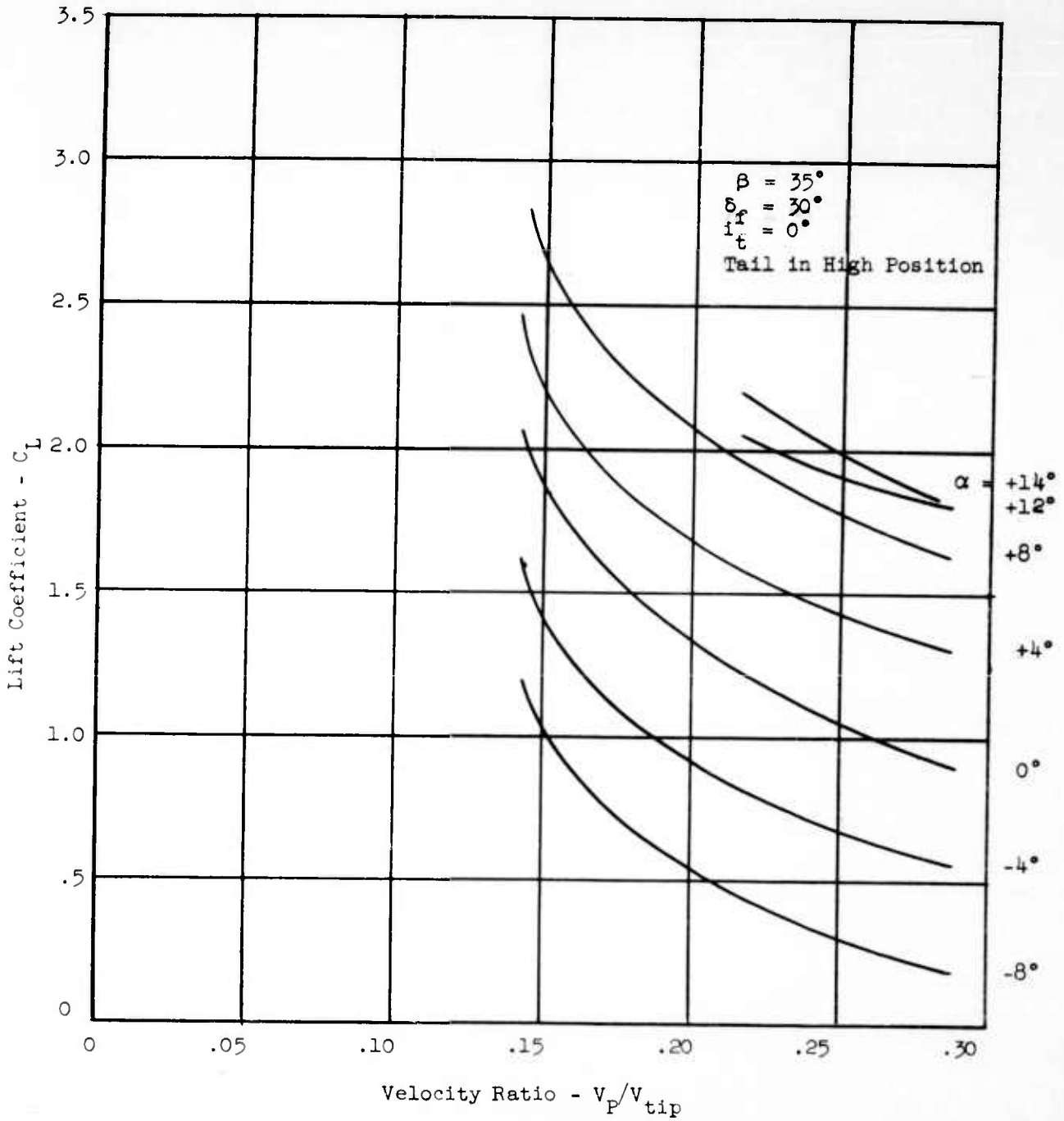

FIGURE 45a - LIFT COEFFICIENT VERSUS VELOCITY RATIO

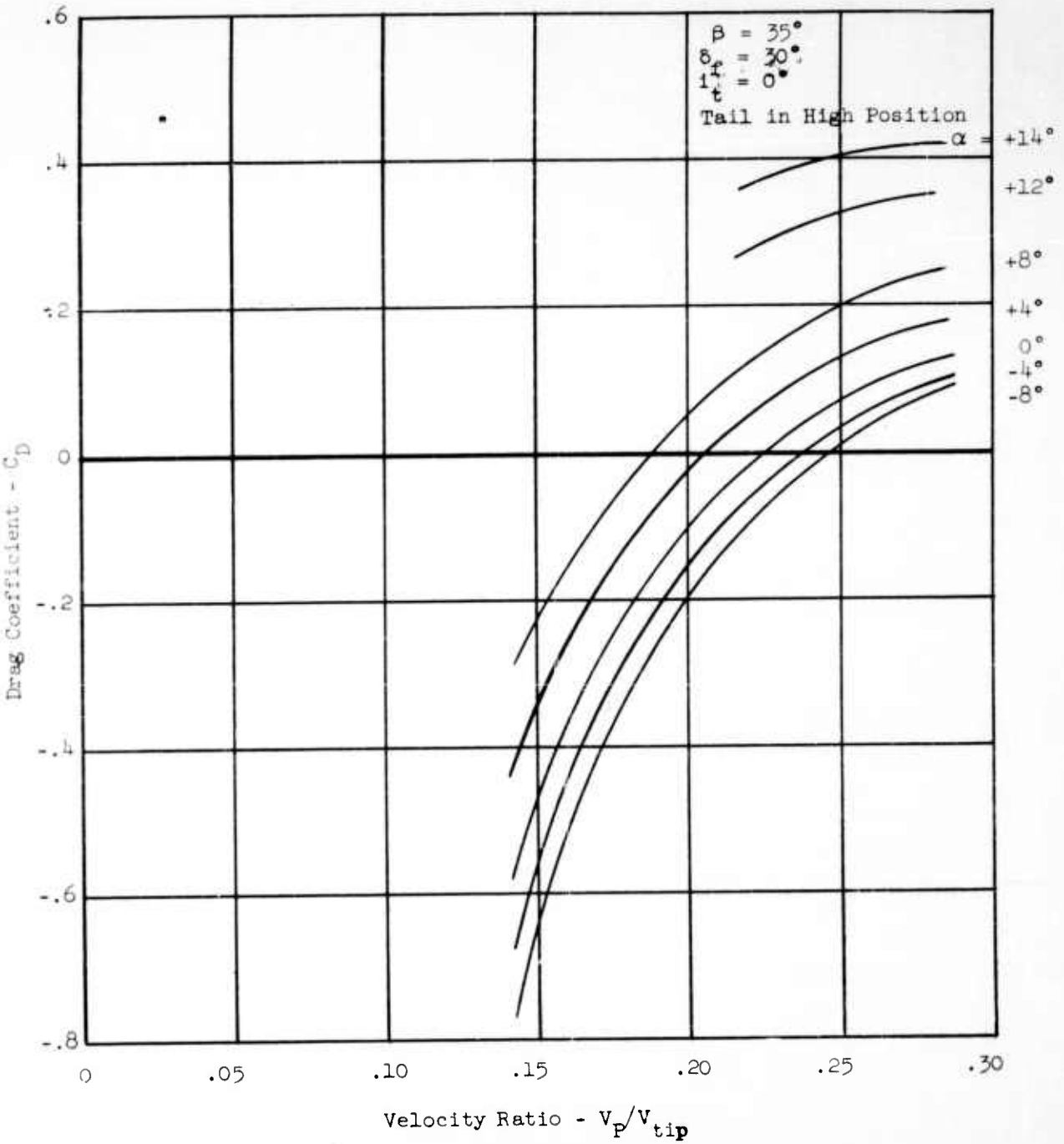

FIGURE 45b - DRAG COEFFICIENT VERSUS VELOCITY RATIO

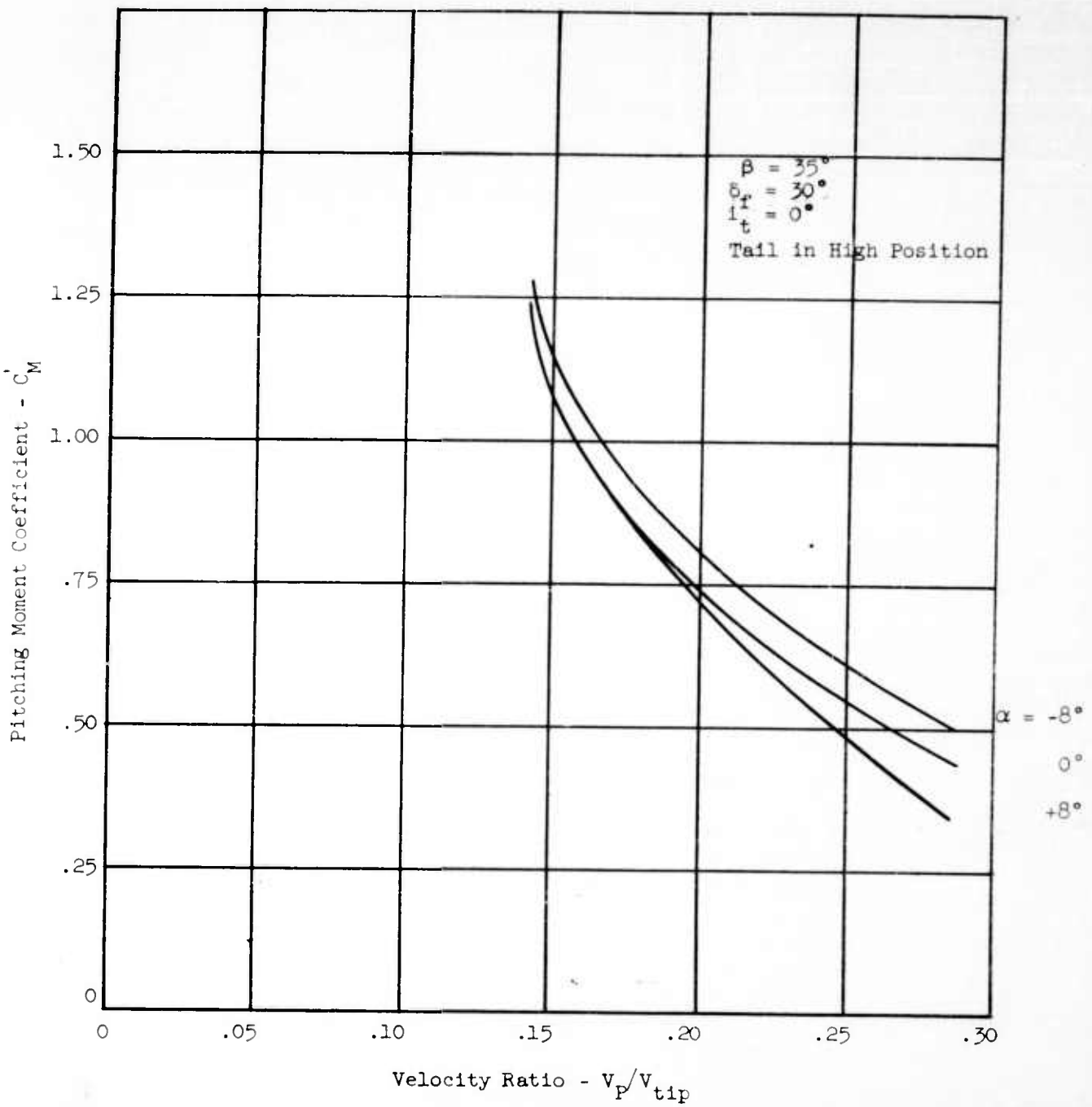

FIGURE 45c - PITCHING MOMENT COEFFICIENT VERSUS VELOCITY RATIO

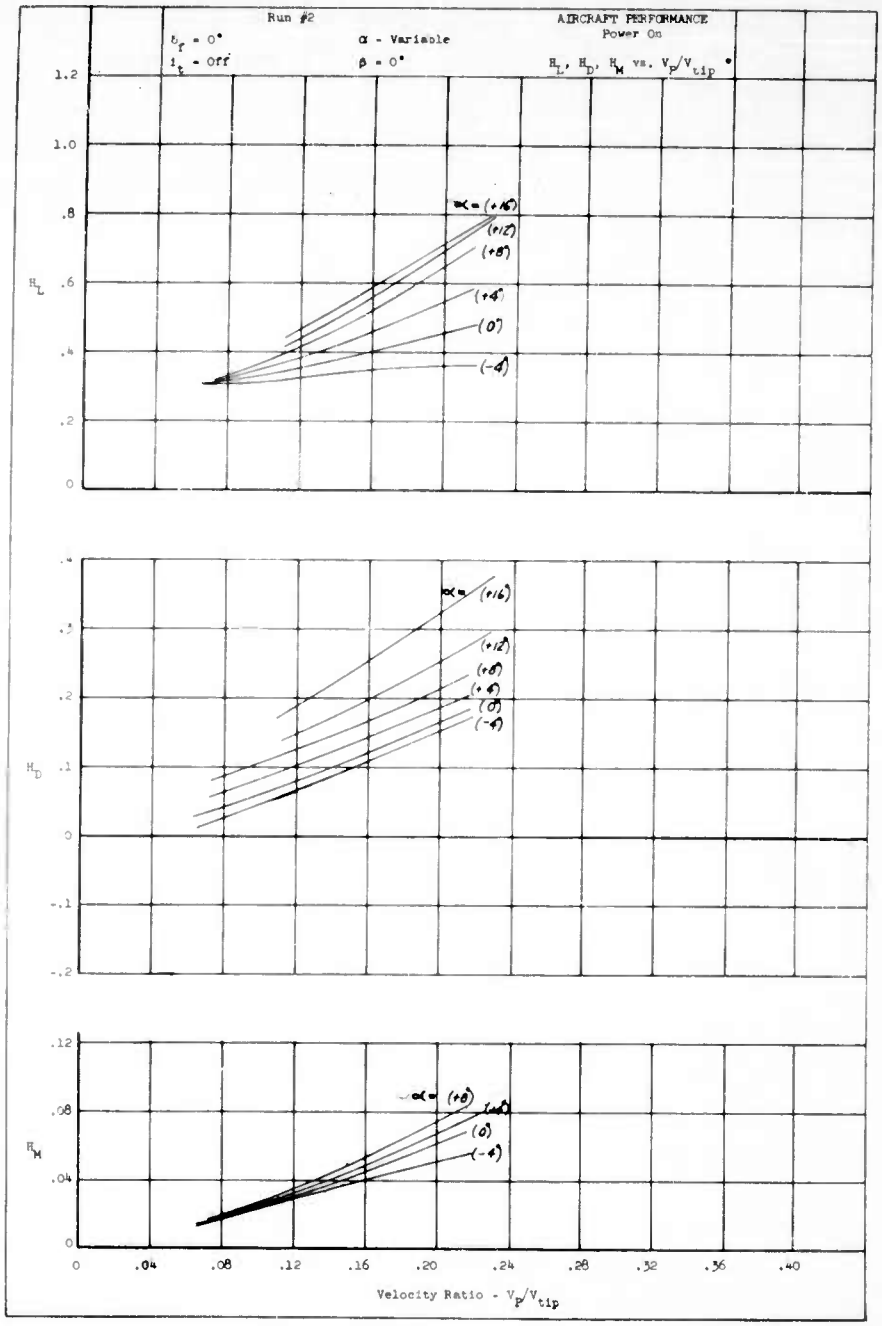

FIGURE 46 - FAN POWERED AIRCRAFT PERFORMANCE

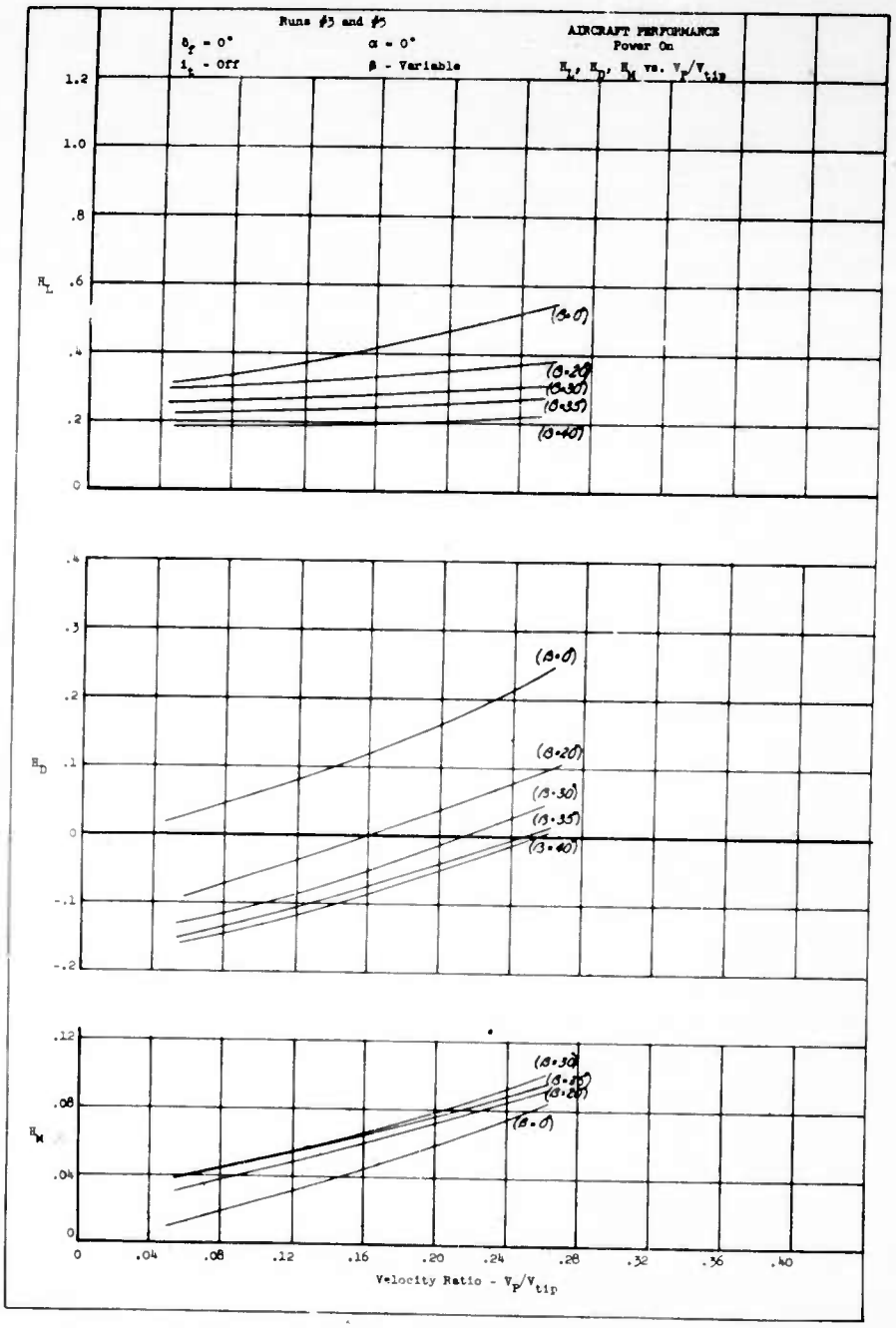

FIGURE 47 - FAN POWERED AIRCRAFT PERFORMANCE

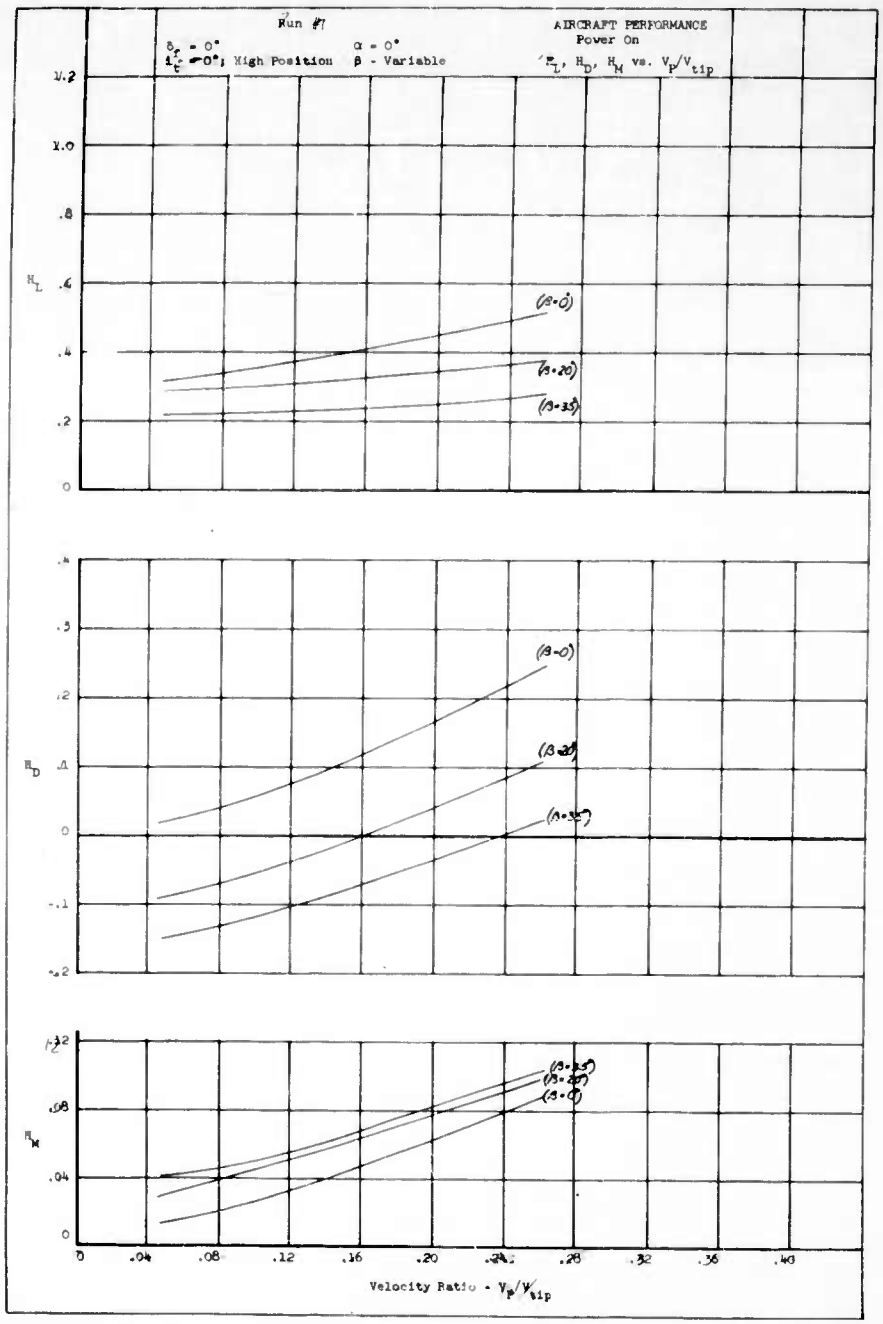

FIGURE 48 - FAN POWERED AIRCRAFT PERFORMANCE

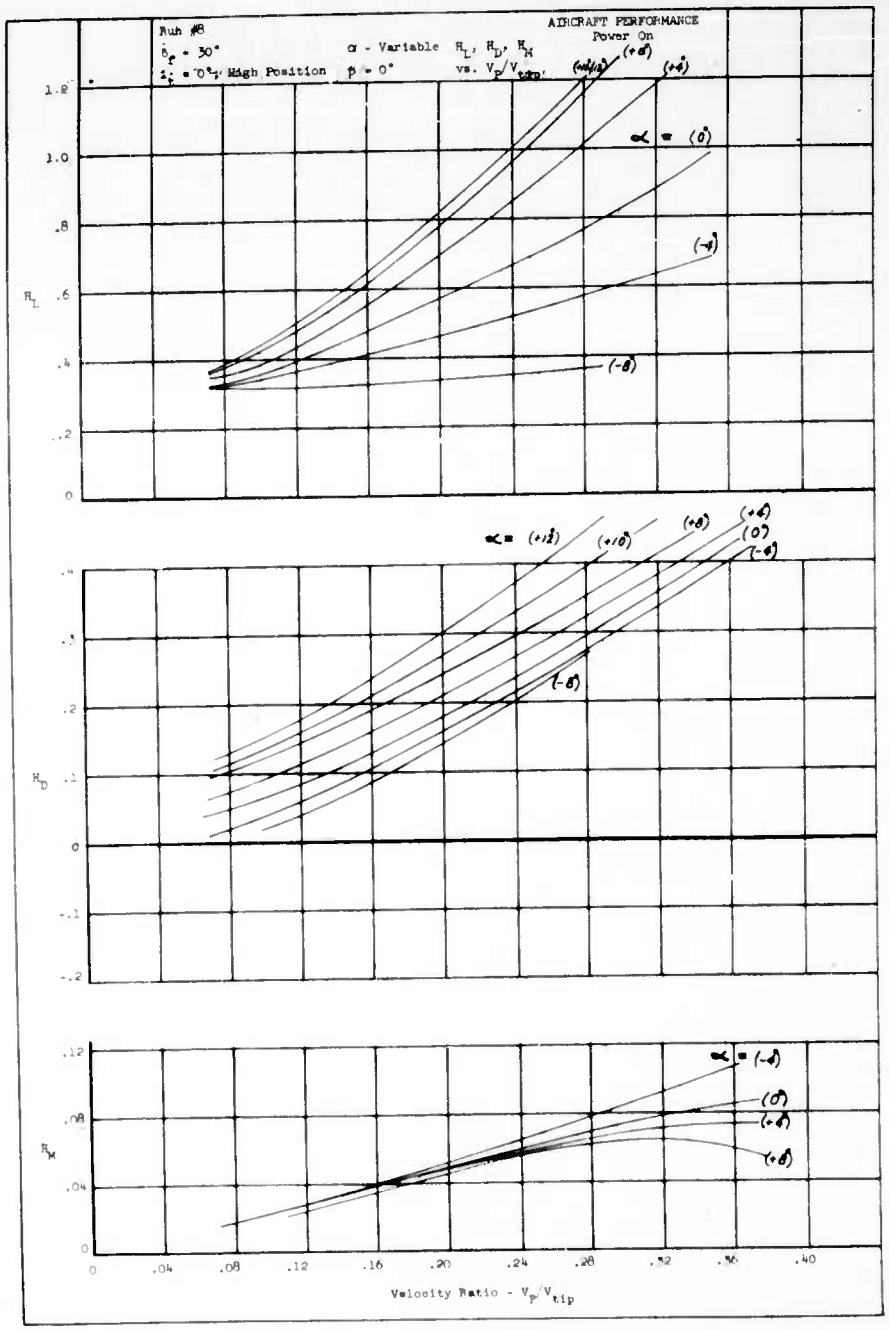

FIGURE 49 - FAN POWERED AIRCRAFT PERFORMANCE

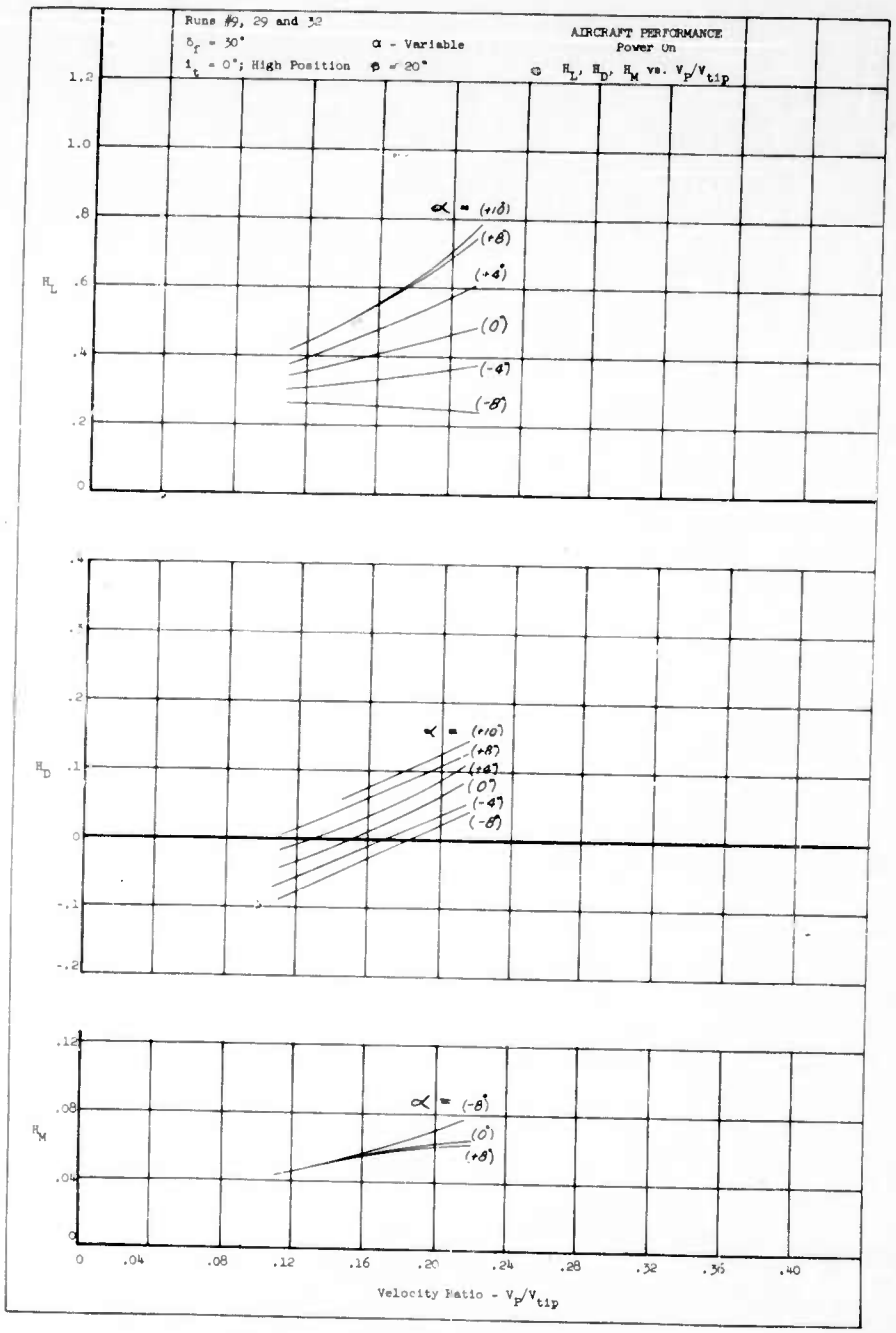

FIGURE 50 - FAN POWERED AIRCRAFT PERFORMANCE

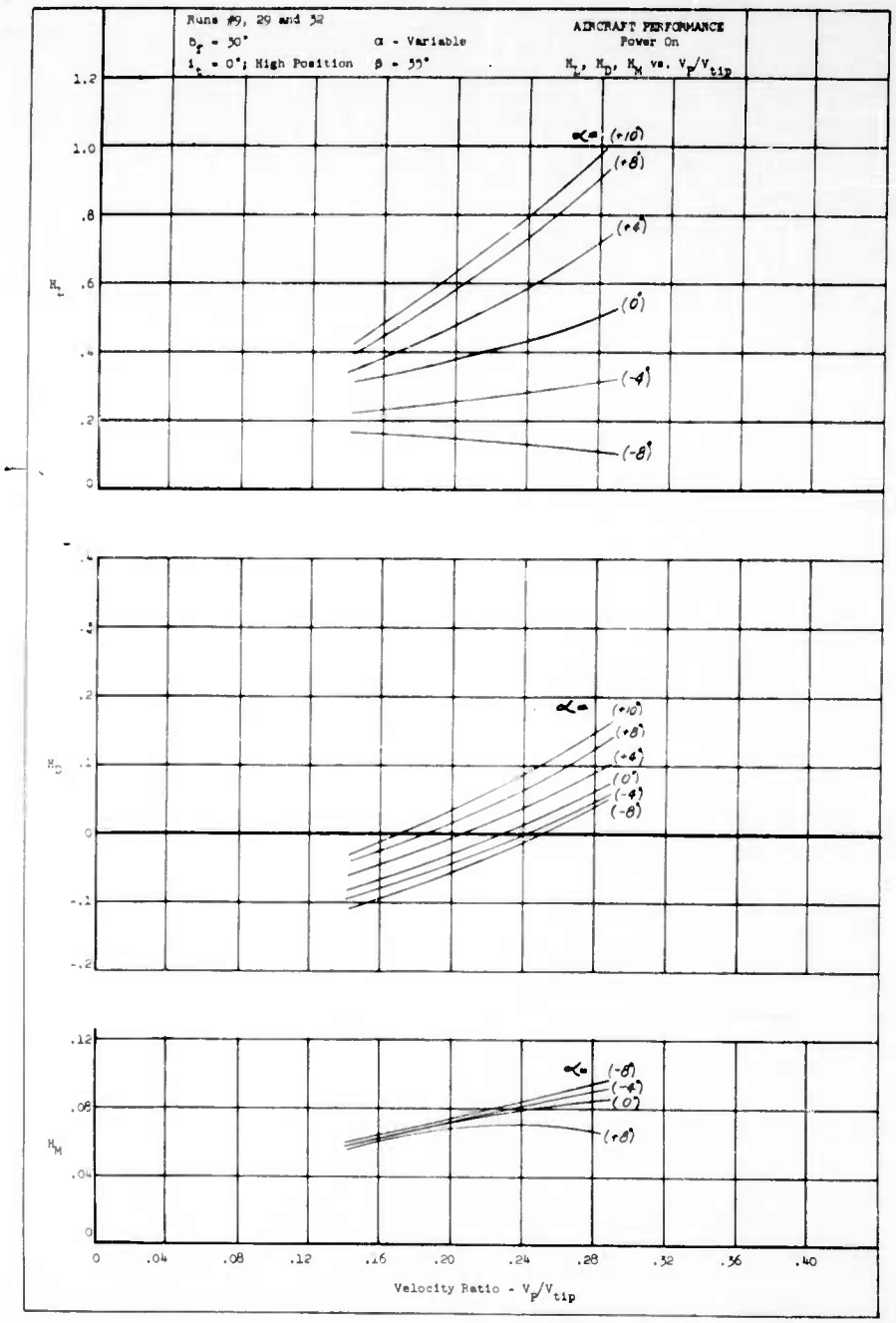

FIGURE 51 - FAN POWERED AIRCRAFT PERFORMANCE

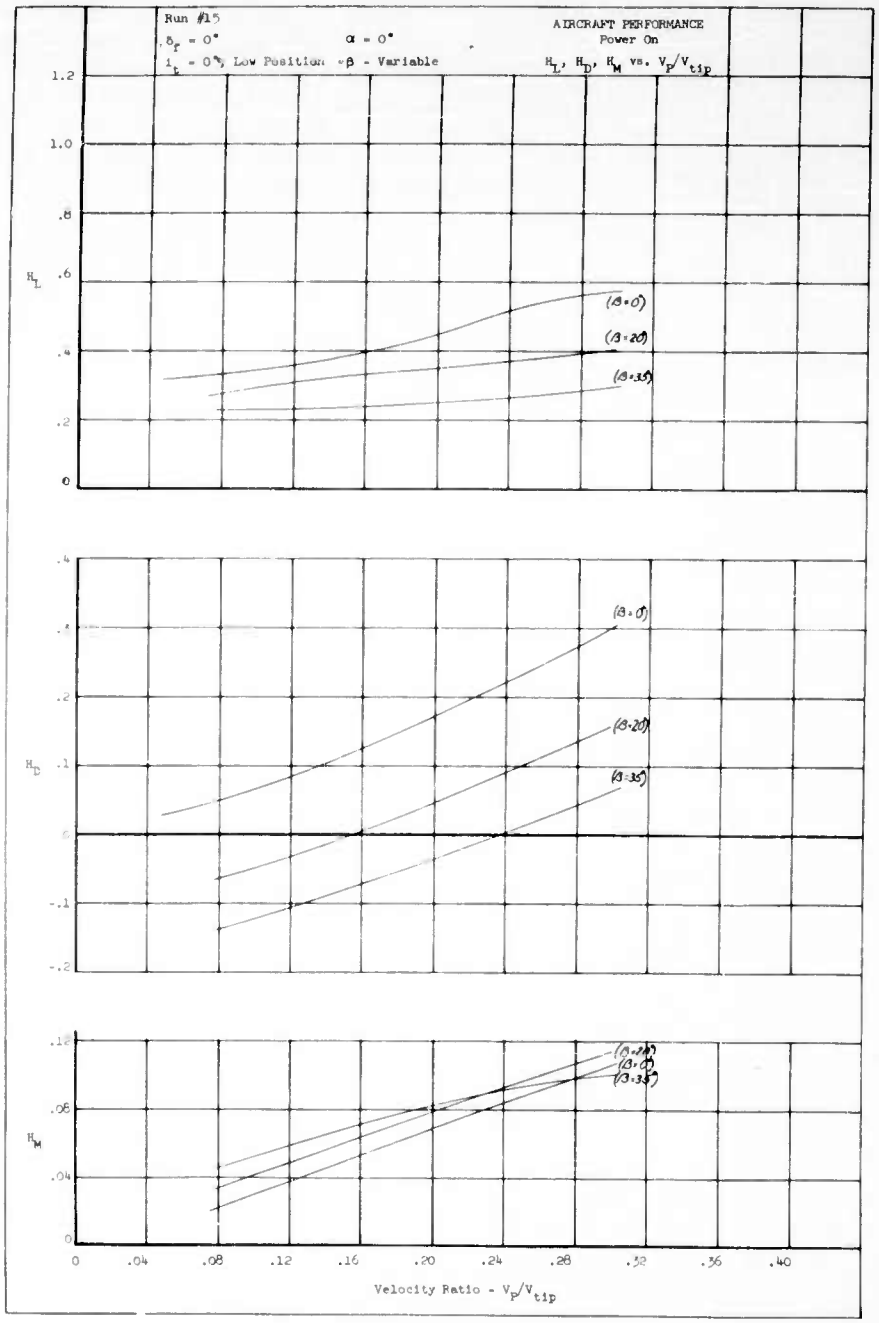

FIGURE 52 - FAN POWERED AIRCRAFT PERFORMANCE

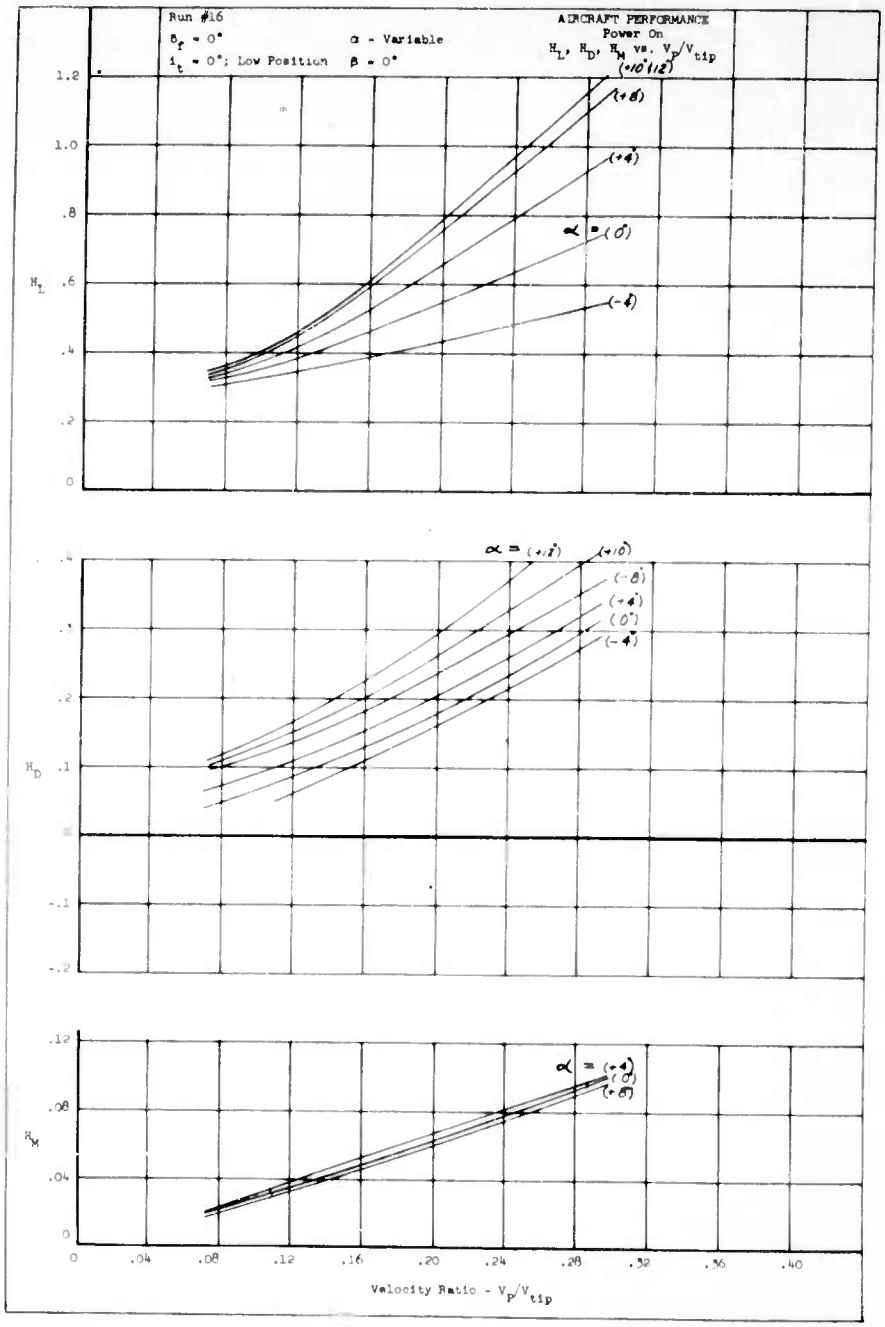

FIGURE 53 - FAN POWERED AIRCRAFT PERFORMANCE

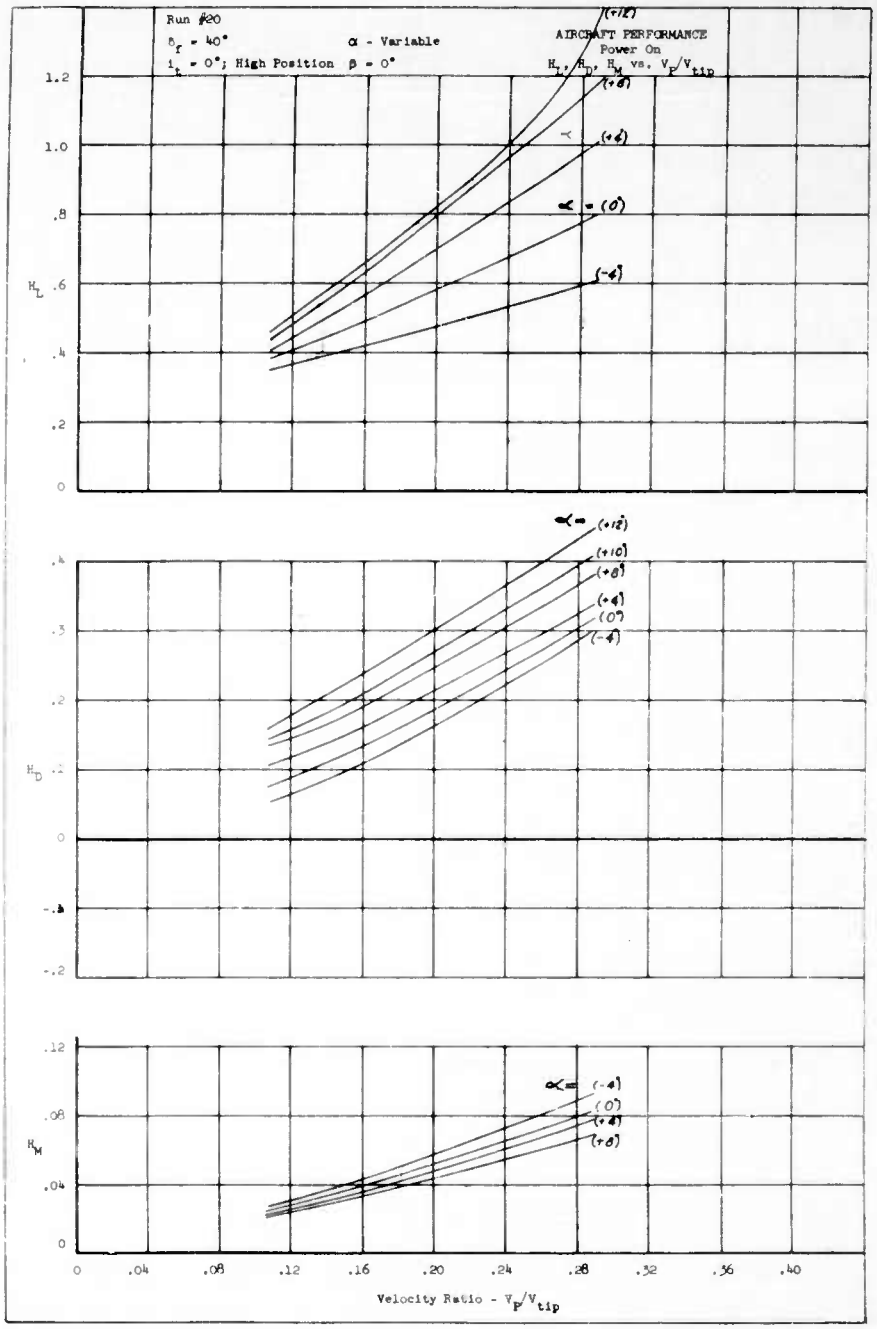

FIGURE 54 - FAN POWERED AIRCRAFT PERFORMANCE

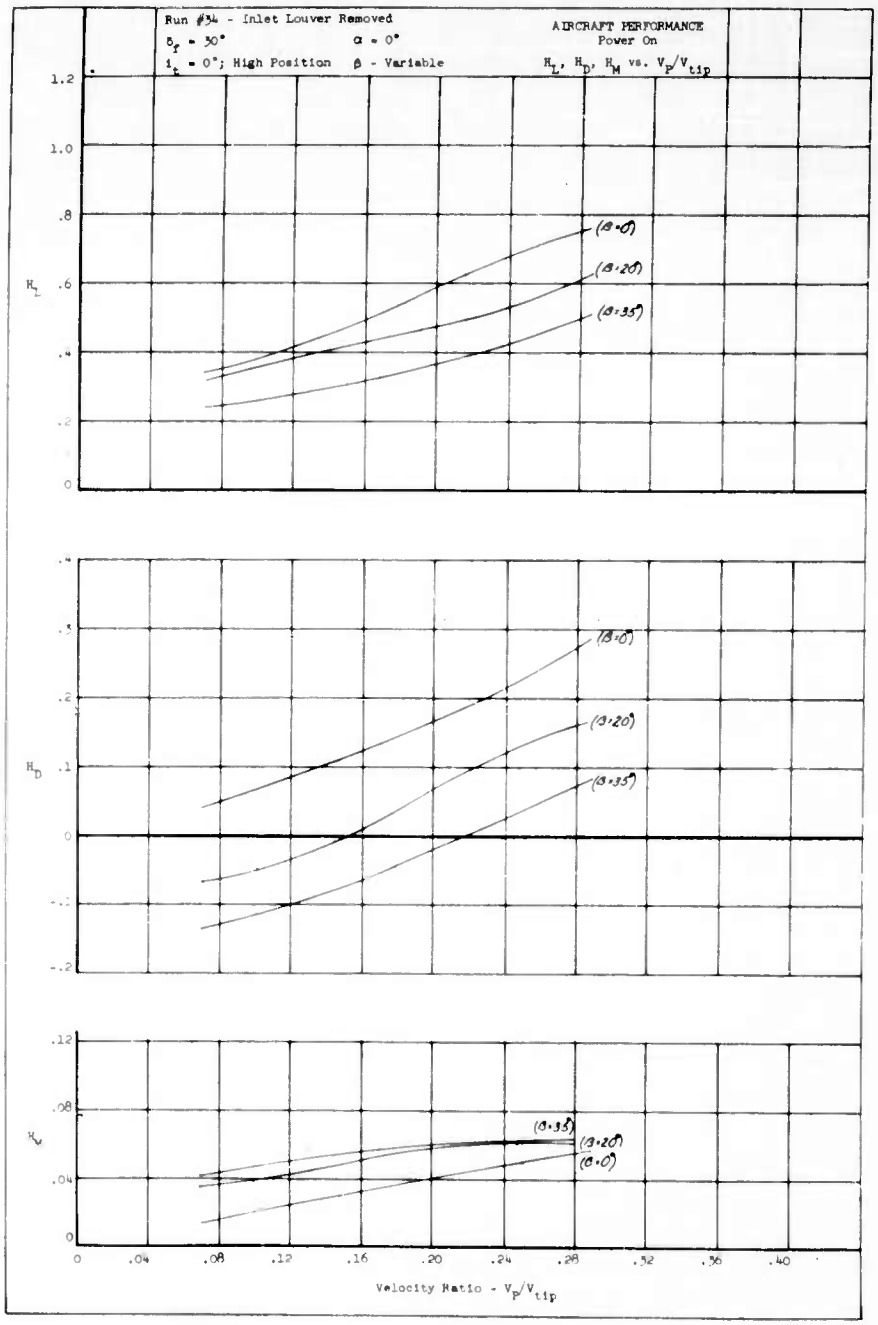

FIGURE 55a - FAN POWERED AIRCRAFT PERFORMANCE

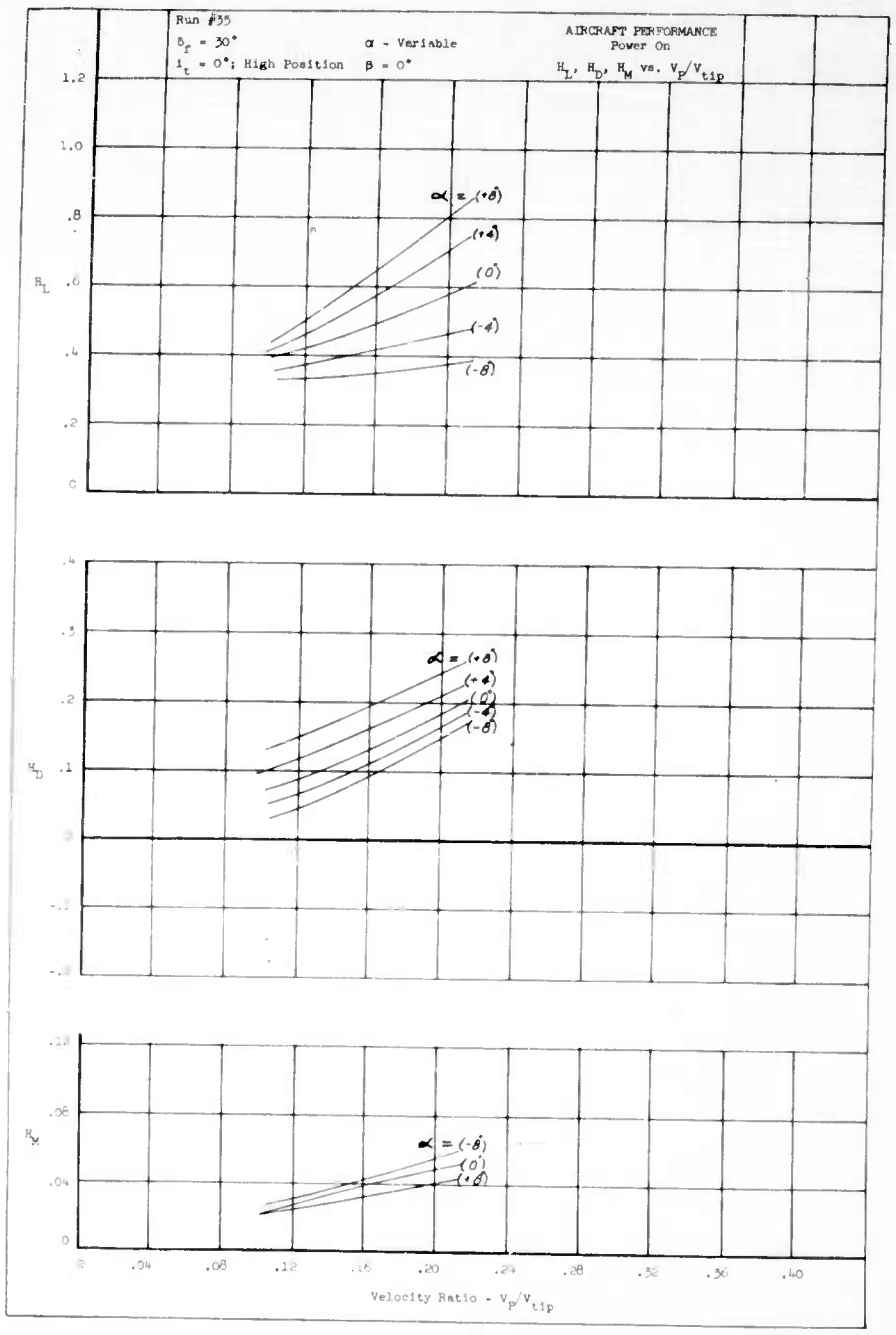

FIGURE 55b - FAN POWERED AIRCRAFT PERFORMANCE

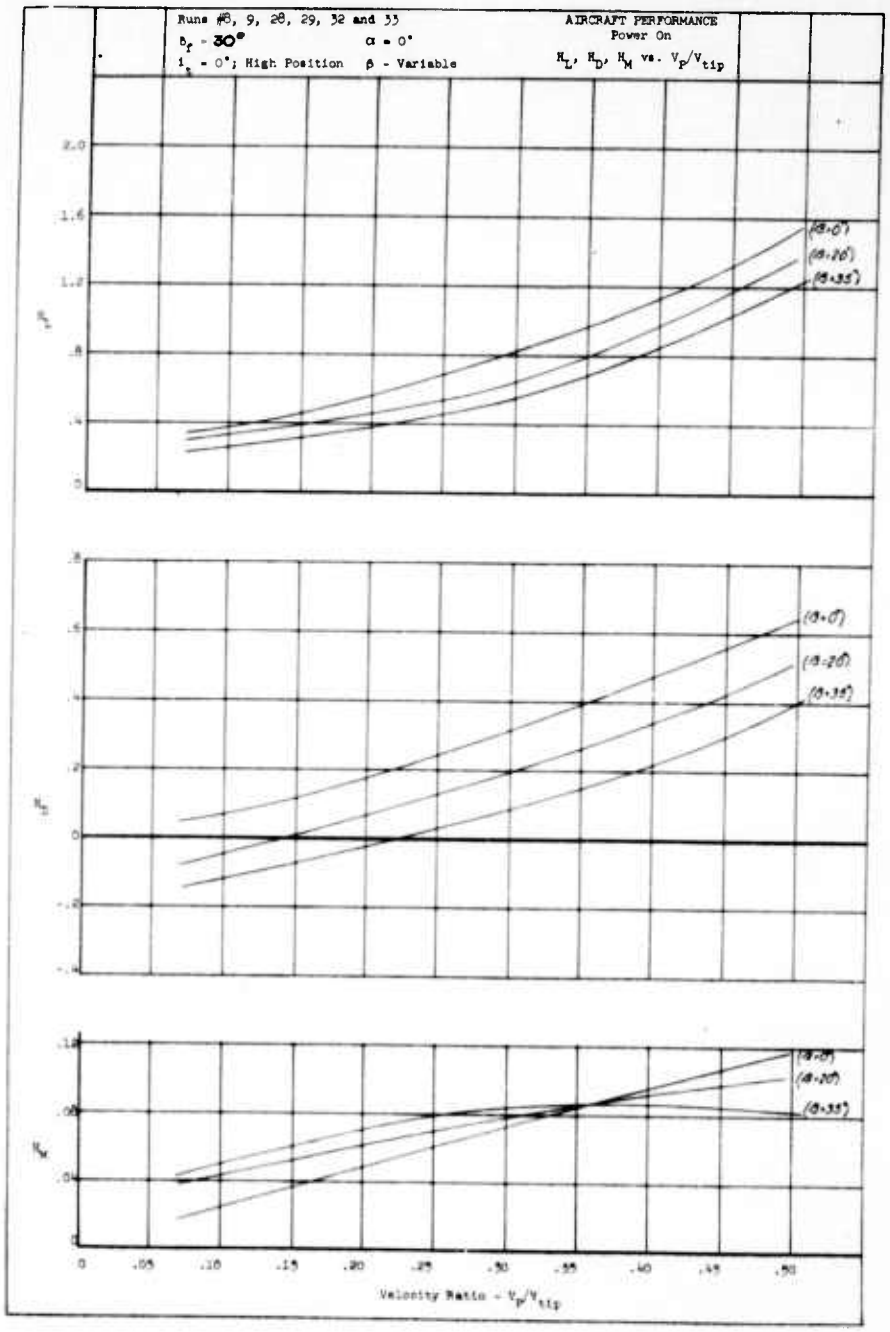

FIGURE 56 - FAN POWERED AIRCRAFT PERFORMANCE

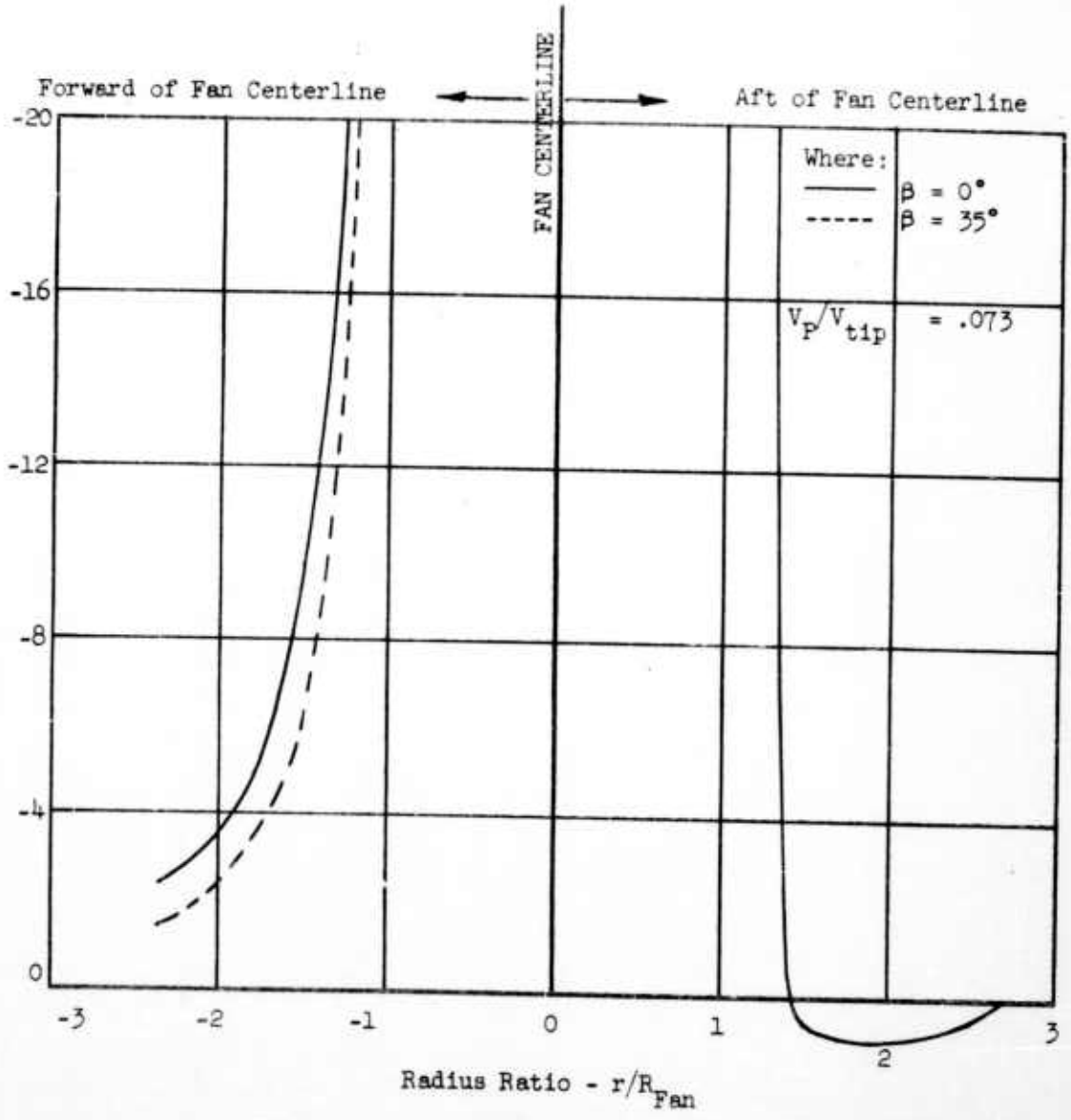

FIGURE 57a - PRESSURE COEFFICIENT ON TOP OF FUSELAGE VERSUS RADIUS RATIO

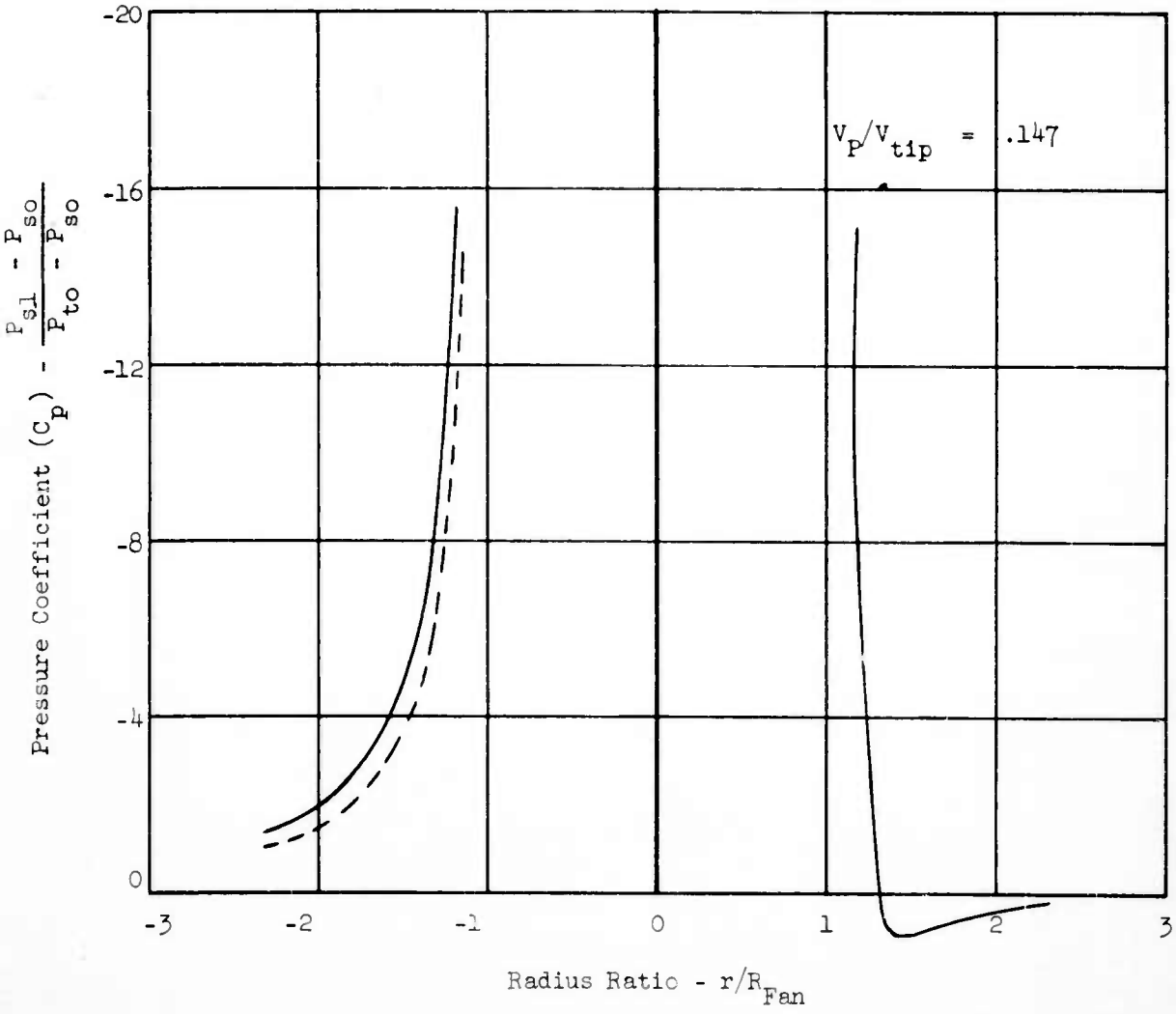

FIGURE 57b - PRESSURE COEFFICIENT ON TOP OF FUSELAGE VERSUS RADIUS RATIO

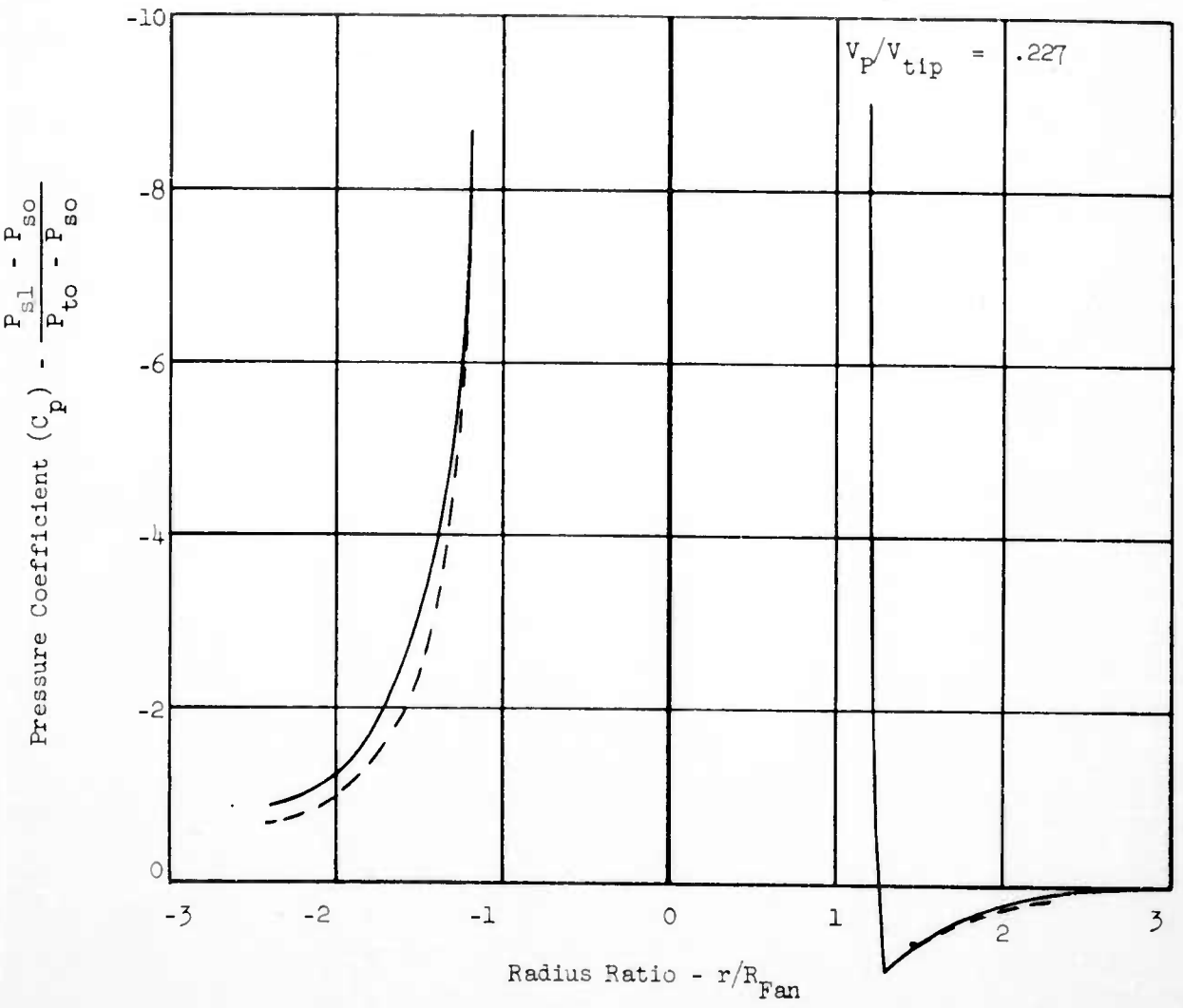

FIGURE 57c - PRESSURE COEFFICIENT ON TOP OF FUSELAGE VERSUS RADIUS RATIO

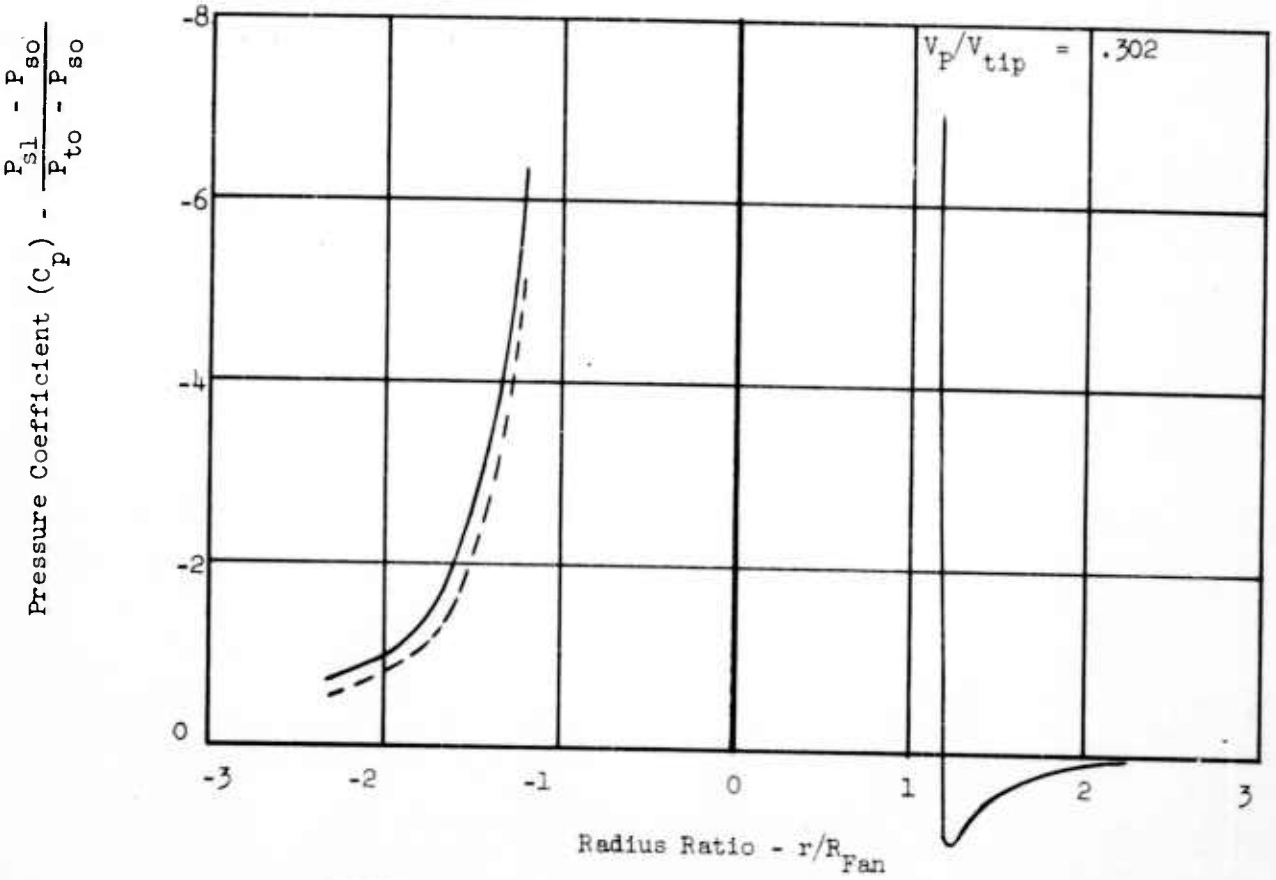

FIGURE 57d - PRESSURE COEFFICIENT ON TOP OF FUSELAGE VERSUS RADIUS RATIO

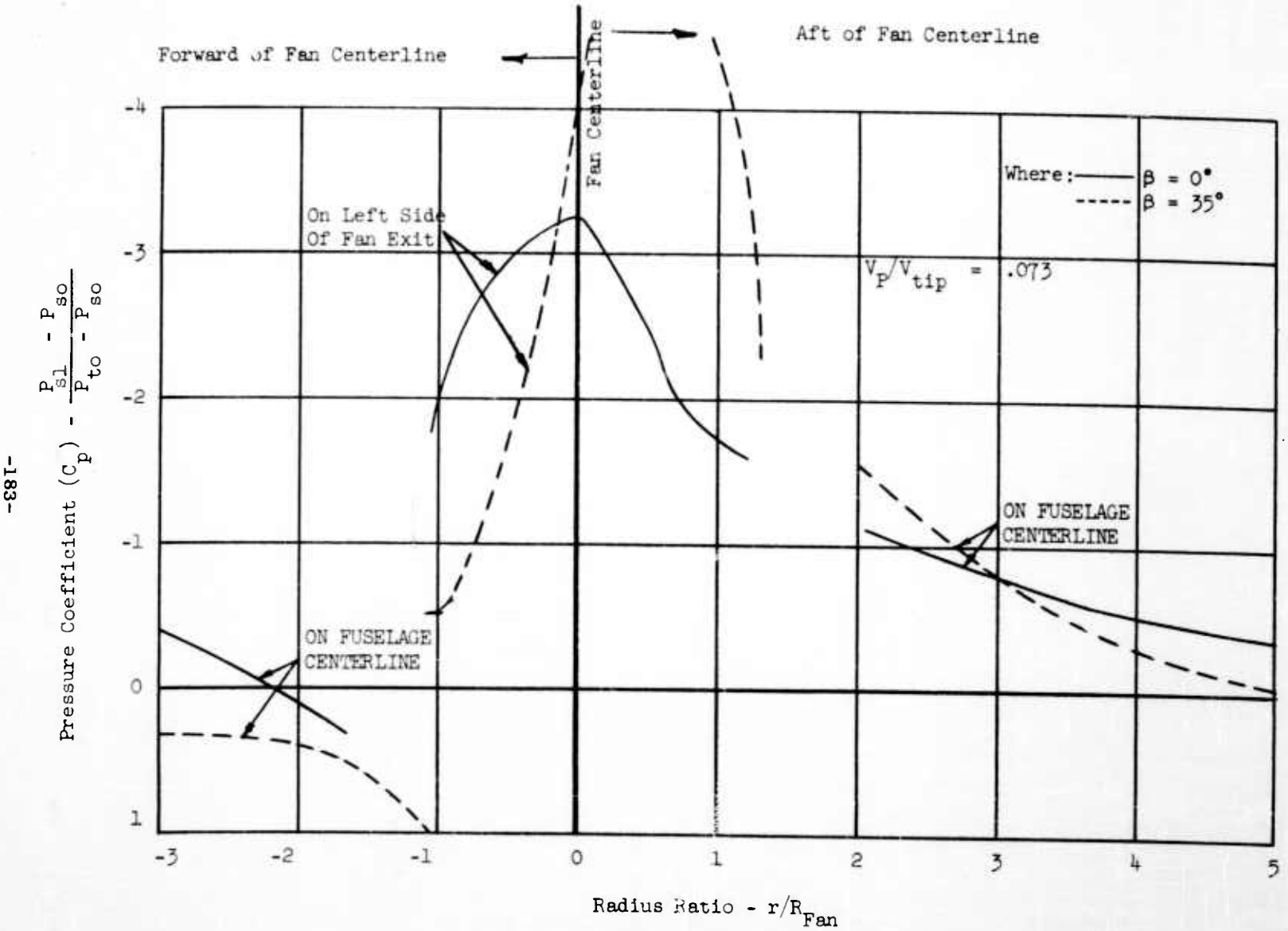

FIGURE 58a - PRESSURE COEFFICIENT ON BOTTOM OF FUSELAGE VERSUS RADIUS RATIO

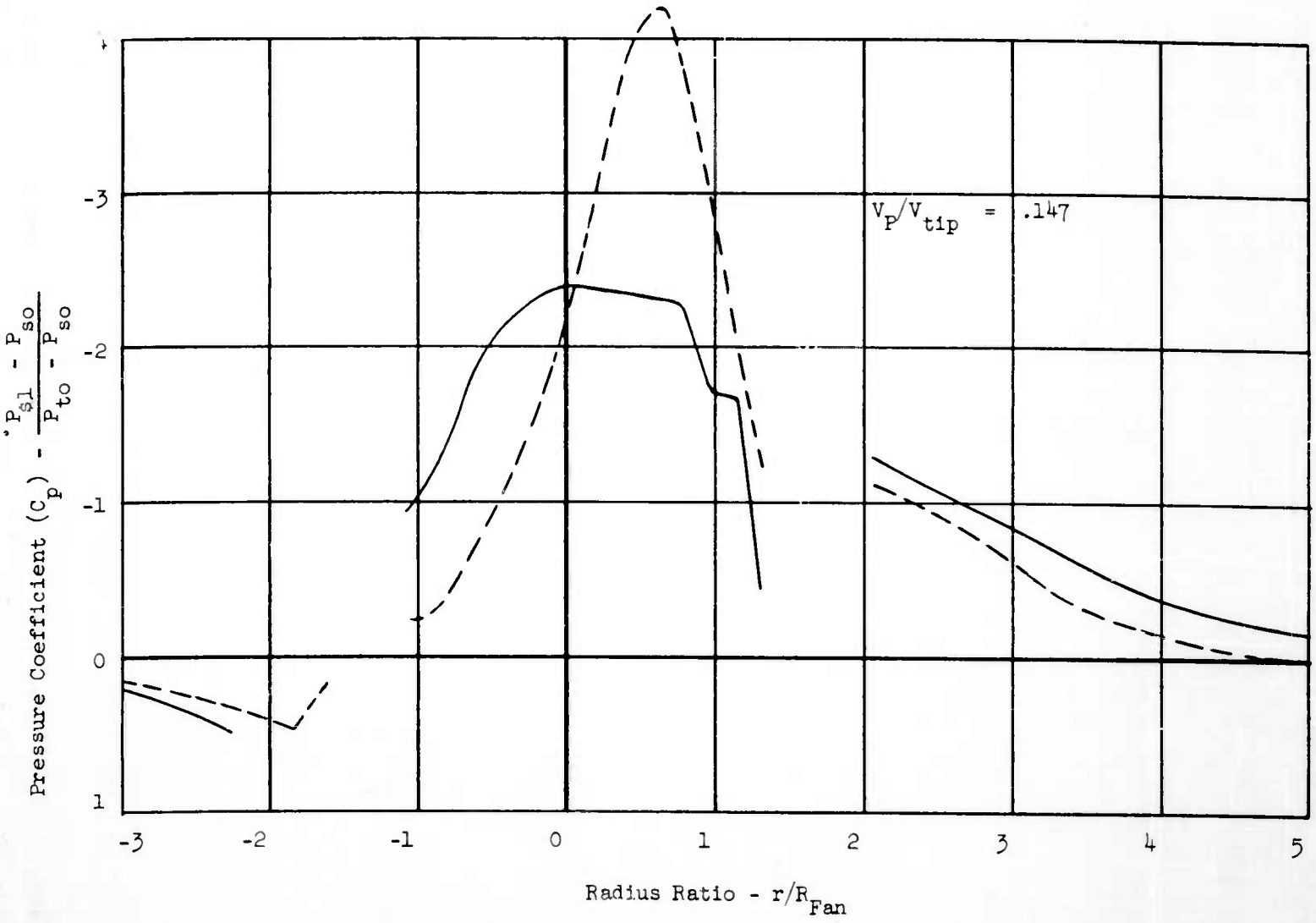

FIGURE 58b - PRESSURE COEFFICIENT ON BOTTOM OF FUSELAGE VERSUS RADIUS RATIO

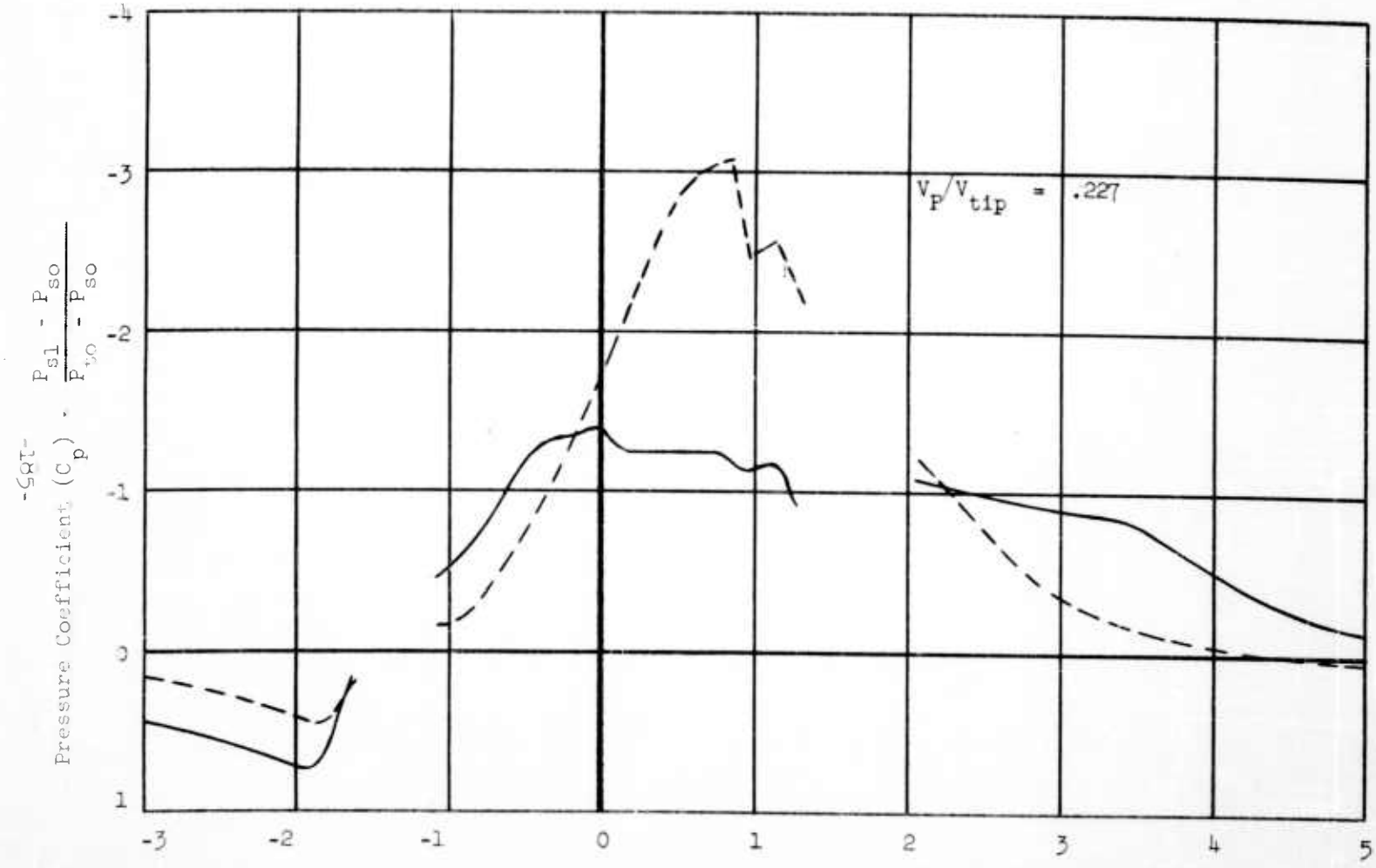

FIGURE 58c - PRESSURE COEFFICIENT ON BOTTOM OF FUSELAGE VERSUS RADIUS RATIO

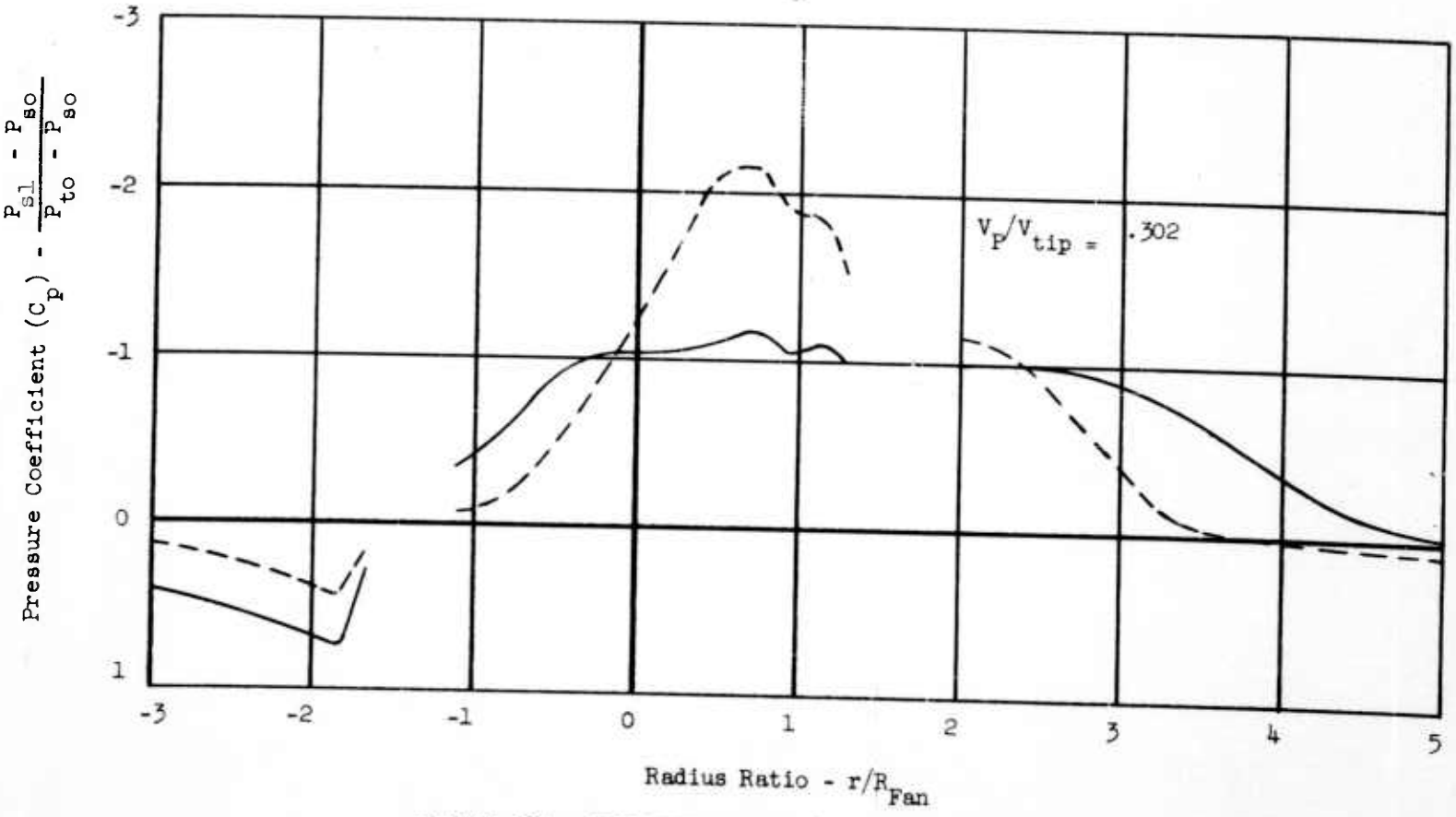

FIGURE 58d - PRESSURE COEFFICIENT ON BOTTOM OF FUSELAGE VERSUS RADIUS RATIO

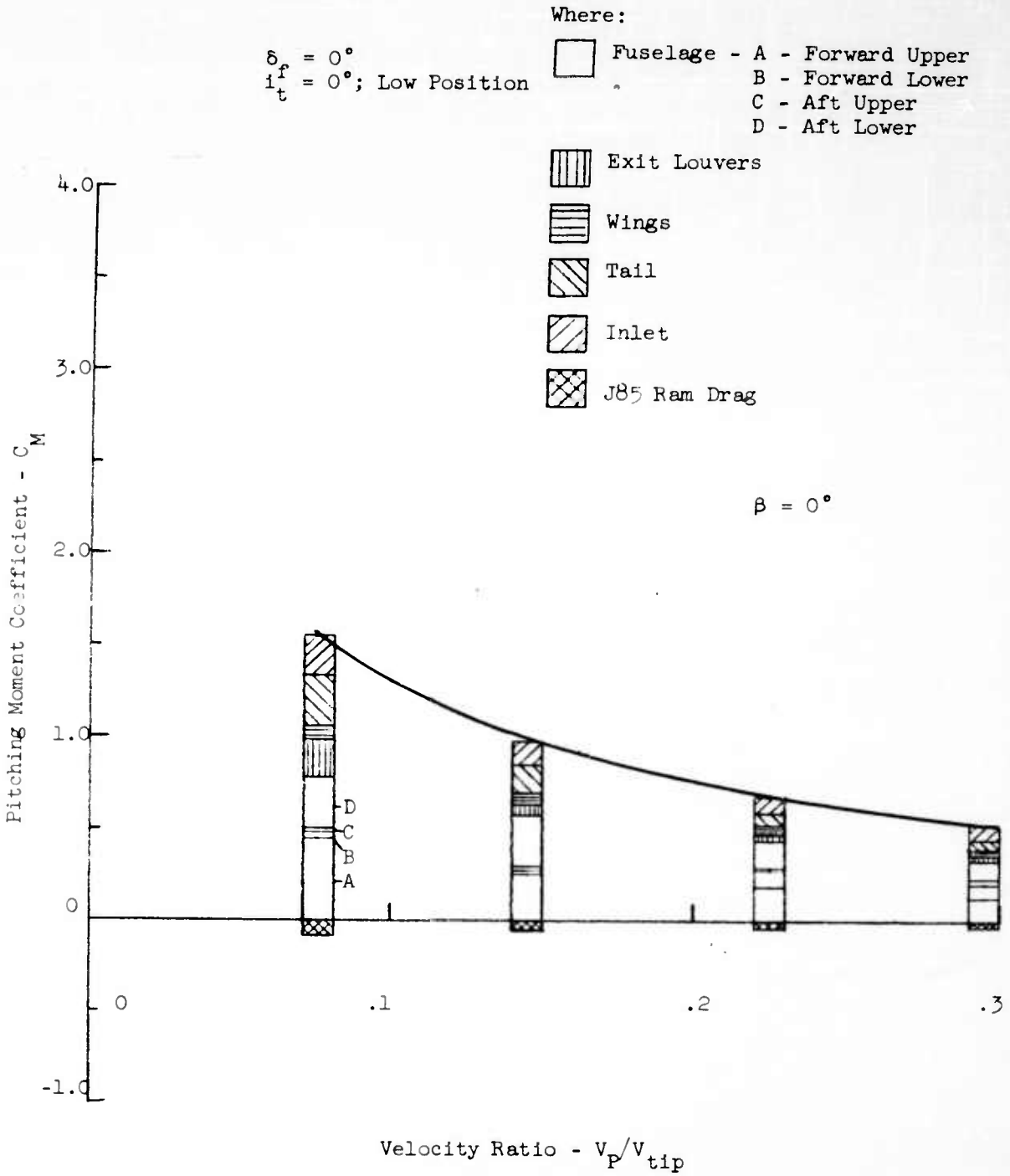

FIGURE 59a - PITCHING MOMENT SOURCE BREAKDOWN VERSUS VELOCITY RATIO

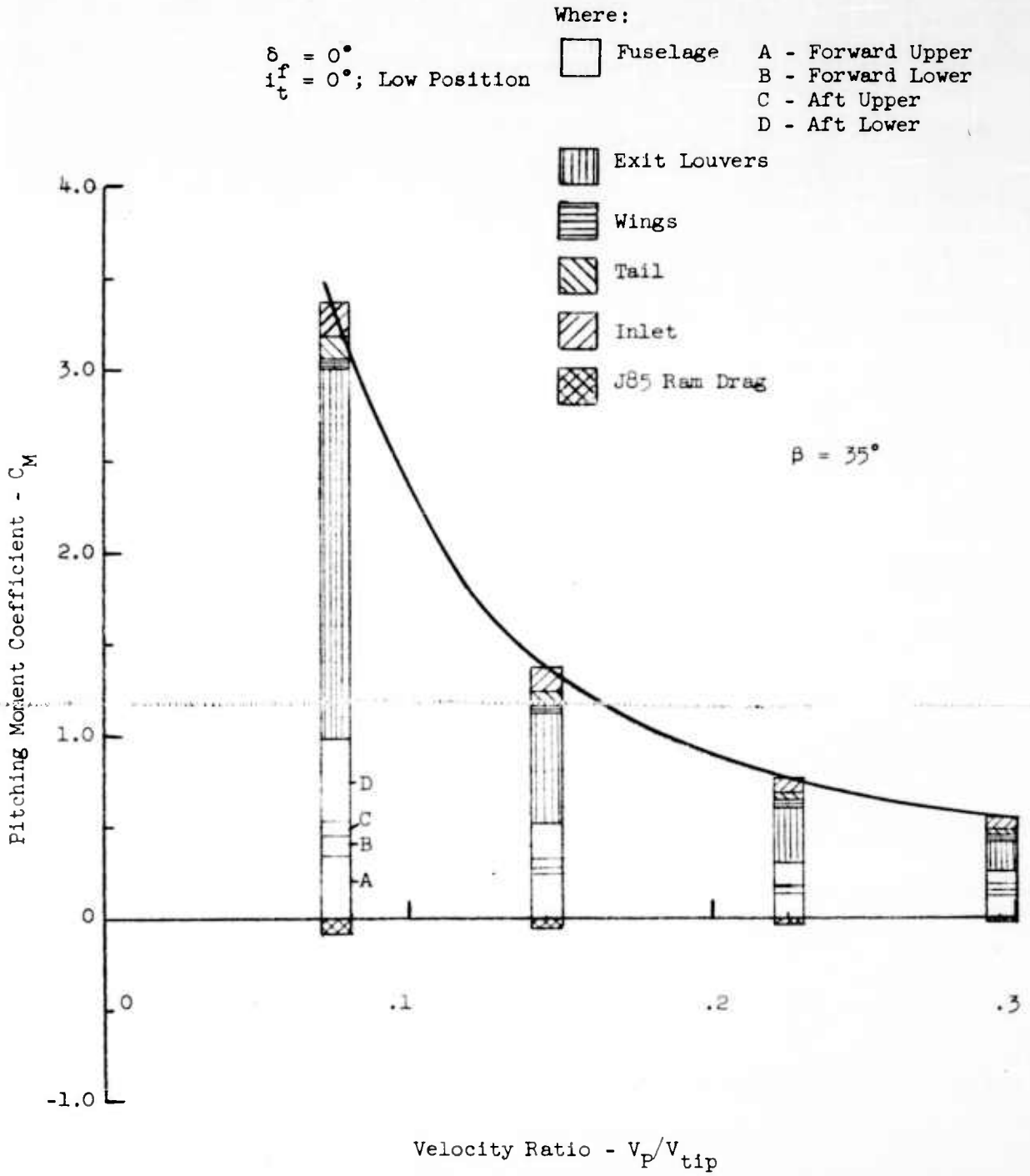

FIGURE 59b - PITCHING MOMENT SOURCE BREAKDOWN VERSUS VELOCITY RATIO

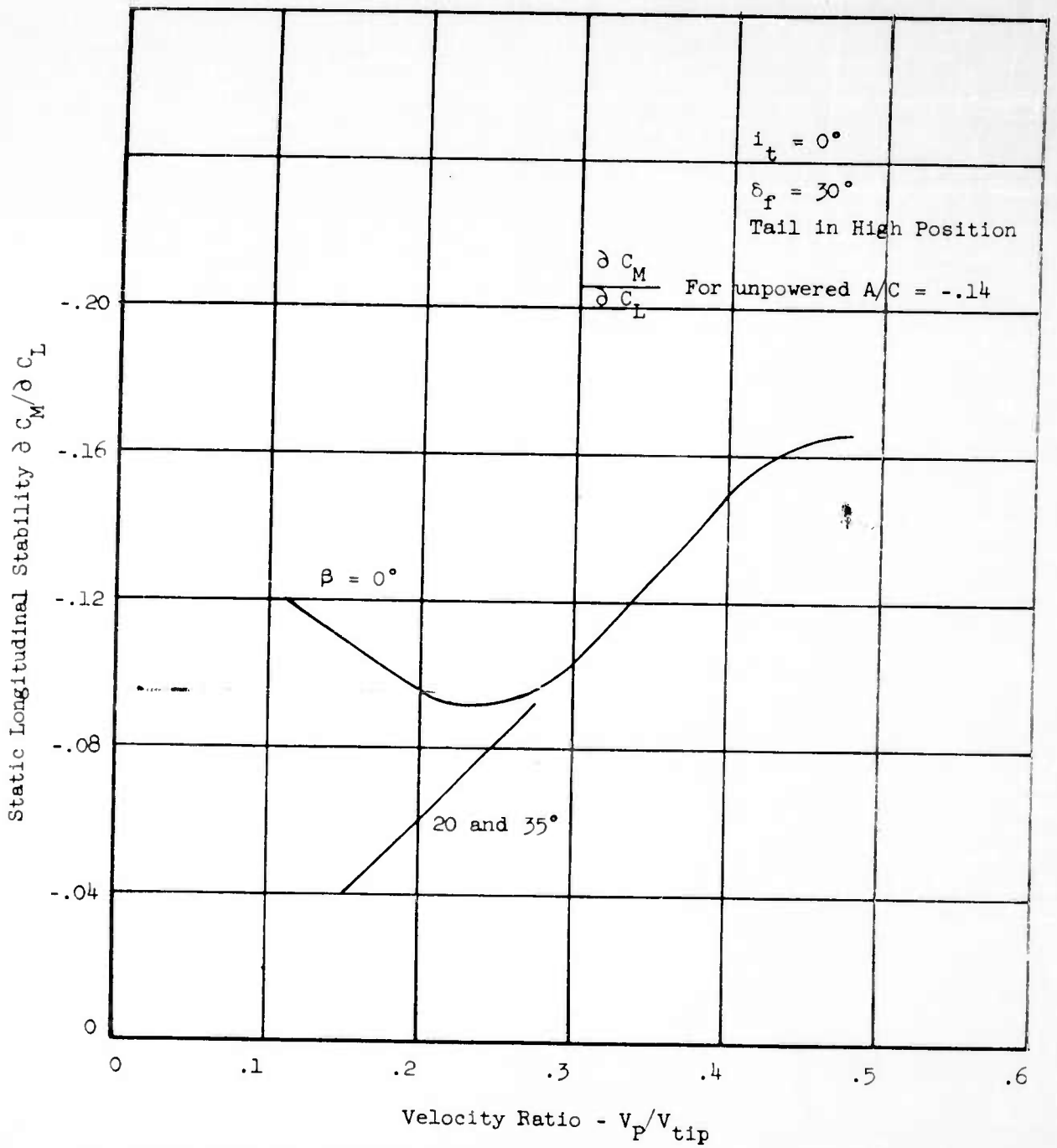

FIGURE 60 - STATIC LONGITUDINAL STABILITY VERSUS VELOCITY RATIO

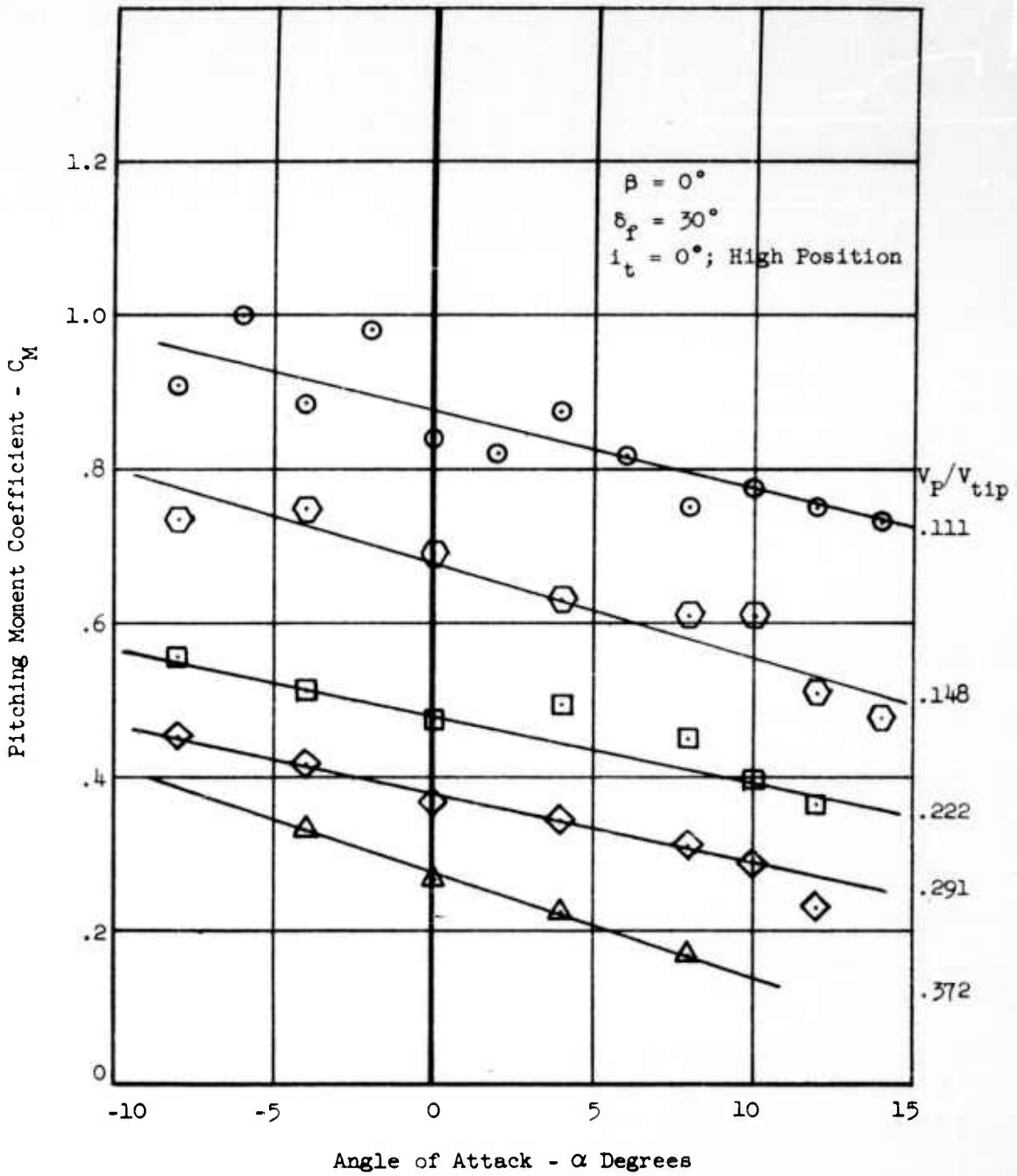

FIGURE 61 - PITCHING MOMENT COEFFICIENT VERSUS ANGLE OF ATTACK AND VELOCITY RATIO

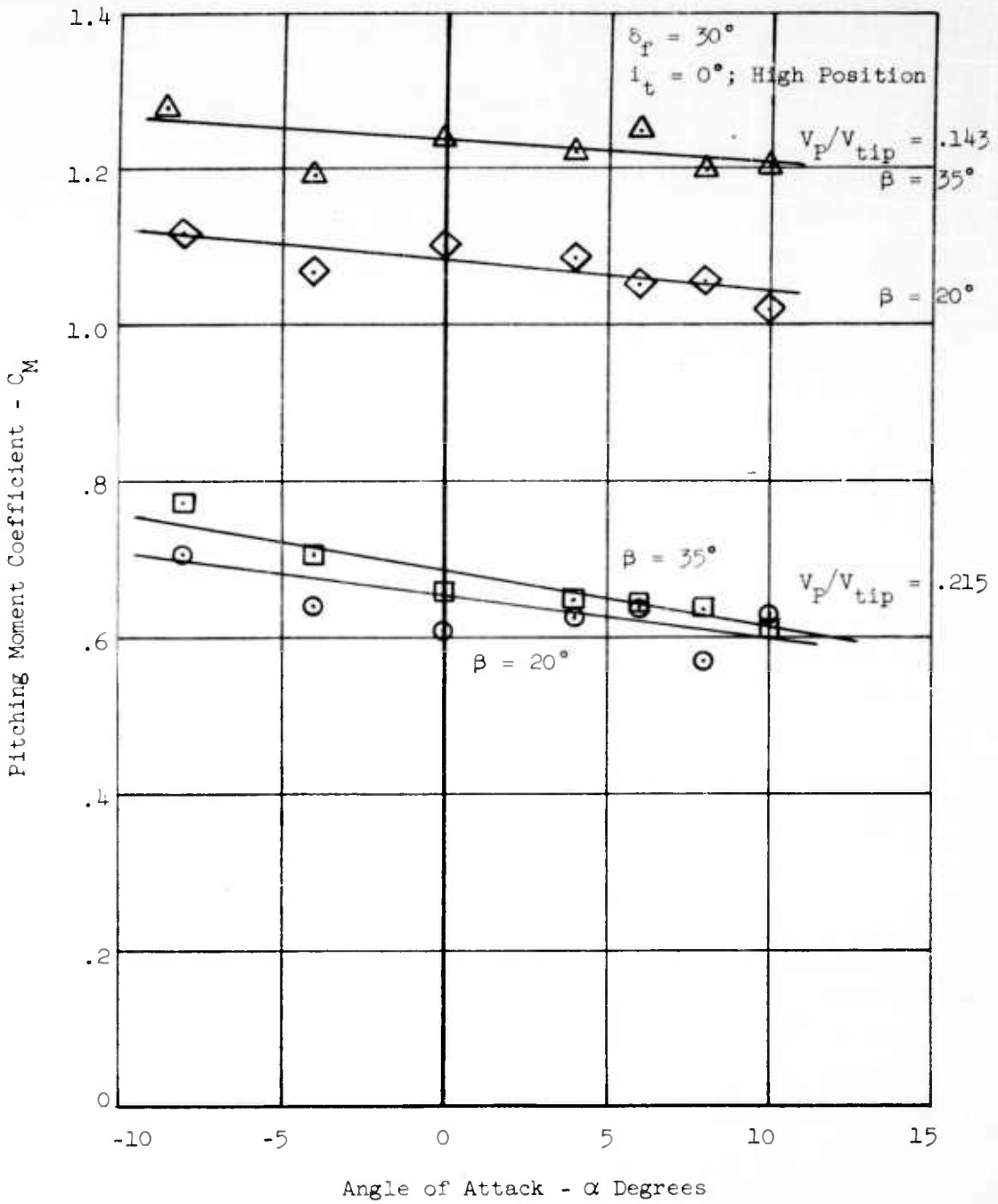

FIGURE 62 - PITCHING MOMENT COEFFICIENT VERSUS ANGLE OF ATTACK AND VELOCITY RATIO

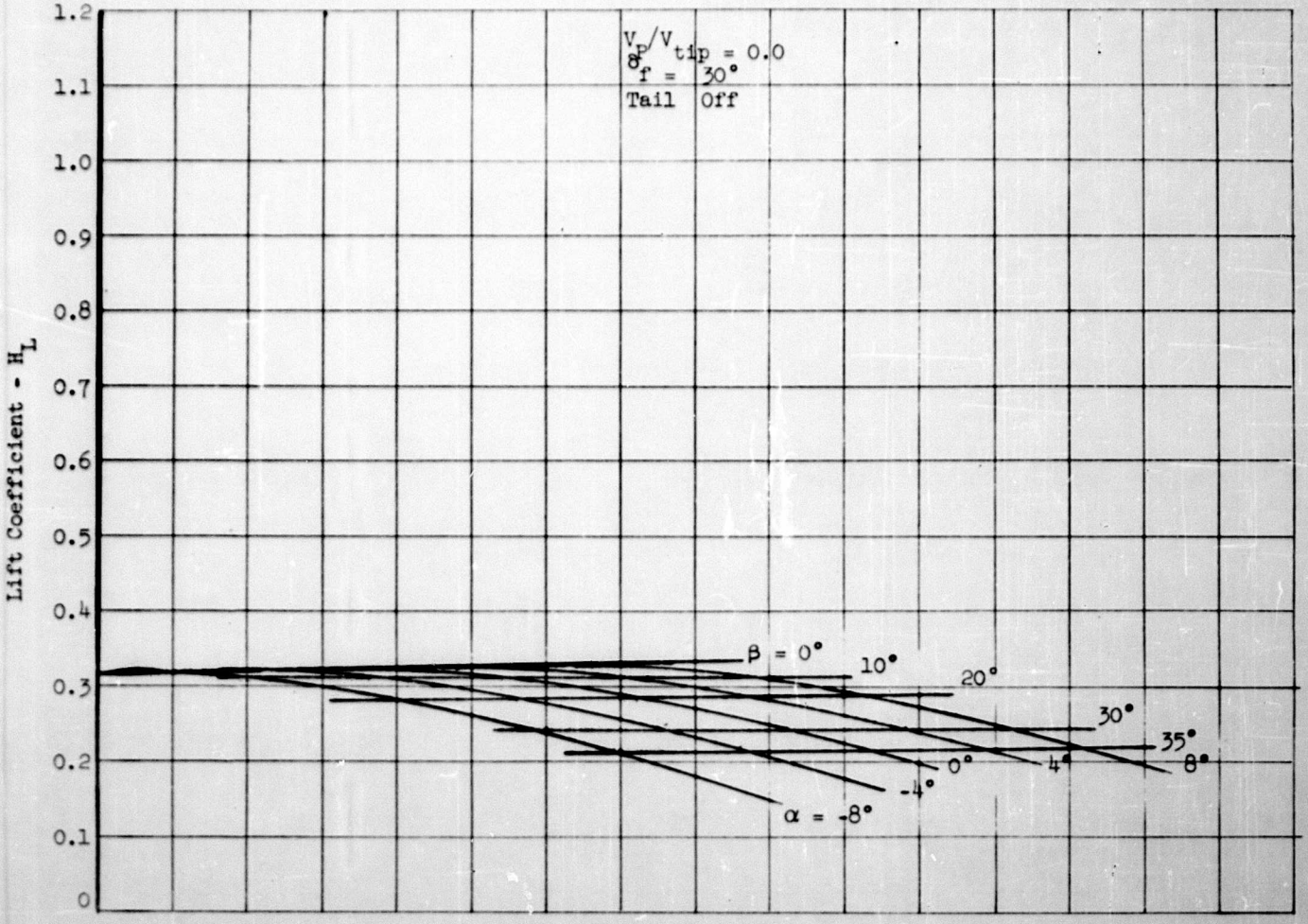

FIGURE 63a - LIFT COEFFICIENT VERSUS ANGLE OF ATTACK AND EXIT LOUVER ANGLE

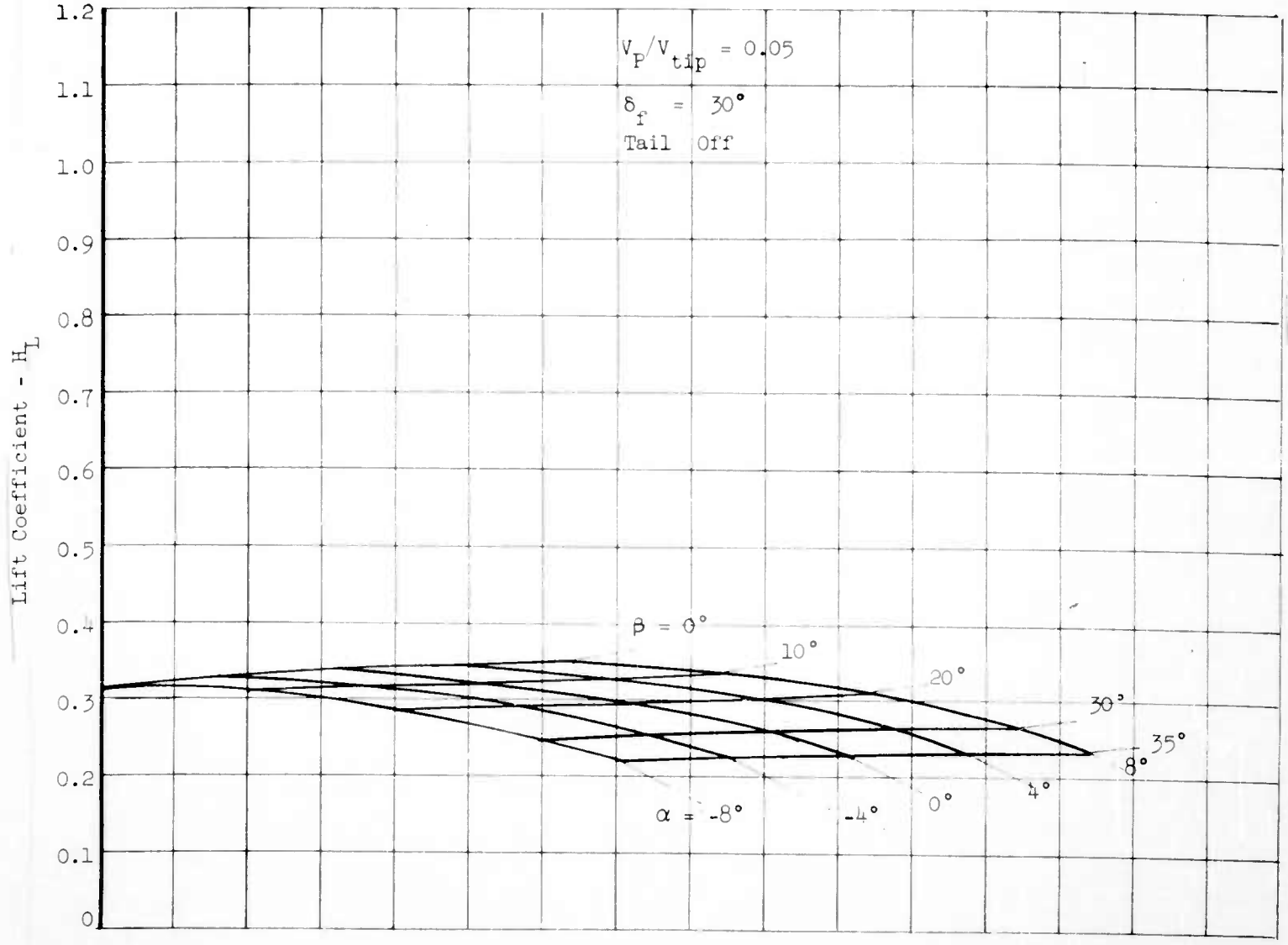

FIGURE 63b - LIFT COEFFICIENT VERSUS ANGLE OF ATTACK AND EXIT LOUVER ANGLE

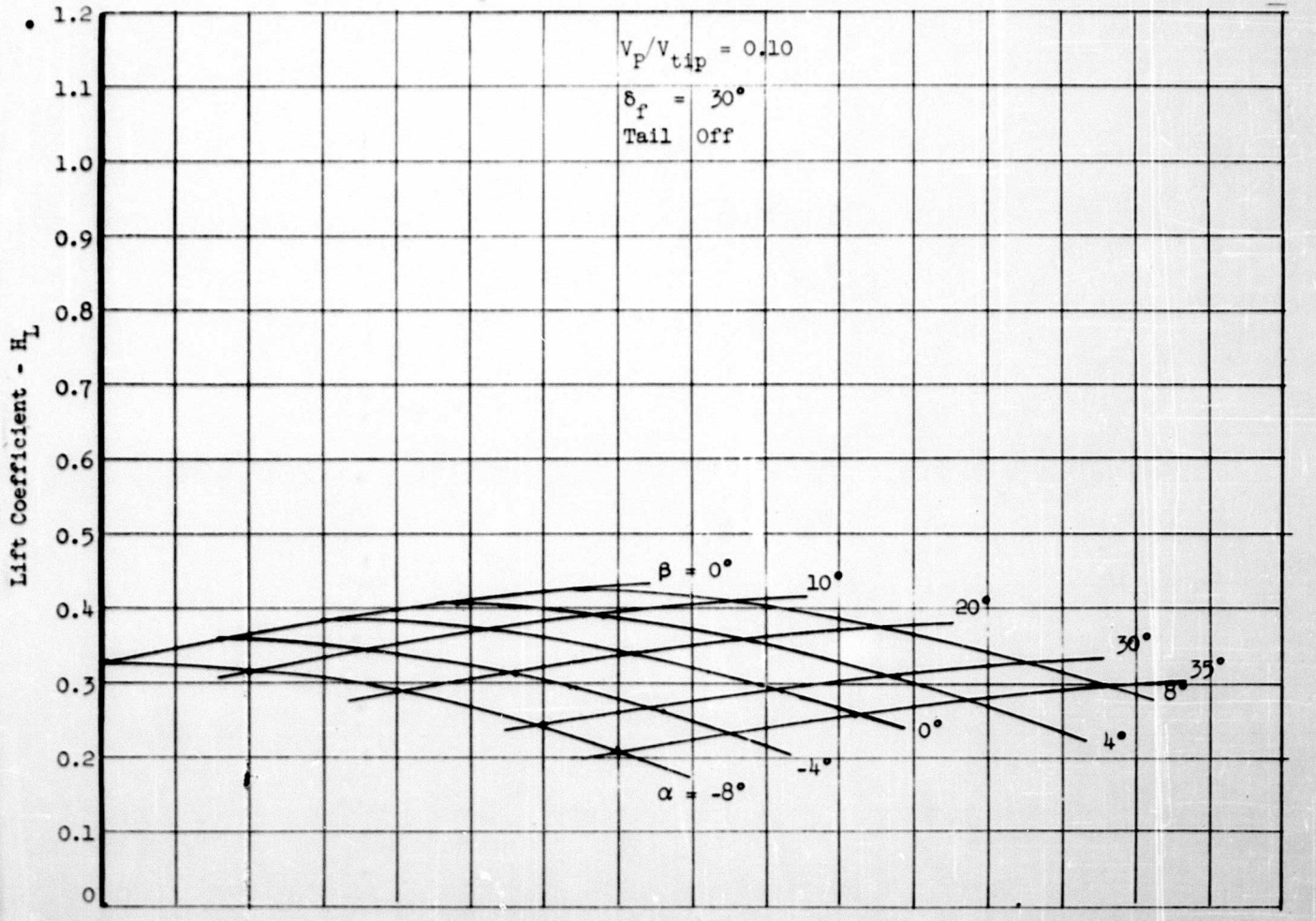

FIGURE 63c - LIFT COEFFICIENT VERSUS ANGLE OF ATTACK AND EXIT LOUVER ANGLE

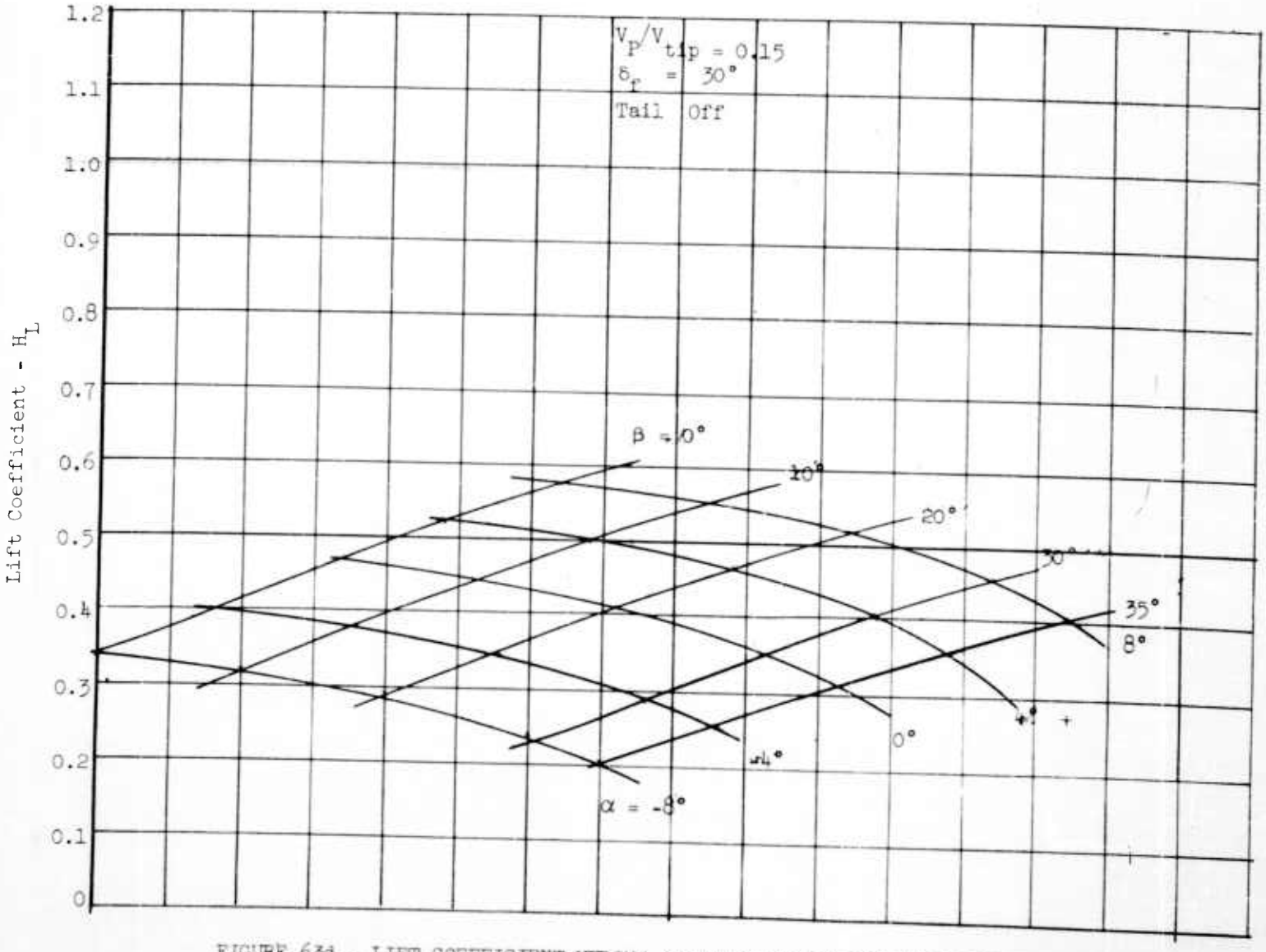

FIGURE 63d - LIFT COEFFICIENT VERSUS ANGLE OF ATTACK AND EXIT LOUVER ANGLE

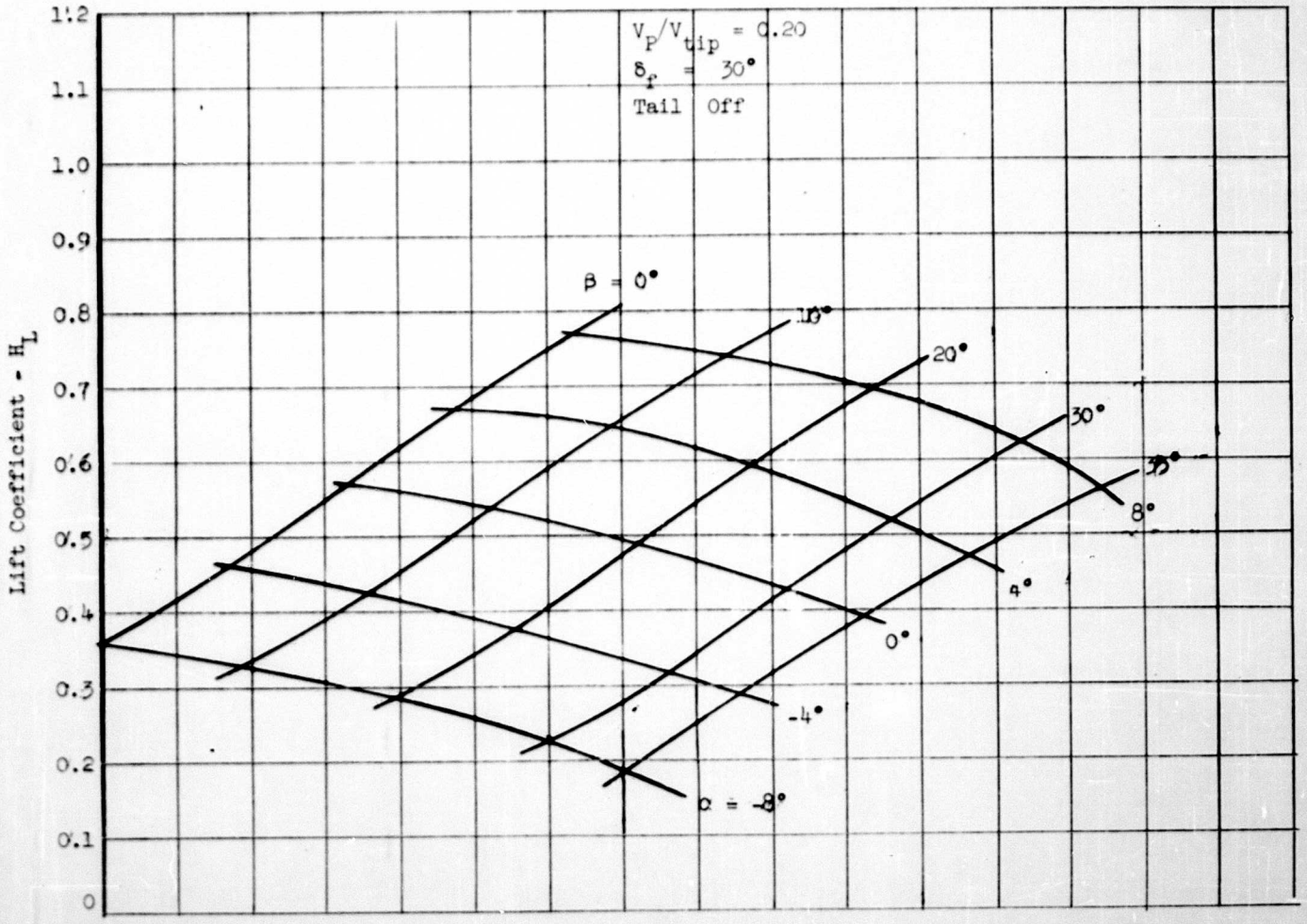

FIGURE 63e - LIFT COEFFICIENT VERSUS ANGLE OF ATTACK AND EXIT LOUVER ANGLE

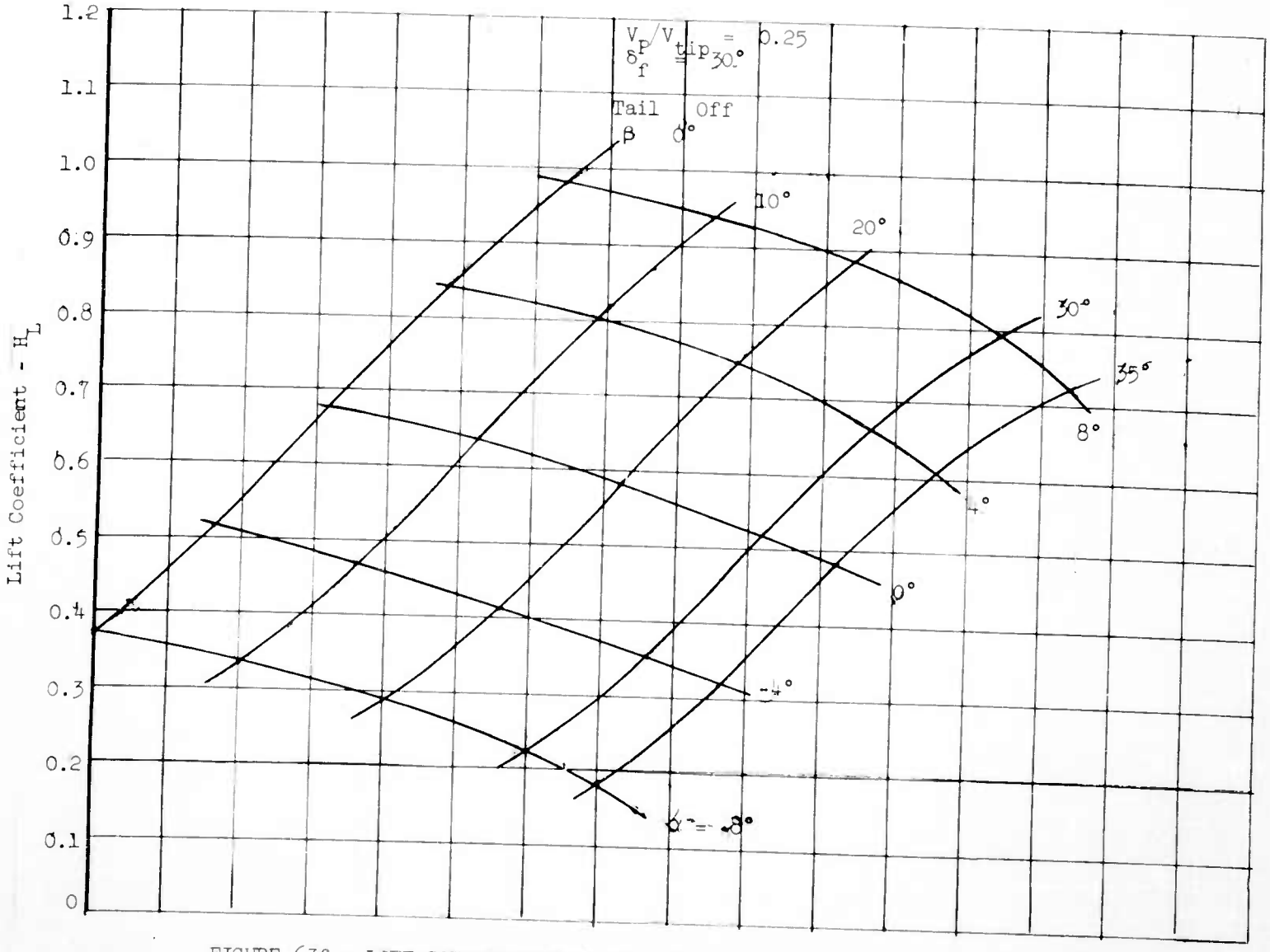

FIGURE 63f - LIFT COEFFICIENT VERSUS ANGLE OF ATTACK AND EXIT LOUVER ANGLE

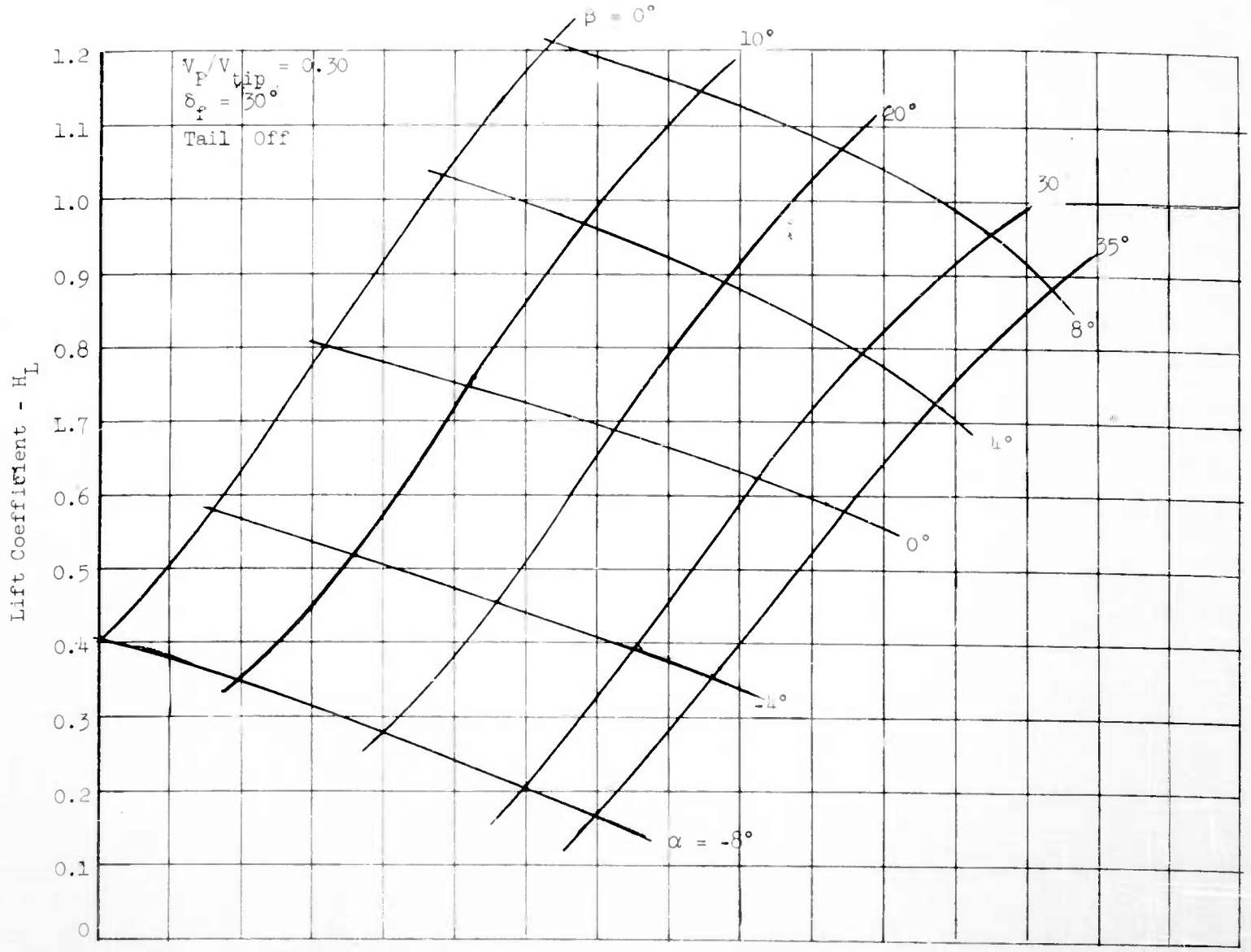

FIGURE 63g - LIFT COEFFICIENT VERSUS ANGLE OF ATTACK AND EXIT LOUVER ANGLE

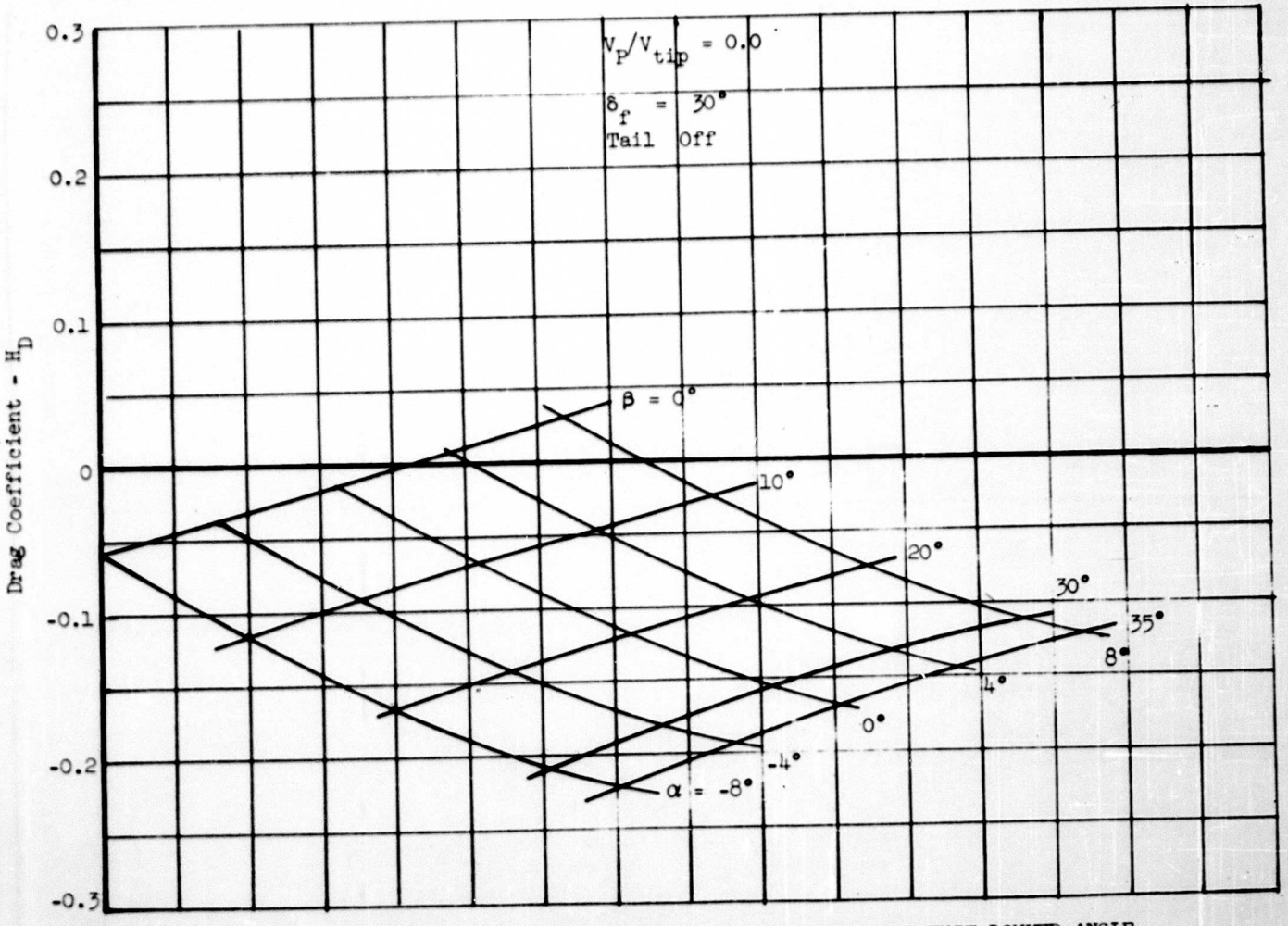

FIGURE 64a - DRAG COEFFICIENT VERSUS ANGLE OF ATTACK AND EXIT LOUVER ANGLE

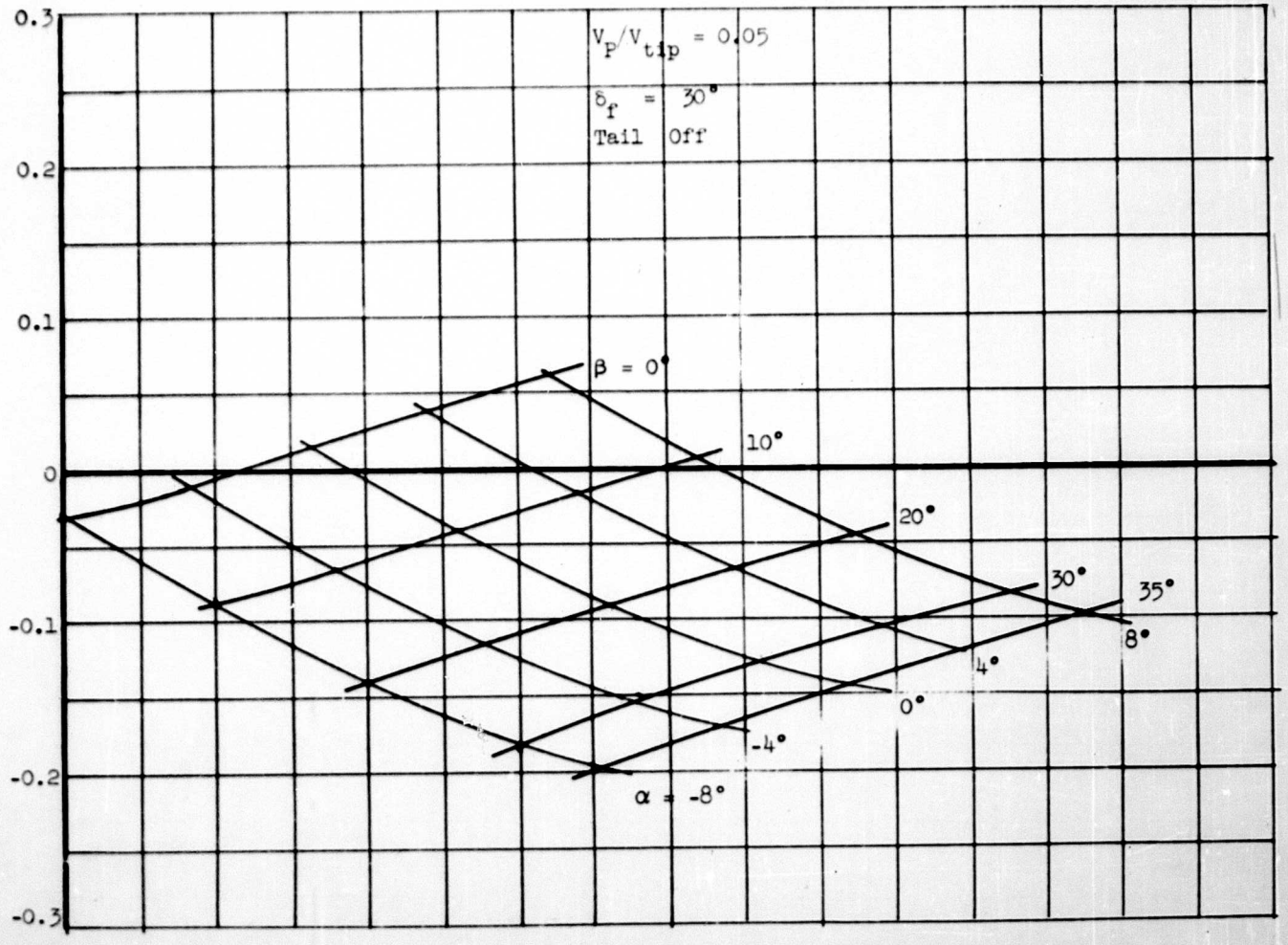

FIGURE 64b - DRAG COEFFICIENT VERSUS ANGLE OF ATTACK AND EXIT LOUVER ANGLE

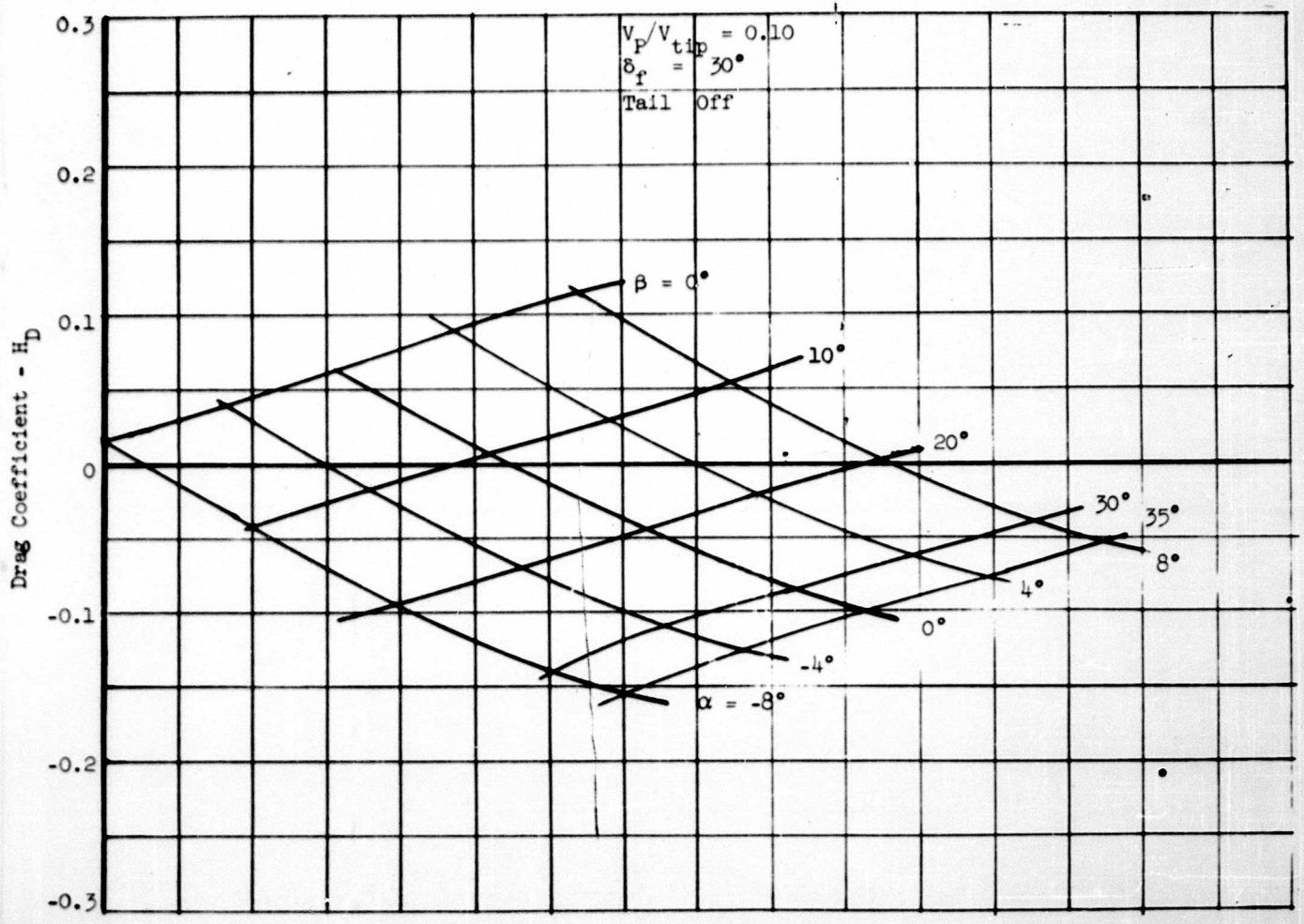

FIGURE 64c - DRAG COEFFICIENT VERSUS ANGLE OF ATTACK AND EXIT LOUVER ANGLE

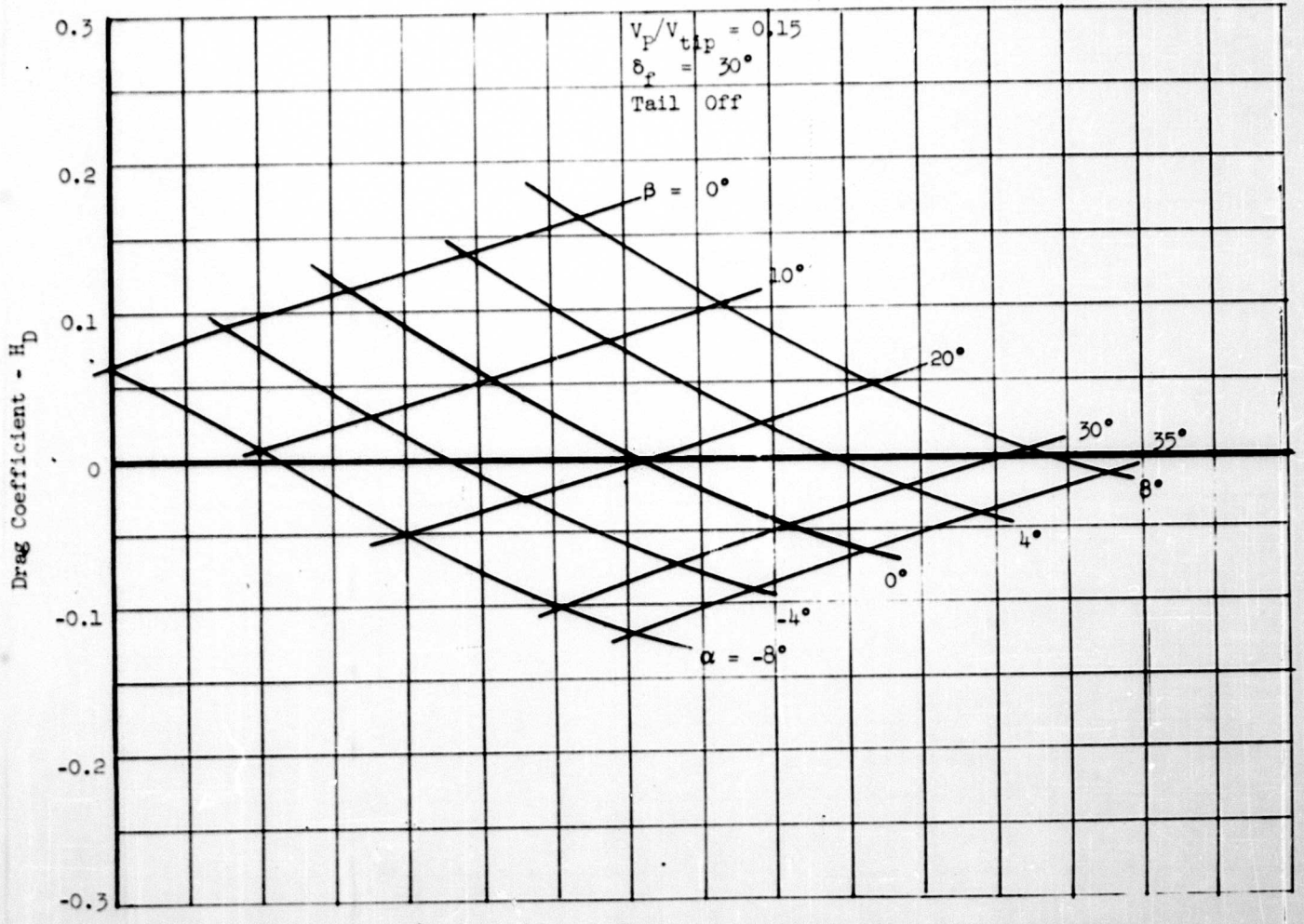

FIGURE 64d - DRAG COEFFICIENT VERSUS ANGLE OF ATTACK AND EXIT LOUVER ANGLE

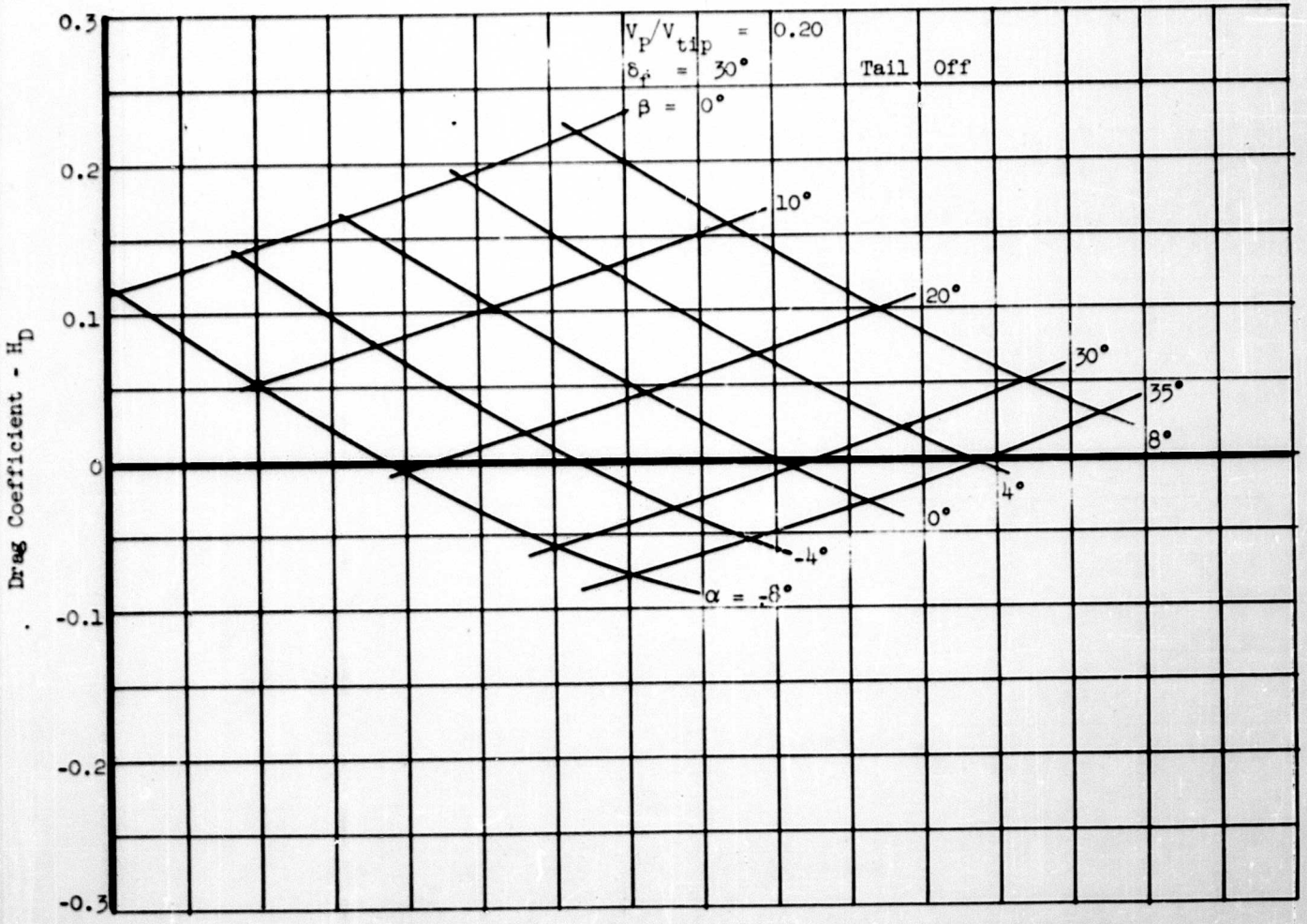

FIGURE 64e - DRAG COEFFICIENT VERSUS ANGLE OF ATTACK AND EXIT LOUVER ANGLE

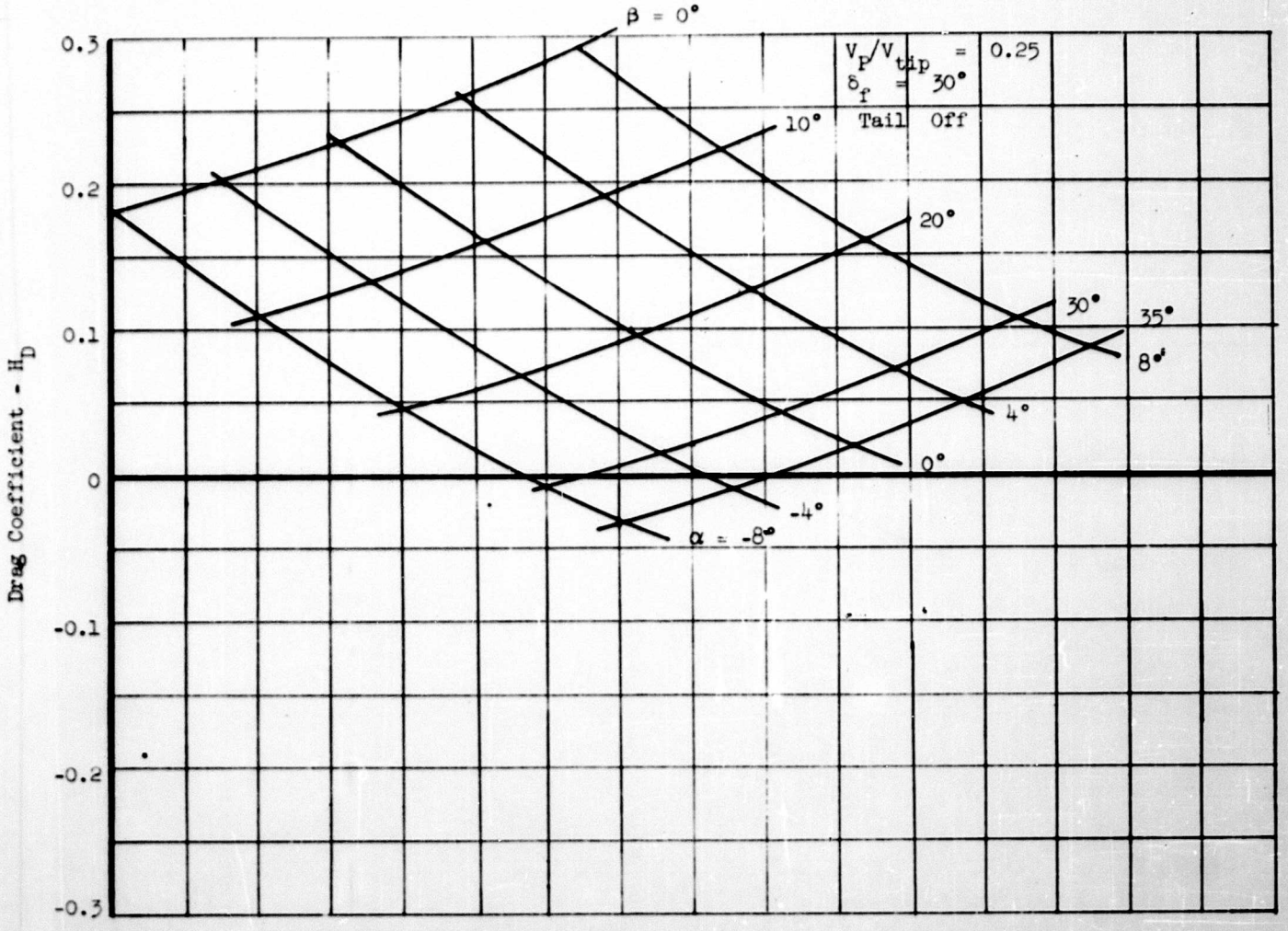

FIGURE 64f - DRAG COEFFICIENT VERSUS ANGLE OF ATTACK AND EXIT LOUVER ANGLE

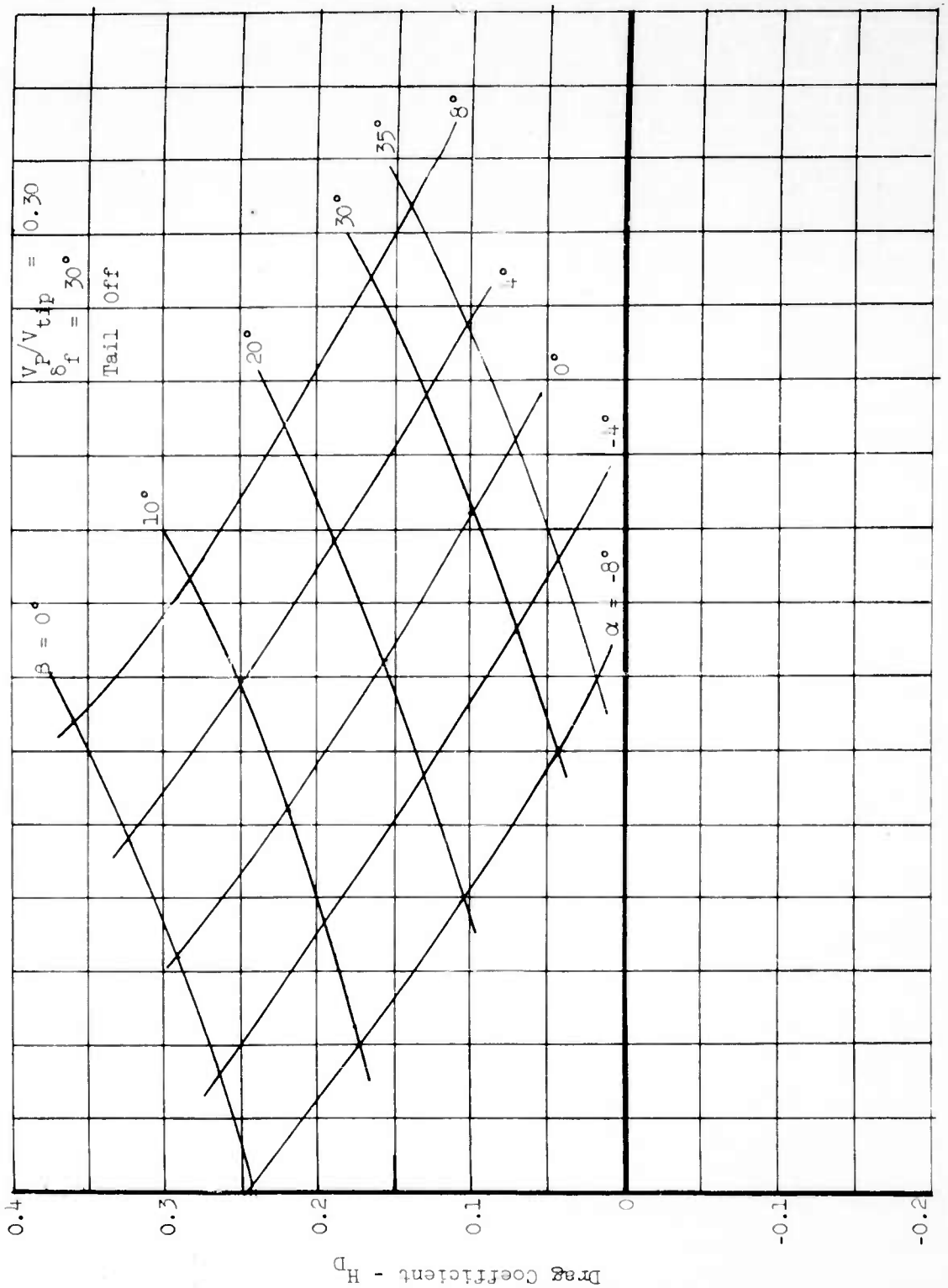

FIGURE 64g - DRAG COEFFICIENT VERSUS ANGLE OF ATTACK AND EXIT LOUVER ANGLE

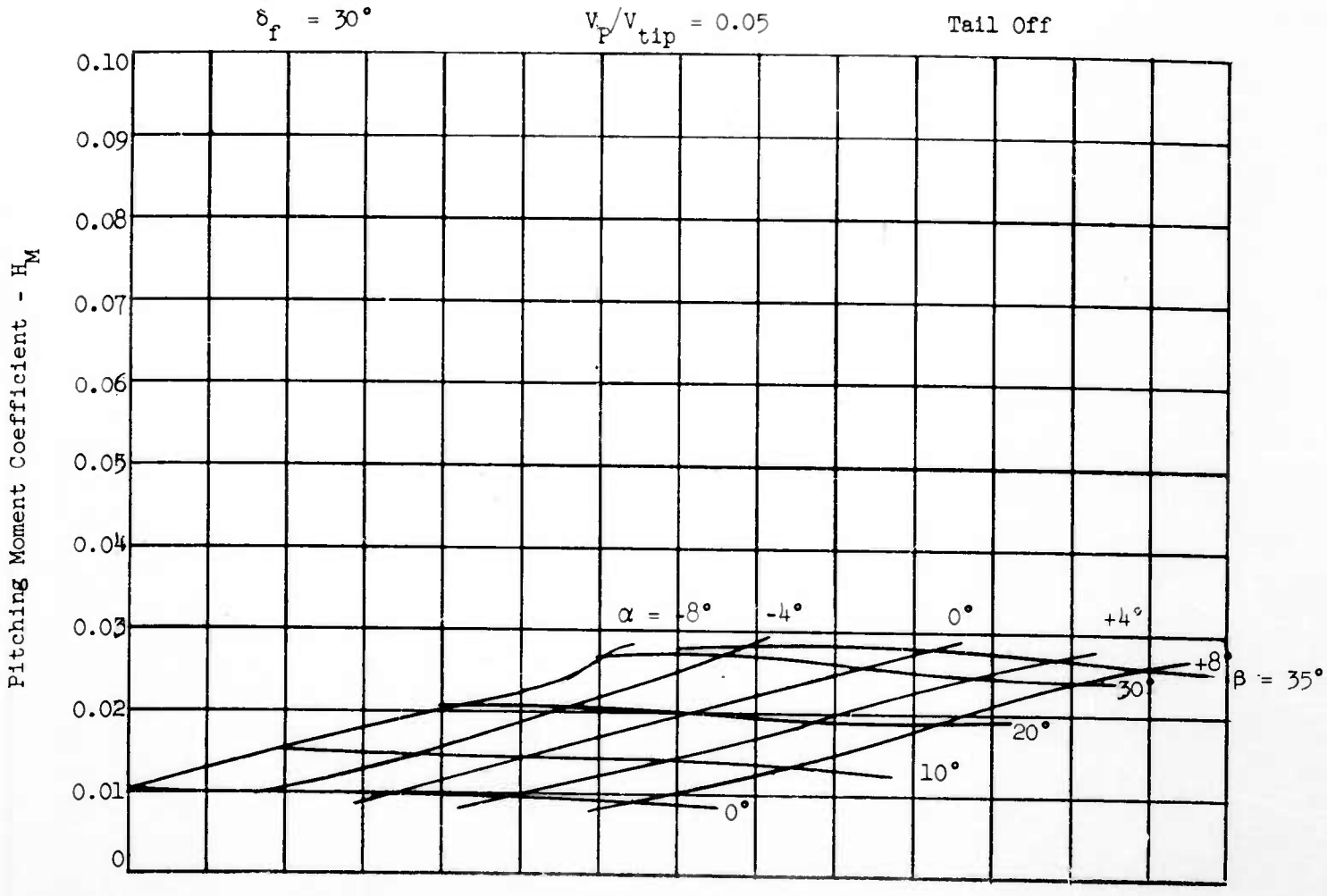

FIGURE 65a - PITCHING MOMENT COEFFICIENT VERSUS ANGLE OF ATTACK AND EXIT LOUVER ANGLE

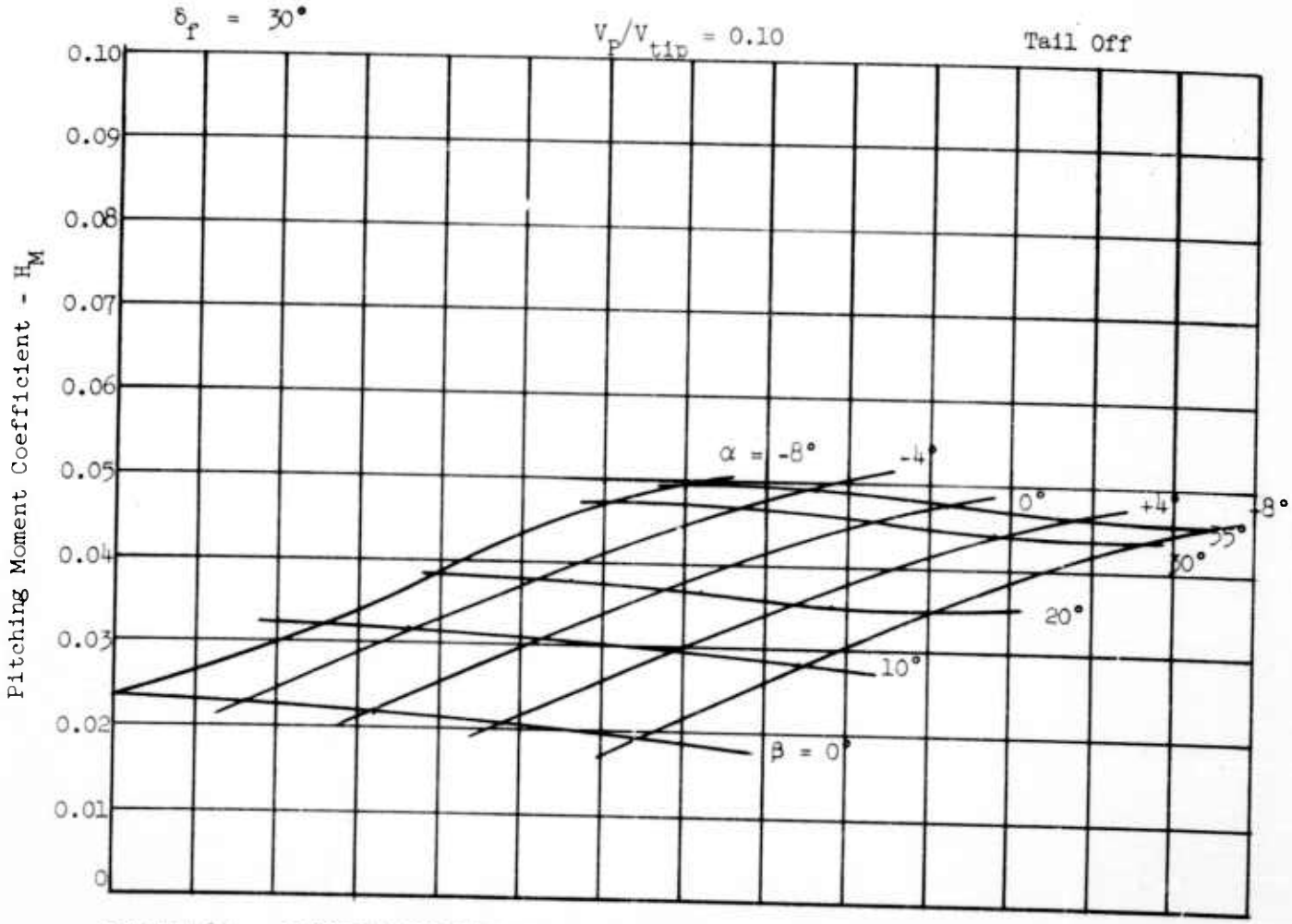

FIGURE 65b - PITCHING MOMENT COEFFICIENT VERSUS ANGLE OF ATTACK AND EXIT LOUVER ANGLE

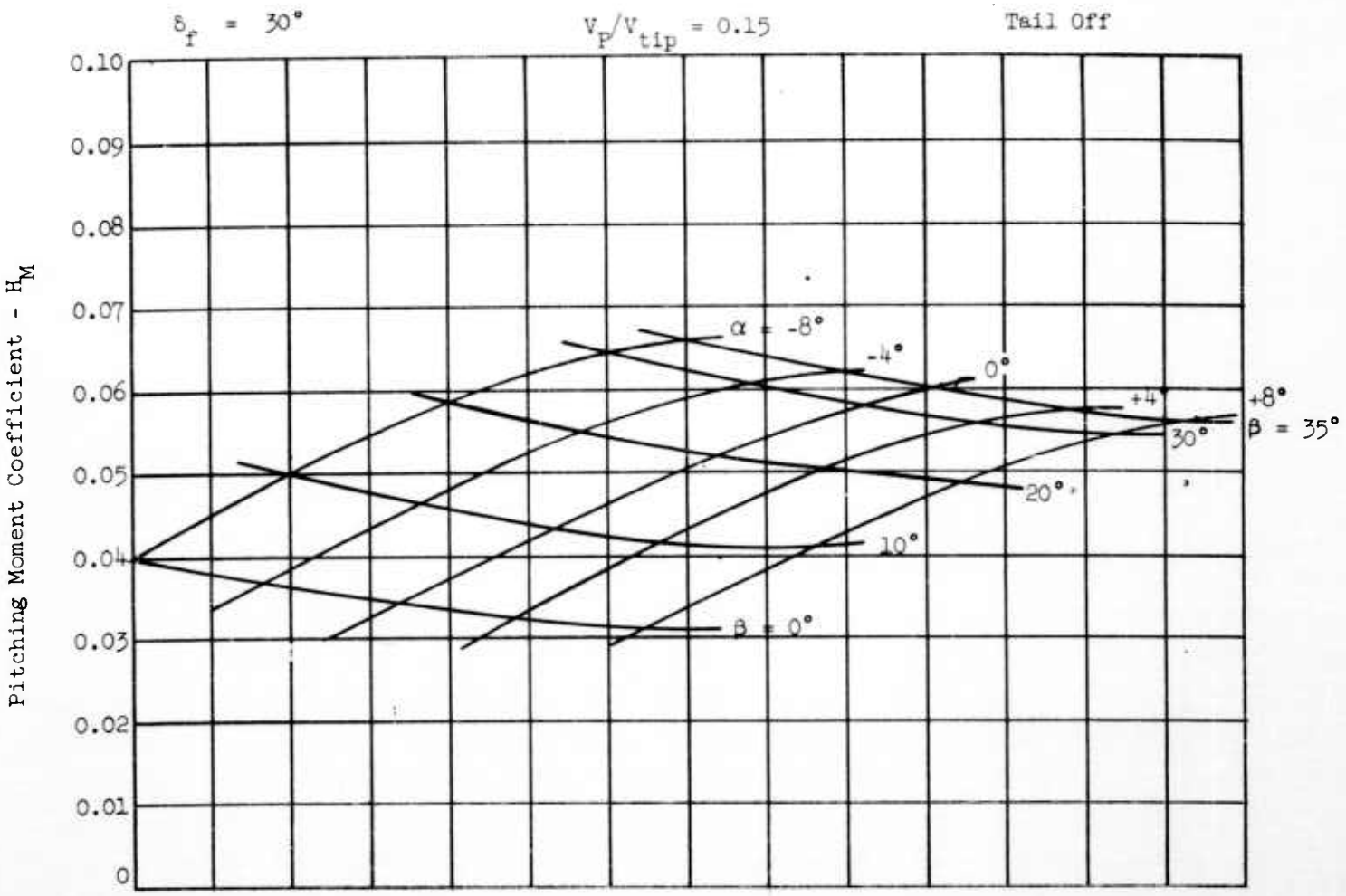

FIGURE 65c - PITCHING MOMENT COEFFICIENT VERSUS ANGLE OF ATTACK AND EXIT LOUVER ANGLE

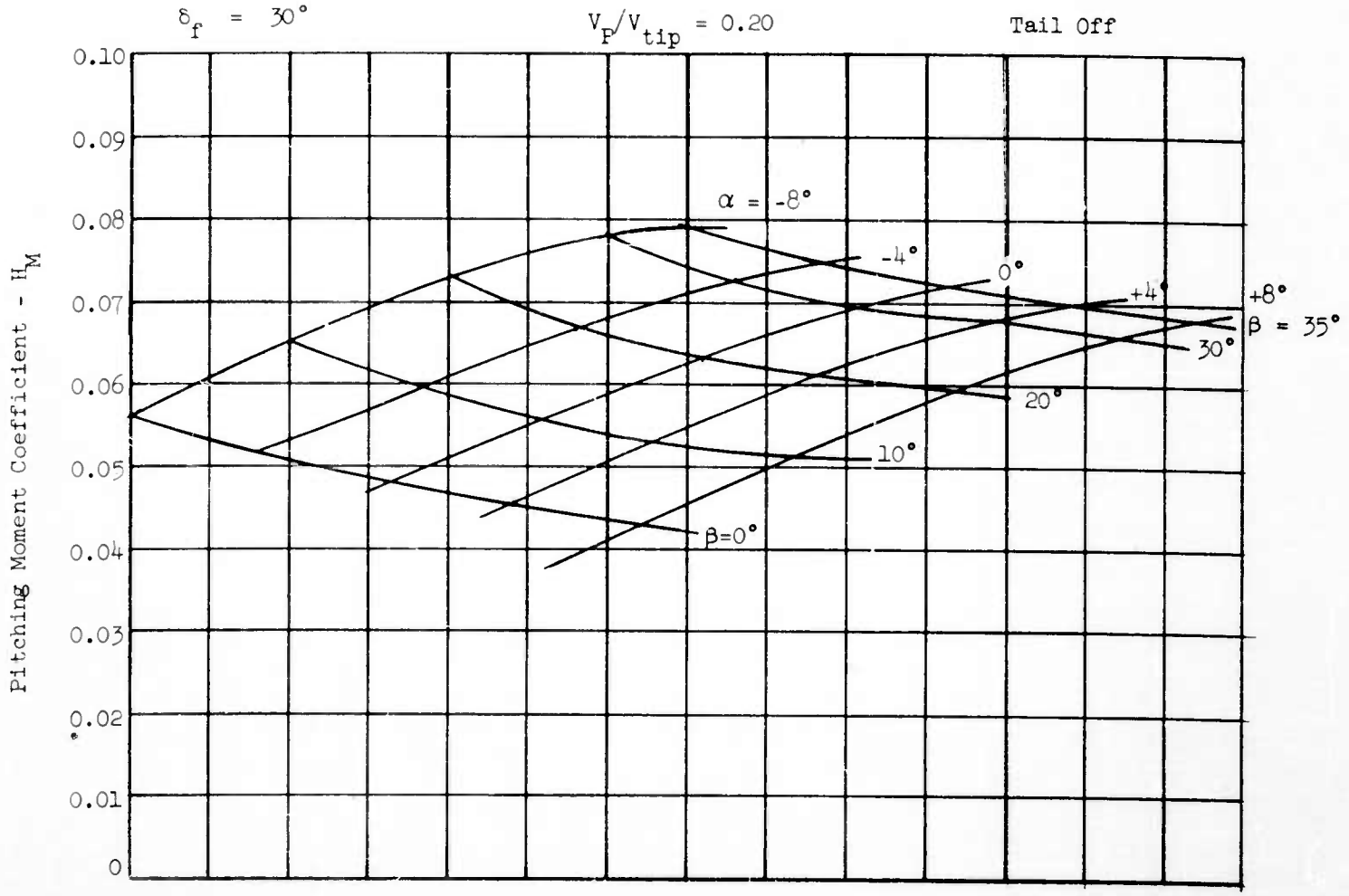

FIGURE 65d - PITCHING MOMENT COEFFICIENT VERSUS ANGLE OF ATTACK AND EXIT LOUVER ANGLE

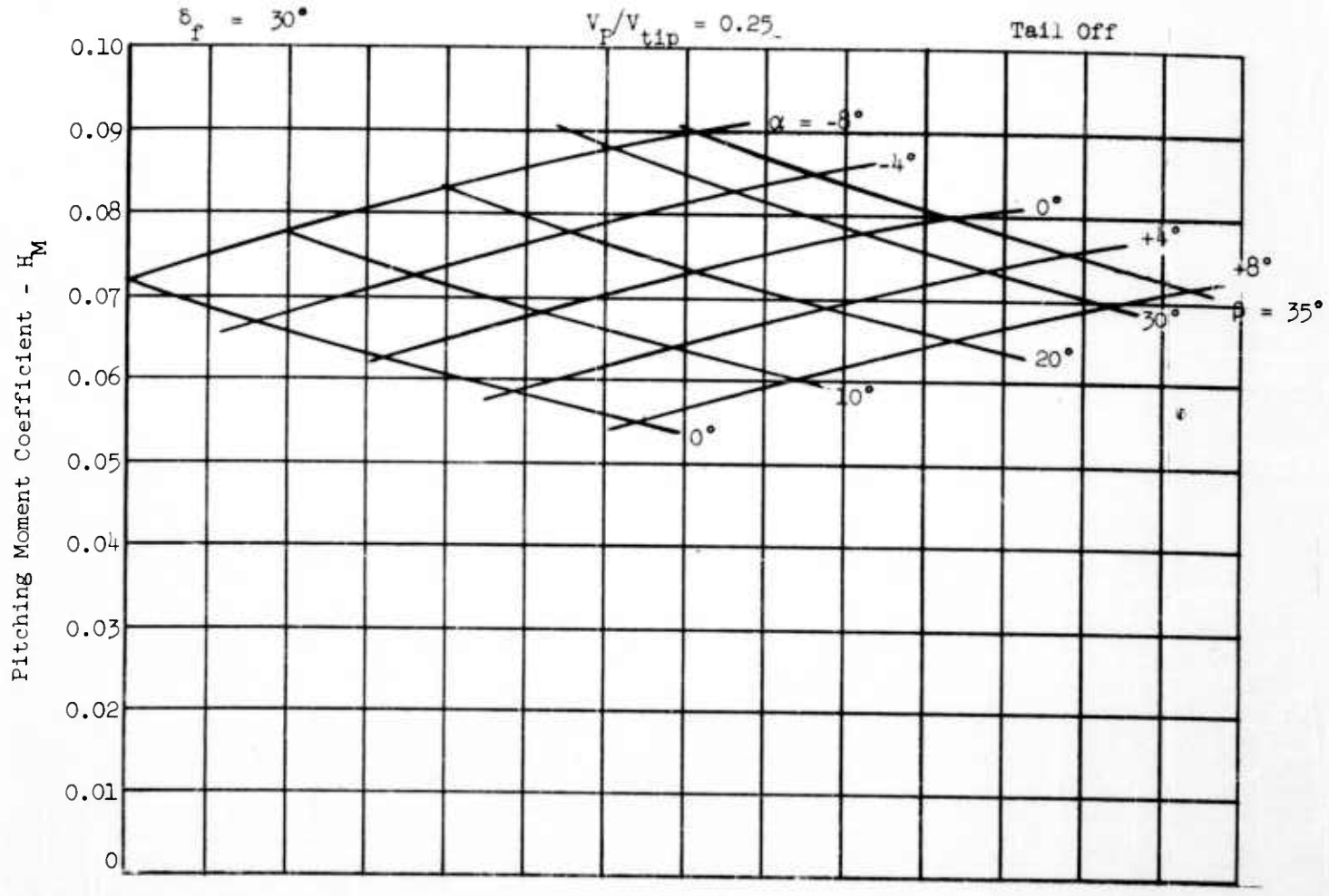

FIGURE 65e - PITCHING MOMENT COEFFICIENT VERSUS ANGLE OF ATTACK AND EXIT LOUVER ANGLE

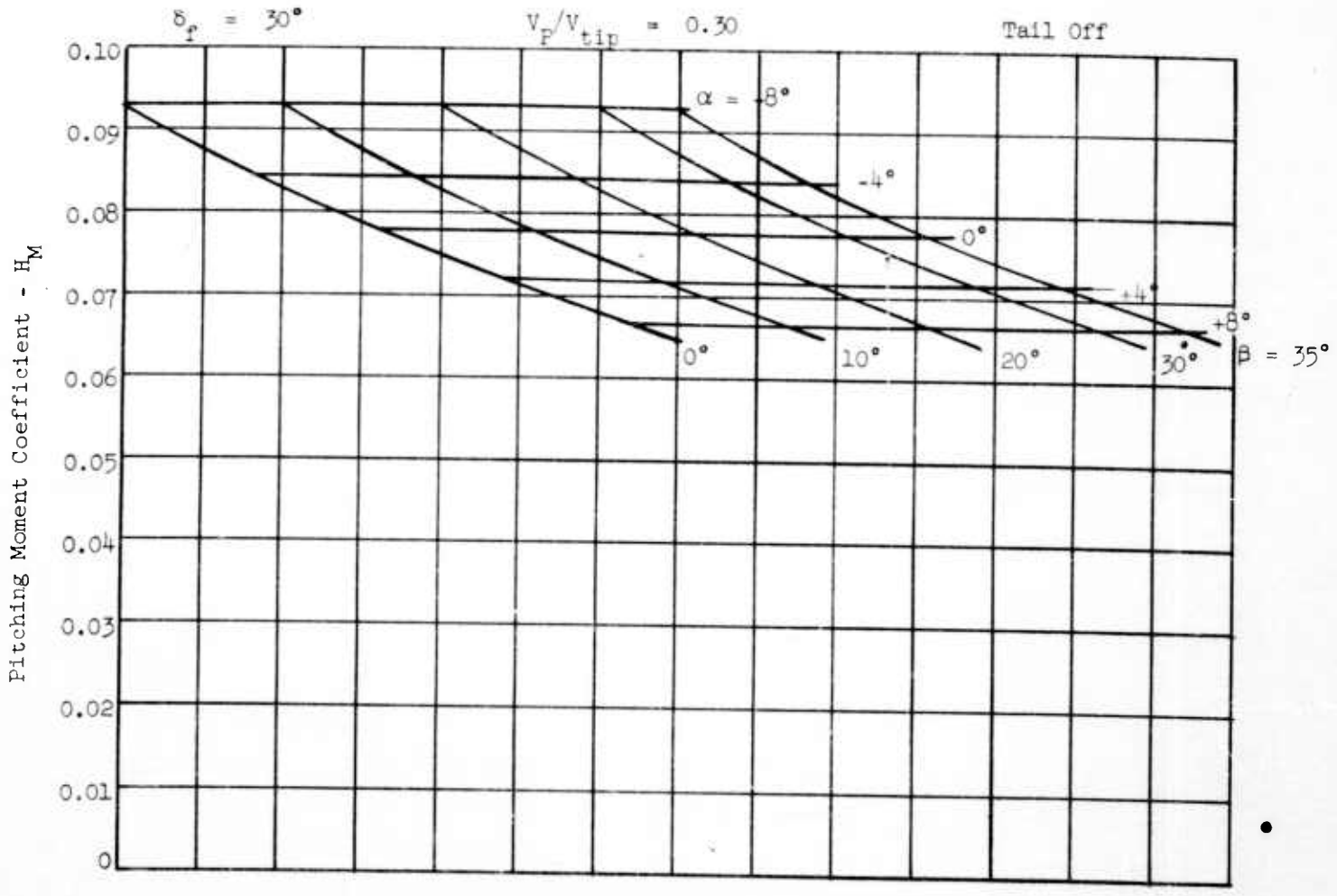

FIGURE 65f - PITCHING MOMENT COEFFICIENT VERSUS ANGLE OF ATTACK AND EXIT LOUVER ANGLE

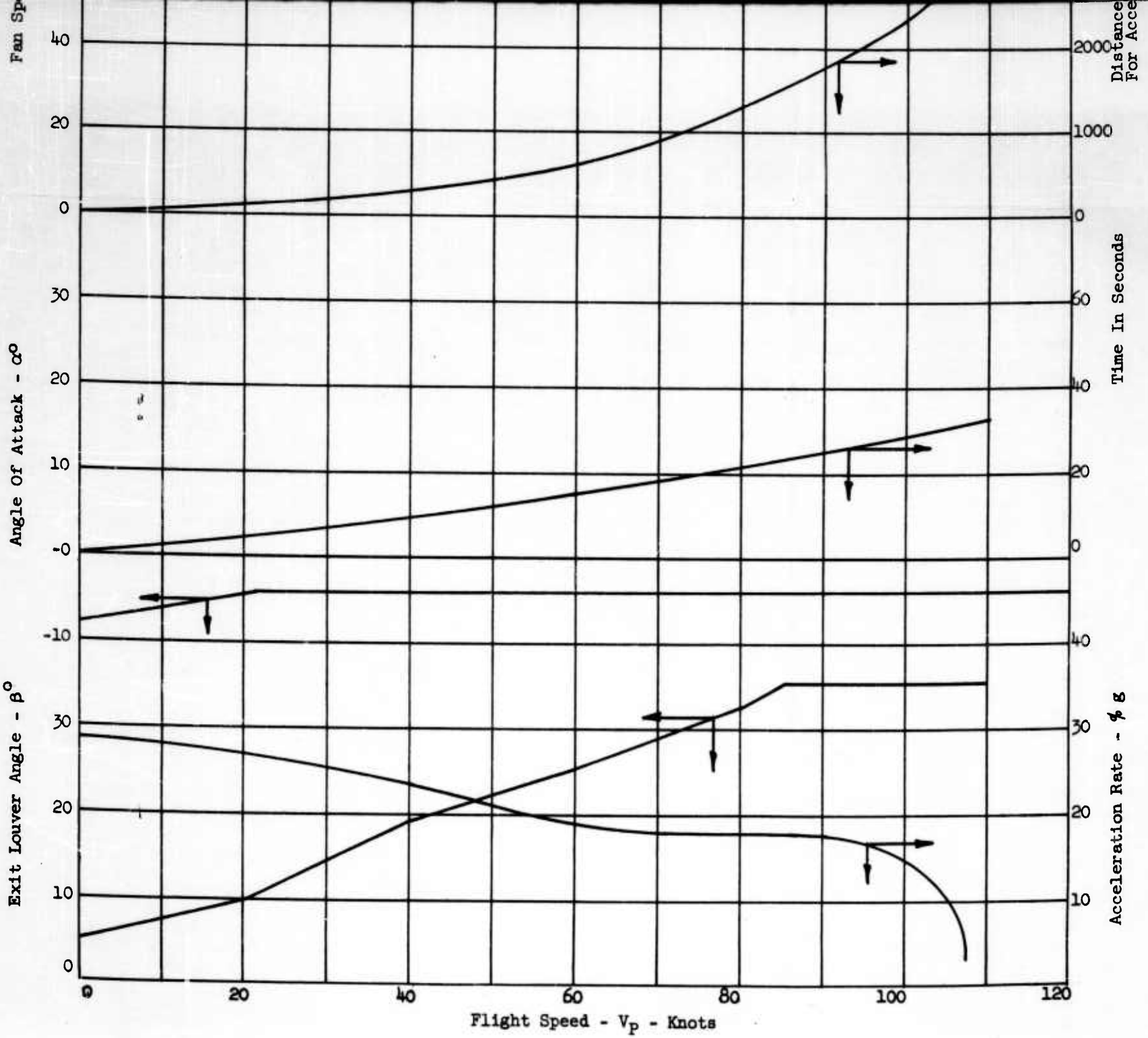

FIGURE 67. TRANSITION CHARACTERISTICS IN LEVEL FLIGHT, WITH MAXIMUM AVAILABLE ACCELLERATION, VERSUS FLIGHT SPEED

Fan Speed - %RPM
30
0
20
40
60
80
100
100%NP
δ f = 30°
Tail off
60
0
1000
2000
3000
4000
0
0.4
0.8
1.2
1.6
Seconds
Distance Required
For Acceleration - Feet
HG. W./HD g

2

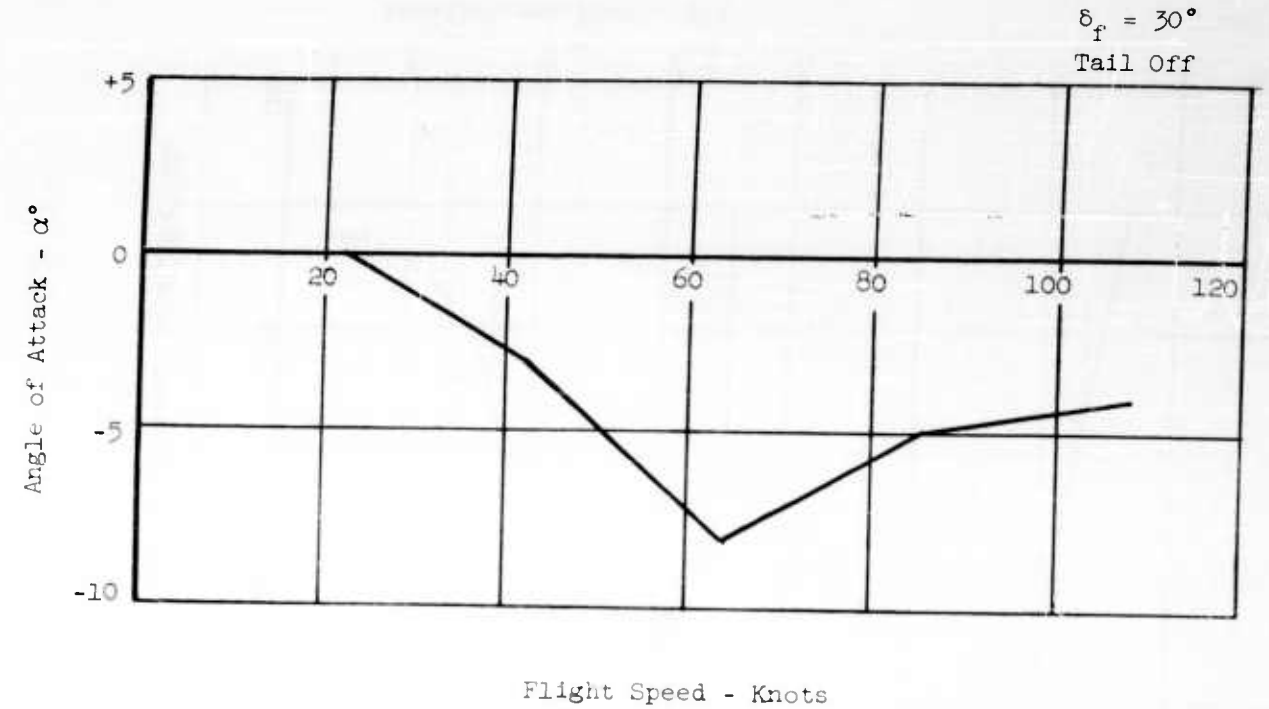

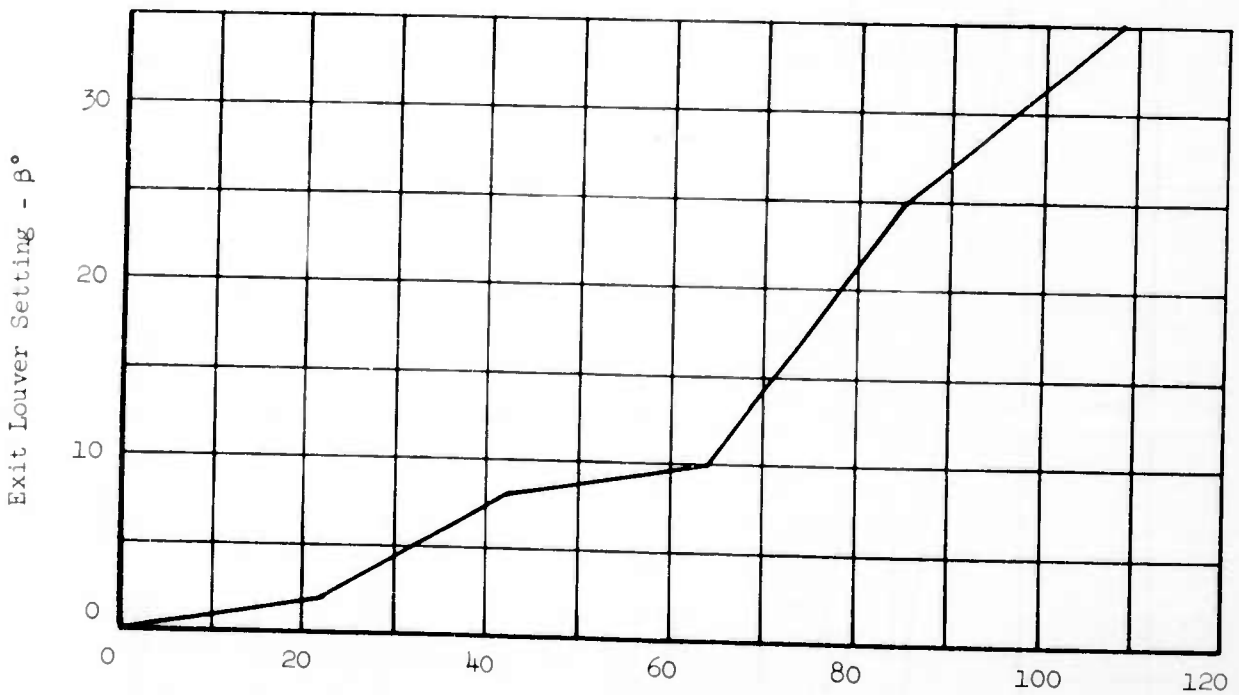

FIGURE 66 - TRANSITION IN UNACCELERATED LEVEL FLIGHT - α and β VERSUS FLIGHT SPEED (N_F = 100%)

Horiz. Distance Required
For Deceleration - Feet
4000
3000
2000
1000
$\delta_f = 30^\circ$
Tail Off
100
80
60
40
20
Fan Speed - % RPM

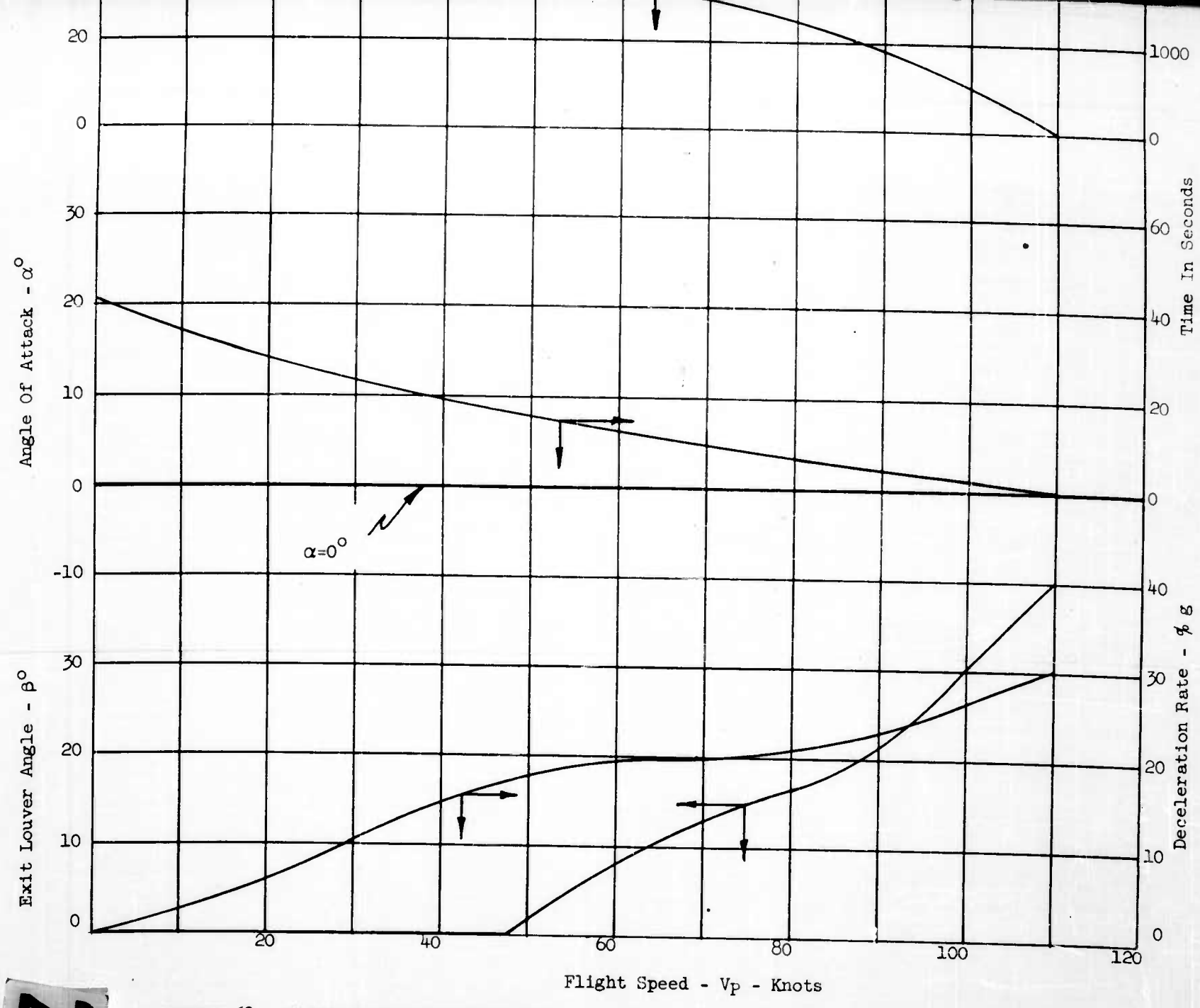

FIGURE 68. TRANSITION CHARAGTERISTICS FOR LEVEL FLIGHT DECELERATION VERSUS FLIGHT SPEED

$\delta_f = 30^\circ$

Tail Off

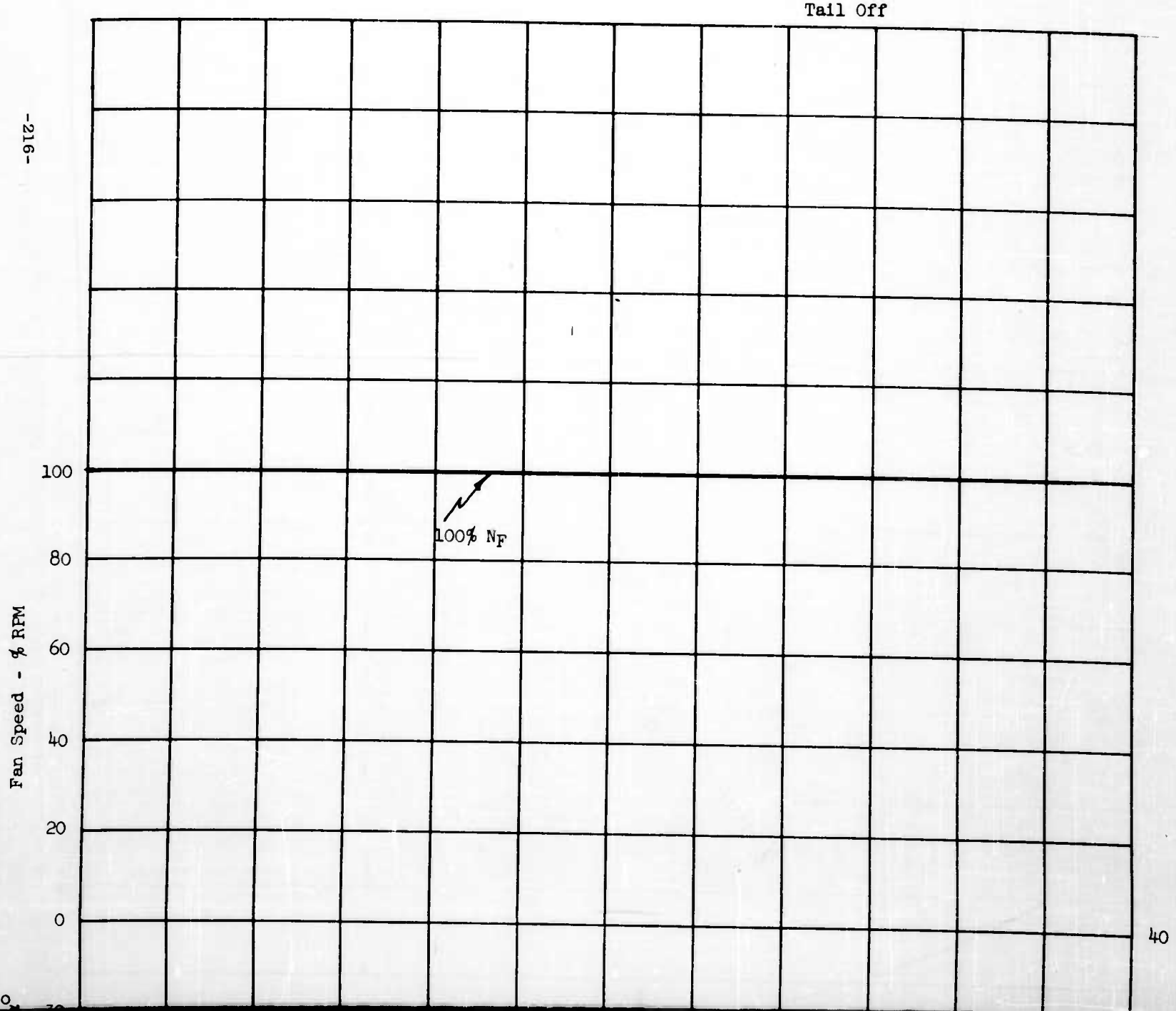

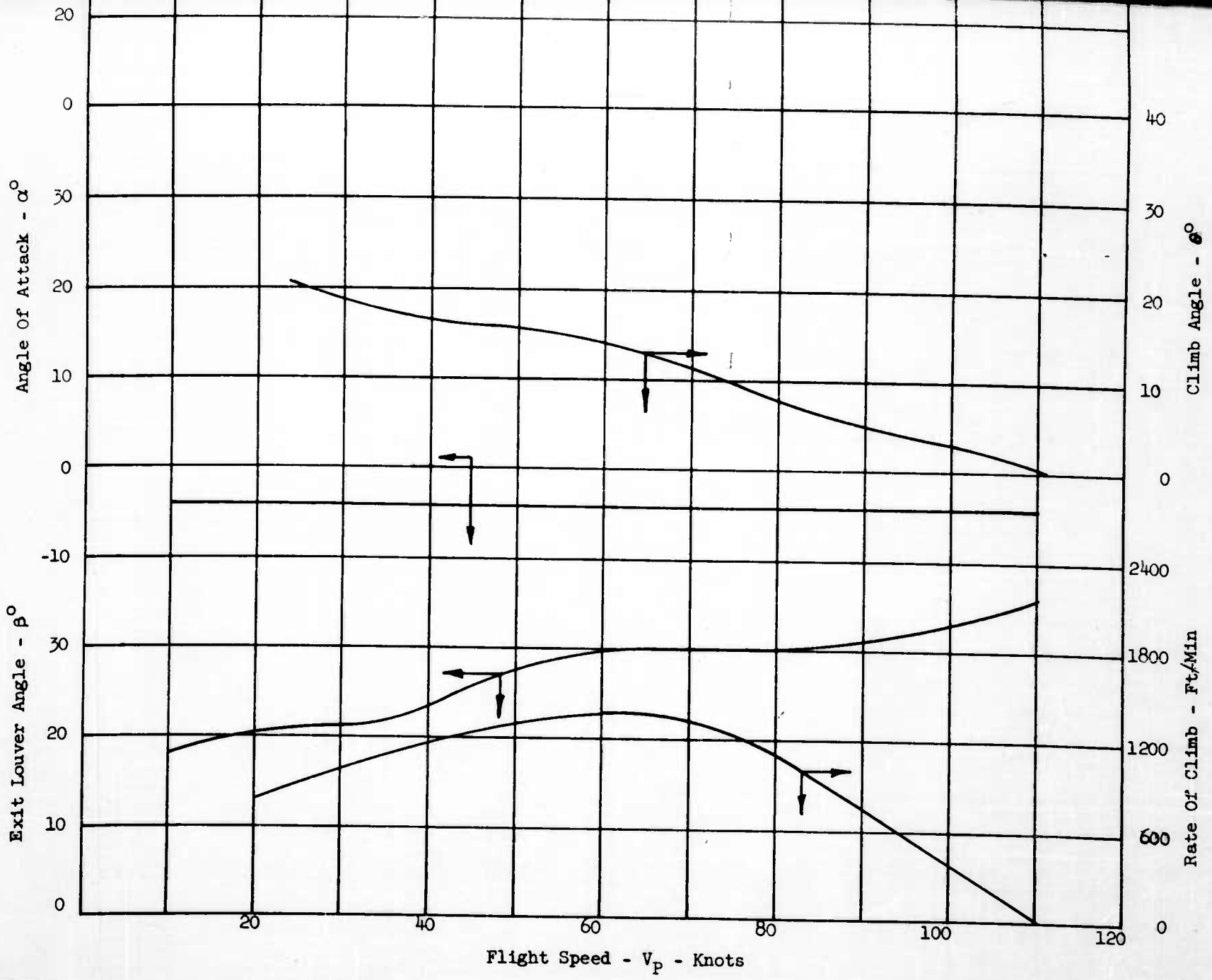

FIGURE 69. TRANSITION CHARACTERISTICS FOR MAXIMUM RATE OF CLIMB AT CONSTANT FLIGHT SPEED VERSUS FLIGHT SPEED

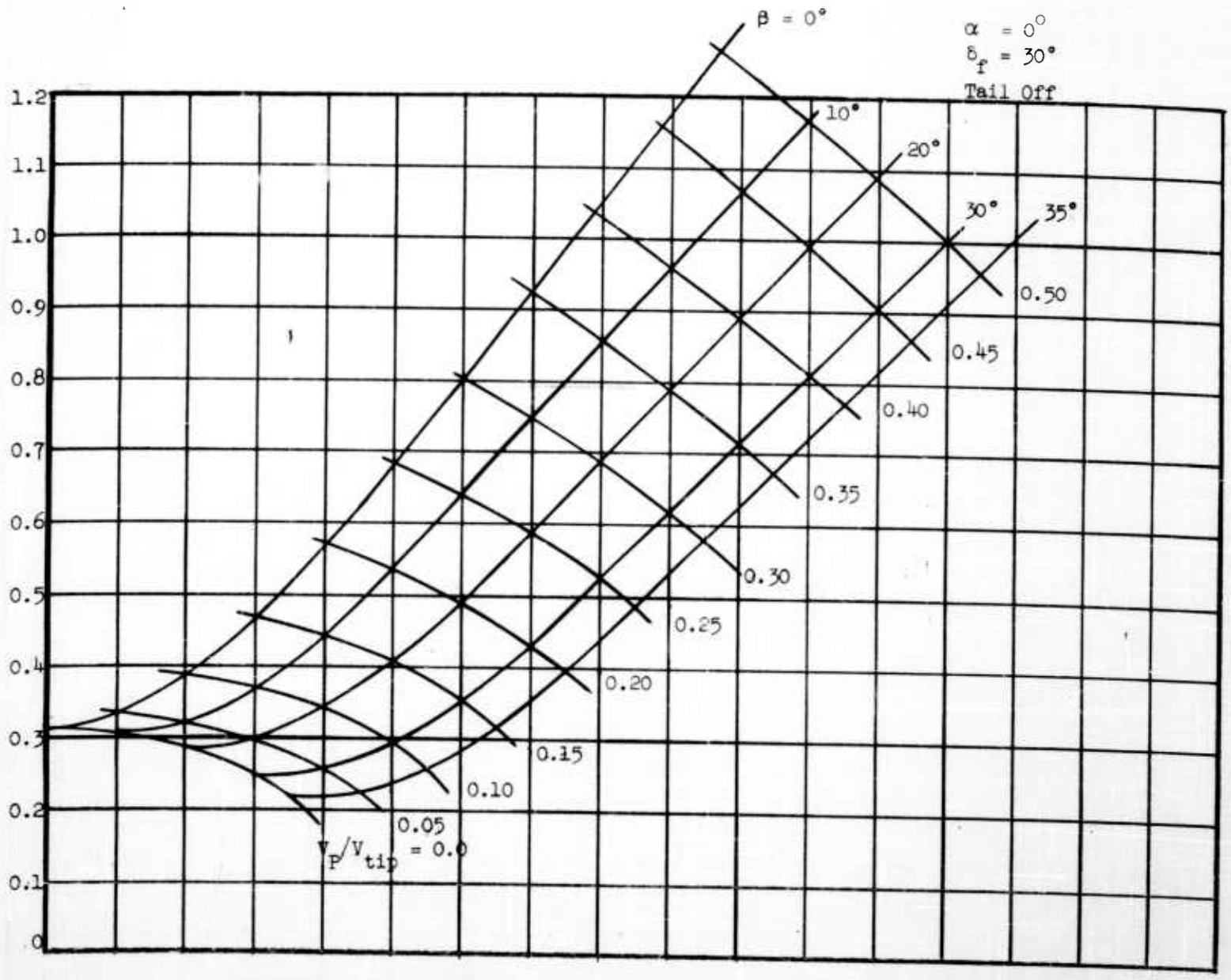

FIGURE 70a - LIFT COEFFICIENT VERSUS VELOCITY RATIO AND EXIT LOUVER ANGLE

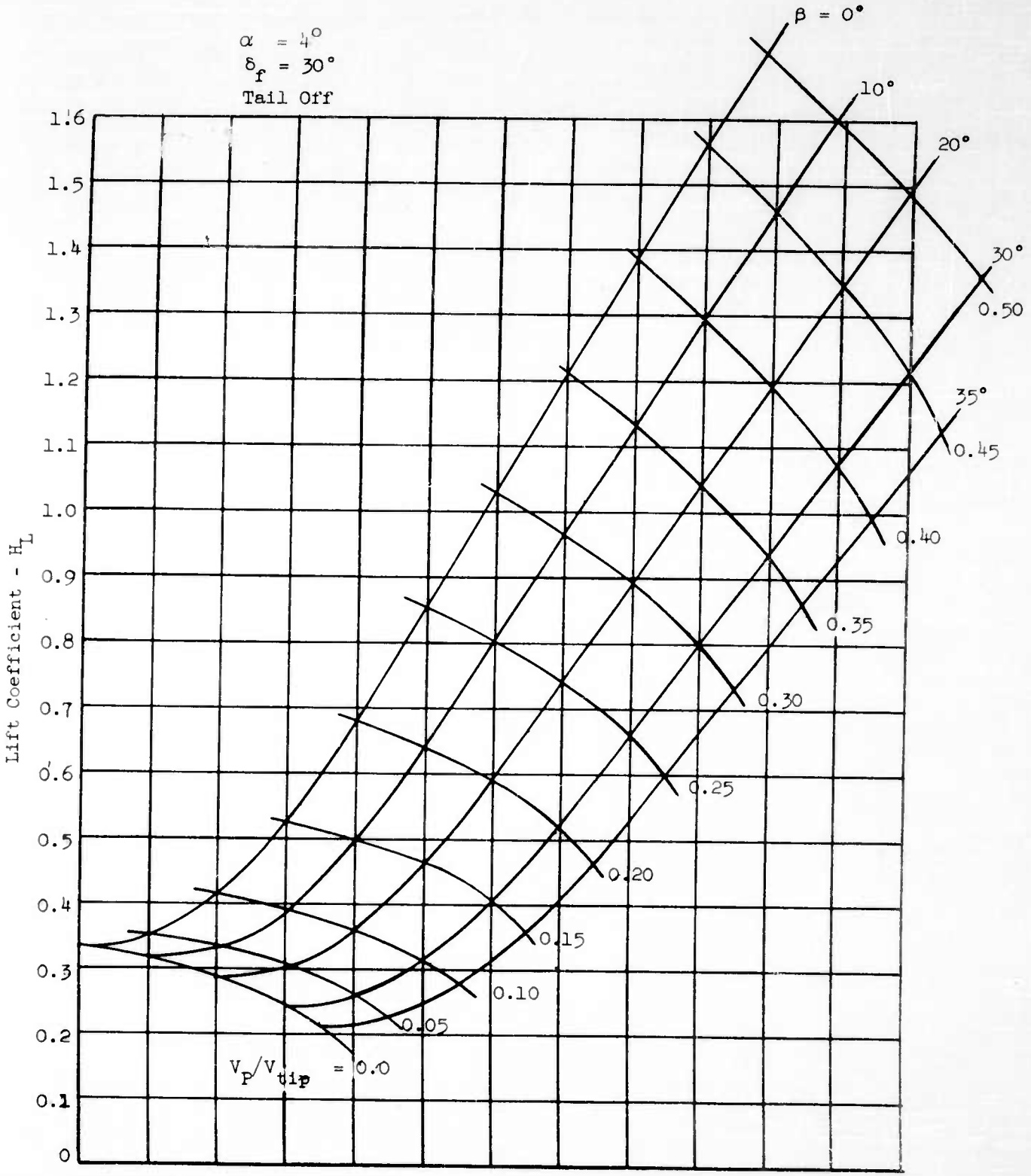

FIGURE 70b - LIFT COEFFICIENT VERSUS VELOCITY RATIO AND EXIT LOUVER ANGLE

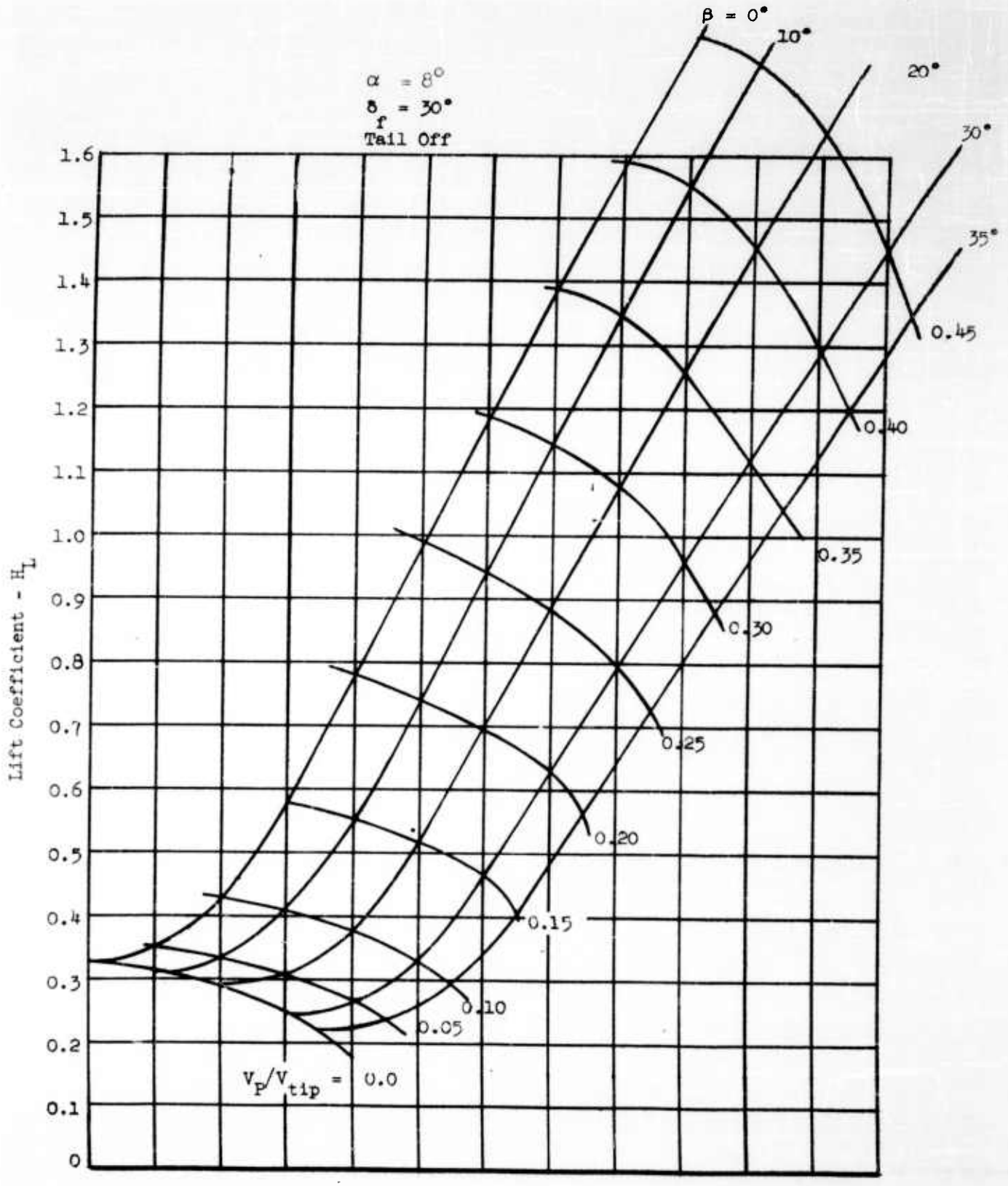

FIGURE 70c - LIFT COEFFICIENT VERSUS VELOCITY RATIO AND EXIT LOUVER ANGLE

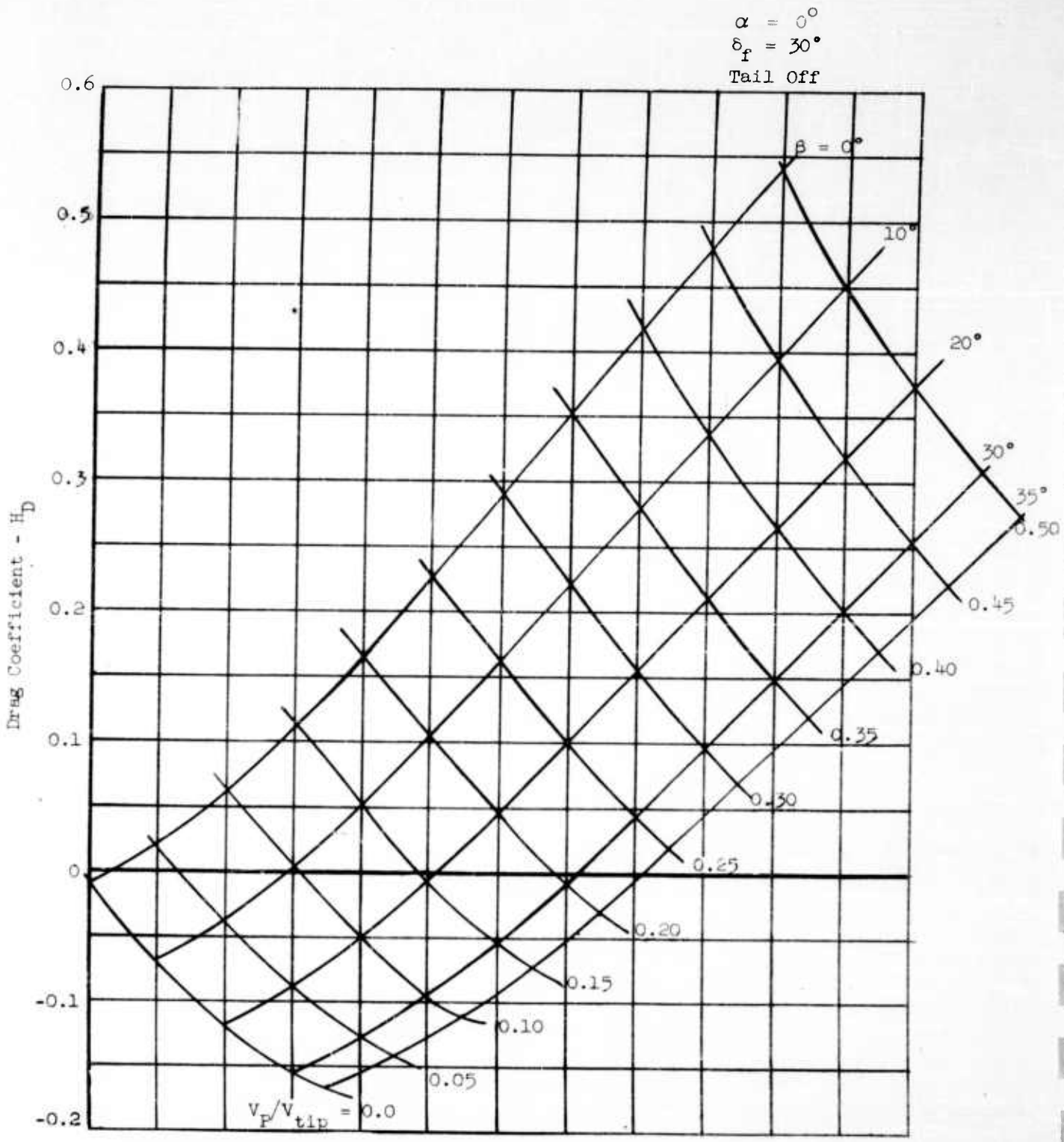

FIGURE 71a - DRAG COEFFICIENT VERSUS VELOCITY RATIO AND EXIT LOUVER ANGLE

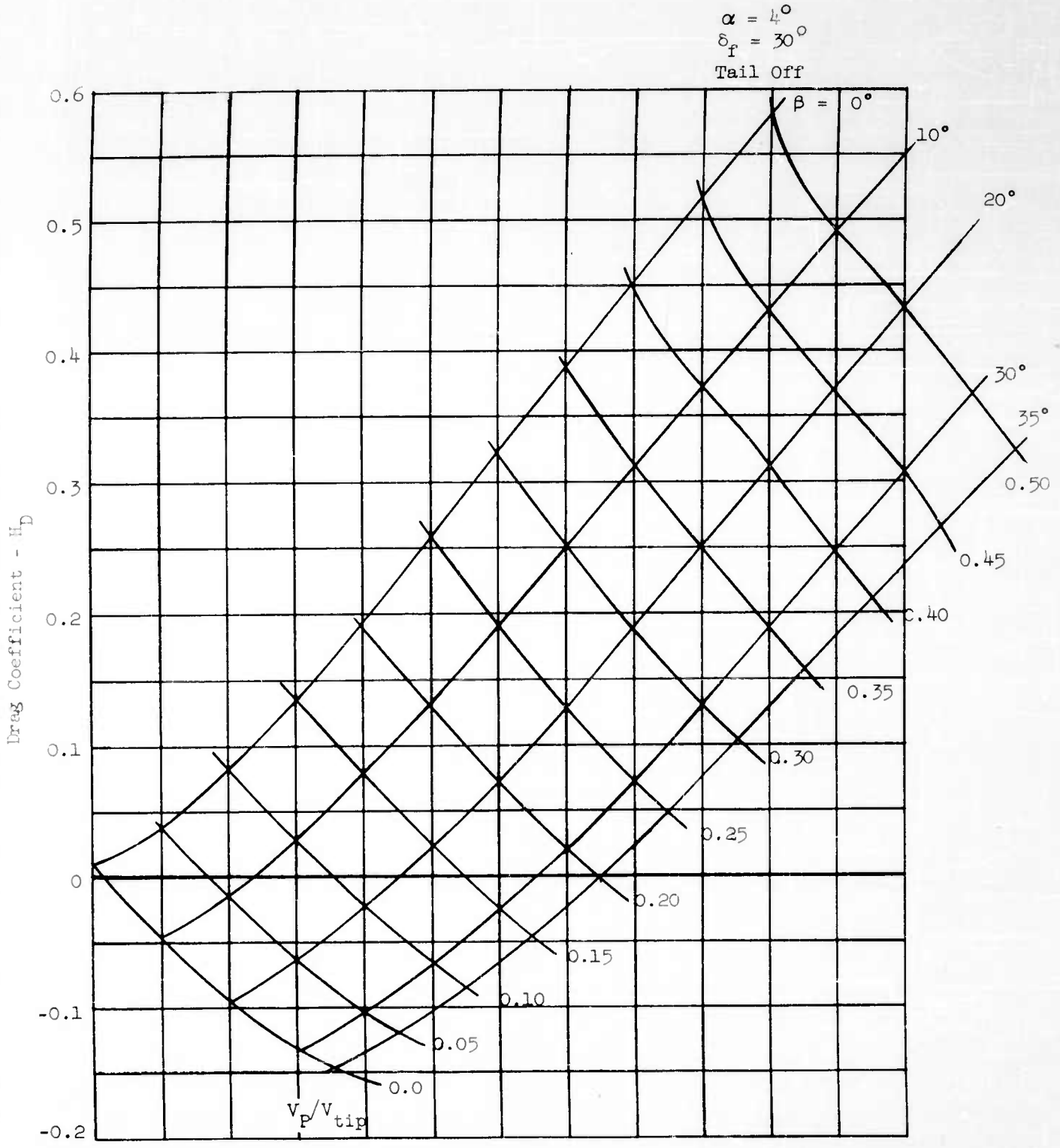

FIGURE 71b - DRAG COEFFICIENT VERSUS VELOCITY RATIO AND EXIT LOUVER ANGLE

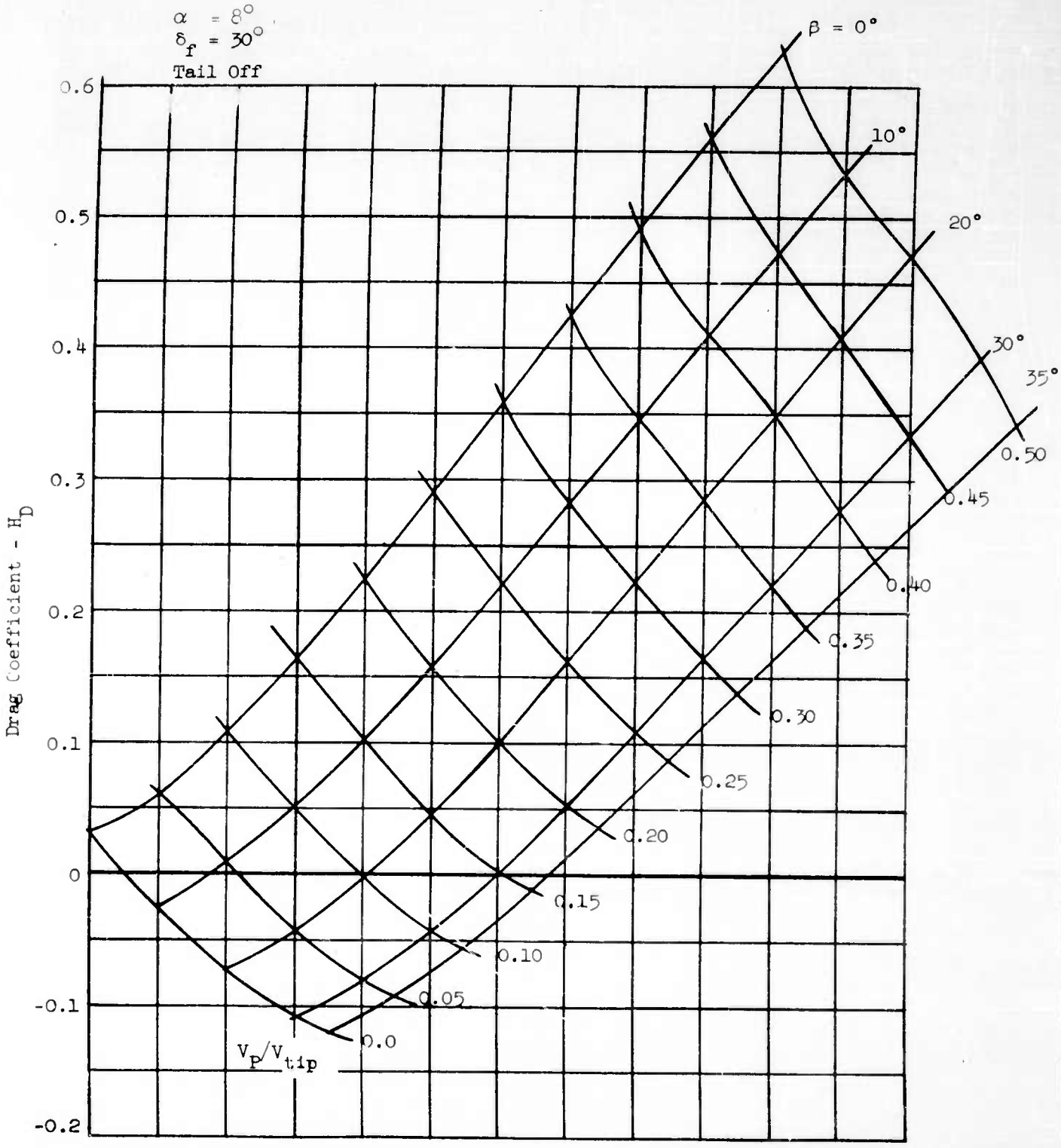

FIGURE 71c - DRAG COEFFICIENT VERSUS VELOCITY RATIO AND EXIT LOUVER ANGLE

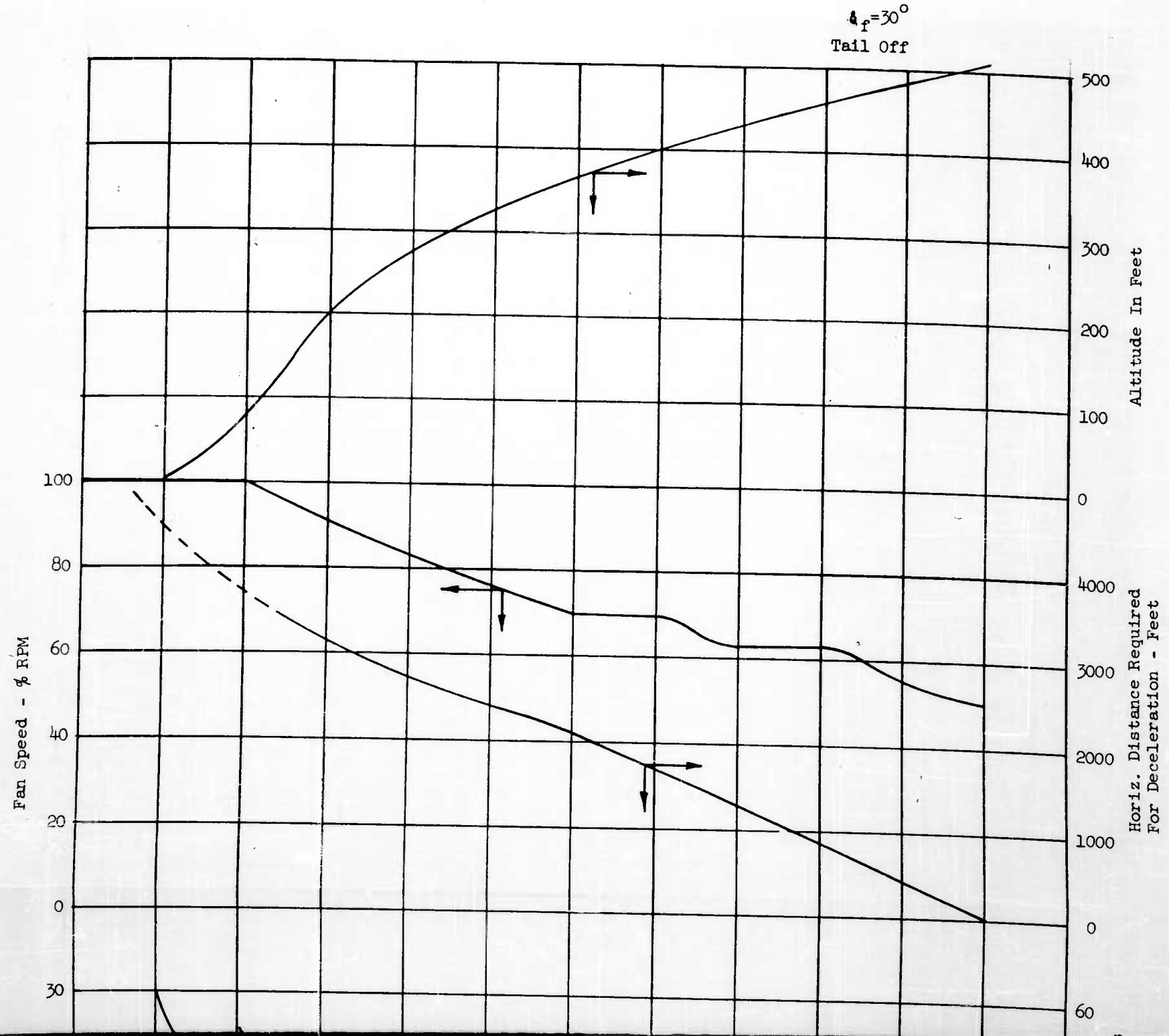
$\delta_f=30^\circ$
Tail Off
Fan Speed - % RPM
100
80
60
40
20
0
30
Altitude In Feet
500
400
300
200
100
0
Horiz. Distance Required
For Deceleration - Feet
4000
3000
2000
1000
0
60

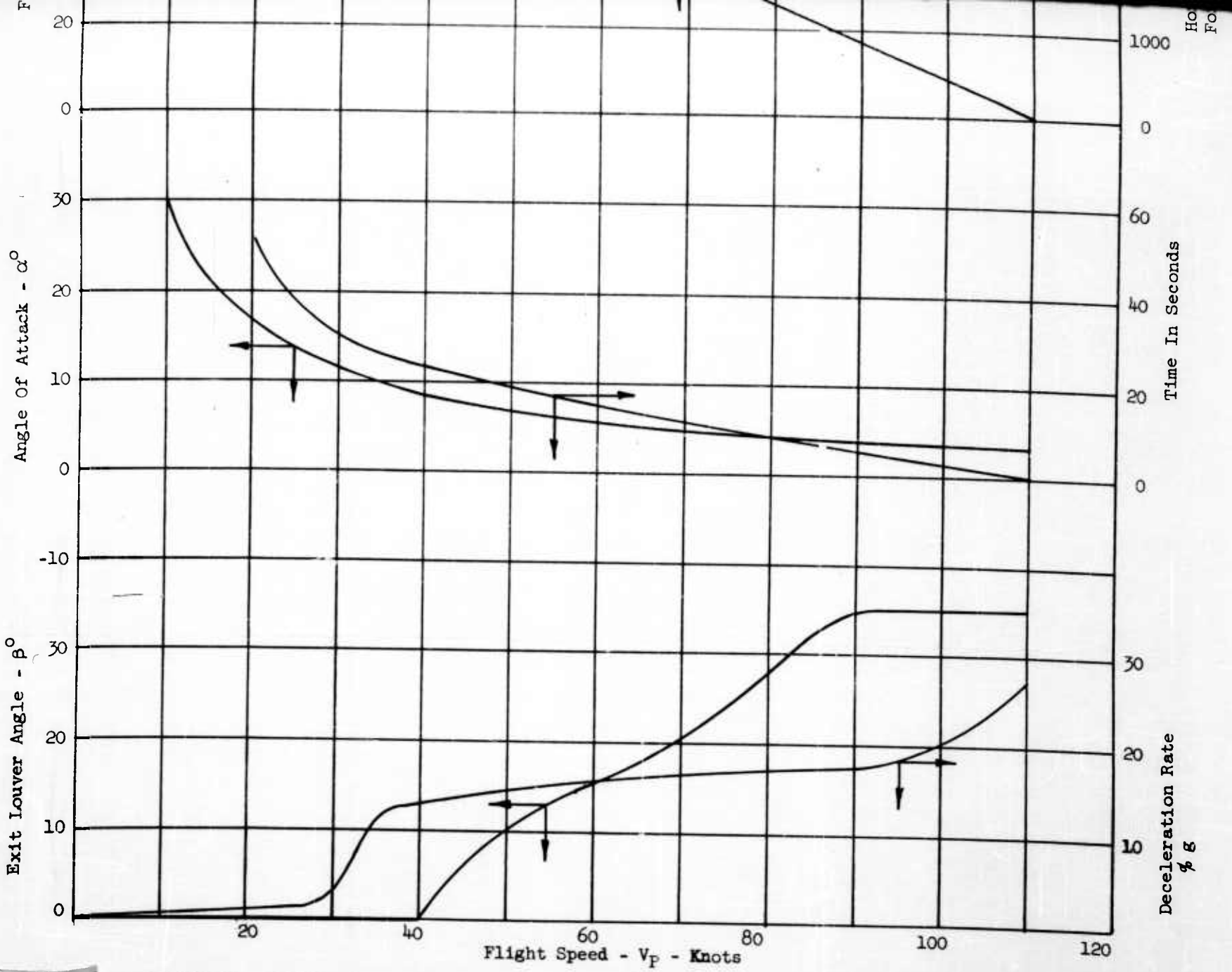

FIGURE 72. TRANSITION CHARACTERISTICS FOR A CONSTANT ATTITUDE DECELERATED DESCENT VERSUS FLIGHT SPEED

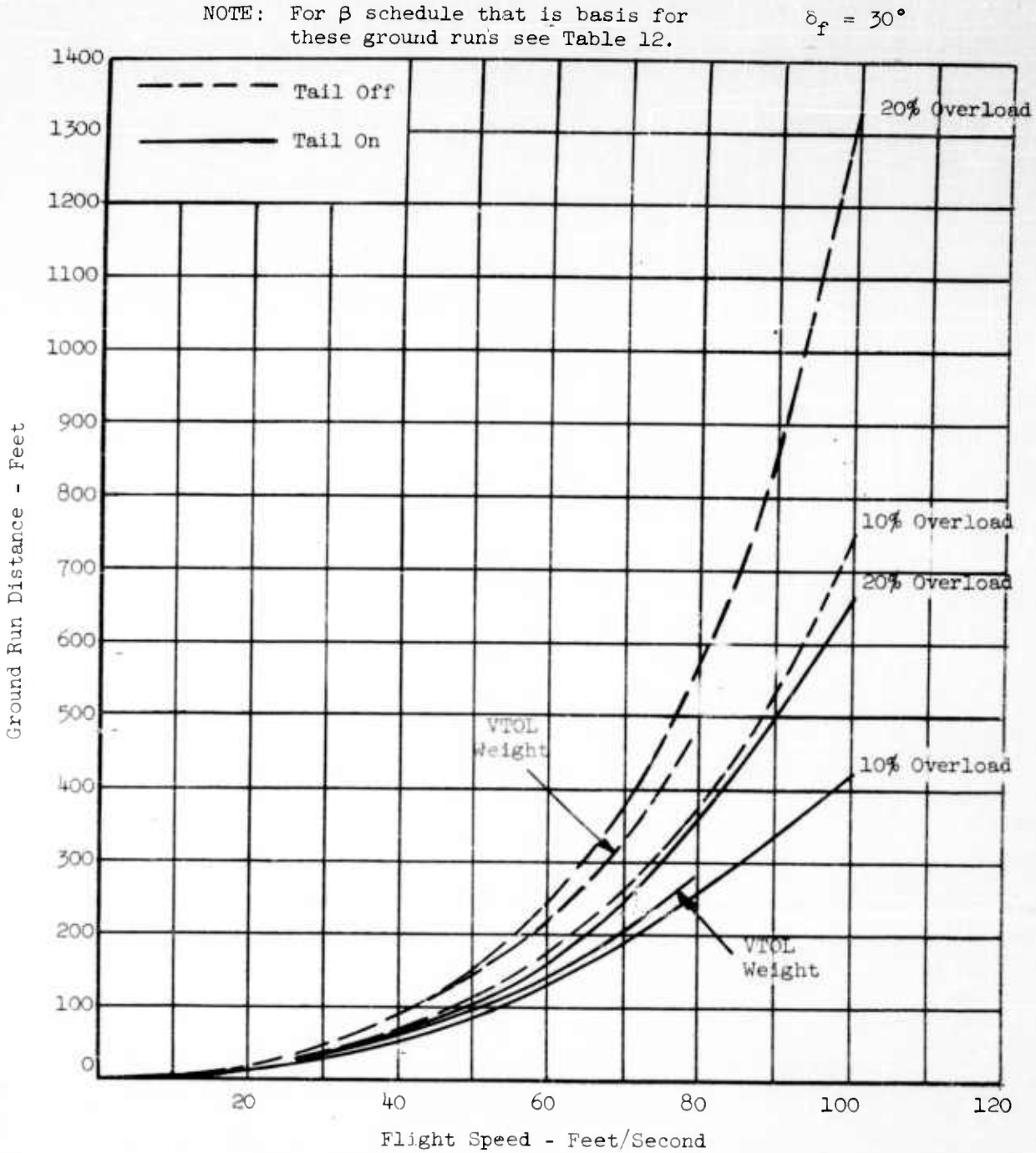

FIGURE 73 - GROUND RUN DISTANCE VERSUS FLIGHT SPEED FOR S.T.O.

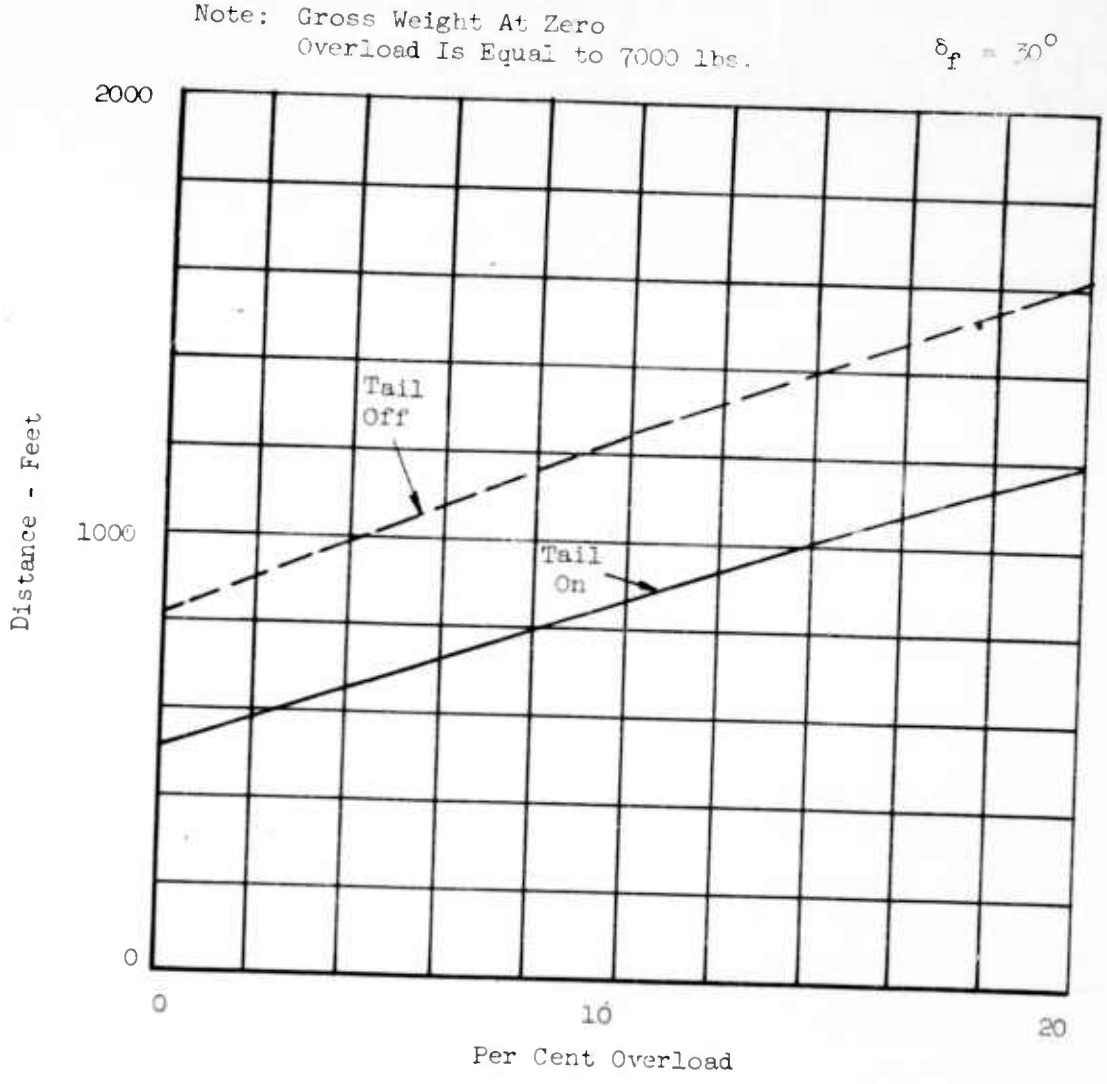

FIGURE 74 - DISTANCE TO CLEAR 50 FOOT OBSTACLE IN STO VERSUS PER CENT OVERLOAD

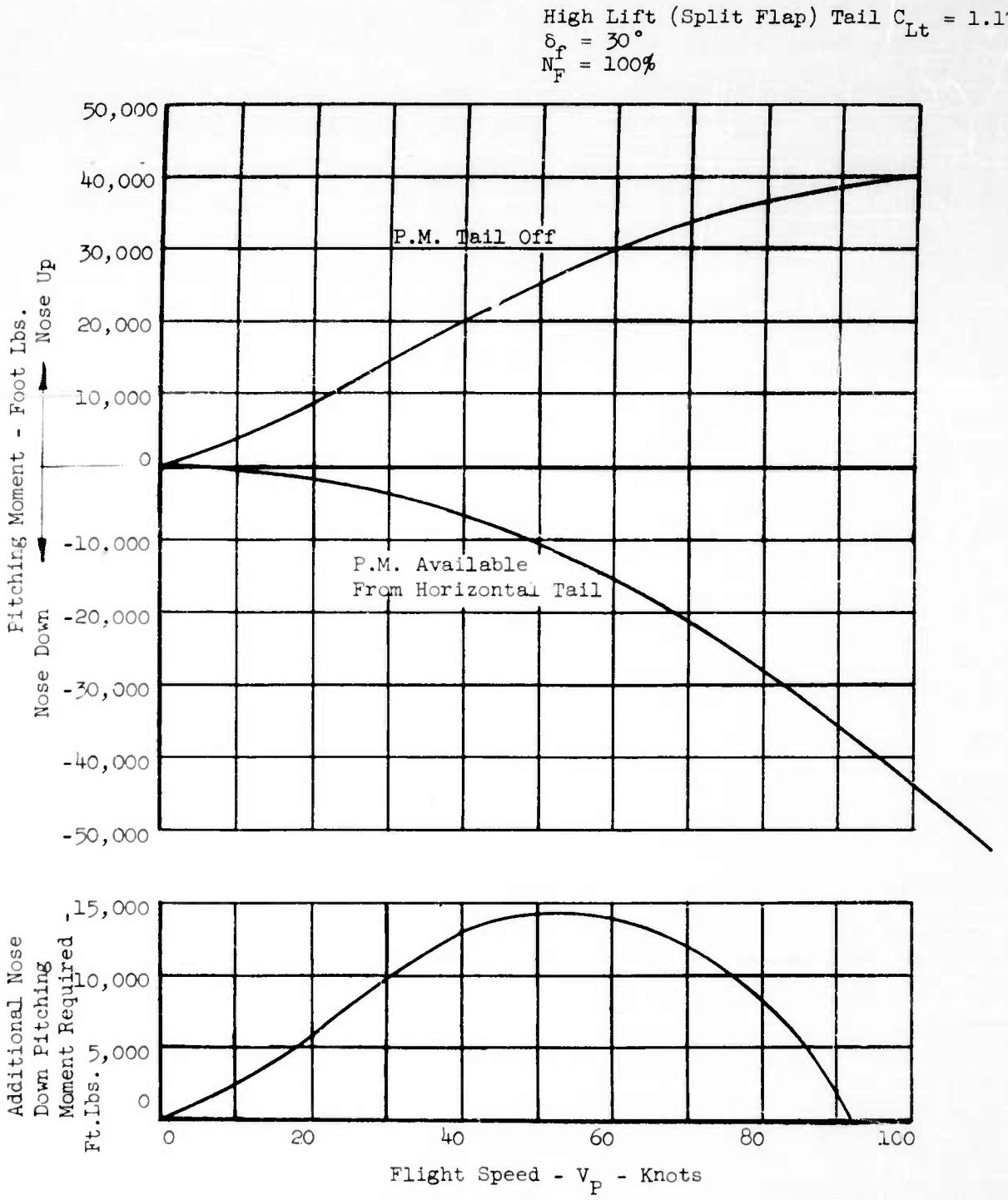

FIGURE 75 - PITCHING MOMENTS IN CONSTANT SPEED CLIMB VERSUS FLIGHT SPEED (SEE FIGURE 69)

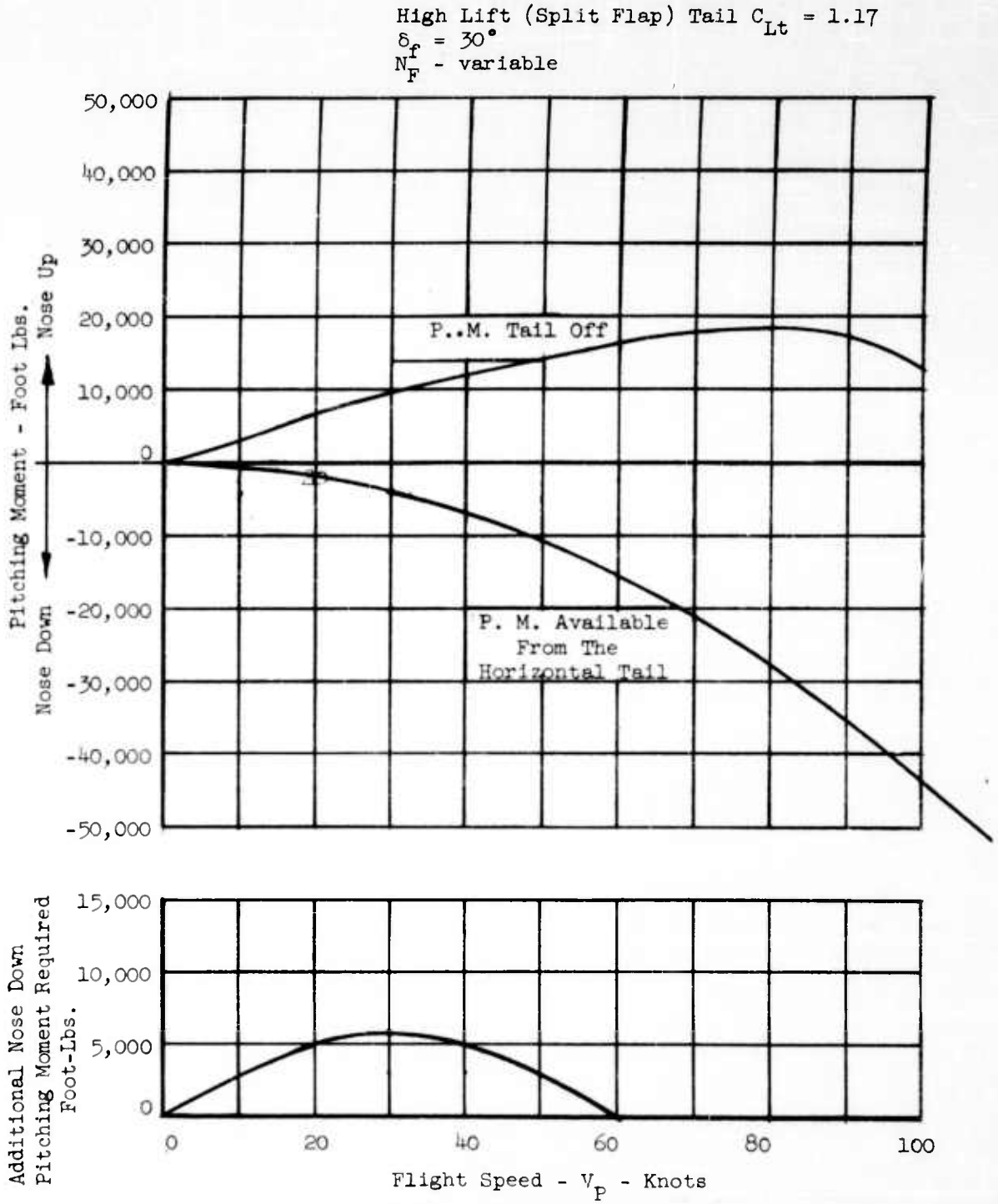

FIGURE 76 - PITCHING MOMENTS IN CONSTANT ATTITUDE DESCENT VERSUS FLIGHT SPEED (VARIABLE FAN SPEED) (SEE FIGURE 72)

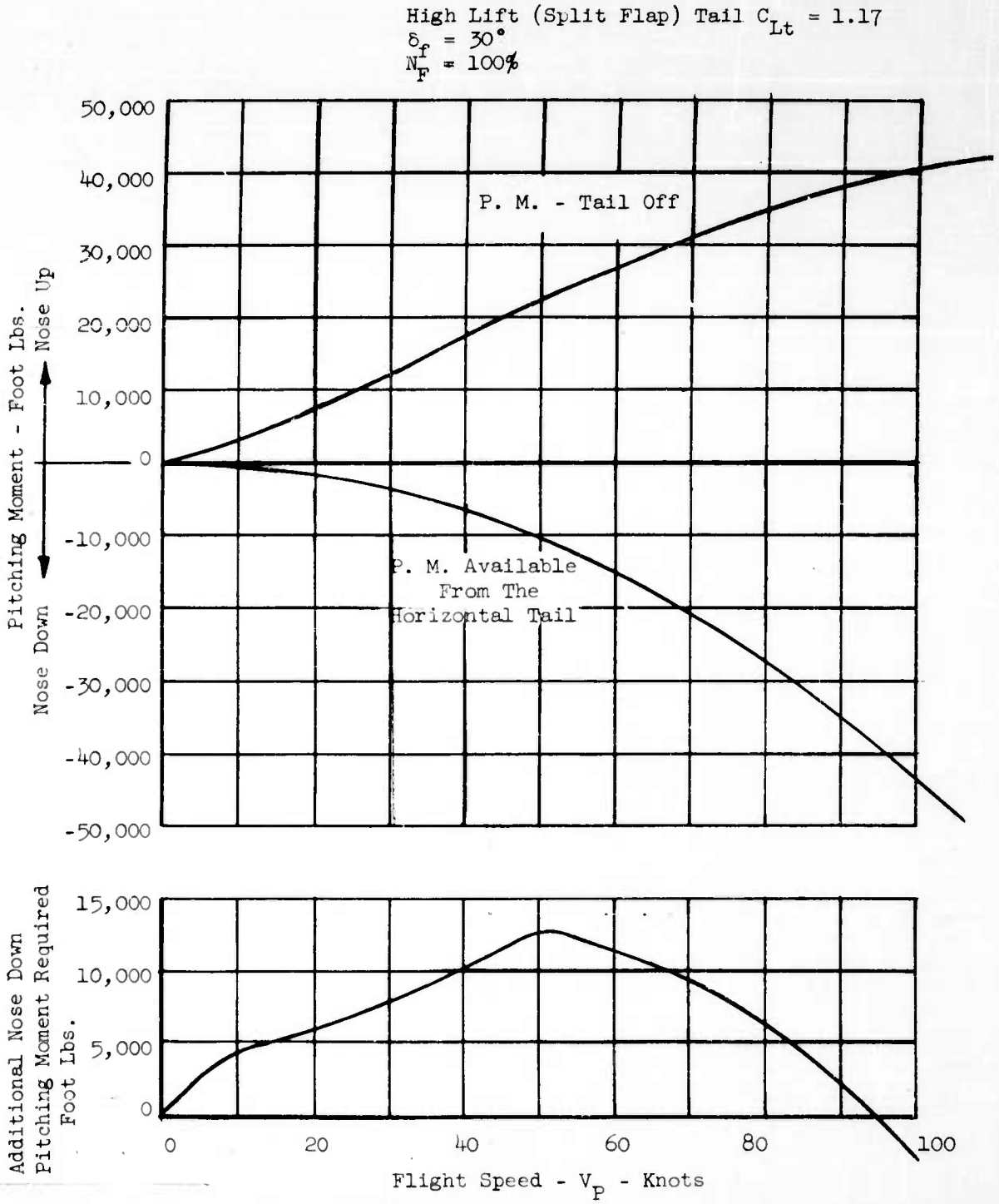

FIGURE 77 - PITCHING MOMENTS IN MAXIMUM ACCELERATION TRANSITION (LEVEL FLIGHT) VERSUS FLIGHT SPEED (SEE FIGURE 67)

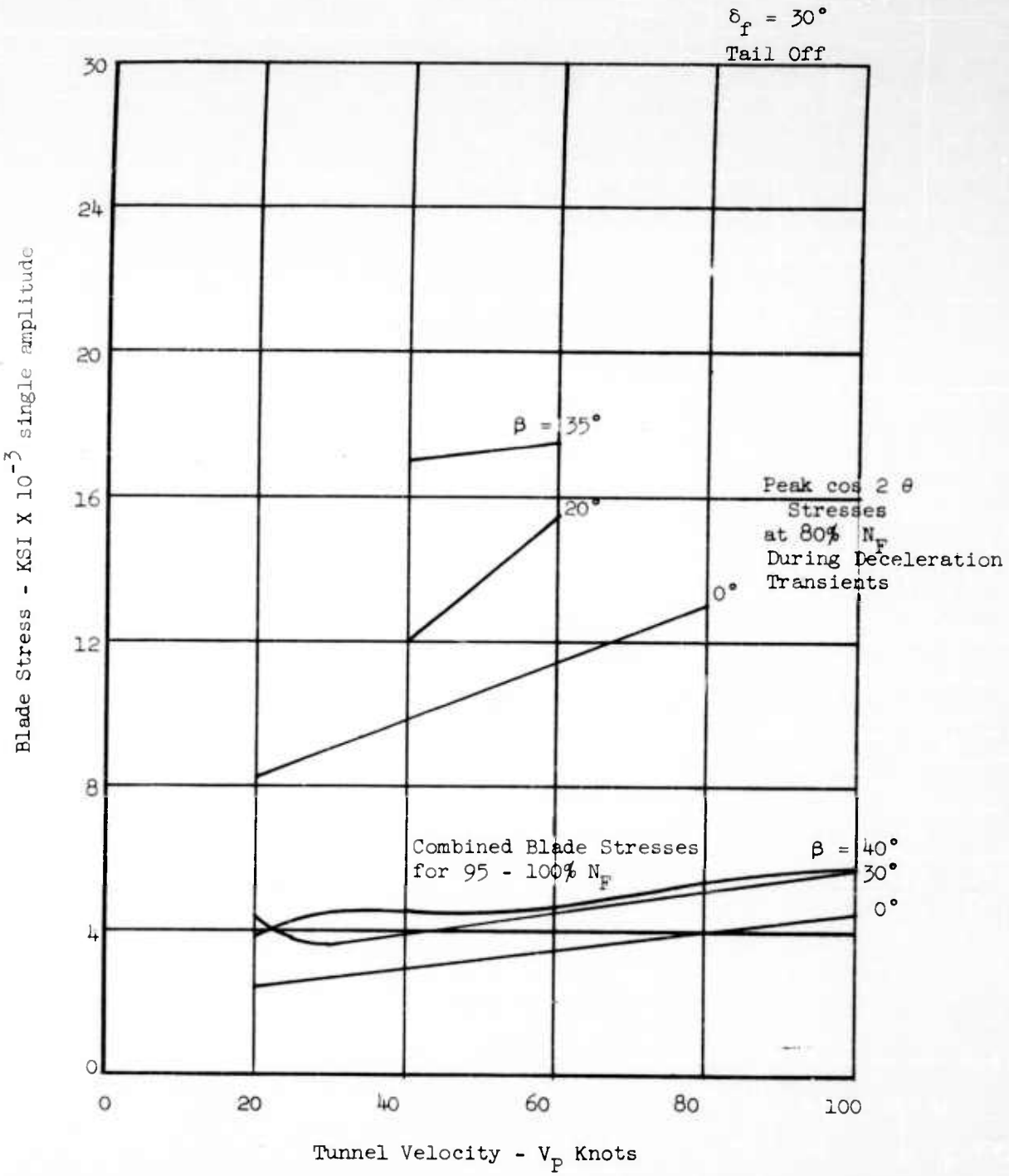

FIGURE 78 - BLADE STRESSES VERSUS TUNNEL SPEED AND EXIT LOUVER ANGLE

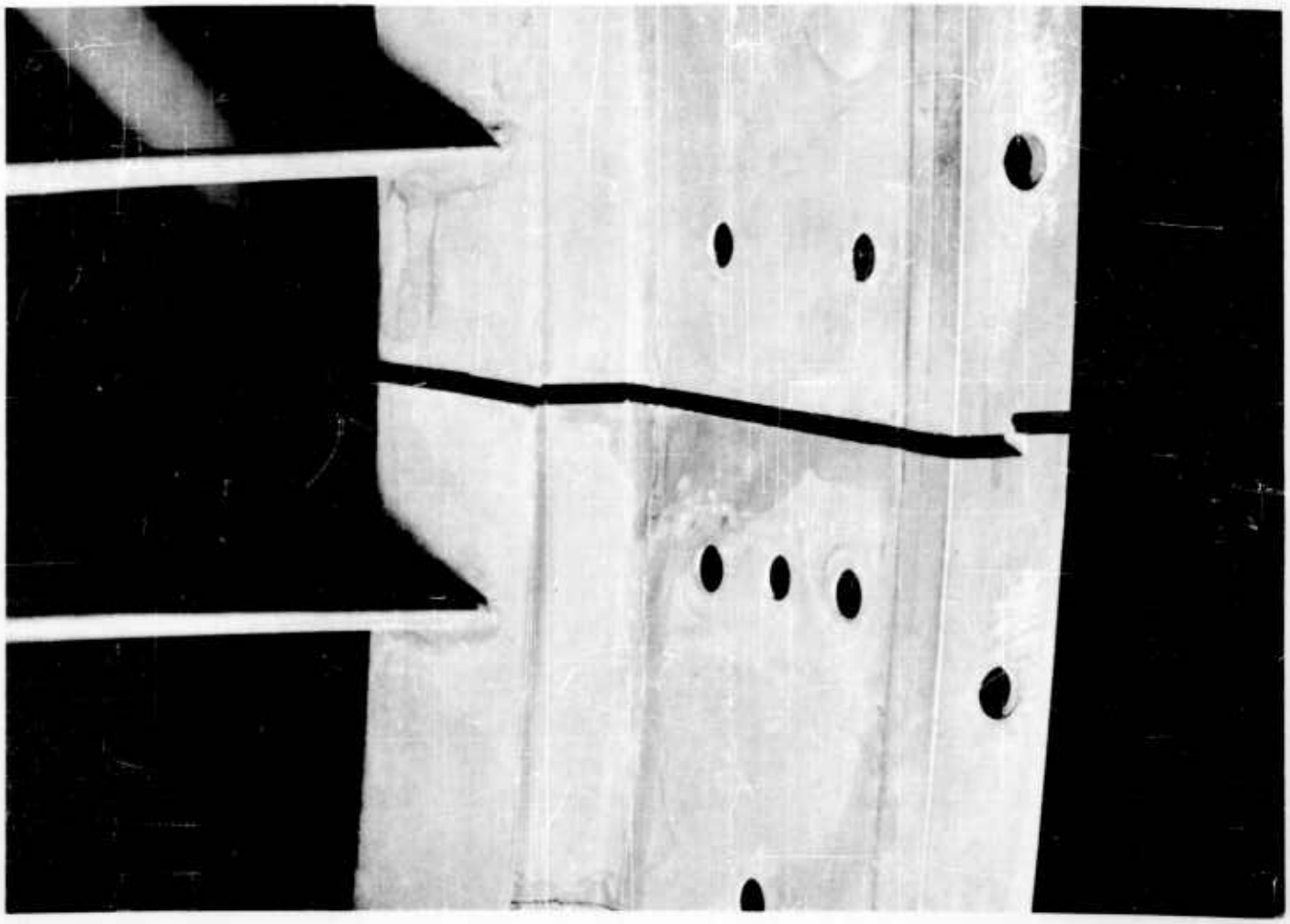

FIGURE 79 - AFT FRAME SAW CUT SEPARATION.

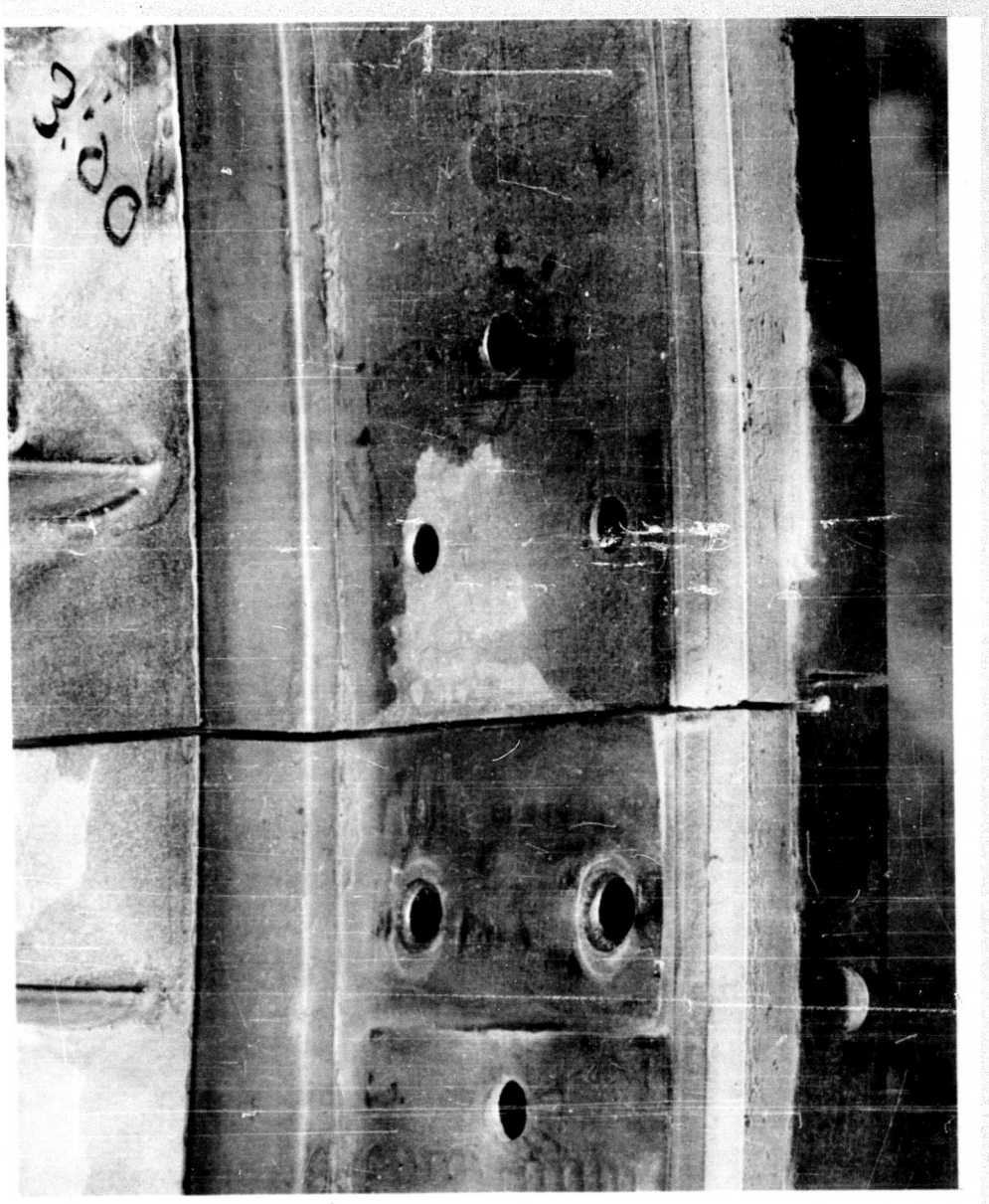

FIGURE 80 - AFT FRAME SAW CUT COMPRESSION

C1011024

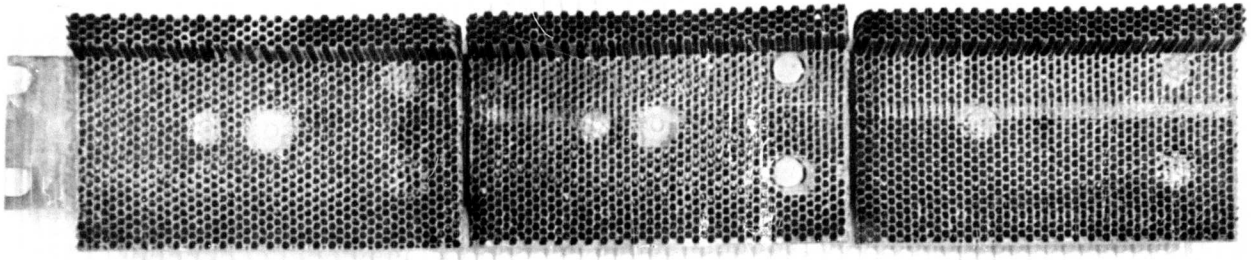

FIGURE 31 - BUCKET SHROUD RUB IN HONEYCOMB SEAL

C1011025

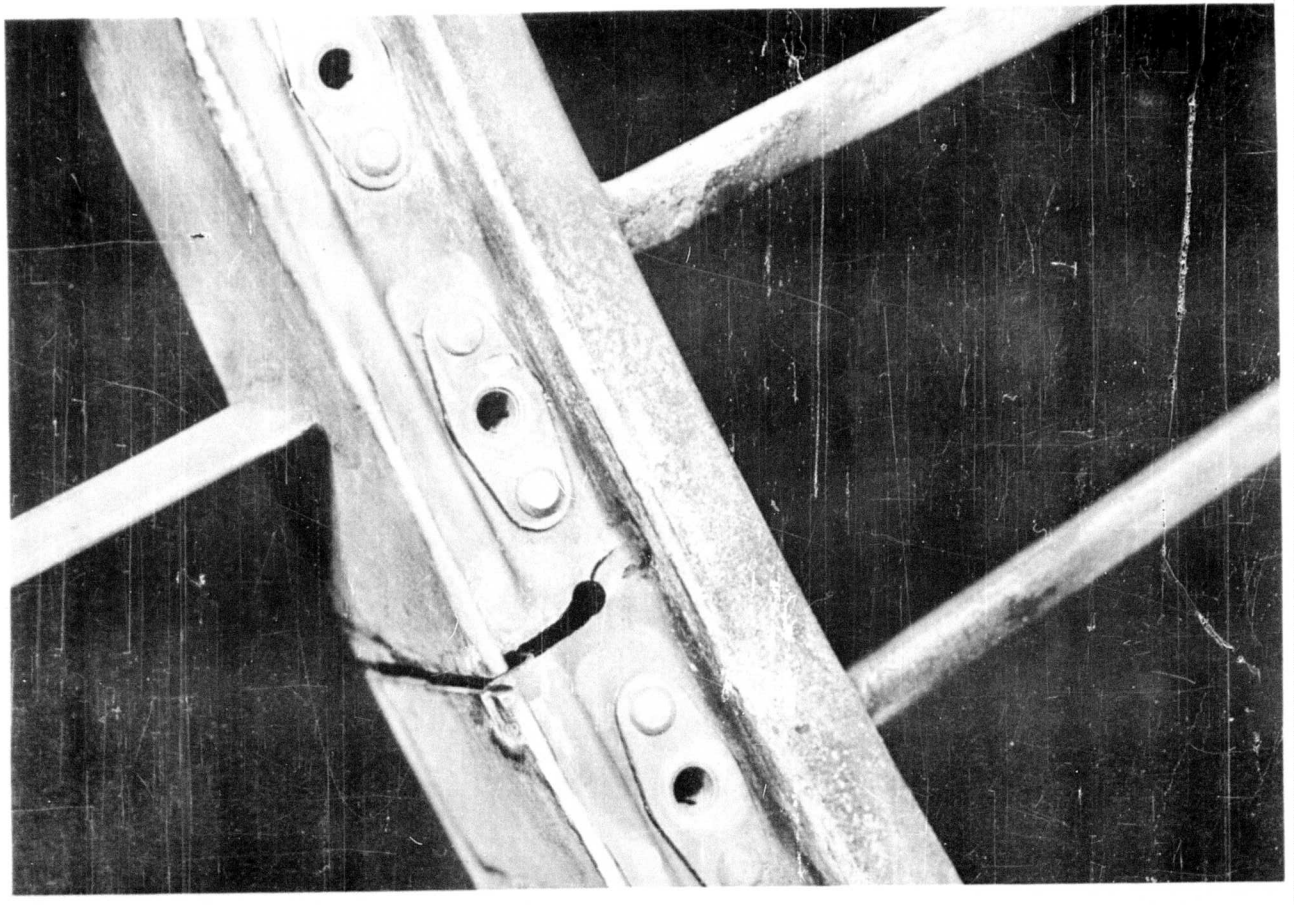

FIGURE 82 - SUPPORT RING CRACK PROPAGATION IN AFT FRAME

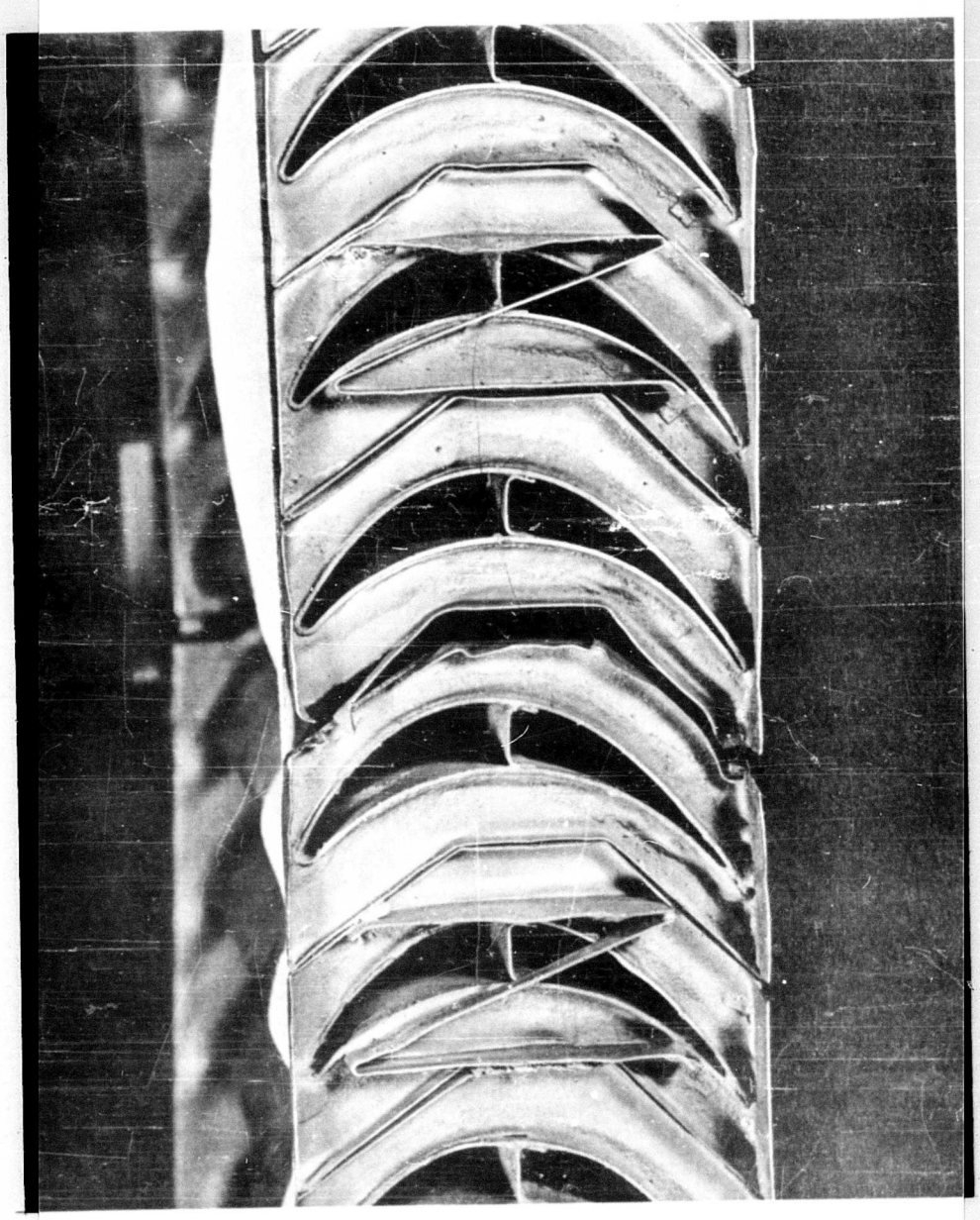

FIGURE 83 - BUCKET SHROUD DETAIL

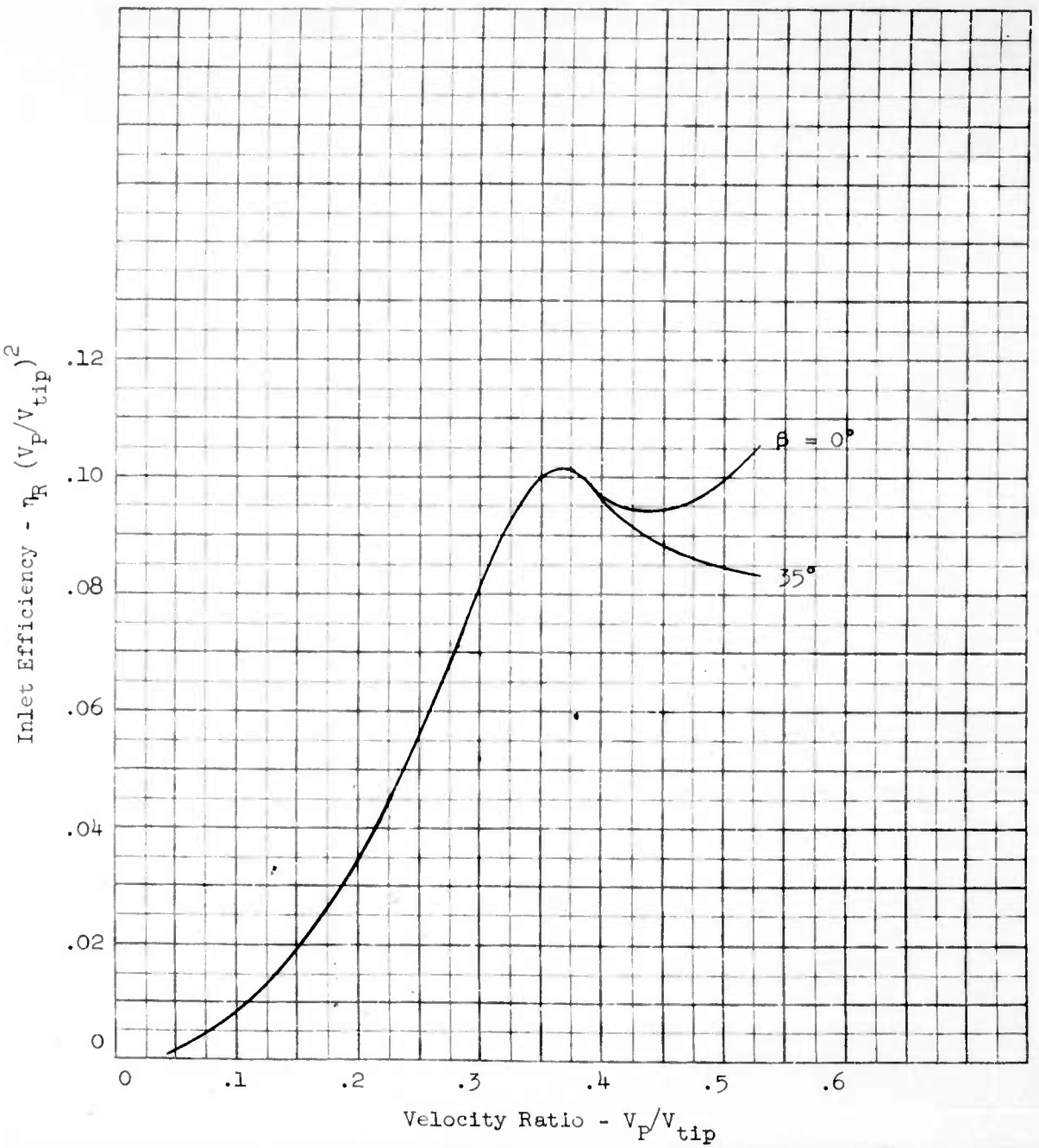

FIGURE 84 - FAN INLET EFFICIENCY VERSUS VELOCITY RATIO

LIST OF DISTRIBUTION

Volume 2

Commanding General
United States Continental Army Command
ATTN: Materiel Developments
Fort Monroe, Virginia (1)

President
United States Army Aviation Board
ATTN: ATBG-DG
Fort Rucker, Alabama (1)

Chief of Transportation
ATTN: TCDRD (1)
ATTN: TCAFO-D (1)
Department of the Army
Washington 25, D. C.

Commander
Aeronautical Systems Division
Air Force Systems Command
ATTN: EWAPEL-(Z) (1)
ATTN: WWRMPT (1)
Wright-Patterson Air Force Base, Ohio

Commanding Officer
U. S. Army Transportation Research Command
ATTN: Research Reference Center (4)
ATTN: Aviation Directorate (1)
ATTN: Military Liaison Office (1)
Fort Eustis, Virginia

Commander
Air Research & Development Command
ATTN: RDR-LA (1)
Andrews Air Force Base
Washington 25, D. C.

Commanding Officer and Director
David Taylor Model Basin
Aerodynamics Laboratory
Washington 7, D. C. (1)

Chief, Bureau of Naval Weapons (R-38)
Department of the Navy
ATTN: RAPP-14 (1)
ATTN: RAAD-32 (1)
Washington 25, D. C.

Chief of Naval Research
Code 461, Maj. L. C. Robertson
Washington 25, D. C. (1)

U. S. Army Standardization Group, U.K.
Box 65, U. S. Navy 100
FPO New York, New York (1)

Director
Operations Research Office
ATTN: Library
The Johns Hopkins University
6935 Arlington Road
Bethesda, Maryland (1)

NASA
ATTN: Bertram A. Mulcahy
Asst. Director for Technical Info.
1520 H Street, N.W.
Washington 25, D. C. (1)

Librarian
Langley Research Center
NASA
Langley Field, Virginia (1)

Ames Research Center
NASA
ATTN: Library
Moffett Field, California (1)

NASA
Lewis Research Center
ATTN: Library
21000 Brookpark Road
Cleveland 35, Ohio (1)

Commander
Armed Services Technical Info. Agency
ATTN: TIPCR
Arlington Hall Station
Arlington 12, Virginia (10)

Office of Chief of R&D
ATTN: Air Mobility Division
Department of the Army
Washington 25, D. C. (1)

Office of the Senior Standardization Representative
U. S. Army Standardization Group, Canada
c/o Director of Equipment Policy
Canadian Army Headquarters
Ottawa, Canada (1)

Canadian Army Liaison Officer
Liaison Group, Room 208
U. S. Army Transportation School
Fort Eustis, Virginia (3)

British Joint Services Mission (Army Staff)
ATTN: Lt. Col. R. J. Wade, RE
DAQMG (Mov & Tn)
3100 Massachusetts Avenue, N. W.
Washington 8, D. C. (3)

Convair
Division of General Dynamics Corporation
San Diego 12, California
ATTN: Library (1)

Grumman Aircraft Engineering Corporation
Bethpage, Long Island, New York
ATTN: Library (1)

Hiller Aircraft Corporation
Palo Alto, California
ATTN: Library (1)

North American Aviation, Inc.
Columbus Division
4300 East Fifth Avenue
Columbus 16, Ohio
ATTN: Library (1)

Republic Aviation Corporation
Farmingdale, Long Island, New York
ATTN: Library (1)

Ryan Aeronautical Company
San Diego, California
ATTN: Library (1)

Vertol Division
Boeing Airplane Company
Morton, Pennsylvania
ATTN: Library (1)

Army Research Office
Office of the Chief of Research and Development
ATTN: Research Support Division
Department of the Army
Washington 25, D. C. (1)

Commanding General
U. S. Army Transportation Materiel Command
ATTN: TCMAC-APU
P.O. Box 209, Main Office
St. Louis 66, Missouri (1)

GENERAL ELECTRIC COMPANY
TECHNICAL INFORMATION SERIES
CONTENTS PAGE

CONTENTS OF REPORT

NO. PAGES TEXT

NO. CHARTS

DRAWING NOS.

PHOTO NOS.

DISTRIBUTION

A. P. Adamson (1)
W. B. Campbell (3)
D. E. Clark (1)
W. R. Collier (2)
R. H. Goldsmith (4)
O. J. Krasner (1)
W. R. Morgan (2)

FOR USE OF G-E EMPLOYEES ONLY

GENERAL ELECTRIC

TECHNICAL INFORMATION SERIES

Title Page

AUTHOR	SUBJECT CLASSIFICATION	NO.
Z.J. Przedpelski	TEST RESULTS FUSELAGE MOUNTED LIFT FAN - VTOL	R61 FPD 427
		DATE April, 1961

TITLE: RESULTS OF WIND TUNNEL TESTS OF A FULL SCALE FUSELAGE MOUNTED, TIP TURBINE DRIVEN LIFT FAN

ABSTRACT: Results of wind tunnel tests of a full scale, fuselage mounted, tip turbine driven lift fan. Volume 2 of 3, April '61, 237 pages-illustrations-tables (Contract DA 44-177-TC584) USA TRECOM Project 9R 38-01-020-02, TREC 61-15. Unclassified Report (Vol. 1 - TIS R61 FPD 210). This report covers 30 hours of testing in the NASA-AMES 40'x80' wind tunnel. Propulsion & aircraft performance and

G.E. CLASS	REPRODUCIBLE COPY FILED AT	NO. PAGES
2	Flight Prop. Division Technical Information Center	237
GOV. CLASS. Unclassified		

Abstract Cont'd: interactions are discussed. Test results indicate that the Lift Fan can proceed to the next phase of the test program.

CONCLUSIONS: (1) Hover Fan lift was 7050 lbs at 100% speed. (2) Short take off analysis of the system shows a distance of 860 feet to clear a 50' obstacle at a gross weight equal to 1.1 of the max. installed lift. (3) Take off & landing transition schedules studied indicated no major control or stability problems. (4) The fan inlet recovered 100% of flight dynamic pressure throughout a flight speed range sufficient for take off transition, and neither angle of attack nor angle of yaw had an appreciable effect on inlet performance over a wide range of the variables

By cutting out this rectangle and folding on the center line, the above information can be fitted into a standard card file.

For list of contents — drawings, photos, etc. and for distribution see next page (GT 2063-B1).

INFORMATION PREPARED FOR Contract DA 44-177-TC-584

TESTS MADE BY Flight Propulsion Laboratory Department

COUNTERSIGNED R.H. Goldsmith OPERATION VTOL

DIVISION Flight Propulsion Div. LOCATION Evendale, Ohio

GT 2063-A1 (10-52)

AP ______________ Accession No. ____________

General Electric Co., Cincinnati, Ohio
FABRICATION, TEST & ANALYSIS OF A TIP TURBINE LIFT FAN VTOL PROPULSION SYSTEM.

Results of wind tunnel tests of a full scale, fuselage mounted, tip turbine driven lift fan.
Volume 2 of 3, April 1961, 237 pages-illustrations-tables (Contract DA 44-177-TC584) USA TRECOM Project 9R 38-01-020-02, TREC 61-15. Unclassified Report.

This report covers 30 hours of testing in the NASA-AMES 40' x 80' wind tunnel.
Propulsion and aircraft performance and interactions are discussed.
Test results indicate that the Lift Fan can proceed to the next phase of the test program.

UNCLASSIFIED

1. VTOL Propulsion System
2. Contract DA 44-177-TC-584

AP ______________ Accession No. ____________

General Electric Co., Cincinnati, Ohio
FABRICATION, TEST & ANALYSIS OF A TIP TURBINE LIFT FAN VTOL PROPULSION SYSTEM.

Results of wind tunnel tests of a full scale, fuselage mounted, tip turbine driven lift fan.
Volume 2 of 3, April 1961, 237 pages-illustrations-tables (Contract DA 44-177-TC584) USA TRECOM Project 9R 38-01-020-02, TREC 61-15. Unclassified Report.

This report covers 30 hours of testing in the NASA-AMES 40' x 80' wind tunnel.
Propulsion and aircraft performance and interactions are discussed.
Test results indicate that the Lift Fan can proceed to the next phase of the test program.

UNCLASSIFIED

1. VTOL Propulsion System
2. Contract DA 44-177-TC-584

AP ______________ Accession No. ____________

General Electric Co., Cincinnati, Ohio
FABRICATION, TEST & ANALYSIS OF A TIP TURBINE LIFT FAN VTOL PROPULSION SYSTEM.

Results of wind tunnel tests of a full scale, fuselage mounted, tip turbine driven lift fan.
Volume 2 of 3, April 1961, 237 pages-illustrations-tables (Contract DA 44-177-TC584) USA TRECOM Project 9R 38-01-020-02, TREC 61-15. Unclassified Report.

This report covers 30 hours of testing in the NASA-AMES 40' x 80' wind tunnel.
Propulsion and aircraft performance and interactions are discussed.
Test results indicate that the Lift Fan can proceed to the next phase of the test program.

UNCLASSIFIED

1. VTOL Propulsion System
2. Contract DA 44-177-TC-584

AP ______________ Accession No. ____________

General Electric Co., Cincinnati, Ohio
FABRICATION, TEST & ANALYSIS OF A TIP TURBINE LIFT FAN VTOL PROPULSION SYSTEM.

Results of wind tunnel tests of a full scale, fuselage mounted, tip turbine driven lift fan.
Volume 2 of 3, April 1961, 237 pages-illustrations-tables (Contract DA 44-177-TC584) USA TRECOM Project 9R 38-01-020-02, TREC 61-15. Unclassified Report.

This report covers 30 hours of testing in the NASA-AMES 40' x 80' wind tunnel.
Propulsion and aircraft performance and interactions are discussed.
Test results indicate that the Lift Fan can proceed to the next phase of the test program.

UNCLASSIFIED

1. VTOL Propulsion System
2. Contract DA 44-177-TC-584